THE ROLE OF MULLERIAN DIFFERENTIATION IN EPITHELIAL OVARIAN CARCINOGENESIS

by

Michelle M.M. Woo

B.Sc., University of British Columbia, 1997
M.Phil., University of Hong Kong, 2000

A THESIS SUBMITTED IN PARTIAL FULFILLMENT OF THE REQUIREMENTS FOR THE DEGREE OF

DOCTOR OF PHILOSOPHY

in

The Faculty of Graduate Studies

(Reproductive & Developmental Sciences)

THE UNIVERSITY OF BRITISH COLUMBIA

January, 2008

ABSTRACT

Ovarian cancer is a fatal disease because of the lack of symptoms and markers for early detection. Most ovarian neoplasms resemble and are classified according to the complex characteristics of Mullerian duct epithelia. We tested the hypothesis that Mullerian epithelial characteristics influence early ovarian neoplastic progression.

The most common type of ovarian cancer is the serous carcinoma which resembles Mullerian-derived oviductal epithelium. We discovered that oviduct-specific glycoprotein (OVGP1), a tubal differentiation marker, was present in inclusion cysts, which are the preferential sites for malignant transformation, and in most low grade serous tumors, but absent in ovarian surface epithelium and most high grade carcinomas. OVGP1 was almost entirely limited to ovarian neoplasms with the notable exception of endometrial hyperplasia and carcinoma. A new antibody against OVGP1 detected elevated serum levels from most women with low grade ovarian cancers compared to normal controls. OVGP1 also identified a subset of patients with high grade serous carcinomas who had a more favorable outcome.

To examine whether the differentiated phenotype of early ovarian neoplasms alters invasiveness, we established the first permanent cell line for serous borderline ovarian tumors (SBOT), which are differentiated but noninvasive. The results revealed a striking phenotypic similarity between two lines regardless of their cytogenetic diversity. They retained Mullerian epithelial characteristics *in vitro*, as demonstrated by their morphologic appearance and the differentiation

markers keratin**,** E-cadherin, CA125 and OVGP1. Neither disruption of the growth pattern nor manipulations of the cadherin profile induced invasivenesss. Induction of invasiveness by SV40 early genes was associated with a loss in morphologic differentiation and of differentiation markers but increased motility. MMP secretion was independent of the invasion status.

Our findings indicate that OVGP1 is an indicator of early ovarian epithelial neoplasia. It can be detected in the sera from women with early ovarian cancer, and thus, may be a new promising diagnostic marker for the early detection of ovarian cancer. In addition, the results show that Mullerian differentiation does not directly prevent invasiveness, but it diminishes in parallel with invasion caused by other factors. The lack of invasiveness by SBOT cells may depend on factors that regulate motility.

TABLE OF CONTENTS

LIST OF TABLES

LIST OF FIGURES

LIST OF ABBREVIATIONS

3-D	three-dimensional
4-HPR	N-(4-Hydroxyphenyl)-retinamide
aCGH	microarray comparative genomic hybridization
AH	atypical hyperplasia of the endometrium
APMA	aminophenylmercuric acetate
ATCC	American Type Culture Collection
ATRA	all-trans retinoic acid
bp	basepair
cDNA	complementary deoxyribonucleic acid
cFN	cellular fibronectin
CGH	comparative genomic hybridization
DMSO	dimethylsulfoxide
DNA	deoxyribonucleic acid
EC	endometrial cancer
ECM	extracellular matrix
EDTA	ethylenediamine tetraacetic acid
EEC	endometrioid endometrial cancer
EGFR	epidermal growth factor receptor
ELISA	enzyme-linked immunoabsorbent assay
EMT	epithelio-mesenchymal transition
EOC	epithelial ovarian cancer
ER	estrogen receptor
ERE	estrogen responsive element
ERK	extracellular regulated kinase
FBS	fetal bovine serum
H	hyperplasia of the endometrium
HGF	hepatocyte growth factor
HOX	homeobox

HSF	hydrosalpinx fluid
FBS	fetal bovine serum
FIGO	International Federation of Gynaecology and Obstetrics
G	grade
IOSE	immortalized OSE, OSE transfected with SV40 LT/ST antigens
ISBOT	immortalized SBOT, SBOT transfected with SV40 LT/ST antigens
kDa	kiloDalton
LMP	ovarian tumors of low malignant potential, a.k.a. SBOT
LT	simian virus 40 large T-antigen
MAPK	mitogen activated protein kinase
mFISH	multicolor fluorescent in-situ hybridization
MMP	matrix metalloproteinase
mRNA	messenger ribonucleic acid
PBS	phosphate-buffered salt solution
pFN	plasma fibronectin
PP2A	protein phosphatase 2A
pRB	retinoblastoma protein
RAR	retinoic acid receptor
RT-PCR	reverse transcription polymerase chain reaction
OSE	ovarian surface epithelium
OVGP1	oviductal glycoprotein 1, oviduct-specific glycoprotein, mucin 9
SBOT	serous borderline ovarian tumor, a.k.a. LMP
SD	standard deviation
SDS	sodium dodecyl sulphate
SF-1	steroidogenic factor-1
siRNA	small interfering ribonucleic acid
ST	simian virus 40 small t-antigen
SV40	simian virus 40

TIC	tubal intraepithelial carcinoma
TBS	tris-buffered salt solution
TBST	tris-buffered salt solution/tween-20
uPA	urokinase plasminogen activator
UPSC	uterine papillary serous carcinoma
WT-1	Wilm's tumour-1
w/v	weight per volume

ACKNOWLEDGMENT

Knowledge, spirit and perserverance has enabled me to complete this thesis. These are traits that Dr. Nelly Auersperg has insisted upon me through her mentorship and leadership. Her enthusiasm for research is truly contagious.

Many thanks to my supervisory committee for their guidance: Dr. C. Blake Gilks, Dr. Steven Pelech, Dr. Calvin Roskelley and Dr. Young S. Moon.

Dr. Gilks has been an incredible collaborator and mentor. Through his mentorship, I have developed a greater understanding of and appreciation for the complexity of ovarian cancer pathology. His patience in guiding me through statistical techniques was a great aid in understanding and interpreting results. My sincere thanks for the numerous and fruitful collaborations.

Dr. Pelech is like an oak tree; unwavering and someone you can always rely on.

Each meeting with Dr. Roskelley has been inspiring: helping me to "think outside the box". His perspectives are enlightening.

Dr. Moon's support of my studies since the beginning has provided much encouragement. His quiet nudges have directed me forward.

Many, many thanks to Dr. Harold G. Verhage and Dr. Robert Molday for their generous gift of the OVGP1 antibodies and for their enthusiasm in my project.

A sincere thank you is extended to Dr. Peter C.K. Leung who trusted in me as an undergraduate in his lab and for his continual trust in me as a graduate student in

the department.

A warm thank you to Sarah Maines-Bandiera, Clara Salamanca, and all my past and present colleagues in the lab. You have made the lab such a wonderful place to be.

A special thank you to Roshni Nair who provided much-needed secretarial and moral support throughout my studies.

Thank you to the Terry Fox Foundation and the National Cancer Institute of Canada, the Michael Smith Foundation for Health Research, and the Child and Family Research Institute for their generous funding and, most importantly, for believing in my ideas and believing in me.

To my family, you have made all of this matter. I thank you for your endearing support.

This is dedicated to all the women and their families whose lives have been affected by ovarian cancer.

1. INTRODUCTION

1.1 Rationale/Objective

Epithelial ovarian cancer (EOC) is the most common form of ovarian cancer. Traditionally, EOC has been thought to arise from the epithelial ovarian lining. Recent studies, however, have suggested an alternate source for EOCs, the fallopian tube epithelium. Embryologically, the ovarian surface epithelium (OSE) and fallopian tube epithelium are closely related. OSE originates from the coelomic epithelium which overlies the gonadal ridge. The coelomic epithelium directly adjacent to this region on the lateral surface of the gonadal ridge undergoes invaginations which eventually coalesce with one another to give rise to the Mullerian ducts, which are the primordia for the epithelia of the fallopian tube, endometrium and endocervix. Thus, Mullerian differentiation refers to the acquisition of characteristics of tubal, endometrial, or endocervical epithelia. Ovarian neoplasia is associated with the complex characteristics of Mullerian duct epithelia. It is believed that as OSE progresses to malignancy, it acquires these differentiated properties. Thus, in contrast to other tissues where carcinogenesis is accompanied by a loss of differentiation, malignant OSE acquires a more highly differentiated epithelial phenotype. The high proportion and consistency of ovarian cancers where such aberrant Mullerian differentiation occurs suggests that this change may confer a selective advantage on the transforming cells. Mullerian differentiation is so frequent in ovarian neoplasms that it serves as the basis for the classification of these cancers. The most common type of ovarian cancer is the serous carcinoma which resembles

oviductal epithelium. Therefore, this study tested the hypothesis that Mullerian epithelial characteristics play a role in early ovarian neoplasia. As ovarian cancer is characterized by few early symptoms and presentation at an advanced stage, it remains the most frequent cause of death from gynecological cancer. Therefore, the general aims were to examine early events in ovarian carcinogenesis and to find new diagnostic markers. The specific aims of this study were:

1. To develop a culture model system for the differentiated but non-invasive serous neoplasms, serous borderline ovarian tumors (SBOT).

2. To characterize SBOTs cultured *in vitro* and to examine whether their differentiated phenotype prevents the progression to invasive cancer.

3. To identify specific markers expressed by normal Mullerian epithelium for use as possible diagnostic/prognostic markers of ovarian cancer in women.

Two additional projects were also undertaken to examine early events in ovarian carcinogenesis but have not yet been completed. The specific aims were:

1. To investigate whether E-cadherin and hepatocyte growth factor play a promoting role in glandular differentiation that is part of the Mullerian differentiation of many ovarian tumors.

2. To determine the effects of retinoic acid, a differentiation factor and chemopreventive agent for ovarian cancer, on proliferation and differentiation of (pre)neoplastic OSE cells.

1.2 Ovarian Cancer

1.2.1 Overview

Ovarian cancer is a disease characterized clinically by vague early symptoms, usual presentation at an advanced stage, and poor survival statistics. The disease will present itself in greater than 190 000 women worldwide and 140 000 women will succumb to the disease this year alone.

Ovarian cancer is the fourth most common cause of death from all cancers in women although it only accounts for about 4% of all cancers in the female population (Jemal *et al.*, 2007). It is certainly the most lethal of all gynecologic malignancies. The lifetime risk of developing ovarian cancer is 1 in 70, compared to 1 in 8 or 9 for breast cancer. The overall five-year survival rate is approximately 50% (Heintz *et al.*, 2006). If the cancer is detected at an early stage when the tumour is limited to the ovary, the five-year survival rate increases dramatically to 90% (Heintz *et al.*, 2006). However, this occurs in less than a fifth of the cases reported. This is in stark contrast to late stage disease when the tumor has spread beyond the pelvis and the five-year survival rate is a dismal 18-47% (Heintz *et al.*, 2006). Resistance to cisplatin-based chemotherapies is a major cause for failure in treatment of ovarian cancer (Fraser *et al.*, 2007). The absence of major symptoms in the early stages and the propensity for recurrence of advanced stage disease clearly points to a need for early detection and better treatment.

1.2.2 Early detection of ovarian cancer

At present, there are no reliable means of early detection for ovarian cancer. There are trials currently underway to screen women in the general population and in

the high-risk population to assess the impact of screening on ovarian cancer mortality (reviewed in Jacobs & Menon, 2004). Two distinct strategies are being employed: (1) transvaginal ultrasound and (2) measurement of the serum tumour marker CA125 with ultrasound as the secondary test (multimodal screening). Transvaginal ultrasound is not capable of differentiating cancerous from benign masses and the cost of screening using this approach would be prohibitive. As such, a two-stage screening strategy would test for abnormal serum tumour marker levels which would subsequently trigger TVS. CA125 has been evaluated the most extensively as a serum tumour marker but it is only detected in 50-60% of early stage disease and is elevated in many conditions other than ovarian cancer, including uterine fibroids, endometriosis, menses, pregnancy and pelvic inflammatory disease (Bast *et al.*, 2002). Current studies are aimed at increasing the sensitivity of the CA125 assay by evaluating other markers in combination with CA125 but these have resulted in decreased specificity (Bast *et al.*, 2002). Novel markers including proteins, genes and metabolites are currently being investigated as possible biomarkers for the early detection of EOC. By far, protein biomarkers have been studied the most extensively as they are the end products of genes and thus, are the driving force for functional change (Williams *et al.*, 2007). The proteins which have sparked the most interest in recent years include but are in no way limited to CA 19-9, CA 72-4, carcinoembryonic antigen (CEA), galactosyl transferase, haptoglobin, HE4, inhibin, the kallikreins, macrophage colony stimulating factor (M-CSF), mesothelin, prostasin, leptin, prolactin, osteopontin, and insulin-like growth factor-II, all of which are elevated with advanced stage disease (reviewed in Bast *et al.*, 2007 and Williams

et al., 2007). There is general consensus that having a single biomarker achieve the required specificity is highly unlikely and thus investigators are now aiming at identifying an optimal combination or panel of biomarkers that are individually up- or down-regulated. Specificity in detecting early ovarian cancer may be improved by identifying markers present only in early ovarian neoplasms or become lost with advanced stage disease. In this study, we have identified such a biomarker for EOC, oviduct-specific glycoprotein (OVGP1) which will be discussed in Section 1.3.1.

1.2.3 Etiology and epidemiology

The etiology and early events in ovarian epithelial carcinogenesis are among the least understood of all major human malignancies. Increasing age (Heintz *et al.*, 2006), ethnicity (Weiss & Peterson, 1978; Grulich *et al.*, 1992; Swerdlow *et al.*, 1995), obesity (Farrow *et al.*, 1989; Li *et al.*, 2007), family history of the disease (reviewed in Lynch & Smirk, 1996 and Boyd & Rubin, 1997), and use of fertility drugs (Whittemore *et al.*, 1992) are all known contributing factors to ovarian cancer. Other factors shown to increase the risk of ovarian cancer include the use of talcum powder on the perineum, which may contain asbestos particles and may ascend upwards into the female genital tract (Piver *et al.*, 1991). In addition, pelvic inflammatory disease may confer an increased risk while tubal ligation reduces the risk (Risch & Howe, 1995). Although the source of EOC is still being debated, epidemiologic risk factors have provided clues to the causes of EOC. Two theories based on epidemiological data were first described in the 1970s. The first theory is associated with the number of ovulatory cycles. Early menarche, late menopause and nulliparity increase the number of ovulatory cycles and are related to an increased

risk of ovarian cancer (American Cancer Society. http://www.cancer.org; Booth *et al.*, 1989; Riman *et al.*, 1998). On the other hand, increasing parity, prolonged breastfeeding and use of oral contraceptives decrease the number of ovulatory cycles and thus, decrease the risk of ovarian cancer. These data support the "incessant ovulation" theory proposed by Fathalla in 1971 (Fathalla, 1971). With repeated ovulation, the ovarian surface epithelium, believed to be the source of EOC, becomes exposed to the estrogen-rich follicular fluid and undergoes frequent periods of rapid cell division, which increases their susceptibility to genetic damage and risk of transformation. The "gonadotropin hypothesis" was suggested by Stadel in 1975 whereby elevated levels of gonadotropins coincide with early menopause and an increased frequency of epithelial ovarian cancer (Stadel, 1975).

1.2.4 Source of epithelial ovarian cancer

It has long been believed that the human ovarian surface epithelium (OSE), a simple mesothelium overlying the ovary, is the major source of EOCs. However, in recent years, the oviductal epithelium has been identified as an alternate source for EOC, specifically the high-grade serous carcinomas (Callahan *et al.*, 2007). Several studies have shown that a significant proportion of women with heritable BRCA1 or 2 mutations undergoing prophylactic salpingo-oophorectomy harbored tumors in their fallopian tube upon careful examination of serial sections of the tube (Powell *et al*., 2005; Lee *et al.*, 2006; Finch *et al.*, 2006; Callahan *et al.*, 2007). The developmental relationship between these two epithelia and the basis for the malignant potential of these two epithelial sources will be discussed in the following sections. Other sources of EOC will also be discussed briefly.

1.2.4.1 Development of the ovarian surface epithelium and the Mullerian ducts

Early in embryonic development, the future OSE forms part of the coelomic epithelium, which in turn gives rise to Mullerian duct-derived epithelia, i.e. the epithelia of the oviduct, endometrium, and endocervix. The OSE overlies the presumptive gonadal area and, by proliferation and differentiation, gives rise to part of the gonadal blastema. The coelomic epithelium undergoes numerous changes during prenatal development and is considered a pleuripotent epithelium because it can give rise to several epithelial tissues.

During embryonic development, the zygote, a totipotent stem cell with the ability to become all the different cell types in the body, divides many times and progressively transforms into a multicellular human being through cell division, migration, growth, apoptosis, and differentiation. The zygote reaches the uterine cavity, and implantation occurs before the end of the first week of gestation. At the end of the second week of embryonic life, the human embryo is bilaminar, with two germ layers (dorsal epiblast and ventral hypoblast) (Moore & Persaud, 1998; Dye, 2000). During the third week of development, the mesodermal cells that give rise to the future OSE develop as an invagination of epiblastic cells from the primitive streak (Fig. 1A) (Auersperg & Woo, 2004). These cells give rise to mesenchymal cells, which migrate between the epiblast and hypoblast and form a layer known as the intraembryonic mesoderm.

Depending on the region from which the epiblastic cells migrated, the mesodermal cells form the paraxial, intermediate, and lateral mesoderm. The

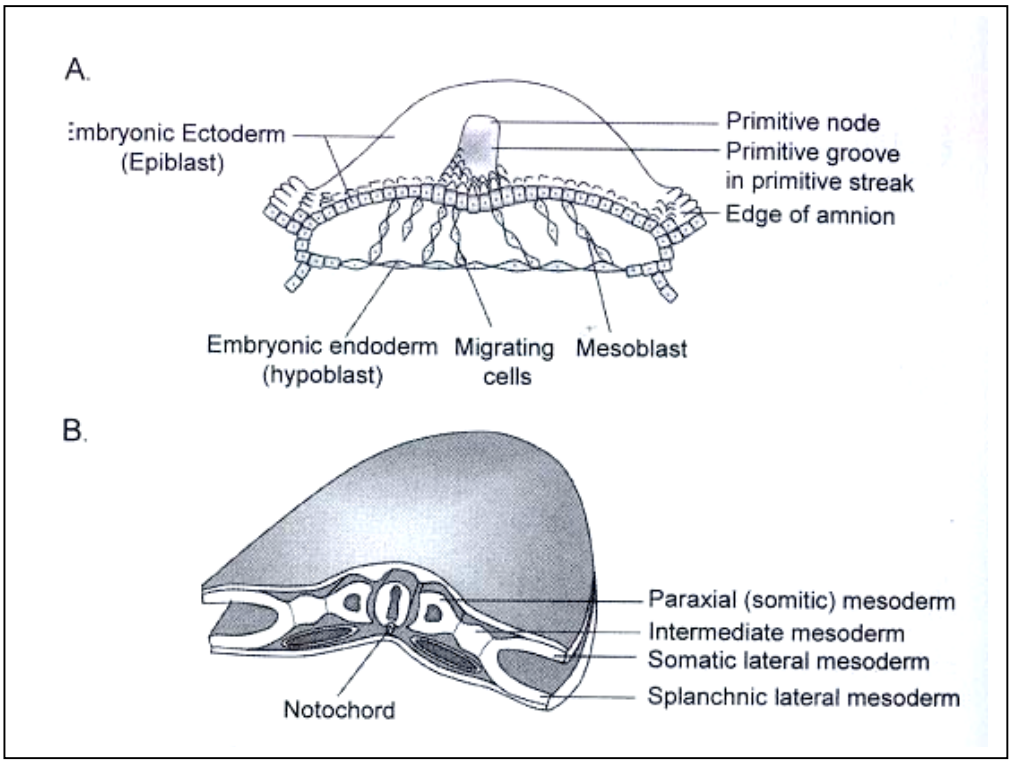

Fig. 1. Early developmental stages of the presumptive gonads and coelomic epithelium. (A) During the third week of embryonic development, gastrulation occurs and epiblastic cells from the primitive streak migrate between the epiblast and hypoblast to form mesoblast or mesenchyme that soon organizes to form the intraembryonic mesoderm. (B) Depending on the region from which the epiblastic cells migrated, the embryonic mesoderm can be subdivided into three layers: the paraxial, intermediate, and lateral plate mesoderm. The urogenital system is derived from the intermediate mesoderm, where the somatic and splanchnic mesoderm diverge, and the overlying mesoderm becomes the ovarian surface epithelium. (Auersperg & Woo, 2004)

coelomic epithelium is derived from the lateral mesoderm, where isolated coelomic spaces or vesicles begin to form, which eventually coalesce to form a single cavity. As lateral folding of the embryo occurs, the intraembryonic coelom is formed. This cavity separates the lateral mesoderm into two layers: (1) a somatic or parietal layer and (2) a splanchnic or visceral layer. The parietal mesoderm layer surrounding the developing intraembryonic coelom is the primordium for the mesothelium (peritoneum) of the peritoneal and pleural cavities. In the region where the parietal and splanchnic mesoderm diverge, the underlying intermediate mesoderm develops into the urogenital system and the overlying mesoderm becomes OSE (Moore & Persaud, 1998) (Fig. 1B).

In the four-week embryo, the first sign of gonadal development is detectable. The first signs of differentiation of the intermediate mesoderm are in the most cranial regions, where the remnants of the earliest form of the kidney, the pronephros, briefly appear. In the latter part of the fourth week, a longitudinal prominence, the pronephric duct, appears on each side of the embryo (Nicosia *et al.*, 1991; Byskov, 1986). This duct is important in organizing the development of much of the adult urogenital system, which forms largely from cells of the caudal portions of the intermediate mesoderm. Development of the duct begins cranially and extends caudally toward the developing mesonephros. The gonads arise from an elongated region of steroidogenic mesoderm along the ventromedial border of the mesonephros. Thus gonadal development is closely associated with the mesonephros, which participates in gonad formation, in the gonad itself, and in association with the Mullerian duct.

Transcriptional factors that are important regulators of gonadal and kidney development include steroidogenic factor-1 (SF-1) and the Wilm's tumour suppressor gene (WT-1). SF-1 is expressed in embryos from the earliest stages of gonadogenesis, when the intermediate mesoderm condenses to form the urogenital ridge (Ikeda *et al.*, 1994). SF-1 can direct pleuripotential embryonic stem cells to differentiate, at least partly, down the steroidogenic pathway, activating expression of the cholesterol side-chain cleavage enzyme (Crawford *et al.*, 1997; Parker & Schimmer, 1997). WT-1 is widely expressed in the coelomic epithelium, the subjacent mesenchyme, and in mesonephric structures, in accordance with a role in gonadal and renal morphogenesis (Kreidberg *et al.*, 1993). WT-1 appears to regulate the transformation from mesenchyme to epithelium during early development of the urogenital system: the differentiation of the metanephric mesenchyme to nephrons, the formation of the mesothelium from the mesenchyme lining the coelom, and the production of sex cords from the mesenchyme of the primitive gonad (Pritchard-Jones *et al.*, 1990). In the adult ovaries, the expression of WT-1 becomes restricted to the granulosa and theca cells.

Another factor that appears to be important in urogenital development is Wnt-4, a member of the Wnt family of locally acting secreted signaling glycoproteins. During development, it is expressed in the mesonephros and in the coelomic epithelium in the region of the presumptive gonad (Vainio *et al.*, 1999). Interestingly, it has been suggested that estrogens can regulate Wnt-4 expression in the adult and thus may also be important in regulation of fetal OSE development (Miller *et al.*, 1998). In addition, homeobox genes are believed to play a key role in the

differentiation of the Mullerian duct. The HOXA cluster, which includes, HOXA9, HOXA10, HOXA11 and HOXA13 is initially dispersed in the developing human paramesonephric duct but subsequently becomes spatially narrowed. In the adult, HOXA9 is expressed in the fallopian tube, HOXA10 is expressed in the uterus, HOXA11 is expressed in the uterus and cervix, and HOXA13 is expressed in the cervix and the upper vagina (Taylor *et al.*, 1997; Cheng *et al.*, 2005; Yoshida *et al.*, 2006). Other genes such as SOX9, DAX-1, GATA-4, and Lhx9 may also play key developmental roles in gonadal differentiation (Sinclair, 1998; Morais da Silva *et al.*, 1996; Pelliniemi *et al.*, 1998; Birk *et al.*, 2000; Oreal *et al.*, 2002).

Just before and during the arrival of primitive germ cells in the urogenital ridge, starting at about five weeks of development, the coelomic epithelial cells covering the primitive gonad undergo marked proliferation, and some of the cells penetrate the underlying mesenchyme, which produces a bulge in the coelomic cavity, the genital ridge. The germinal component of the ovary (oocytes) in the adult derives from primordial germ cells, which appear first in the wall of the endoderm yolk sac. By week five, the urogenital ridge consists of several different kinds of somatic cells, a proliferating coelomic epithelium covering the developing gonad, and an underlying compartment containing mesenchymal cells, blood vessels, and cells of the neighbouring mesonephros (Byskov, 1986; Nicosia *et al.*, 1991).

In the six-week embryo, the paramesonephric or Mullerian ducts begin to develop on each side from invaginations of coelomic epithelium, in the mesonephric region (Parr & McMahon, 1998; Vainio *et al.*, 1999). The edges of these invaginations approach each other and fuse together to form the Mullerian ducts.

The cranial ends of the ducts open into the coelomic cavity as funnel-shaped structures, which later develop into the fallopian tubes. The paramesonephric ducts also run caudally and approach each other in the future pelvic region of the embryo, where they fuse together to form a Y-shaped structure. This crossing and ultimate meeting in the midline are caused by the medial swinging of the entire urogenital ridge. The region of midline fusion of the paramesonephric ducts ultimately becomes the uterus and endocervix, while the ridge tissue that is carried along with the paramesonephric ducts forms the broad ligament of the uterus (Moore & Persaud, 1998). Thus the coelomic epithelium in the vicinity of the presumptive gonads has the competence to create the Mullerian ducts (i.e., the primordia for the epithelia of the oviduct-endometrium, and endocervix). Interestingly, although the coelomic epithelium is the precursor of OSE, extraovarian peritoneum (EP), and Mullerian epithelia, the differentiation marker CA-125 is expressed in the adult in EP and Mullerian epithelia, but not in the OSE (Kabawat *et al.*, 1983). It has been suggested that this difference is evidence of divergent differentiation between OSE and EP, which leads to the cessation of CA125 production by OSE before birth (Kabawat *et al.*, 1983). An alternative interpretation is that the part of the coelomic epithelium that gives rise to OSE never reaches the stage of differentiation where CA125 is expressed, which is attained by the other epithelia in the first trimester of gestation.

At later stages of development, some of the germ cells have migrated to the urogenital ridge and are intermingling with the surface epithelial cells. A delicate basal lamina with scanty collagen fibrils separates these cells from the underlying mesenchyme. The coelomic epithelium continues to proliferate and forms a

multistratified, papillary epithelium overlying a basal lamina and in some areas a nascent tunica albuginea. The tunica albuginea in the future ovary is a collagenous connective tissue layer that separates the OSE from the underlying ovarian stroma. As shown by electron microscopy, continued growth of the coelomic epithelium into the underlying mesenchyme gives rise to finger-like epithelial cortical cords, which subsequently break up into isolated cell clusters, each surrounding one or more primitive germ cells (Gondos, 1975; Byskov, 1986; Nicosia *et al.*, 1991). These surrounding epithelial cells are the follicular or pregranulosa cells of the primordial follicles. Therefore, the fetal OSE is also likely a progenitor of the ovarian granulosa cells (Pan *et al.*, 1992).

During the late stages of fetal development, the coelomic epithelium reverts to one layer in the now elongated, lobular ovary. Common features on the apical surface of the epithelial cells now include microvilli, blebs, ruffles, and solitary cilia. The tunica albuginea is well developed. It is composed of bundles of collagen fibres and elongated fibroblasts. The germ cells (oogonia or oocytes), now surrounded by a single layer of flattened pregranulosa cells, detach themselves from the finger-like epithelial cords to form isolated primordial and primary developing follicles (Byskov, 1986).

In summary, during development of the coelomic epithelium, the fetal OSE changes from a flat-to-cuboidal simple epithelium with a fragmentary basement membrane to a multistratified, papillary epithelium on a well-defined basement membrane. Subsequently, it reverts to a monolayer of cuboidal cells covering the ovary. Thus the coelomic epithelium in and near the gonadal area represents an

embryonic field with the competence of capacity to differentiate along many different pathways. In addition to its likely role as a progenitor of granulosa cells, the coelomic epithelium in the gonadal region can also differentiate along Mullerian duct epithelial lines. The factors involved in the development and differentiation of the coelomic epithelium are not fully understood. This phenotypic plasticity of the coelomic epithelium during development appears to be retained in the adult OSE because it can alter its state of differentiation under physiologic and pathologic conditions (Auersperg & Woo, 2004).

1.2.4.2 Ovarian surface epithelium in the adult

The ovarian surface epithelium, also referred to in the literature as normal ovarian epithelium (Bast *et al.*, 1998) or ovarian mesothelium (Nicosia *et al.*, 1991; Nicosia *et al.*, 1997), is the part of the pelvic peritoneum that covers the ovary (Auersperg *et al.*, 2001). It is an inconspicuous tissue with no known major function, but it is of great importance in gynecologic pathology because it is believed to be the source of epithelial ovarian carcinomas. Specific aspects in the development and differentiation of OSE may contribute to the tendency of this simple epithelium to undergo malignant transformation and to create cancers that are structurally and functionally among the most complex of all human neoplasms (Auersperg & Woo, 2004). *In vitro* transfection studies and animal models of ovarian cancer support OSE as a source of ovarian neoplasms.

In addition to the changes that occur in the OSE during embryonic development, important changes also occur during adulthood. The adult human OSE retains the potential to differentiate along several pathways. These include

conversion to mesenchymal (stromal) phenotypes (epithelial-mesenchymal transition, EMT) under physiologic conditions, and the assumption of characteristics of the Mullerian duct-derived oviductal, endometrial, and endocervical epithelia, which are closely related to OSE developmentally, in metaplasia, and in the course of neoplastic progression (Auersperg & Woo, 2004).

After ovulation ruptures the ovarian surface, OSE cells adjacent to the ovulatory defect flatten, assume mesenchymal shapes, and become migratory, but retain some epithelial characteristics, such as polarization and intercellular contact (Nicosia *et al.*, 1991; Nicosia *et al.*, 1997). Preliminary evidence suggests that OSE can assume mesenchymal characteristics if they are dispersed within the ovarian cortex: sections through newly formed corpora lutea in postovulatory human ovaries have revealed fibroblast-like cells that contain keratin, identifying them as OSE (Auersperg *et al.*, 2001). This is reflected in *in vitro* cultures, whereby OSE cells at first form keratin-positive epithelial monolayers, but concurrently initiate synthesis of the stromal collagen type III (Dyck *et al.*, 1996). Subsequently, they modulate to more mesenchymal phenotypes, which are characterized by anterior-posterior polarity, secretion of collagen types I and III, and loss of epithelial markers (Auersperg *et al.*, 2001). *In vivo*, fragments of OSE may be trapped in the ovarian cortex by two mechanisms: (1) at the time of ovulation, as a result of rupture and repair of the ovarian surface, or (2) as a result of conformational changes of the ovary, which lead to entrapment of the OSE within invaginations (clefts) that can become separated from the surface. If such trapped OSE cells survive within the stroma, they may undergo EMT as a form of homeostasis, which leads to their

integration into the ovarian connective tissues as normal, functional stromal cells. Alternatively, they may fail to undergo EMT, in which case they would remain epithelial and form epithelial inclusion cysts. OSE lining inclusion cysts and clefts is prone to metaplasia and to neoplastic transformation as suggested by the "incessant ovulation" theory. This is also observed in culture where the capacity of OSE to undergo EMT is greatly reduced with malignant progression and, to a lesser degree, in women with a genetic predisposition to develop ovarian cancer (Auersperg *et al.*, 1994; Wong *et al.*, 1999).

On the ovarian surface, OSE normally exists as a simple nonproliferative mesothelium, where the cells undergo reversible shape changes to accommodate alterations in the contours of the ovary and bursts of localized proliferation to repair ovulatory damage. In contrast, OSE that is physically removed from the ovarian surface but retains its epithelial phenotype as the lining of inclusion cysts and surface clefts (invaginations) frequently undergoes metaplastic changes, which are most commonly of a tubal (oviductal) type. Early neoplastic changes with the potential to progress to carcinomas also appear preferentially in epithelial inclusion cysts. The basis for the propensity of OSE to undergo such changes when removed from the ovarian surface is unknown, but it is tempting to speculate that this propensity is related to the improved blood supply and exposure to paracrine stromal influences within the ovarian cortex (Auersperg & Woo, 2004).

An unusual aspect of epithelial ovarian carcinogenesis are the changes in differentiation that accompany neoplastic progression (Fig. 2). Whereas normal OSE is a simple epithelium with some stromal features, it acquires characteristics of the

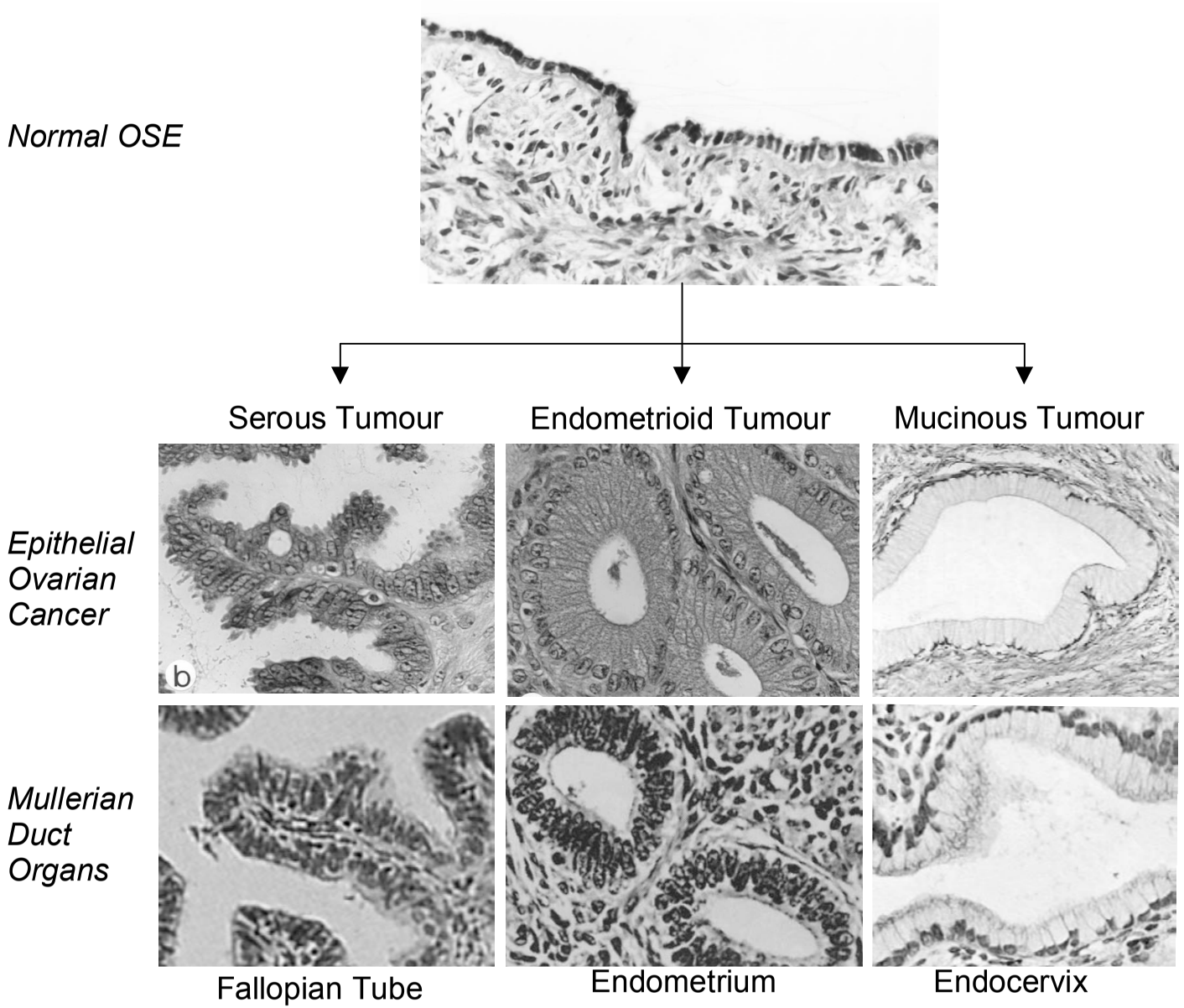

Fig. 2. Histologic appearance of normal ovarian surface epithelium (OSE), epithelial ovarian carcinomas derived from OSE, and normal epithelia derived from the Mullerian ducts. OSE is a simple mesothelium overlying the ovary. With neoplastic transformation, it frequently assumes the complex epithelial characteristics of either the fallopian tube, endometrium, or endocervix. The resulting carcinomas are classified as serous, endometrioid, and mucous, respectively. Note the resemblance of the carcinomas to the normal Mullerian duct-derived tissues and their complex architecture compared to OSE. Hematoxylin and Eosin, x200. (Auersperg & Woo, 2004)

Mullerian duct-derived (oviductal, endometrial, and endocervical) epithelia in the course of tumorigenesis. Like these epithelia, differentiated ovarian carcinomas lack the stromal markers of normal OSE and are more highly differentiated, as shown, for example, by high-molecular-weight keratins, mucus, cilia, the formation of glands and papillae, CA125 and the epithelial differentiation marker, E-cadherin (Auersperg *et al.*, 2001). It was previously shown that a hybrid ovarian carcinoma cell line expressing E-cadherin, in the presence of hepatocyte growth factor (HGF), was able to undergo branching morphogenesis, which mimics the formation of glands *in vivo* (Wong *et al.*, 2004). Therefore, one of the aims of this study was to examine whether the presence of E-cadherin in OSE was sufficient to induce the differentiated phenotype of well-differentiated ovarian carcinomas. Thus, in contrast to other epithelia where neoplastic progression results in loss of differentiation, OSE progresses to a more highly differentiated phenotype, which is lost again only in late stages (Auersperg *et al.*, 2001; Young *et al.*, 1998). Inappropriate expression of Mullerian differentiation by OSE in the course of neoplastic progression occurs so frequently and consistently as to suggest that it may confer a selective advantage on the transforming cells, perhaps in the form of altered responses to their environment.

Recent experimental models of epithelial ovarian carcinogenesis have lent support to OSE as the source of ovarian tumours. Investigators have successfully transformed human OSE cells by disrupting pathways, such as p53 and pRB, as well as by introducing activated HRAS or KRAS, that are often dysregulated in human ovarian cancer (Liu *et al.*, 2004; Yang *et al.*, 2007a; Yang *et al.*, 2007b). In addition, mouse models for ovarian cancer have also been developed. One such model was

described by Orsulic *et al.* (2002) who used an avian retroviral gene delivery technique for the introduction of multiple genes. Primary mouse ovarian cells from p53-deficient mice expressing a combination of the oncogenes, c-myc, K-ras, and Akt, were able to form tumours in immunocompromised mice (Orsulic *et al.*, 2002). In another approach, Connolly *et al.* (2003) showed that by using the Mullerian inhibitory substance type II receptor, which targets the epithelium of the female mouse reproductive tract including OSE, to direct the transforming region of SV40, bilateral, poorly differentiated ovarian tumours formed in the female transgenic mice. A more recent study took advantage of the enclosed anatomical location of the mouse ovary (Flesken-Nikitin *et al.*, 2003). Using a single intrabursal administration of recombinant adenovirus expressing Cre, they were able to demonstrate that concurrent inactivation of p53 and Rb1 was sufficient to induce epithelial ovarian carcinogenesis in the immunocompromised mice, which included the development of multiple serous cysts lined by neoplastic cells, as well as papillary structures, in addition to poorly differentiated carcinomas (Flesken-Nikitin *et al.*, 2003). Using the same methodology, a combination of oncogenic KRAS and PTEN deletion induces the formation of invasive endometrioid ovarian adenocarcinomas (Dinulescu *et al.*, 2005). The same phenotype could also be demonstrated via inactivation of the PTEN and APC tumor suppressor genes which alters the PI3K/PTEN and Wnt/β-catenin signaling pathways (Wu *et al.*, 2007). Naora's laboratory demonstrated that ectopic expression of homeobox genes, which normally controls differentiation of the Mullerian duct, in tumorigenic mouse OSE cells were able to induce ovarian tumors

with morphologic heterogeneity and the assumption of Mullerian-like features (Cheng *et al.*, 2005).

Thus, the adult OSE represents a relatively uncommitted epithelium with the capacity to alter its state of differentiation. It appears to have retained the pleuripotential nature of its mesodermal embryonic precursor, the coelomic epithelium. Preliminary data suggest that epithelio-mesenchymal transition may be a means of maintaining homeostasis of OSE that is displaced into the ovarian cortex, whereas a loss of the capacity to undergo this conversion may contribute to the development of pathologic changes. Under pathologic conditions, and in particular with metaplasia or neoplastic progression, the OSE undergoes Mullerian differentiation, which leads to increasingly stable and complex epithelial characteristics resembling the Mullerian duct-derived epithelia. Thus the close developmental relationship between the Mullerian epithelia and OSE is an important aspect of ovarian carcinogenesis and suggests that OSE is the precursor of epithelial ovarian carcinomas (Auersperg & Woo, 2004).

1.2.4.3 Fallopian tube epithelium

The shift towards studying the fallopian tube as a potential source of ovarian or pelvic serous carcinomas began with the discovery of fallopian tube carcinomas in women with heritable BRCA1 or 2 mutations undergoing prophylactic salpingo-oophorectomy. In the cases where occult carcinoma was detected, 42-100% of them involved the fallopian tubes (tubal intrapepithelial carcinoma or TIC) (Powell *et al.*, 2005; Lee *et al.*, 2006; Finch *et al.*, 2006; Callahan *et al.*, 2007). TIC is believed to be an early manifestation of serous carcinoma as it is frequently the only neoplasm

observed in these cases (Crum *et al.*, 2007). Thorough examination of the entire fallopian tube revealed that the majority of the tumours were localized to the fimbria in both familial and sporadic serous carcinoma cases (Cass *et al.*, 2005; Medeiros *et al.*, 2006). In a prospective study, TIC was identified in 19 of 39 consecutive serous carcinomas classified as primary ovarian carcinoma with identical p53 mutations detected in both tumors (Kindelberger *et al.*, 2007). As the fimbrial end of the tube lies in close proximity to the ovarian surface, it is conceivable that proposed mechanisms by which ovulation may induce transformation of OSE may also hold true for oviductal epithelium. In addition, there is a high incidence of these carcinomas in the ovulating hen and a high frequency of preinvasive disease in the oviduct in hens with ovarian cancer (Campbell, 1951; Wilson, 1958; Rodriguez-Burford *et al.*, 2001). In women, it is believed that in addition to the close proximity of the fimbrial end to the ovary which can seed cells directly on the ovarian surface, retrograde menstrual flow may deposit neoplastic tubal epithelial cells onto the ovary and eventually cause ectopic tumours (Piek *et al.*, 2004).

1.2.4.4 Other putative sources of ovarian carcinomas

Endometriotic lesions, which are part of the secondary Mullerian system, are believed to give rise to some of the endometrioid EOCs (Sainz de la Cuesta *et al.*, 1996; Jimbo *et al.*, 1997). Although there is currently very little literature to support this, some investigators have proposed that the secondary Mullerian system may be a source of EOCs (Dubeau, 1999; Piek *et al.*, 2004). The secondary Mullerian system refers to structures lined by Mullerian epithelium found outside the cervix, uterus, and fallopian tubes (Lauchlan *et al.*, 1972; Lauchlan *et al.*, 1994) which include

paraovarian/paratubal cysts, rete ovarii, endosalpingiosis, endometriosis, and endomucinosis. It has been observed that serous epithelial tumours arose from cysts of the secondary Mullerian system in both humans (Genadry *et al.*, 1977; Dalrymple *et al.*, 1989; Fromm *et al.*, 1990; Karseladze, 2001) and in some animal strains (Quattropani *et al.*, 1977; Quattropani, 1978; Quattropani, 1981; Gelberg *et al.*, 1984; Rutgers *et al.*, 1988).

1.2.5 Classification

Ovarian cancers are a heterogeneous group of neoplasms and differ widely with respect to their clinical presentation, treatment and outcome. Epithelial ovarian neoplasms account for about two-thirds of all ovarian tumours with their malignant forms accounting for approximately 90% of all ovarian cancers in the Western world. There also exists the non-epithelial ovarian tumours but they are relatively rare. The classification of epithelial ovarian neoplasms is based on their histological resemblance to Mullerian epithelia and is further subdivided in terms of patterns of growth. This classification system was formulated by the World Health Organization and the International Society of Gynecological Pathologists. Thus, EOCs differentiating along tubal lines become the serous tumours, those following an endometrial pathway are the endometrioid tumours and those following an endocervical route form the mucinous tumours. These are subclassified into benign, borderline (of low malignant potential) and malignant tumours which is based on their biological and clinical behavior (reviewed in Scully *et al.*, 1996; Prat, 2004).

The serous group of neoplasms are the most common and account for 30 to 40 percent of all ovarian neoplasms. Approximately 70% are benign, 5-10% borderline,

and 20-25% carcinomas. Together, the borderline and malignant groups account for about 30 percent of all ovarian cancers. Much of the research to date has focused on the invasive or malignant form of this disease. Despite their common lineage in terms of serous differentiation, borderline tumours are less aggressive clinically but have the capacity to become invasive. Therefore, one of the aims of this study was to examine whether the differentiated phenotype of serous borderline ovarian tumours are retained *in vitro* and to investigate whether differentiation hinders their capacity to invade. The characteristics of serous tumours, and in particular the borderline category (SBOT), will be discussed below.

1.2.5.1 Serous tumours

Serous tumours are characterized by cells resembling those of the fallopian tube. They grow in a distinctive pattern, forming extensive, often complex papillary structures. Since the inception of the serous borderline or low malignant potential category of ovarian neoplasms over 30 years ago, the pathogenesis of these tumors and their relation to invasive carcinoma remains elusive. Histopathologically and clinically, ovarian serous borderline tumours (SBOT) are neither clearly benign nor overtly malignant (Fig. 3). Unlike benign tumours, they exhibit histologic features of malignancy including nuclear atypia, cellular stratification, mitotic activity and, in some cases, stromal microinvasion, but they lack the destructive stromal invasion seen in malignant tumours (McKenney *et al.*, 2006; Gilks *et al.*, 2005). Clinically, most SBOT are confined to the ovary when discovered but in about one-third of patients, non-invasive implants are present in the pelvis and/or abdomen. SBOTs grow slowly and have been considered as relatively indolent tumours with an overall

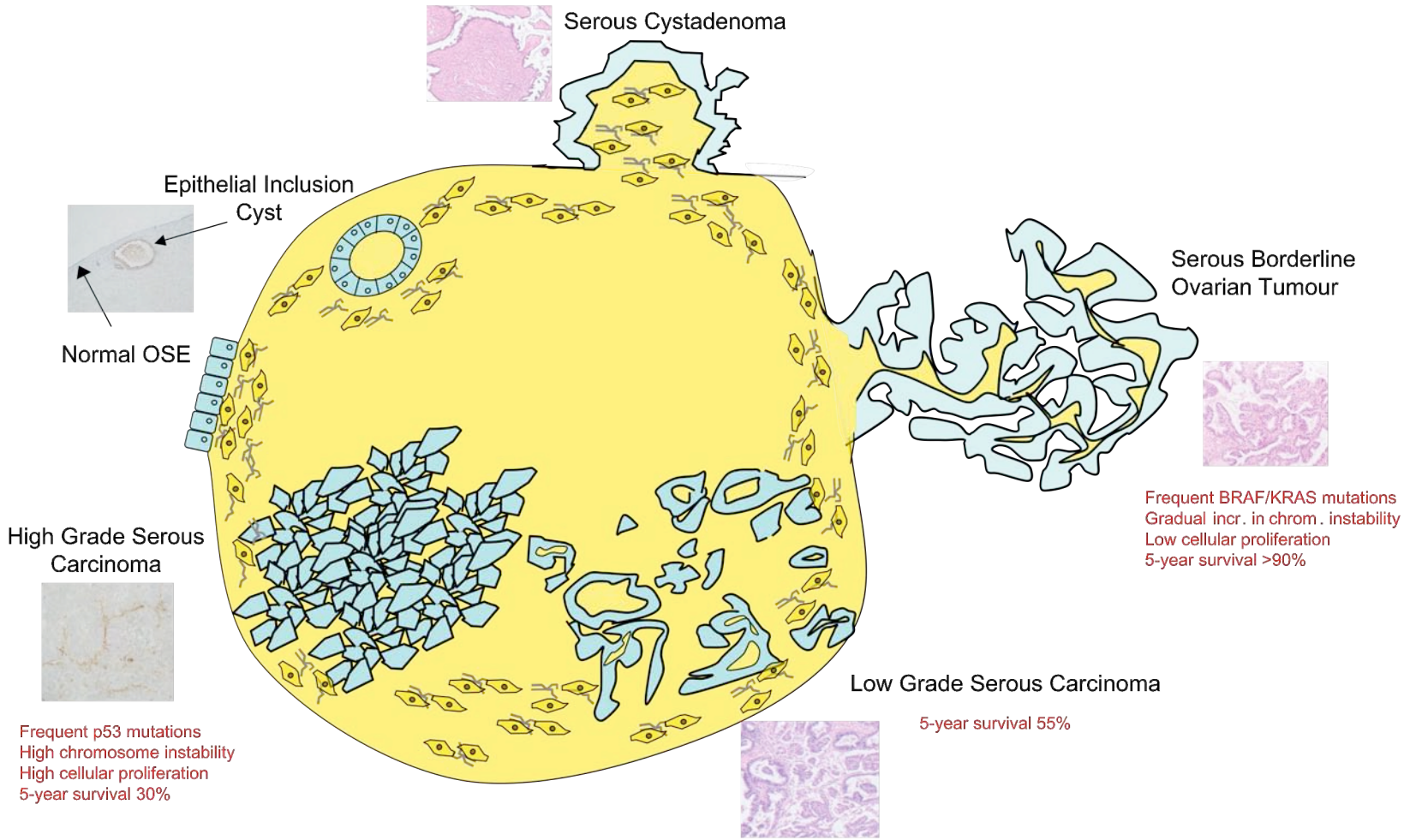

Fig. 3. Pathogenesis of epithelial ovarian cancer.

10-year survival rate of 83-91% (Crispens *et al.*, 2002). Although the incidence of SBOT is low (approximately 1.4 per 100 000 women per year in the United States), these tumours usually affect younger women who must make decisions regarding risks associated with treatment that spares fertility (Mink *et al.*, 2002; Sherman *et al.*, 2004). According to a recent report by Silva *et al.*, recurrence of the disease occurs in 44% of the patients over a period of 15 years (Silva *et al.*, 2006). Prognosis is excellent if the tumour recurs as an SBOT but in approximately three-quarters of the patients, the tumours recur as low-grade serous carcinomas and of these, 47-74% of the women will die of the disease (Crispens *et al.*, 2002; Silva *et al.*, 2006). For these women, response to therapy is minimal (Crispens *et al.*, 2002). It remains a conundrum as to whether SBOT are a distinct clinicopathologic entity or a precursor of invasive carcinoma. There are increasing data supporting the theory that a subset of SBOT progress to low-grade invasive carcinomas but only rarely to high-grade serous carcinomas (Singer *et al.*, 2003; Tibiletti *et al.*, 2003; Parker *et al.*, 2004; Bonome *et al.*, 2005; Shih *et al.*, 2005; Osterberg *et al.*, 2006). Recent studies have shown that a high proportion of SBOT and low-grade serous carcinomas harbour oncogenic mutations in KRAS or BRAF, which are uncommon in high-grade invasive tumours (Singer *et al.*, 2003; Sieben *et al.*, 2004; Shih et al., 2005) while high-grade serous carcinomas frequently harbour p53 mutations which occur infrequently in SBOT and low-grade cancers (Kmet *et al.*, 2003; Singer *et al.*, 2005). In addition to p53 mutations, high-grade serous carcinomas are associated with both germline and somatic BRCA1 and BRCA2 abnormalities suggesting that genomic

and in particular chromosomal instability is a fundamental feature of such cancers (Hilton *et al.*, 2002).

The characteristic phenotype of SBOTs provides an opportunity to examine the early steps in ovarian carcinogenesis. However, due to a lack of culture systems and animal models information about the properties of SBOT and their changes in these early events is extremely limited (Sherman *et al.*, 2004). Recently, Lee *et al.* (2005) described a new ovarian cancer model through the establishment of subrenal capsule xenografts of primary human ovarian tumours in immunodeficient mice, including one SBOT, which demonstrated a strong histopathological and immunohistochemical resemblance to the original tissues. As part of a larger study of primary ovarian tumours, Bertolero's group evaluated the response of two SBOTs to cis-platinum treatment *in vitro* (Balconi *et al.*, 1988). Crickard *et al.* (1986) demonstrated that in 5 primary cultures of SBOT grown on corneal endothelial extracellular matrix, the SBOT cells exhibited protease activity. In two studies, the properties of longer-term SBOT cultures were described: In one, one case of SBOT underwent 15 passages and expressed cytokeratins, intercellular adhesion molecule-1, epidermal growth factor receptor (EGFR), and polymorphic epithelial mucin (Ramakrishna *et al.*, 1997). The most extensive study of cultured SBOT to date was by Luo *et al.* (1997) where long-term cultures were established via infection with adenoviruses containing the SV40 T antigen. These cells were found to express keratin, BRCA1, estrogen and gonadotropin receptors. The SBOT cultures resembled invasive ovarian carcinoma cultures in their production of matrix metalloproteinases (MMP) and MMP inhibitors, but lacked urokinase plasminogen activator (uPA) and

tissue plasminogen activator (tPA) which were produced by almost all invasive tumours (van der Burg *et al.*, 1996). These studies contributed to the characterization of SBOT, but the relationship of their phenotypes to their genetic makeup, as well as the basis for their lack of invasiveness remained undefined. In this study, we characterized the phenotype and genotype of one long-term and one short-term SBOT cell line, in an attempt to further define the basis for the major clinically important differences between SBOT and invasive serous ovarian carcinomas.

1.3 Mullerian epithelial differentiation markers

Mullerian differentiation is so frequent in ovarian neoplasms that it serves as the basis for the classification of these tumours. As described earlier, the most common type of ovarian cancer are the serous neoplasms which resembles oviductal epithelium. Except for CA125, there are at present no molecular markers that characterize tubal differentiation and serve as predictive or diagnostic markers in ovarian cancer (Bast *et al.*, 1998; Mazurek *et al.*, 1998; Hellstrom *et al.*, 2003). Based on the histologic resemblance of serous carcinomas to tubal epithelium, we hypothesized that markers present in normal fallopian tube epithelium may be ectopically expressed in OSE undergoing Mullerian differentiation and neoplastic progression. On the other hand, if serous carcinomas originate in the fallopian tube epithelium, it would indicate that the differentiated properties of the tubal epithelium are retained during neoplastic progression and are lost only in advanced stage disease. In either scenario, tubal differentiation markers may help us to better identify ovarian neoplasms in women.

The fallopian tube is a highly vascularized, muscular tube with three distinct, anatomically and functionally different regions: the infundibulum, ampulla and isthmus. The open end is the infundibulum comprised of fringed projections called fimbria which helps to capture the oocyte following ovulation. The middle region is the ampulla where fertilization and embryonic development takes place and is the site of major biosynthetic activity. Near the region of the uterus is the isthmus which functions as a sperm reservoir. The mucosa consists of two cell types: ciliated and non-ciliated secretory cells. Hundreds of macromolecules are actively biosynthesized and secreted by the secretory cells (Buhi *et al.*, 2000) (Fig. 4). Some of these appear to be hormonally regulated by ovarian steroids, most importantly, estrogen. This occurs during late follicular development and estrus as a means for optimizing the microenvironment for fertilization and early cleavage-stage embryonic development.

Based on the literature, the only specific tubal differentiation marker identified to date is oviduct-specific glycoprotein (OVGP1) (Rapisarda *et al.*, 1993; Arias *et al.*, 1994; Leese *et al.*, 2001). Therefore, in this study, we tested the hypothesis that OVGP1 may be a marker expressed during the aberrant Mullerian epithelial differentiation of ovarian neoplasms.

1.3.1 Oviduct-specific glycoprotein

OVGP1, also known as oviductin or mucin 9 (MUC9), is normally secreted specifically and exclusively by the secretory epithelial cells of the oviduct (O'Day-Bowman *et al.*, 1995; Lapensee *et al.*, 1997). OVGP1 expression correlates with the differentiated state of the epithelium lining the lumen of the oviduct, which occurs in

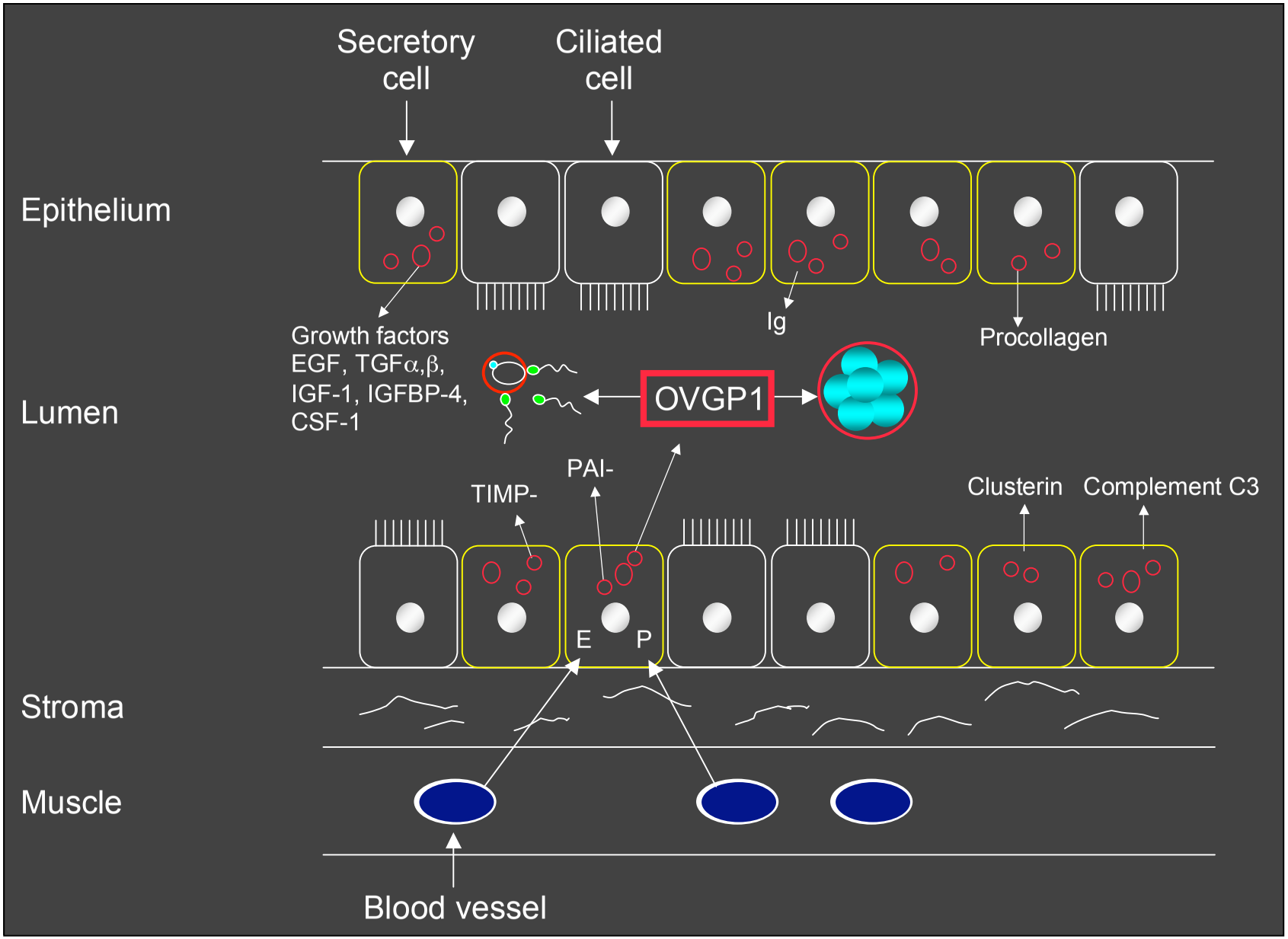

Fig. 4. Macromolecules synthesized and secreted by the oviduct. Oviduct-specific glycoprotein (OVGP1) is synthesized and secreted specifically by the secretory cell of the oviduct close to the time of ovulation. It is believed to play a role in fertilization and early embryonic development. Adapted from Buhi *et al.*, 2000.

the presence of elevated estradiol levels unopposed by progesterone (Verhage *et al.*, 1990; Brenner & Slayden, 1994). The human genome contains a single copy of the OVGP1 gene located on chromosome 1p13 (Lapensee *et al.*, 1997). The human cDNA encoding human OVGP1 is 2216 base pairs in length, encoding for a 654 amino acid protein with a predicted molecular weight of 72.9 kDa (Verhage *et al.*, 1998; Arias *et al.*, 1994). In one-dimensional gels, OVGP1 has a molecular mass of 110 to 130 kDa, attributed to differing degrees of glycosylation (Verhage *et al.*, 1988). OVGP1 is highly conserved among mammalian species with greater than 90% homology among primates (human, baboon, and rhesus) (Donnelly *et al.*, 1991; Verhage *et al.*, 1997) at both the nucleotide and amino acid levels, and between 57-73% homology among other species (Sendai *et al.*, 1994; DeSouza & Murray, 1995; Marshall *et al.*, 1996; Buhi *et al.*, 1996; Suzuki *et al.*, 1995; Paquette *et al.*, 1995; Sendai *et al.*, 1995). A higher degree of similarity among species exists in the amino terminal end when compared to the carboxy terminal end. In the human gene, exon 11 encodes for the carboxy terminal region (Jaffe, 1996). This region contains at least one potential *N*-linked glycosylation site. In addition, examination of the human deduced amino acid sequence reveals that OVGP1 possesses contiguous Ser/Thr rich repeated units of 15 amino acids, clustered in its carboxy-terminal portion (Malette *et al.*, 1995; Paquette *et al.*, 1995). These are mucin-type motifs providing potential *O*-linked glycosylation sites of which the human clone contains three complete units and four truncated ones (Arias *et al.*, 1994). The carboxy terminal region also contains many terminal sialic residues, typical of sialomucins. These findings suggest that OVGP1 may be a secretory mucin and/or a sialomucin (DeSouza & Murray, 1995;

Satoh *et al.*, 1995). In addition, the N-terminal end of the protein contains a string of 11 hydrophobic residues which may represent a signal peptide. Furthermore, all of the OVGP1s sequenced to date share identities with a variety of chitinases classified as Family 18 glycosyl hydrolases (Jaffe *et al.*, 1996) but differ in one or two amino acids which are believed to be essential for enzymatic activity (Watanabe *et al.*, 1993; Bleau *et al.*, 1999). Molecular characterization of the OVGP1 promoter region reveals eight half estrogen-responsive elements (ERE) and an imperfect ERE (Agarwal *et al.*, 2002). By electromobility shift assay and specific estrogen receptor antibodies, the imperfect ERE has been shown to bind estrogen receptor β in a human oviductal cell line but not in other cell types (Agarwal *et al.*, 2002). A recent *in silico* analysis of the OVGP1 gene demonstrates a clathrin box present for endocytosis, in addition to ubiquitinylation signals. Additionally, the analysis also indicates the presence of a Class III PDZ-domain ligand motif, which together with those of GRB2-like src homology 2 (SH2) and Src-family SH2 domain binding motifs, and SH3 2, 3 motifs implicate OVGP1 as a PDZ ligand protein and possibly as a component of a multi-protein complex or focal adhesion points such as tight junctions in epithelial cells (Kadam *et al.*, 2007).

Functionally OVGP1 is believed to play a role in fertilization and early embryonic development (Boice *et al.*, 1990; Boatman *et al.*, 1994; O'Day-Bowman *et al.*, 1996; Schmidt *et al.*, 1997). Numerous studies have shown that OVGP1 is synthesized and secreted during the mid- to late-proliferative phase when estrogen levels are high (Rapisarda *et al.*, 1993; Arias *et al.*, 1994). OVGP1 can bind to the zona pellucida of human and baboon oocytes and can increase the number of sperm

binding to hemizonae which can be blocked by antibodies against OVGP1 (Schmidt *et al.*, 1997). However, OVGP1-null mice are fertile suggesting that OVGP1 is not an absolute requirement for successful fertilization (Araki *et al.*, 2003). In addition, it is believed that the highly glycosylated and charged protein may play a protective role in the oviduct by preventing ectopic implantation. This may be through its association with the zona pellucida, the early embryo, and the oviductal epithelium and thus, provide repulsive forces that allow the free movement of the egg within the oviduct (Malette *et al.*, 1995; Paquette *et al.*, 1995). This type of adhesive property may also be beneficial in the protection against infection as OVGP1 may bind to adhesins of potentially pathogenic microorganisms which eventually get flushed away by the oviductal fluid (Lapensee *et al.*, 1997).

Most of the research to date has only focused on the role of OVGP1 in normal fallopian tube function. In this study, we characterized the expression of OVGP1 in ovarian tumor tissues using a tissue microarray and a rabbit polyclonal antibody against human OVGP1 generated by Dr. Harold G. Verhage's laboratory at the University of Illinois in Chicago. Our data suggested the potential of using OVGP1 as a serum biomarker for the early detection of ovarian cancer and thus, a monoclonal antibody was generated in collaboration with Dr. Bob Molday's laboratory at the University of British Columbia to develop a serum-based assay for OVGP1.

1.4 Endometrial Cancer

In an initial study of the expression of OVGP1, different tissues were screened using tissue microarrays. Preliminary results showed that 3 of 56 cases of

endometrial cancer and 6 of 17 cases of atypical endometrial hyperplasias stained positively for OVGP1 based on examination of 0.6-mm tissue cores. On the basis of these observations, it was hypothesized that OVGP1 may also be a marker of the development and progression of atypical hyperplasias, which are known precursors of endometrial cancer.

Endometrial cancer is the most common malignancy of the female genital tract. In the lifetime of a woman, the probability of developing endometrial cancer is 1 in 38 (Jemal *et al.*, 2007). During carcinogenesis, the endometrium undergoes many phenotypic changes, reflecting the variable cellular differentiation in the Mullerian system (Lax, 2004). Endometrial adenocarcinomas are classified into two predominant histologic groups, endometrioid carcinomas, which account for 80% of endometrial adenocarcinomas, and the nonendometrioid types (Kurman *et al.*, 1994). Nonendometrioid endometrial carcinomas, including uterine papillary serous carcinomas and clear cell carcinomas, are infrequent; however, they are high-grade, aggressive tumours with a poor clinical outcome (Cirisano *et al.*, 2000; Grice *et al.*, 1998; Sherman *et al.*, 1992). Uterine papillary serous carcinomas and clear cell carcinomas are not estrogen-responsive and arise from precancerous lesions that develop in atrophic endometrium (Sivridis & Giatromanolaki, 2001). In contrast, endometrioid carcinomas are driven by estrogen stimulation and are often preceded by or coexist with endometrial hyperplasia, which is believed to be a precursor lesion (Mutter, 2002). Histologically, it is difficult to differentiate nonatypical hyperplasias from atypical hyperplasias and atypical hyperplasias from well-differentiated endometrioid carcinoma. Both atypical hyperplasia and low-grade endometrioid

carcinoma show cytological atypia, and are distinguished primarily by architectural features (Longacre *et al.*, 1995). There is high intra- and interobserver variability in the histologic diagnosis of these lesions (Kendall *et al.*, 1998; Dietel, 2001; Silverberg, 2000). Accurate classification of these precursor lesions is of great clinical importance because it allows for appropriate preventative measures to be taken. Therefore, in addition to the morphologic classification of endometrial neoplasia, recent reports have identified possible precursor lesions with immunohistochemistry, molecular analysis, comparative genomic hybridization, and DNA microarray technology (Dietel, 2001).

Thus, one of our specific aims was to examine the expression of OVGP1 in whole sections of normal, hyperplastic, and malignant endometrium. To determine whether OVGP1 can predict clinical outcome, immunohistochemistry was also carried out on a tissue microarray of endometrial cancer cases with follow-up data. Because OVGP1 is an estrogen-regulated protein and because hyperplasias and endometrioid carcinomas are estrogen driven, we examined the expression of estrogen receptor (ER) in the endometrial tumours. We also examined the expression of PTEN, the loss of which has been proposed as a marker of endometrial neoplasia (Mutter *et al.*, 2001).

In summary, this study provides new information regarding the roles of E-cadherin and hepatocyte growth factor in Mullerian differentiation, examines potential mechanisms by which retinoic acid acts as a chemopreventive agent,

presents the first experimental model to study SBOT, and has provided a new marker for histochemical analysis and, likely, a new serum marker for ovarian cancer.

2. MATERIALS AND METHODS

2.1 Cell Culture

Institutional approval for experimentation with human tissues was obtained prior to this study.

2.1.1 Normal human ovarian surface epithelial cells

Normal human OSE cells were obtained from ovarian biopsies and at laparoscopic procedures from women with no family histories of breast/ovarian cancer, having surgery for non-malignant gynecologic conditions. Immortalized OSE (IOSE) and E-cadherin expressing (IOSE-EC) lines were obtained by immortalization of normal OSE with the simian virus early region and E-cadherin genes as previously described (Maines-Bandiera *et al.*, 1992; Auersperg *et al.*, 1997). Cells were maintained in medium 199/MCDB 105 (1:1) (M199/105) (Sigma, St. Louis, MO) supplemented with 10% fetal bovine serum (FBS) (Hyclone, Logan, UT) for OSE cells, and with 5% FBS for IOSE lines, at 37^{o}C in a humidified incubator with 5% CO_2:95% air. Cells were subcultured with 0.06% trypsin/0.01% ethylenediamine tetraacetic acid (trypsin/EDTA) (Invitrogen, Burlington, ON) in Ca^{2+}, Mg^{2+}-free Hanks' balanced salt solution (Invitrogen).

2.1.2 Serous borderline ovarian tumours

Fresh tissue samples of three serous borderline ovarian tumours (SBOT-1, SBOT-3, and SBOT-4) and one SBOT-derived low-grade carcinoma (SBOT-2) were obtained from four women aged 38 to 46 years. Patient 1 was a 46-year old woman, diagnosed in 2003 with a primary serous borderline tumour of the left ovary with

surface involvement (stage IC) (SBOT-1). Patient 2 was diagnosed in 1995 with stage III SBOT with non-invasive implants. At the age of 45, eight years after initial presentation, the patient had recurrence in the form of a low-grade serous carcinoma (SBOT-2) at which time the specimen was obtained. Patient 3 first presented in 1994 with SBOT of the peritoneum. The tumour recurred as SBOT in 1997, 1999 and again in 2003 when the women was 38 years old and at which time the tumor specimen was obtained for this study (SBOT-3). Based on the hospital records, two years following the collection of the specimen, the patient was diagnosed with recurrence of the disease and the tumour had progressed to a low-grade serous carcinoma. Case 4 is a woman who had an initial presentation of SBOT in the right ovary (stage IA). Two years later in 2005, this 43-year old woman was diagnosed with recurrence of the disease in the left ovary with surface involvement (SBOT-4). The specimen was obtained at this time.

The tissue explants were minced and dissociated with trypsin/EDTA in trypsinizing flasks at 37^{o}C. Single cells and tissue fragments were cultured in M199/105, supplemented with 10% FBS. Cells from each tumor specimen, designated SBOT-1, SBOT-2, SBOT-3 and SBOT-4, were seeded into several culture dishes, labeled SBOT-1.1-1.9, SBOT-2.1- 2.3, SBOT-3.1-3.3 and SBOT-4.1-4.11, respectively. The cultures initially contained a mixture of fibroblasts and epithelial cells as determined by keratin expression, but over 75% of the cells were cancer cells. Homogeneous epithelial populations were selected by differential adhesion: they were trypsinized with 0.12% trypsin for approximately 5-10 min, followed by trypsin/EDTA for about 15-25 min. With this procedure, fibroblasts detached more

rapidly than SBOT cells and could be selectively removed. As the epithelial cells were damaged by complete dissociation, they were subcultured as mixtures of single cells and small cell clusters by trypsinizing with 0.12% trypsin, followed by brief exposure to trypsin/EDTA, and seeded onto plastic coated with cellular (cFN; Fibrogenex, Morton Grove, IL) or plasma fibronectin (pFN; Invitrogen) (Zand *et al.*, 2000). Pure epithelial cultures were not obtained in the SBOT-1 and SBOT-2 cases as they were eventually overgrown by fibroblasts. Therefore, only a limited number of experiments, which did not require pure epithelial populations, were performed on these two lines. After approximately 3-4 passages, pure populations of epithelial cells were obtained in the SBOT-3 culture. The SBOT-3 cells attached poorly to plastic after subculture. Therefore they were propagated, in part, from cells that were left over after partial trypsinization and repopulated the culture vessels. One of the SBOT-3 cultures, SBOT-3.1, continued to proliferate and has currently reached about 100 population doublings (PDs). Several sublines of SBOT-4 have been propagated for about 10-12 PDs, but at that stage they ceased proliferating and eventually died, on plastic as well as on fibronectin substrata.

The SV40 virus early genes were introduced into SBOT-1, SBOT-2 and SBOT-3 lines by transfection with FuGENE 6 (Roche Diagnostics, Laval, QC, Canada), generating lines, ISBOT-1.5, -2.2, and -3.3.

2.1.3 Cell lines

The ovarian cancer cell lines, CAOV-3, OVCAR-3 and SKOV-3, and the human embryonic kidney cell line, HEK-293, were obtained from American Type Culture Collection (ATCC). Ovarian cancer lines, OVCAR-5 and OVCAR-8, were

kindly provided by Dr. T.C. Hamilton (Fox Chase Cancer Center, Philadelphia). These lines were maintained in M199/105 supplemented with 5% FBS. OVCA429 ovarian carcinoma cells were obtained from Dr. Robert C. Bast (M.D. Anderson Cancer Center, Houston. TX) and maintained in MEM supplemented with 5% FBS. All cells were trypsinized at subconfluence with trypsin/EDTA. The human cervical cancer cell line, C-4II, was maintained in M199/105 supplemented with 5% FBS and passaged with trypsin alone (Auersperg, 1969).

2.2 3-dimensional Collagen Gel Culture

The capacity of cells to form branching tubules in collagen gel was examined (Brinkmann *et al*., 1995). In brief, collagen gel solution was polymerized by adding a mixture containing 7 parts of rat tail type-I collagen stock solution, 1 part each of 10x medium 199, 10% NCS and 22 mg/mL $NaHCO_3$ on ice. The solution was then neutralized with 0.34 M NaOH. 300 μL/well of the cold neutralized collagen gel solution was plated onto 24-well plates and allowed to gel at 37°C. For each well, $2x10^4$ cells were resuspended in 300 μL neutralized collagen solution and then seeded on top of the first layer. The collagen was allowed to gel before 1 ml culture medium containing 2% NCS was added. Cultures were treated with: (1) recombinant hepatocyte growth factor (HGF) (20 ng/mL), (2) all-trans retinoic acid (ATRA) (1μM), and (3) HGF and ATRA at their respective concentrations. For experiments involving HGF only, phosphate-buffered saline (pH 7.4) (PBS: 137 mM NaCl, 2.7 mM KCl, 4.3 mM $Na_2HPO_4.7H_2O$, 1.4 mM KH_2PO_4) was added to the control

cultures while for experiments involving ATRA, 0.1% dimethyl sulfoxide (DMSO; Sigma) was added to the control cultures. The cultures were maintained for 21 days in an atmosphere of 5% CO_2/air with medium changes every 3 days. Representative fields were photographed.

2.3 Western Blot Analysis

Cells were washed with ice-cold PBS and lysed in RIPA buffer (50 mM Tris-HCl, pH 7.4, 1% NP-40, 1% sodium deoxycholate, 0.1% SDS, 150 mM NaCl, 5 mM EDTA) containing a cocktail of protease inhibitors (Sigma). The cell lysates were incubated on ice for 10 min and cell debris was removed by centrifugation at $\geq$13 000xg for 10 min at 4^{o}C. Protein concentrations of the lysates were determined using a Bradford protein assay (Bio-Rad Laboratories, Richmond, CA). Conditioned media were collected and stored at -70^{o}C. The cellular extracts and conditioned media were then diluted to the correct concentrations using RIPA buffer and sample loading buffer (2.5% w/v sodium dodecyl sulphate, 10% v/v glycerol, 50 mM HCl, pH 6.8, 0.5 M β-mercaptoethanol and 0.01% w/v bromophenol blue). Samples were loaded and separated on an 8% SDS-polyacrylamide gel and transferred onto nitrocellulose membrane by electrophoresis at 100V for 1-2 h. For all primary antibodies membranes were blocked with 5% skim milk in 0.05-0.1% Tween-20 Tris-buffered saline (TBS: 10 mM Tris-HCl, pH7.4, 150 mM NaCl) for 1 h, and incubated with primary for 1 h at room temperature or overnight at 4^{o}C. Primary antibodies used are listed in Table 1. After extensive washing, immunoreactive bands were visualized with peroxidase-conjugated anti-rabbit or anti-mouse immunoglobulin (1:3000; Bio-

Rad Lab.) for 1 h, followed by enhanced chemiluminescence (Pierce, Nepean, ON) using X-ray film (Kodak).

Table 1: Antibodies used for Western blot analysis

Antigen	Clone	Supplier	Dilution	Incubation Time
E-cadherin	36	BD Transduction Lab.	0.25μg/mL	1 h
N-cadherin	32	BD Transduction Lab.	0.1μg/mL	1 h
6x histidine	EH23	ABM	1:1000	1 h
Rhodopsin	1D4	R. Molday	1:1000	1 h
OVGP1	7E10	R. Molday	1:3	O/N
OVGP1	Polyclonal	H.G. Verhage	0.3μg/mL	O/N
p44/42 MAP kinase	-	Cell Signaling	1:1000	1h
Phospho-p44/42 MAP kinase	E10	Cell Signaling	1:1000	1h

Abbreviations: h, hour; O/N, overnight

2.4 Reverse Transcription-Polymerase Chain Reaction (RT-PCR)

Total ribonucleic acid (RNA) was extracted using the RNeasy Mini kit according to the manufacturer's protocol (Qiagen Inc., Mississauga, Ontario, Canada). The concentration and purity of RNA were determined based on absorbance at 260 nm measured by a spectrophotometer. Complementary DNA (cDNA) was synthesized from total RNA using the First Strand cDNA synthesis kit (Pharmacia Biotech, Morgan, Canada) The reaction mixture (15 μl) containing 1-5 μg RNA, 5 μl bulk first-strand cDNA reaction mix, 20 pmole oligo-dT primer and 6 mM dithiothreitol was incubated at 37^{o}C for 60 min and terminated by heating at 90^{o}C for 5 min.

To amplify the cDNA, 5 μl reverse-transcribed cDNA was subjected to PCR in a 50 μL reaction mixture containing 10 mM Tris-HCl, pH 8.3, 50 mM KCl, 2.5 mM $MgCl_2$, 0.001% w/v gelatin, 200 mM each of dATP, dCTP, dGTP, and dTTP, 2.5 units of Taq polymerase (Invitrogen); and 0.5 pmole of each sense and antisense appropriate primers for HGF and its receptor (c-Met):

HGF: 5'-AGTACTGTGCAATTAAAACATGCG-3' and

5'-TTGTTTGGGATAAGTTGCCCA-3';

c-Met: 5'-GGTGAAGTGTTAAAAGTTGGA-3' and

5'-ATGAGGAGTGTGTACTCTTG-3'

All PCR primers span the introns to detect specific messenger RNA sequences. With these primers, the PCR products for HGF and c-Met were 378-bp (nucleotides 841-1219 GenBank M29145) and 324-bp (nucleotides 2667-2991 GenBank J02958), respectively. The amplification reaction was carried over 35 cycles. For HGF and c-Met, each cycle consisted of denaturation at 94°C for 30 s; primer annealing at 55°C for 45 s (HGF) or at 56°C for 30 s (c-Met); extension at 72°C for 30 s. This was followed by a final extension at 72°C for 15 min in a DNA thermal cycler (Perkin Elmer, Norwalk, CT). PCR controls were performed in the absence of cDNA to ensure that cross-contamination of samples did not occur. Twenty microlitres of the PCR products were then loaded on 1% agarose gels and stained with ethidium bromide.

2.5 Growth Assay

The effects of retinoic acid on growth of OSE and IOSE cells were determined using the DNA Hoechst assay (Papadimitriou & Lelkes, 1993). Cells were cultured in 96-well plates for 6 days in M199:105 supplemented with 5% FBS and in the presence of 1μM ATRA or 0.1% DMSO (control). Cells were washed with serum-free medium, fixed in ice-cold methanol for 20 min and stained with 0.5μg/mL Hoechst 33258 (Sigma). Fluorescence was measured using the FL600 Plate Reader at an excitation of 360/40 and emission of 460/40. Values were converted to percentage of control for each case and represent the mean $\pm$ S.D. of 8 wells. Experiments were repeated three times.

SBOT cells were cultured in 12 or 24-well plates under varying conditions. To determine whether different growth surfaces alter the rate of proliferation, cells were cultured in plates with regular and high attachment surfaces (Corning Cat. #3336), with or without plasma fibronectin coating. In addition, to determine whether stromal influences alter the growth potential of the SBOT cells, the cells were cocultured with irradiated NIH-3T3 cells. Seven thousand irradiated NIH-3T3 cells/cm^2 were seeded into the wells one day prior to seeding SBOT cells. After 2-3 weeks, cells were fixed with methanol at -20^oC for 20 min and stained for keratin and nuclei as described in section 2.6. The number of keratin-positive cells was analyzed using the Cellomics High-Content Screening Reader (Cellomics Inc., Pittsburgh, PA). Three hundred fields/well and 225 fields/well were analyzed for 12- and 24-well plates, respectively, which accounts for greater than 40% and 60% of the well,

respectively. The data are presented as the mean number of cells per field ± S.D. of triplicate wells. Experiments were repeated three times.

2.6 Immunostaining of Cultured Cells

Immunofluorescent staining for keratin, SV40 large T-Antigen, E-cadherin, and N-cadherin was performed. Cells were cultured on coverslips, washed with serum-free medium, fixed in methanol at –20°C for 20 min or more, post-fixed in cold methanol/acetone (1:1) for 5 min and dried. Following rehydration in PBS, the coverslips were blocked with Dako Protein Block (Dako, Mississauga, ON, Canada) for 30-60 min, and incubated with primary antibodies at room temperature for 1 h. The primary antibodies used are listed in Table 2.

Table 2: Antibodies used for immunostaining of cultured cells

Antigen	Clone	Supplier	Dilution
Keratin	Polyclonal	DakoCytomation	1:1000
SV40 T-antigen	Abl-1	Oncogene Science	1μg/mL
E-cadherin	36	BD Transduction Lab.	0.5μg/mL
N-cadherin	32	BD Transduction Lab.	0.83μg/mL

The anti-keratin wide spectrum screening antibody labels a variety of keratins representing a wide range of molecular weight proteins. The anti-SV40 T antigen antibody recognizes the 94 kDa SV40 large T antigen and the 21 kDa SV40 small T antigen. The anti-E-cadherin antibody targets the cytoplasmic domain of E-cadherin and recognizes a 120 kDa band by Western blot analysis. The anti-N-cadherin antibody recognizes a 130 kDa band by Western blot analysis. Alexa 594-labeled goat anti-mouse (1:800) or Alexa 488-labeled goat anti-rabbit IgG (1:400) (Jackson

Immunoresearch Laboratories Inc., West Grove, PA) were used as secondary antibodies. Cells were counterstained with Hoechst 33258 (0.5μg/mL; Sigma, Oakville, Ontario), rinsed with PBS, mounted with Gelvatol and examined using a Zeiss Axiophot microscope equipped with a digital camera (Q Imaging, Burnaby, B. C., Canada).

2.7 Telomerase Assay

Telomerase activity was measured in cellular extracts from SBOT-3.1 and -4 cells using the telomerase PCR-ELISA (Roche Molecular Biochemicals, Indianapolis, IN), according to the manufacturer's instructions. All reagents are provided in the kit. In brief, 2 x 10^5 cells were harvested and lysed in 200μL of the Lysis reagent. 1-3 μL of the cell extract (corresponding to 1 x 10^3-3 x 10^3 cell equivalents) was added to 25 μL of the Reaction mixture in an Eppendorf tube for PCR. As a negative control, the cell extracts were heat-treated for 10 min at 65^{o}C prior to the TRAP reaction to inactivate telomerase protein. Sterile water was added to a final volume of 50 μL. Tubes were then transferred to a thermal cycler and a combined primer/elongation reaction was performed as follows: primer elongation (10-30 min, 25^{o}C, step 1), telomerase inactivation (5 min, 94^{o}C, step 2), amplification (denaturation at 94^{o}C for 30 s, annealing at 50^{o}C for 30 s, polymerization at 72^{o}C for 90 s, cycles 1-30), extension at 72^{o}C for 10 min (step 3), and hold at 4^{o}C. For each sample, 20 μL of the Denaturation reagent was added to 5 μL of the amplification product and incubated at 15-25^{o}C for 10 min, followed by the addition of 225 μL of the Hybridization buffer. After mixing, 100 μL of the mixture was added per well of the precoated MTP

modules and covered with the self-adhesive cover foil to prevent evaporation. The plate was then incubated at 37°C on a shaker (300 rpm) for 2 h. The wells were washed 3 times with 250 μL of washing buffer per well for at least 30 s, followed by the addition of 100 μL of Anti-DIG-POD. After incubation at 15-25°C for 30 min, 300 rpm, the wells were rinsed 5 times with 250 μL of washing buffer, followed by incubation with 100 μL of TMB substrate solution for colour development at 15-25°C for 10-20 min while shaking at 300 rpm. The color development was stopped by adding 100 μL of the Stop reagent. The absorbance of the samples were read at 450 nm (with a reference wavelength of approx. 690 nm) using a Microtiter plate (ELISA) reader (model). The data are presented as the absorbance [$A_{450nm} - A_{690nm}$].

2.8 BRAF and KRAS DNA Mutation Analysis

DNA mutation analysis was performed by Dr. Carla Oliveira (University of Porto, Porto, Portugal) to examine whether the SBOT-3.1 and SBOT-4 cultures had mutations in *BRAF* and *KRAS*, which are common in low-grade serous tumours. Genomic DNA was extracted from SBOT-3.1 and SBOT-4 cells using standard methods. Analysis of *BRAF* exon 15 and *KRAS* exon 1 mutational hotspots were performed by Single Stranded Conformation Polymorphism and Heteroduplex Analysis (SSCP/HA), followed by direct sequencing (Oliveira *et al.*, 2004). Briefly, the fragment encompassing BRAF exon 15 and KRAS exon 1 were amplified by PCR using the following cycling conditions: 30 seconds at 94°C, 30 seconds at 60°C, and 45 seconds at 72°C for 35 cycles (primer sequences available upon request). PCR products from samples and a normal control were analysed by SSCP/HA.

Samples displaying aberrant migrating patterns in comparison to normal controls were sequenced. All mutations found were confirmed in a second independent PCR.

2.9 Multicolor Fluorescent In-Situ Hybridization

Multicolour fluorescent in-situ hybridization (mFISH) was performed by Dr. David Huntsman's laboratory (Department of Pathology, UBC) to examine the karyotype of the SBOT-3.1 and SBOT-4 cultures. The SBOT-3.1 and SBOT-4 cells were grown and harvested to generate metaphases using standard cytogenetic protocols. Fresh slides were prepared and mFISH was performed as described previously (Maines-Bandiera *et al.*, 2001). Briefly, mFISH was performed using the 24XCyte MetaSystems DNA probe kit which utilizes combinatorial fluorescent labeling to uniquely label each chromosome of the human karyotype. The mFISH procedure was performed according to manufacturer's protocols (MetaSystems GmbH, Altlussheim, Germany). mFISH analysis was performed on 10 quality metaphases using a Zeiss microscope (Axioplan 2; Zeiss, Toronto, Canada) equipped with appropriate filters (4',6-diamino-2-phenylindole (DAPI), fluorescein isothiocyanate (FITC), Spectrum Orange, tetramethyl rhodamine isothiocyanate (TRITC), Cy5, diethyl aminomethyl coumarin). Imaging was performed using the MetaSystems ISIS imaging software.

2.10 Comparative Genomic Hybridization

Microarray comparative genomic hybridization (aCGH) was performed by Dr. David Huntsman's laboratory to examine changes in gene copy numbers of SBOT-

3.1 and SBOT-4 cells in an attempt to identify genes which may be important in the development of these tumours. Array CGH was performed using the GenoSensor Array 300 system following the manufacturer's instructions (Vysis, Downer's Grove, IL, USA). The microarray contains 861 spots representing 287 chromosomal regions commonly altered in human cancers. Briefly, DNA extracted from the SBOT-3.1 and SBOT-4 cells were labelled by random priming for 2 hours with Cy3 and male reference DNA was labelled with Cy5. Following labelling, the DNA was digested with DNase for 1 hour at 15°C. Probes were precipitated by ethanol precipitation and the probe size was then confirmed by gel electrophoresis. Tumour and reference DNA were mixed with hybridization buffer and denatured at 80°C for 10 minutes followed by incubation at 37°C for 45 minutes. The hybridization mixture was then applied to the array, coverslipped and incubated in a humid chamber containing 50% formamide/2X SSC at 37°C for approximately 3 days. After hybridization, the microarrays were washed at 58°C in a 1X SSC/0.1% NP-40 solution for 4 minutes followed by 4 minutes in a 0.1X SSC/0.1% NP-40 solution. The microarrays were then transferred to 1X SSC at room temperature for 1 minute and then rinsed in distilled water. The array was counterstained with DAPI for 45 minutes then analyzed using the Genosensor scanner and software. Fluorescence ratios were calculated by comparing sample DNA fluorescence to reference DNA fluorescence. A fluorescence ratio of >1.2 was considered a gain and a ratio of <0.8 was considered a loss. Single target clones showing gain or loss were not included.

2.11 CA125 Assay

CA125 is an important clinical marker, as well as differentiation marker of ovarian cancer and therefore, cultured SBOT cells were examined for the secretion of this protein. Conditioned media from confluent cultures were collected and assayed twice for CA125 using the microparticle enzyme immunoassay as per manufacturer's specifications (Abbott) at the B.C. Cancer Agency, which routinely performs the CA125 assay for measuring levels in the serum from patients. The reference level is <35 kU/L, with a borderline range of 35-65 kU/L.

2.12 Matrigel™ Invasion Assay

The invasion assay was performed in Boyden chambers (Albini *et al.*, 1987) with minor modifications (Woo *et al.*, 2007). Filters (8 μm pore size, 24-well) were coated with 40 μL of 1 mg/mL growth-factor-reduced Matrigel™ (Fisher, Nepean, ON, Canada). Cells in M199/105 supplemented with 0.1% FBS or 1% FBS were incubated for 16 h or 40 h against a gradient of 10% FBS or 5% FBS with 5μg/mL cellular fibronectin, respectively. For E-cadherin blocking studies, cells were incubated with a neutralizing E-cadherin monoclonal antibody (MB2; Abcam, Cambridge, MA). Cells on the top of the filters were removed with a cotton swab and cells that penetrated the membrane were fixed with ice-cold methanol for 20 min, air dried, rehydrated with PBS and stained with 0.5 μg/mL Hoechst 33258. For samples containing a mixture of cell types, the epithelial cells were identified by staining for keratin, as described in Section 2.6. The membranes were then mounted onto glass slides with Gelvatol and the number of nuclei stained with Hoechst 33258 or the

number of keratin positive cells was counted using Northern Eclipse 6.0 software from Empix Imaging (Mississauga, ON, Canada). Results are presented as the number of invading cells per filter ± SD of at least 5 fields and is representative of three separate experiments.

2.13 Migration Assay

Confluent monolayers were serum starved overnight and scratched using a micropipette tip. The migration of the cells into the scratch was measured at 0h, 6h and 24h by capturing images using a monochromatic digital CCD camera (Retiga 1300; Qimaging, Surrey, BC) connected to an inverted microscope (Zeiss). The Northern Eclipse 6.0 software was used to analyze the area covered by the migrating cells. The area of the wound is outlined using the "TRACE" tool and the output is expressed in pixels. Using the 10X objective, one pixel is equivalent to 1.12 μm. The results are presented as the mean area covered by the migrating cells in one field (mm^2) ± SD of at least five fields and is representative of three separate experiments.

2.14 Analysis of Protease Expression

The expression of proteases in cultured SBOT cells was examined to determine whether a lack of protease expression in SBOT cells is a determinant of their non-invasive phenotype. Analysis of MMP-2, MMP-9 and uPA expression was performed by Dr. Jaime Symowicz in Dr. M. Sharon Stack's laboratory (Northwestern University Feinberg School of Medicine, Chicago, IL). Confluent

dishes of SBOT-3 and SBOT-4 cells were cultured in serum-free M199/105 for 24 h. The conditioned media were collected and analyzed for proteinase expression.

2.14.1 Analysis of MMP-2 and MMP-9 activity

For gelatin zymography, cells were cultured with or without treatment with 1mM aminophenylmercuric acetate (APMA) (Sigma, St Louis, MO) for the last h prior to electrophoresis. The conditioned media were electrophoresed under non-reducing conditions on a 9% SDS-polyacrylamide gel containing ~0.1% gelatin (Heussen & Dowdle, 1980). Zones of gelatin clearance in the gel indicated enzyme activity. OVCA429 ovarian carcinoma cells (cell line provided by Dr. Robert Bast, M.D. Anderson, Houston, TX) were cultured in serum free MEM for 24 h and their conditioned media were used as a positive control for proMMP2 and proMMP9. To determine total MMP-2, conditioned media were analyzed with the Quantikine human/mouse MMP-2 (total) immunoassay kit (R&D Systems, Minneapolis, MN) according to manufacturer's specifications. Each sample was analyzed in duplicate.

2.14.2 Analysis of uPA activity

Net plasminogen activator activity in conditioned media was quantified using a coupled assay to monitor plasminogen activation and the resulting plasmin hydrolysis of a colorimetric substrate (VLKpNA) (Stack *et al.*, 1990). Each sample was analyzed in triplicate in two separate assays.

2.15 Assay of Anchorage-Independent Growth

Anchorage-independence is a well-known *in vitro* indicator of malignancy and therefore, was used to assess the malignancy of SBOT cells in culture. Growth in

soft agar was assayed by suspending 1.3 X 10^4 cells in 2 mL of complete medium with 0.33% agarose (Invitrogen Canada Inc., Burlington, Ontario) and placing the suspension on top of 5.0 mL of solidified 0.5% agarose/medium in 60 mm culture dishes. Triplicate cultures for each cell type were maintained for 3 weeks at 37°C in 5% CO_2/air with 2 mL of fresh medium added once a week. The colonies were then sized and counted.

2.16 Determination of *in Vivo* Tumorigenicity

Female BALB/c severely compromised immunodeficient mice, 4 to 6 weeks old, were obtained from the Terry Fox Laboratory (Vancouver, Canada). Four mice were injected intraperitoneally with approximately 4 X 10^5 SBOT-3.1 or ISBOT-3.3 cells per animal in 0.2 mL of CO_2-independent medium. As tumours usually arise in less than six months and tumour formation was not evident in any of the mice , the experiments were terminated at six months and the animals examined for gross evidence of tumours or ascites.

2.17 N-cadherin Adenovirus Construction and Infection

The N-cadherin adenovirus was constructed from the human full-length N-cadherin cDNA clone (Origene, Rockville, Maryland). The N-cadherin cDNA plasmid was transformed into E. coli by incubation of the plasmid and competent cells (Invitrogen) on ice for 30 min, heat shock at 42°C for 30, followed by incubation at 37°C, 225 rpm for 1 h in SOC medium. Single colonies were selected and cultured in Luria-Bertani (LB) broth containing 50μg/mL of ampicillin. Plasmid extractions

were performed using the miniprep or midiprep kits from Qiagen (Mississauga, ON, Canada), according to the manufacturer's procedure. The N-cadherin cDNA was excised from the pCMV6-XL6 vector using the restriction enzymes StuI and SpeI (New England Biolabs, Inc.; NEB) generating a 5.2 kb fragment which was subsequently run in a 1% agarose gel (Invitrogen). The correct sized band was cut out, and gel purified using the Qiagen gel purification kit. The 5.2 kb N-cadherin fragment was subsequently cut with NotI (NEB) and gel purified, generating a 4.5 kb fragment and subcloned into the pShuttle(+) vector (Applied Biological Materials Inc., ABM, Vancouver, BC, Canada) using T4 DNA ligase (NEB). Colonies were cultured in LB containing 25μg/mL of kanamycin. A clone in the correct orientation was selected and sequenced for verification. The N-cadherin pShuttle(+) vector was subsequently subcloned into the pAdenoviral vector DNA (ABM) by double digesting with PI-SceI/I-Ceu I (NEB), followed by ligation and digestion with Swa I (NEB), phenol:chloroform:isoamyl alcohol (25:24:1) extraction, and transformation. The recombinant N-cadherin adenoviral vector was packaged into infectious adenovirus by transfecting HEK-293 cells. For infection, cells were trypsinized, infected with recombinant adenoviruses (either EGFP-virus or N-cadherin virus) for 1 h in suspension, replated and cultured for 24-72 hours. The infection efficiency was nearly 100% as determined by immunofluorescence staining for N-cadherin. Matrigel^{TM} invasion assays were carried out 72 h post-infection.

2.18 Paraffin Embedded Tissues and Array Construction

Archival formalin-fixed paraffin-embedded normal and tumor tissues were collected from the Departments of Pathology of Vancouver Hospital and Health Science Center and Stanford Medical Center. Tissue arrays were prepared by members in the Departments of Pathology at UBC and Stanford University. Representative normal and tumour regions were identified from hematoxylin- and eosin-stained sections. From each specimen, duplicate tissue cores with a diameter of 0.6 mm were punched and arrayed on a recipient paraffin block (Alkushi *et al.*, 2003). The multitissue microarrays were constructed using a Beecher Instruments Micro Tissue Arrayer. Sections of the completed tissue array blocks were cut at 3-4μm and placed on silanized glass slides. We used these sections for immunohistochemical analysis.

2.18.1 Normal oviduct, normal tissue and multi-tumour tissue arrays

Normal oviduct tissue sections were used as controls in immunohistochemistry for OVGP1. The mid- and late-proliferative phase oviduct stains positively while the secretory phase oviduct stains negatively for OVGP1. The multitissue and multitumour tissue arrays consisted of 433 cases representing 45 normal tissues and 51 benign and malignant tumour types from 37 different tissues.

2.18.2 Normal ovary and ovarian tumours

Whole tissue sections from 19 normal ovaries and 14 benign serous cystadenomas and an ovarian tumour array were examined for the expression of OVGP1. The ovarian tumour array consisted of 3 benign mucinous cystadenomas, 89

borderline, and 283 malignant ovarian tumours. Table 3 is a summary of the cases used in this study showing their histologic classification (WHO) and malignancy.

Table 3: Summary of ovarian cases used for immunohistochemical staining

Histological feature	Total no. of cases
Tissue sections	33
Normal	19
Benign serous cystadenoma	14
Tissue microarray	375
Serous tumour	248
Borderline	65
Malignant	183
Seromucinous tumour	6
Borderline	5
Malignant	1
Mucinous tumour	32
Benign	3
Borderline	14
Malignant	15
Endometrioid tumour	44
Borderline	5
Malignant	39
Undifferentiated carcinoma	9
Clear cell carcinoma	34
Transitional cell carcinoma	1
Krukenberg carcinoma	1

2.18.3 Normal endometrium and endometrial tumours

Paraffin-embedded tissues from 290 hysterectomy specimens were examined for the expression of OVGP1, ER and PTEN (Table 4). These included whole tissue sections from 15 cases of normal endometria, of which 5 were proliferative, 5 were secretory, and 5 were menstrual phase endometria. There were 43 cases of hyperplasias, 16 nonatypical, and 27 atypical. Of the endometrioid carcinomas (*n* =

24), 15 were low-grade (International Federation of Gynecologists and Obstetricians (FIGO) grade 1), and 9 were high-grade (FIGO grade 3). The rest were uterine papillary serous carcinomas (n = 8). Two hundred cases were used to construct an endometrial cancer tissue microarray. None of the included cases received preoperative radiotherapy or chemotherapy. One hundred fifty-six cases were of the endometrioid type, whereas the rest were nonendometrioid carcinomas.

Table 4: Summary of endometrial cases used for immunohistochemical staining

Histological feature	Total no. of cases
Tissue sections	90
Normal	15
Proliferative	5
Secretory	5
Menstrual	5
Hyperplasia	43
Typical	16
Atypical	27
Endometrioid carcinoma	24
Grade 1	15
Grade 3	9
Papillary serous carcinoma	8
Tissue microarray	200
Endometrioid carcinoma	156
Nonendomerioid carcinoma	44

2.19 Immunostaining of Paraffin-Embedded Tissues

The avidin-biotin method was used for immunohistochemical staining and applied to formalin fixed and paraffin embedded tissue. Sections of the recipient paraffin blocks were cut, deparaffinized with xylene, and rehydrated through a series of graded alcohols

2.19.1 Staining for oviduct-specific glycoprotein

For comparison of OVGP1 in different normal and tumour tissue sections and tissue microarrays, a polyclonal antibody generated in rabbits was kindly provided by Dr. Harold G. Verhage. Following rehydration, the sections were treated with 30% H_2O_2 for 5 min, and then submitted to antigen retrieval by microwave oven treatment for 10 min or steamer for 30 min in 10 mM citrate buffer at pH 6.0. Slides were subsequently washed twice in distilled water, and once in TBS. Tissues were incubated in normal goat serum for 30 min followed by staining for human OVGP1 using the rabbit polyclonal antibody at a dilution of 1:1000 overnight at 4^{o}C. After three washes in TBS for 15 min each, tissues were incubated with biotinylated anti-rabbit immunoglobulins at 1:200 dilution (Vector Laboratories, Inc., Burlington, ON) at room temperature for 1 h followed by avidin-biotin peroxidase complexes (Vectastain ABC kit; Vector Laboratories, Inc.) for 1 h. The sections were developed with 3,3'-diaminobenzidine tetrahydrochloride (DAB; Vector Lab., Inc.), counterstained lightly with hematoxylin (Sigma), and dehydrated with graded ethanol concentrations, followed by xylene and mounting with Permount. Mid- or late-proliferative stage oviductal tissues were used as positive controls while secretory phase oviductal tissues were used as negative controls. Pre-immune serum also served as a negative control.

2.19.2 Staining for estrogen receptor and PTEN

Staining for ER and PTEN was carried out by Dr. Abdulmohsen Alkushi (Department of Pathology, Vancouver General Hospital, Vancouver, B.C.) and Dr. Anthony Magliocco (University of Calgary, Calgary, AB), respectively, with an

automated stainer (Ventana, Tucson, AZ), according to the manufacturer's guidelines. Antigen retrieval was carried out as indicated in Table 5.

Table 5: Antibodies used for immunohistochemical staining of formalin fixed paraffin embedded tissues

Antigen	Clone	Supplier	Dilution	Antigen Retrieval
OVGP1	Polyclonal	H.G. Verhage	1μg/mL	M/S
OVGP1	7E10	R. Molday	-	S
PTEN	Polyclonal	H.C. Cheng	2.63μg/mL	V
ER	6F11	Novocastra	1:50	M

Abbreviations: M, microwave; S, steamer; V, as per Ventana protocol Benchmark MBK iView DAB system

2.20 Oviduct-Specific Glycoprotein Production and Development of a Monoclonal Antibody

A monoclonal antibody was generated for the purpose of developing a serum-based assay for the detection of OVGP1 in patients with ovarian cancer. In an attempt to produce a monoclonal antibody, collaborations were started with Dr. Robert Molday, University of British Columbia, Vancouver, BC and one fee-for-service company (A&G Pharmaceuticals). A monoclonal antibody, 7E10, was successfully developed in the laboratory of Dr. Robert Molday using a recombinant fusion protein produced in *E. coli*. To assay the hybridoma clones, OVGP1 was overexpressed in mammalian cells and conditioned media were collected as described below.

2.20.1 Oviduct-specific glycoprotein production

The OVGP1 cDNA was kindly provided by Dr. Randall Jaffe (University of Illinois at Chicago, Chicago, IL). The OVGP1 cDNA was tagged with either 6x-

histidine by Bio S&T, Montreal, QC or the C-terminal of Rhodopsin (T-E-T-S-Q-V-A-P-A) by Dr. Robert Molday's laboratory. Recombinant protein was produced using the FreeStyle™ 293 Expression System (Invitrogen), designed to allow large-scale transfection of suspension 293 human embryonic kidney cells (HEK-293F cells) in a defined, serum-free medium (Freestyle™ 293 Expression Medium). HEK-293F cells were seeded at 3 x 10^5 viable cells/mL and subcultured when the density was approximately 2-3 x 10^6 viable cells/mL. The cells were maintained in 125 mL or 500 mL polycarbonate, disposable Erlenmeyer flasks and incubated at 37°C containing a humidified atmosphere of 5% CO_2 in air in an orbital shaker platform rotating at 125rpm. Transfection of HEK-293F cells with OVGP1-his or OVGP1-Rho was scaled up or down depending on the number of cells. In brief, on the day of transfection, the total number of viable cells was determined and diluted to 1.1 x 10^6 viable cells/mL with fresh, pre-warmed FreeStyle™ 293 Expression Medium. For every 30 mL of cell suspension (3 x 10^7 cells), 30 μg of plasmid DNA in 1 mL of Opti-MEM (Invitrogen) and 40 μL of 293fectin™ in 1 mL of Opti-MEM were used. The plasmid DNA and 293fectin™ were incubated separately for 5 min at room temperature and then mixed together and incubated for 20-30 min at room temperature to allow the DNA-293fect™ complexes to form. The conditioned media and cell lysates were harvested every day for 5 days or cumulatively for 5 days post-transfection to determine the optimal expression of the recombinant protein. Overexpression of the protein in conditioned media and cell lysates were determined by Western blot analysis using the polyclonal OGP antibody and 6x histidine

monoclonal antibody (EH23; ABM, Vancouver, BC), and the Rho 1D4 monoclonal antibody (Dr. Robert Molday) as described in Section 2.3 (Table 1).

2.20.2 Development of a monoclonal antibody

Monoclonal antibodies were generated in Dr. Robert Molday's laboratory by injecting mice with recombinant protein generated in *E. coli* against the N-terminal and C-terminal regions of OVGP1 tagged with Rhodopsin. Serum was tested by Western blot analysis using OVGP1 conditioned medium. Mice with a positive signal had their spleens fused with a leukemia cell line to generate hybridomas. Hybridoma clones were first screened using a dot blot assay. Positive clones were subsequently tested further by immunblotting against conditioned medium containing OVGP1 as described in Section 2.3. The clones yielding a correct sized band in immunoblotting was further tested by immunohistochemistry which was performed by Mrs. Sarah Maines-Bandiera in our laboratory. As OVGP1 is normally expressed in the secretory cells of the oviduct when estrogen levels are high, sections of formalin-fixed paraffin-embedded mid-late proliferative phase oviduct were probed with the different clones as described in Section 2.19 with some modifications. In addition, ovarian tumour tissue arrays were screened for the presence of OVGP1 using the clone, 7E10, which gave a positive and specific result by Western blot analysis and immunohistochemical staining of the oviduct. Following rehydration, sections were treated with 3% H_2O_2 for 30 min, and then submitted to antigen retrieval by steaming for 30 min in Target Retrieval Solution (DAKO). Tissues were blocked with DAKO protein block for 1 h, followed by incubation with the supernatant from the hybridomas overnight at 4^{o}C. The sections were washed,

followed by incubation with Envision Labelled Polymer/ HRP (DAKO) and development in DAB (DAKO). The sections were then counterstained, dehydrated and mounted as in Section 2.19.

2.21 Development of a Serum-Based Assay for Oviduct-Specific Glycoprotein

A sandwich ELISA assay for OVGP1 is currently being developed in our lab using the clone 7E10 and the polyclonal OGP antibody. The 7E10 clone was purified and bound to the bottom of a plate well by coating the wells overnight at 4^{o}C. After blocking, serum samples are added to the wells and incubated for 1-2 h at room temperature to allow for binding of the antigen to the 7E10 antibody. The rabbit polyclonal OGP antibody is subsequently used as the second antibody which binds to the antigen. After incubation with horseradish peroxidase-linked anti-rabbit secondary antibody (Biorad), the assay is then quantitated through the use of a colorimetric substrate, ABTS (Sigma), and read at 405 nm minus 490 nm (background) using a microplate photoreader (Bio-Tek Instruments Inc.).

2.22 Scoring and statistical analysis

Tissues and tissue arrays stained for OVGP1, ER and PTEN were scored microscopically after immunohistochemical staining. Scoring of the OVGP1 staining was performed in conjunction with Dr. C. Blake Gilks. Scoring of the ER and PTEN staining was performed by Dr. Abdulmohsen Alkushi.

OVGP1 expression in the normal tissue and multi-tumour tissue arrays was assigned a negative score of 0 for no staining and a positive score of 1 for positive

staining, regardless of staining intensity or the percentage of positive cells stained. Staining for OVGP1 in the normal ovaries was scored based on intensity as strong, moderate, or absent. The ovarian tumours were given a negative or positive score for no staining and positive staining, respectively, to examine the overall distribution of OVGP1 in different histologic subtypes and grades of benign, borderline, and invasive ovarian tumours. A more detailed analysis of the staining was performed on the ovarian carcinomas. The localization (apical or cytoplasmic), intensity (weak or strong), and percentage of positive cells/case (<20%, 20-80%, >80%) were determined for each case of ovarian carcinoma.

Using the 7E10 clone, ovarian carcinomas were assigned according to the following staining categories: no staining, weak diffuse staining, strong patchy staining, and strong diffuse staining. The Kaplan-Meier method was used to construct a disease-specific survival curve for subgroups of patients based on oviduct-specific glycoprotein expression profile as assessed on the tissue microarray. Comparison of curves was done using log-rank statistic. Time-to-event was defined as disease-specific survival from initial diagnosis to date of death due to ovarian carcinoma, with all others considered censored.

For the endometrial tissue sections, scores for the expression of OVGP1 were assigned semiquantitatively according to the percentage of cells stained (no positive cells, score 0; <5%, score 1; 5 to 50%, score 2; >50%, score 3) and the intensity of staining (no staining, score 0; weak, score 1; moderate, score 2; and strong, score 3). The two scores were then multiplied to get the staining index. For the endometrial tissue microarrays, staining for oviduct-specific glycoprotein was scored by staining

intensity as either (*a*) absent or weak or (*b*) strong. Sections stained for ER and PTEN were scored by percentage of positive cells with a three-point scale where 0 = 0 to 50% of cells staining, 1 = >50% of cells staining, and 5 = uninterpretable score. Technically unsatisfactory samples (24 for OVGP1 staining, 42 for the comparison of ER and OVGP1, and 49 for the comparison of PTEN and OVGP1) were eliminated from additional consideration. As OVGP1 staining in endometrial tissues is focal, score results for duplicate cores from the same case were consolidated into one score where positive staining always superceded a negative or uninterpretable result. Statistical analyses were done with SSPS, version 11.0 software (Chicago, IL). Either Mann-Whitney *U* rank sum or Kruskal-Wallis nonparametric tests were used to evaluate the correlation between OVGP1 expression and endometrial tissue categories. These tests are commonly used when dealing with data distributed in categories. The Kaplan-Meier method was used to construct a disease-specific survival curve for subgroups of patients based on oviduct-specific glycoprotein expression profile as assessed on the tissue microarray. Comparison of curves was done using log-rank statistic. Time-to-event was defined as disease-specific survival from initial hysterectomy to date of death due to endometrial carcinoma, with all others considered censored. Correlation between OVGP1, PTEN and ER expression was compared by either χ^2 or Fisher's exact test. For all analyses, two-sided tests of significance were used with α of 0.05.

3. RESULTS

3.1 Genotypic and Phenotypic Characterization of Cultured SBOT Cells

3.1.1 Morphological characterization and growth potential of cultured SBOT cells

To further study the role of differentiation in ovarian neoplasia, we examined the phenotypic and genotypic characteristics of SBOTs, a highly differentiated epithelial tumour type which lacks the capacity to invade. Only a few *in vitro* cultures of SBOT cells have as yet been characterized, while we have found no descriptions of permanent SBOT cell lines. Therefore, we established a culture model to allow in-depth functional characterization of SBOT. Tissues were obtained at surgery from four different patients and designated as SBOT-1, SBOT-2, SBOT-3 and SBOT-4. The tissues were dissociated and were plated into multiple 60 mm culture dishes. Pure populations of epithelial cells were obtained in lines SBOT-3 and SBOT-4, while fibroblast contamination outgrew the cancer cells in lines SBOT-1 and SBOT-2. Therefore, SBOT-1 and SBOT-2 were only examined for the expression of keratin, E-cadherin, and CA125. A permanent cell line was obtained in a subline of the SBOT-3 culture, SBOT-3.1. SBOT-3.1 has been propagated for greater than 100 population doublings (PDs) without undergoing crisis or senescence. For the first 24 months, SBOT-3.1 cells grew at doubling times of about 4-6 days. SBOT-3.1 cells initially adhered to tissue culture plastic very poorly, which problem was partially alleviated by coating growth surfaces with fibronectin. With time, cells were selected that adhered to plastic more readily, but the growth rate became reduced to PDs of approximately 4 weeks. The growth rate was increased by co-

culturing the SBOT-3.1 cells with lethally irradiated NIH-3T3 fibroblasts (Fig. 5). Cells cultured on high attachment plastic and on fibronectin-coated surfaces spread better, but this did not alter their growth rate. In contrast to the SBOT-3 cells, the SBOT-4 cells proliferated rapidly for 2-3 passages (approximately 10-12 PDs) but then became stationary and eventually died. Co-culture with 3T3 cells amplified the growth potential of SBOT-4 cells only slightly (data not shown). Thus, despite the presence of telomerase activity in both lines (Fig. 6), it appears that the SBOT-3.1 cells were capable of adapting to long-term culture conditions while the SBOT-4 cells did not. Morphologically, the epithelial cells from all four lines formed whorl-like colonies (Fig. 7, A) and were elongated and irregularly shaped, sometimes with long cytoplasmic projections (B), resembling cultured metaplastic ovarian surface epithelium (OSE) and low-grade ovarian epithelial neoplasms rather than normal OSE, which forms cobblestone monolayers of compact epithelial cells (Wong *et al.*, 1998; Wong *et al.*, 1999). With passage in culture, the SBOT-3.1 cells formed small epithelial colonies comprised of large, flattened cells but with increasing confluence, they became tightly packed and columnar (C, D).

3.1.2 Mutational and cytogenetic analysis of cultured SBOT cells

Activating mutations in *KRAS* and in one of its downstream mediators, *BRAF*, have been identified in over 60% of serous borderline ovarian tumors (Singer *et al.*, 2003). Analysis by Dr. Carla Oliveira (University of Porto, Porto, Portugal) showed that the SBOT-3.1 cell line contained no mutations in either the *KRAS* or *BRAF* genes while the SBOT-4 line, although negative for *KRAS* mutations, displayed the *V600E*

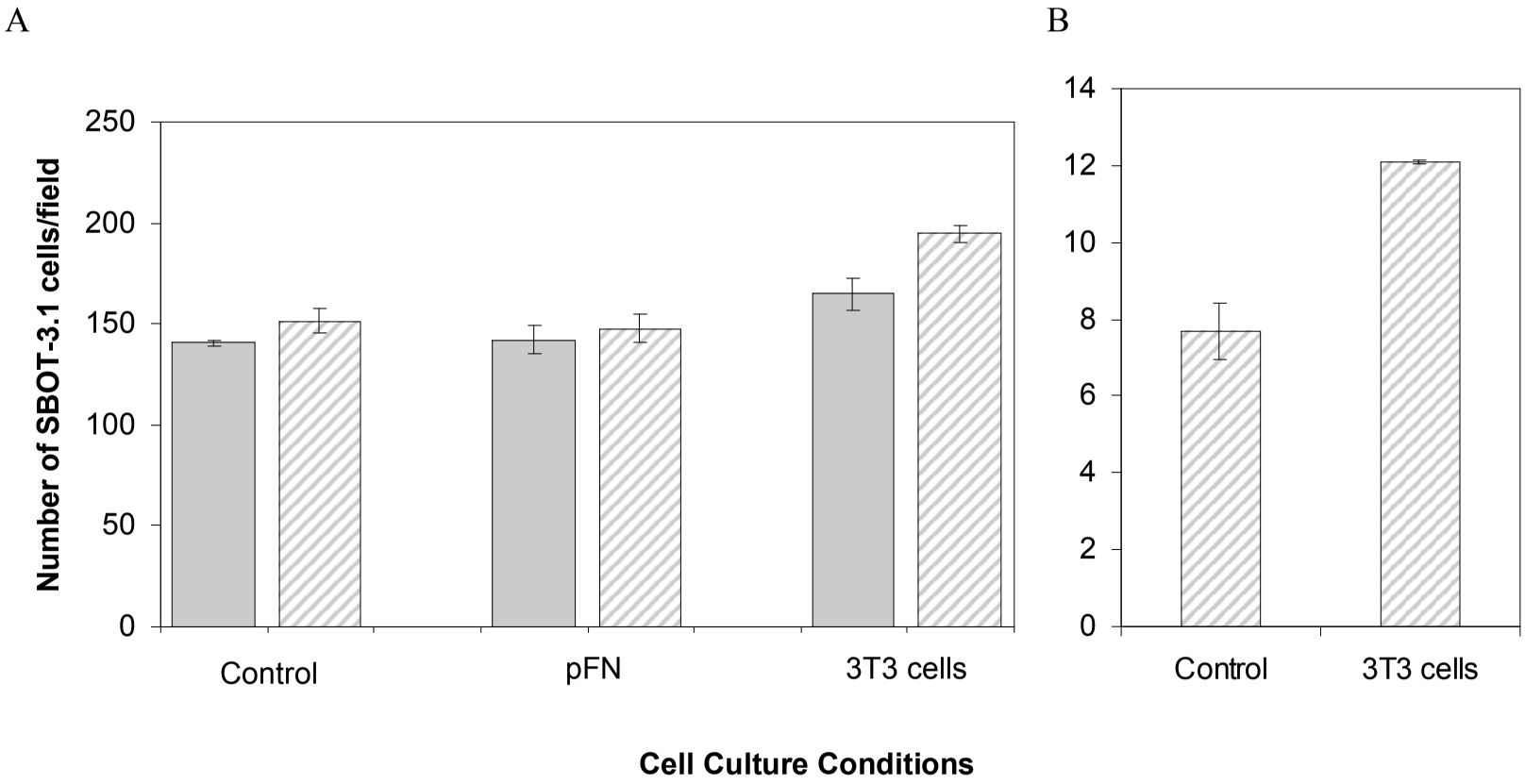

Fig. 5. Growth of SBOT-3.1 cells on different substrata. (A) Low passage SBOT-3.1 cells, and (B) high passage SBOT-3.1 cells. Solid bars, regular tissue culture plastic. Striped bars, high attachment plastic (Corning, Catalogue # 3336). Plastic coated with plasma fibronectin (pFN) did not alter cell growth on either regular or high attachment plates. Cell growth was stimulated when plated on plastic with irradiated NIH-3T3 cells seeded as a feeder layer. The effect was more prominent in high attachment plates. A larger increase in cell growth was observed with the high passage SBOT-3.1 cells. Mean $\pm$ S.D. of triplicate cultures. Representative of 3 individual experiments.

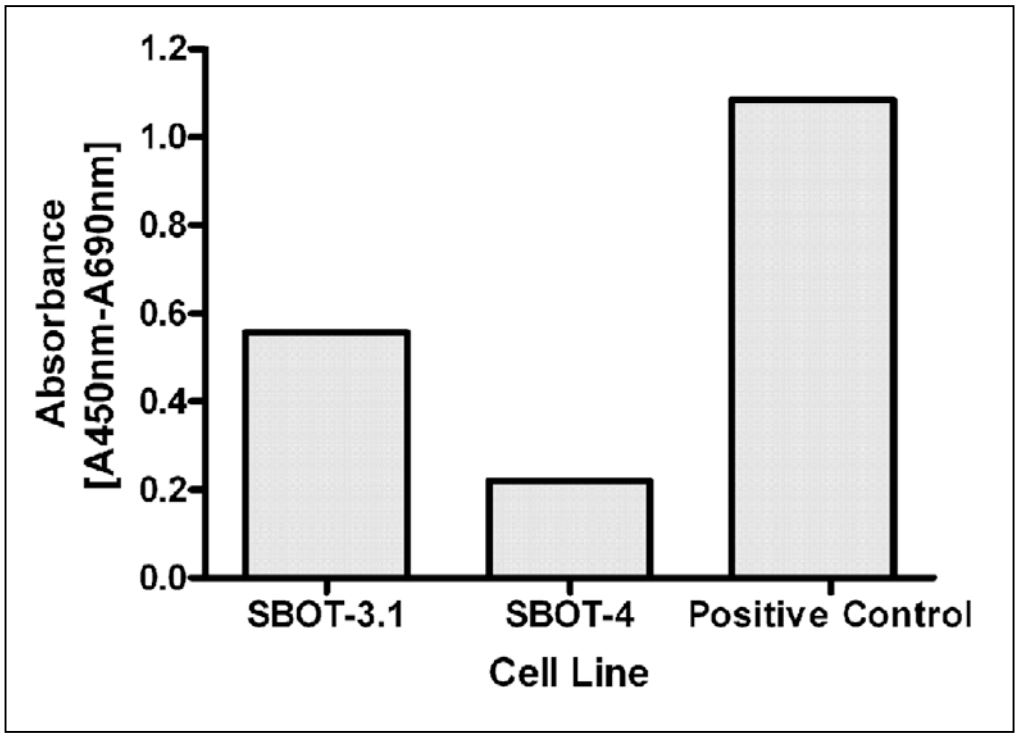

Fig. 6. Telomerase activity was detected in both the permanent cell line, SBOT-3.1, and low-passage SBOT-4 cells. Volumes of extracts equivalent to 3000 cell equivalents were incubated in the presence of dNTPs and the elongated oligonucleotides were amplified and detected by PCR ELISA as described in the kit protocol. The results are expressed in arbitrary absorbance units.

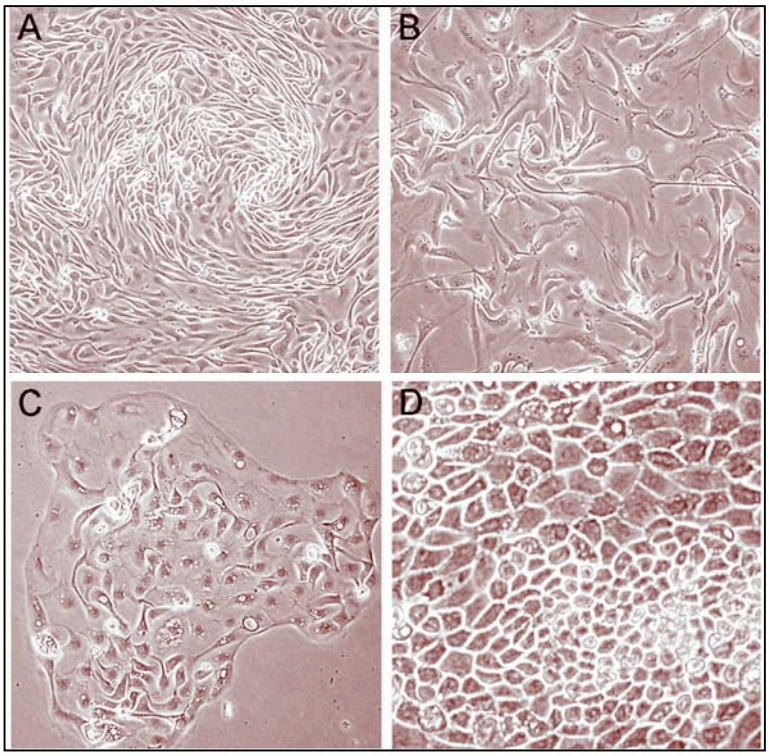

Fig. 7. Morphology of SBOT cells. (A), whorly growth pattern in primary culture and (B), long cytoplasmic extensions in low passage culture, resembling cultured metaplastic OSE and low-grade serous ovarian carcinomas. The permanent SBOT-3.1 line forms colonies of flattened epithelial cells under sparse conditions (C), while at high cell densities, the cells became tightly packed and columnar in shape (D). Phase microscopy.

mutation, which accounts for at least 80% of *BRAF* mutations (Fig. 8) (Rajagopalan *et al.*, 2002; Pollock *et al.*, 2003; Singer *et al.*, 2003). Multicolor-FISH karyotyping of the SBOT-3.1 cell line, carried out in Dr. Huntsman's lab of the B.C. Cancer Agency, identified a 51 chromosome set with both numerical and structural aberrations: 51, XX, +8, +12, +14, +14, t(15;16)(q25;p11), +16, -18, +20 (Fig. 9), which was also revealed by conventional cytogenetic analysis (data not shown). The translocation was observed in all metaphases analyzed. Consistent with these findings, the low-resolution CGH profile (Table 6) showed gains in chromosomes 8, 12, 14, 16, and 20, and reduced copy numbers in 1p, 9 and 18. Multicolor-FISH analysis and array CGH analysis of the SBOT-4 cell line revealed no major structural or numerical abnormalities other than a subpopulation of <25% of tetraploid cells. As the abnormality in this subpopulation was balanced it was not detectable by array CGH.

Table 6 shows the results of copy number abnormalities of SBOT-3.1 and SBOT-4 cells detected by array-based CGH. The results indicate that the cytogenetics of SBOT cells are less complex in comparison to high grade ovarian cancers as demonstrated in this study *in vitro.* In addition, the findings of this study correlate with previous studies performed by others in SBOT tissue specimens. Array CGH analysis identified a loss of chromosomes 1p36 and 9 in the SBOT-3.1 cell line, which was beyond the resolution of mFISH. The SBOT-4 cells had significantly fewer gains or losses compared to the SBOT-3.1 cell line. The two lines shared common chromosomal copy number abnormalities in only a few regions or loci. Array-based CGH detected copy number gains common to both cell lines at several

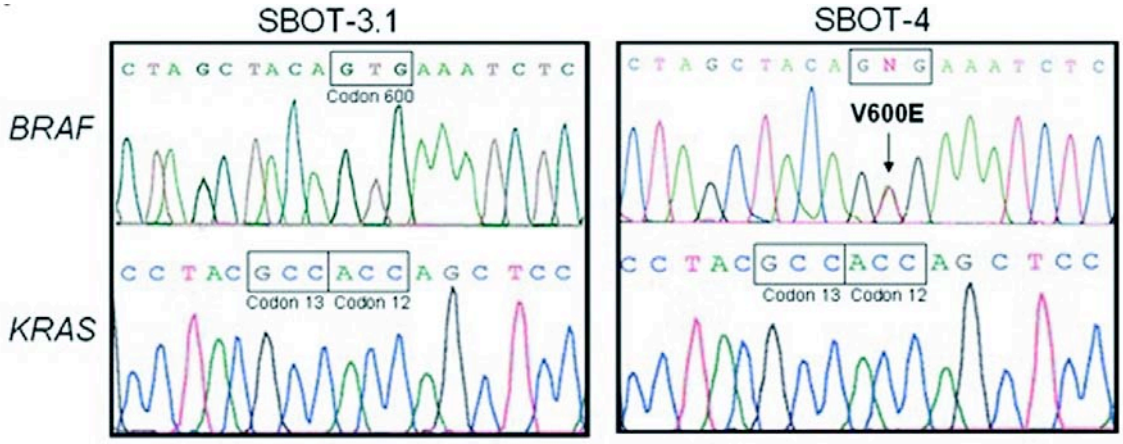

Fig. 8. BRAF and KRAS mutational analysis in the SBOT-3.1 and SBOT-4 cell lines. A BRAF mutation was found in the SBOT-4 cells: in exon 15, position 600, subtitution of A for the T. GTG ⟶ GAG. No BRAF or KRAS mutations were found in the SBOT-3.1 cells. Genomic DNA was extracted and analysed for BRAF exon 15 and KRAS exon 1 mutational hotspots by Single Stranded Conformation Polymorphism and Heteroduplex Analysis, followed by direct sequencing.

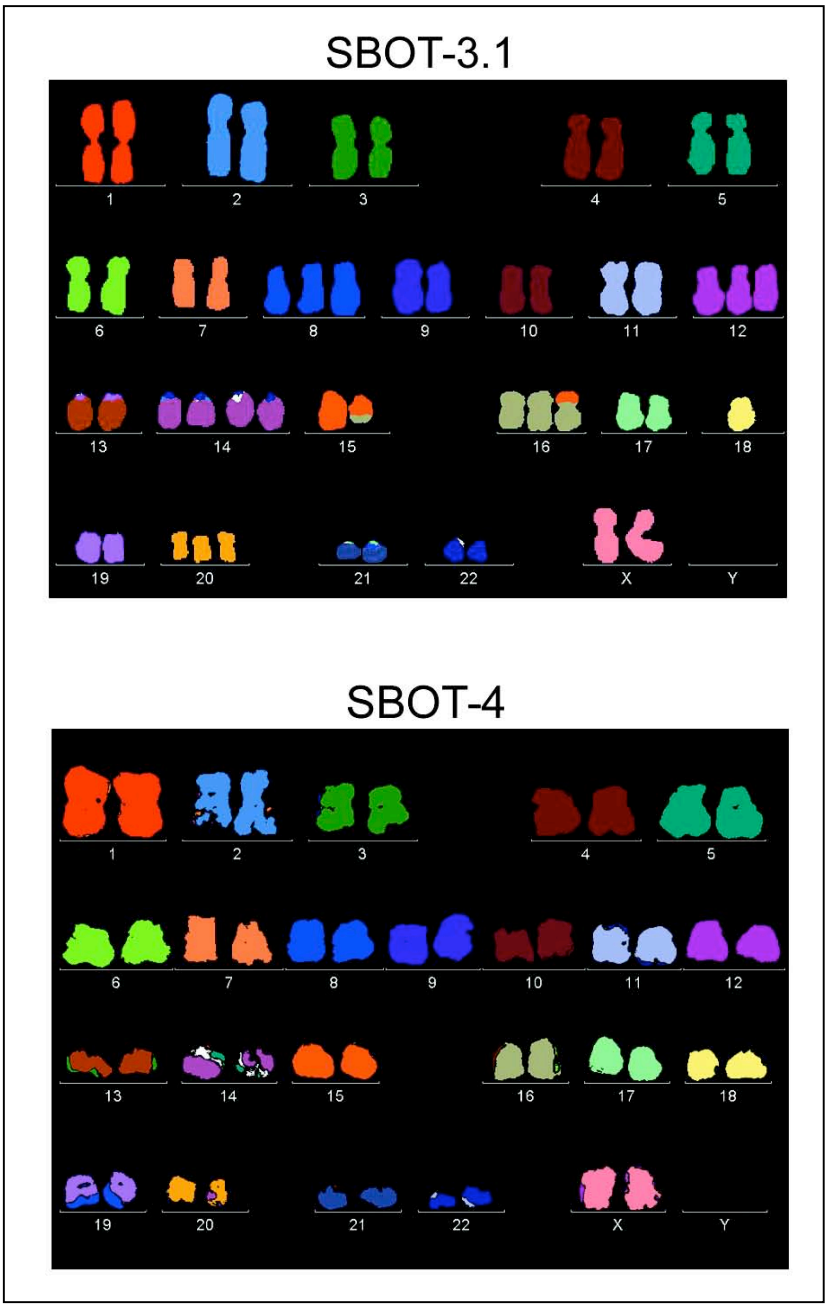

Fig. 9. MFISH analysis of the SBOT-3.1 and SBOT-4 cells. The SBOT-3.1 cell line has the following karyotype: 51, XX, +8, +12, +14, +14, t(15;16)(q25;p11), +16, -18, +20, while no abnormalities were observed in SBOT-4 cells. MFISH was performed using the 24XCyte MetaSystems DNA probe kit (MetaSystems GmBH) which utilizes combinatorial fluorescent labeling to uniquely label each chromosome of the human karyotype.

Table 6. A comparison of the copy number abnormalities between the SBOT-3.1 and -4 cell lines as detected by array-CGH analysis

Note: Empty spaces represent loci with no change in copy number. Text in bold represent loci which are commonly involved in ovarian carcinogenesis.

			SBOT-3.1			SBOT-4		
Chromosome no.	Locus name	Cytogenetic location	Mean ratio	±	Non-modal (p<x)	Mean ratio	±	Non-modal (p<x)
1	CDC2L1(p58)	1p36				0.81	--	0.001
1	D1S214	1p36.31	0.58	--	0.001			
1	D1S1635	1p36.22	0.57	--	0.001			
1	D1S199	1p36.13	0.69	--	0.01			
1	FGR(SRC2)	1p36.2-p36.1	0.58	--	0.001	1.20	++	0.005
1	TGFB2	1q41	1.59	++				
2	MSH2,KCNK12	2p22.3-2p22.1				1.29	++	0.0002
2	LRP1B	2q21.2	0.75	--				
2	D2S447	2q tel	0.71	--	0.005	1.35	++	0.0002
4	DDX15	4p15.3				1.20	++	0.005
5	C84C11/T3	5p tel				1.20	++	0.01
5	5QTEL70	5q tel	0.70	--	0.005			
6	CCND3	6p21				1.21	++	0.01
7	G31341	7p tel	0.77	--				
7	**EGFR**	**7p12.3-p12.1**				**1.29**	**++**	**0.0002**
8	D8S504	8p tel	1.26	++				
8	D8S596	8p tel	1.31	++				
8	**PDGRL**	**8p22-p21.3**	**1.29**	**++**				
8	LPL	8p22	1.22	++				
8	**FGFR1**	**8p11.2-p11.1**	**1.27**	**++**				
8	**MOS**	**8q11**	**1.27**	**++**				
8	**E2F5**	**8p22-q21.3**	**1.23**	**++**				
8	**EXT1**	**8q24.11-q24.13**	**1.37**	**++**	**0.01**			
8	**MYC**	**8q24.12-q24.13**	**1.25**	**++**				
8	U11829	8q tel	1.36	++				
9	D9S913	9ptel	0.64	--	0.001			
9	AFM137XA11	9p11.2	0.73	--		0.82	--	0.002
9	D9S166	9p12-q21	0.79	--				
9	PTCH	9q22.3	0.69	--	0.005			
9	DBCCR1	9q33.2	0.72	--	0.005			
9	TSC1	9q34	0.69	--	0.005			
9	ABL1	9q34.1	0.75	--				
9	H18962	9q tel	0.71	--	0.005			
9	D9S325	9q tel	0.58	--	0.001			
10	WI-2389,D10S1260	10p14-p13	1.24	++				
11	INS	11p tel				1.57	++	0.0001
11	HRAS	11p15.5	0.76	--				
12	8M16/SP6	12p tel	1.29	++				
12	SHGC-5557	12p tel	1.22	++				
12	CCND2	12p13	1.30	++				
12	**CDKN1B(p27)**	**12p13.1-p12**	**1.24**	**++**				

Chromosome no.	Locus name	Cytogenetic location	SBOT-3.1 Mean ratio	±	SBOT-3.1 Non-modal (p<x)	SBOT-4 Mean ratio	±	SBOT-4 Non-modal (p<x)
12	**SAS,CDK4**	**12q13-q14**	**1.21**	**++**				
12	**MDM2**	**12q14.3-q15**	**1.26**	**++**				
12	DRIM,ARL1	12q23	1.24	++				
12	U11838	12q tel	1.28	++				
13	D13S327	13q tel				1.20	++	0.01
14	PNN(DRS)	14q13	1.37	++	0.01			
14	TCL1A	14q32.1	1.61	++	0.001	1.23	++	0.005
14	**AKT1**	**14q32.32**	**1.34**	**++**	**0.01**			
14	IGH(D14S308)	14q tel	1.85	++	0.001			
14	IGH(SHGC-36156)	14q tel	1.39	++	0.01			
15	PACE4C	15q tel				1.29	++	0.0005
16	CREBBP	16p13.3	1.24	++				
16	CYLD	16q12-q13	1.26	++				
16	**CDH1**	**16q22.1**	**1.32**	**++**				
16	FRA16D	16q23.2	1.34	++	0.01			
16	**CDH13**	**16q24.2-q24.3**	**1.39**	**++**	**0.005**			
18	D18S552	18p tel	0.75	--				
18	SHGC17327	18p tel	0.68	--	0.001			
18	YES1	18p11.31-p11.21	0.79	--				
18	LAMA3	18q11.2	0.60	--	0.001			
18	DCC	18q21.3	0.73	--	0.01			
18	MADH4(DPC4)	18q21.1	0.80	--				
18	**BCL2 3'**	**18q21.3**	**0.79**	**--**				
18	CTDP1,SHGC-14582	18q tel	0.48	--	0.001			
18	18QTEL11	18q tel	0.75	--				
20	20PTEL18	20p tel	1.32	++		1.23	++	0.005
20	SOX22	20p tel	1.21	++				
20	JAG1	20p12.1-p11.23	1.32	++				
20	MKKS, SHGC-79896	20p12.1-p11.23	1.36	++	0.01			
20	TOP1	20q12-q13.1	1.27	++				
20	CSE1L(CAS)	20q13	1.22	++				
20	**STK6(STK15)**	**20q13.2-q13.3**	**1.34**	**++**	**0.01**			
20	**ZNF217(ZABC1)**	**20q13.2**	**1.23**	**++**				
20	CYP24	20q13.2	1.31	++				
X	STS 3'	Xp22.3	1.40	++	0.005			
X	STS 5'	Xp22.3	1.42	++	0.005	1.40	++	0.0001
X	KAL	Xp22.3	1.30	++		1.32	++	0.0001
X	DMD exon 45-51	Xp21.1	1.55	++	0.001	1.44	++	0.0001
X	DXS580	Xp11.2	1.26	++		1.28	++	0.0002
X	DXS7132	Xq12	1.26	++				
X	AR 3'	Xq11-q12	1.59	++	0.001	1.55	++	0.0001
X	XIST	Xq13.2	1.30	++		1.39	++	0.0001
X	OCRL1	Xq25	1.46	++	0.002	1.96	++	0.0001
Y	SRY	Yp11.3	0.72	--		0.61	--	0.0001
Y	AZFa region	Yq11				0.59	--	0.0001

loci on Ch. X and at TCL1A at Ch.14q. and 20PTEL18 at Ch.20p. The only loss in copy number common to both cell lines was the locus AFM137XA11 at Ch9p. Other copy number gains and losses observed in the SBOT-3.1 cell line, which are known to be important in ovarian neoplastic progression, are listed in Table 6. It is noteworthy that five such loci (PDGRL, FGFR1, MOS, E2F5, EXT1 and MYC) were amplified at Ch.8 which is a common site of abnormalities in SBOT and that gains also included genes involved in growth factor signaling (EGFR, ERBB3), p53 regulation and PI3K signaling (AKT1, MDM2) as well as WNT1, and ZNF217 which is commonly amplified in ovarian cancer. There was a loss in chromosome 18q21.3 which contains the locus for BCL2, an important member of the anti-apoptotic family. In addition, there was a gain in the gene encoding E-cadherin, CDH1, which is commonly upregulated in well-differentiated ovarian tumours. In contrast to high grade EOCs, there was a gain in chromosome region 16q24.2-q24.3 which contains the locus for CDH13, encoding H-cadherin.

3.1.3 Cultured SBOT cells express epithelial differentiation markers

In contrast to normal OSE cells which adhere to one another by N-cadherin and do not secrete CA125, metaplastic and neoplastic OSE often express the epithelial cell-adhesion molecule E-cadherin and secrete the epithelial differentiation marker CA125 (Maines-Bandiera *et al.*, 1997; Bast *et al.*, 1998; Wong *et al.*, 1999). All four SBOT cultures expressed abundant keratin filaments, as well as E-cadherin in areas of cell-cell adhesion (Fig. 10, data not shown for SBOT-1 and SBOT-2 lines). They expressed no N-cadherin, or a little in the perinuclear

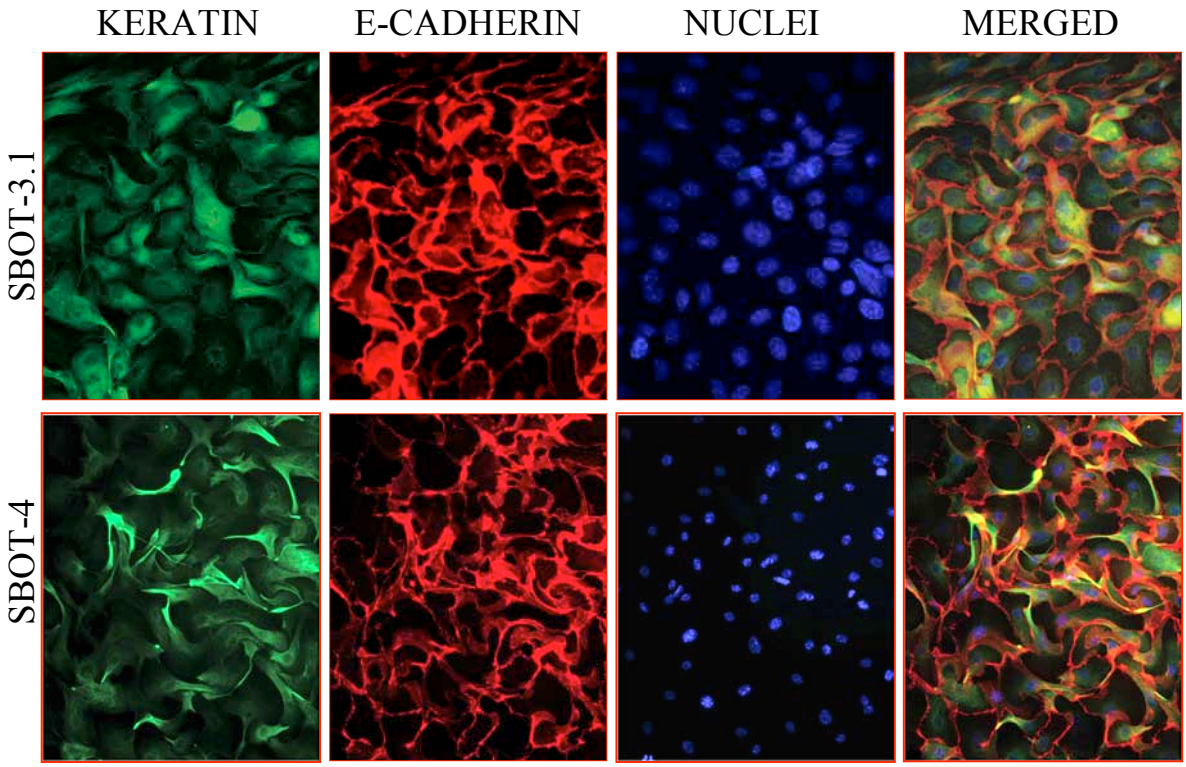

Fig. 10. Immunofluorescence microscopy of cultured SBOT cells stained for the epithelial markers keratin and E-cadherin. SBOT cells express abundant keratin filaments and E-cadherin is localized at the cell to cell junctions. Cells were cultured on coverslips, fixed in methanol and labeled with a rabbit polyclonal antibody against keratin (wide-spectrum) and a mouse monoclonal antibody against E-cadherin. Nuclei were stained with Hoechst 33258.

regions (Fig. 11). Conditioned medium from the SBOT cultures revealed very high levels of CA125 as shown in Table 7. In addition, SBOT-3.1 and SBOT-4 cultures were examined for the secretion of the differentiation marker, oviduct- specific glycoprotein (OVGP1), which we demonstrated to be a marker of early ovarian neoplasia and low grade ovarian tumours (Woo *et al.*, 2004). Both cultures secreted OVGP1 into the conditioned media (Fig. 12).

Table 7. CA125 levels in conditioned medium of SBOT cells

Cell line	CA125 kU/L
SBOT-1	304-639
SBOT-2	N.D.
SBOT-3	1700-1741
SBOT-4	6400-10 000

CA125 was assayed by microparticle enzyme immunoassay as per manufacturer's specifications (Abbott). The reference level is <35kU/L, with a borderline range of 35-65kU/L. N.D., not determined.

3.1.4 SBOT cells are noninvasive in culture and have limited migratory capacity

By definition, serous borderline ovarian tumours lack stromal invasion, which distinguishes these neoplasms from invasive carcinomas. To determine whether SBOT cells retain this characteristic *in vitro*, their invasiveness was measured using the *in vitro* Matrigel^{TM} invasion assay, a method which strongly correlates with invasive behavior *in vivo* (Shaw, 2005). As shown in Fig. 13, SBOT-3.1 and SBOT-4 cells have very limited invasive capacity as compared to the weakly invasive CAOV-3 cell line and the highly invasive SKOV-3 cell line. To determine whether the limited invasive ability of the SBOT cells was attributable to a limitation in migratory capacity, the scratch assay was used to determine the rate at which the cells covered

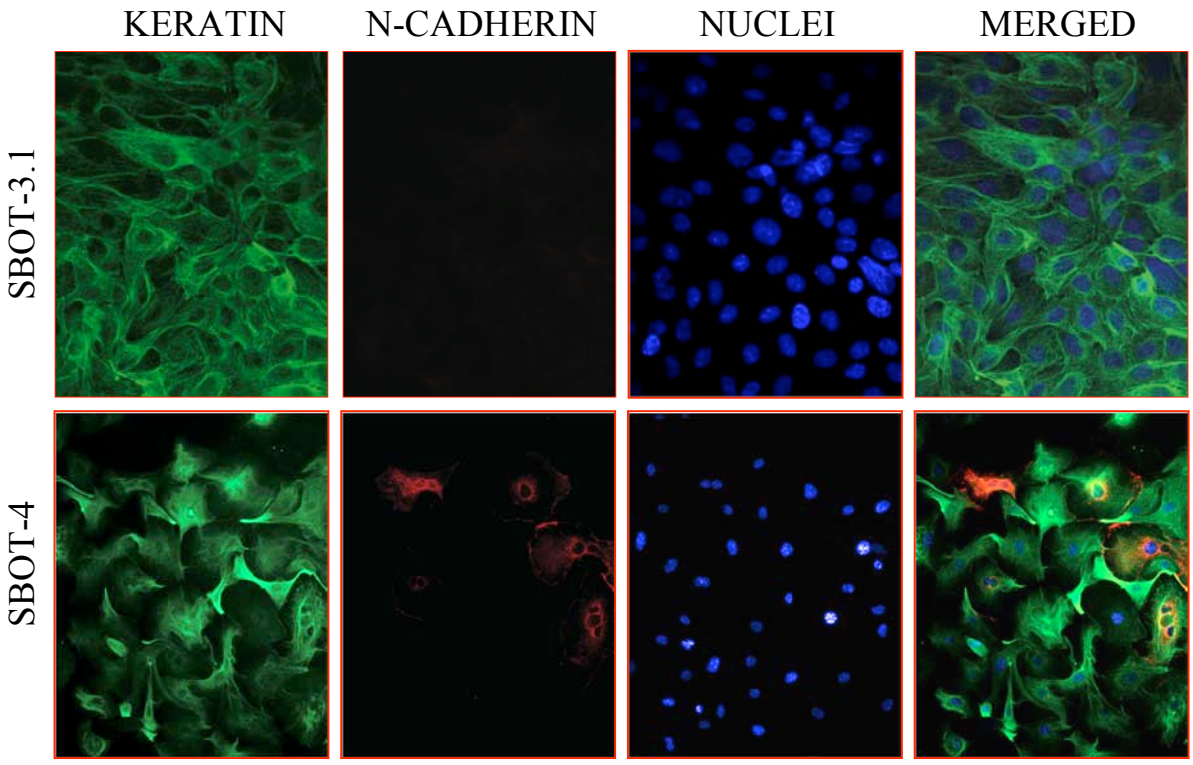

Fig. 11. Immunofluorescent staining for N-cadherin in cultured SBOT cells. SBOT cells express little or no N-cadherin. Cells were cultured on coverslips, fixed in methanol and labeled with a rabbit polyclonal antibody against keratin (wide-spectrum) and a mouse monoclonal antibody against N-cadherin. Nuclei were stained with Hoechst 33258.

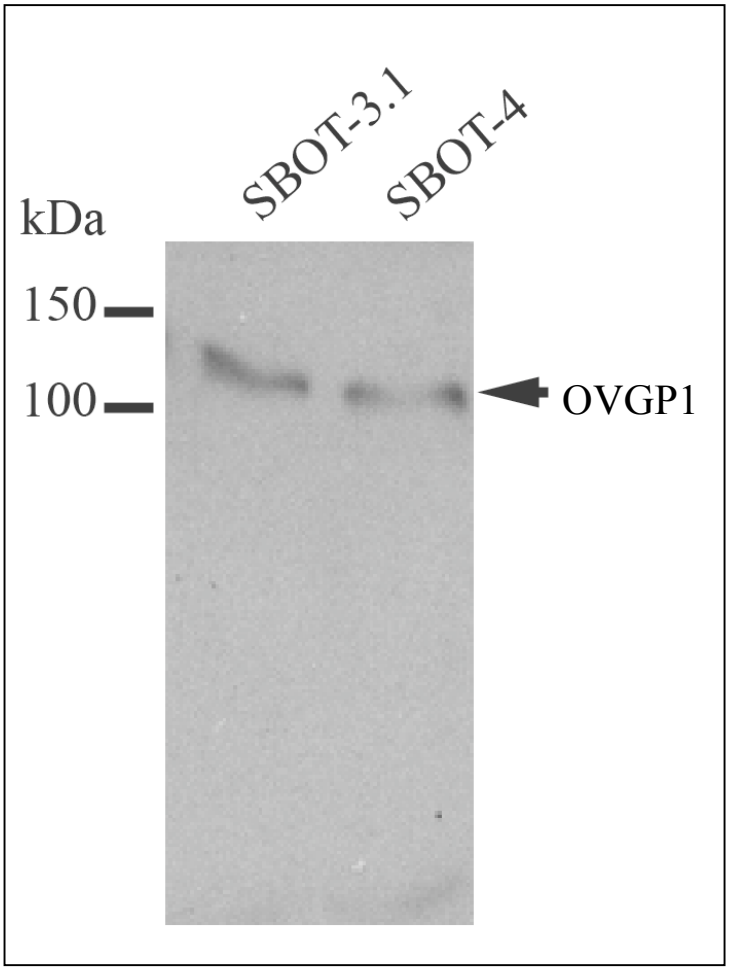

Fig. 12. SBOT cells secrete oviduct-specific glycoprotein (OVGP1), an indicator of early ovarian neoplasia. Conditioned media were collected from confluent cultures, concentrated, and analyzed by SDS-PAGE using a rabbit polyclonal antibody against OVGP1. A band between 110-130kDa is observed in both the SBOT-3.1 and SBOT-4 lines.

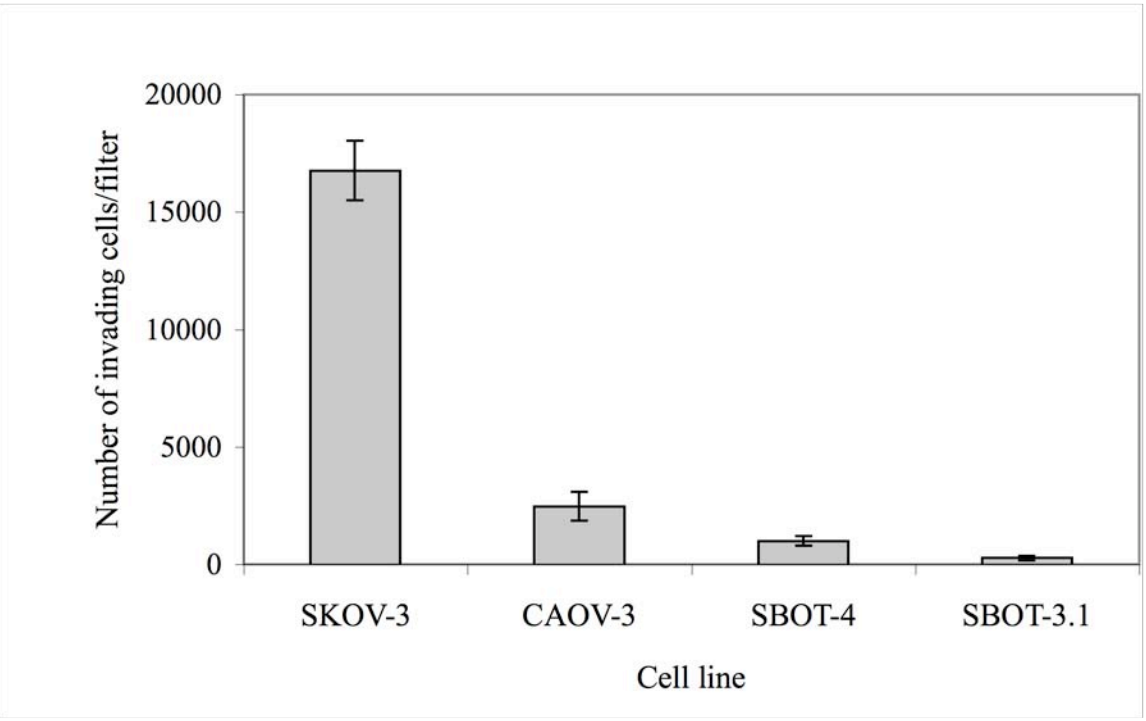

Fig. 13. Invasive capacity of SBOT cells in culture. SBOT cells have limited invasive capacity as compared to the invasive ovarian cancer cell lines, SKOV-3 and CAOV-3. SBOT-4 cells are slightly more invasive compared to the SBOT-3.1 cell line. SKOV-3 cells are highly invasive compared to the moderately invasive CAOV-3 line. Approximately 10^5 cells were plated onto Matrigel-coated Boyden chambers. After 24 h, the number of cells traversing the filter was determined by staining with Hoechst 33258. Values shown are the mean of the total number of cells per filter for triplicate transwells from one experiment and are representative of three separate experiments. Bars represent SD.

the wound area. Both SBOT lines migrated significantly less than the two ovarian cancer lines (Fig. 14).

3.1.5 Cultured SBOT cells secrete extracellular matrix degrading enzymes

To determine whether the inability to degrade the extracellular matrix contributed to the limited invasive phenotype of the SBOT cells, conditioned media were analyzed by Dr. Jaime Symowicz in the laboratory of Dr. M. Sharon Stack (Northwestern University Feinberg School of Medicine, Chicago, IL) for the expression and secretion of extracellular matrix degrading enzymes. Using gelatinase zymography, both the SBOT-3.1 and SBOT-4 cells expressed proMMP2 and proMMP9, which were both activated following treatment with the MMP activator APMA (Fig. 15). Slight differences in the gel mobility of proMMP9 in the control OVCA429 CM sample and SBOT samples were likely due to differential glycosylation of proMMP9 in the OVCA429 cells (Van den Steen *et al.*, 2001; Kotra *et al.*, 2002). SBOT-3.1 cells also expressed very low levels of active uPA, while uPA activity was at least 70X greater in the SBOT-4 cells (Fig. 15), perhaps contributing to their slightly increased invasiveness as shown in Fig. 13.

3.1.6 SBOT cells are anchorage dependent and are non-tumourigenic

As the SBOT-3.1 and SBOT-4 cells were derived from tumours which can progress to invasive carcinomas *in vivo,* they were tested for anchorage independence as an *in vitro* indicator of malignancy. Over three weeks, no colonies formed in soft agar indicating a continuiing requirement for growth factors and/or extracellular matrix components lacking in *in vitro* conditions, that are essential for anchorage-

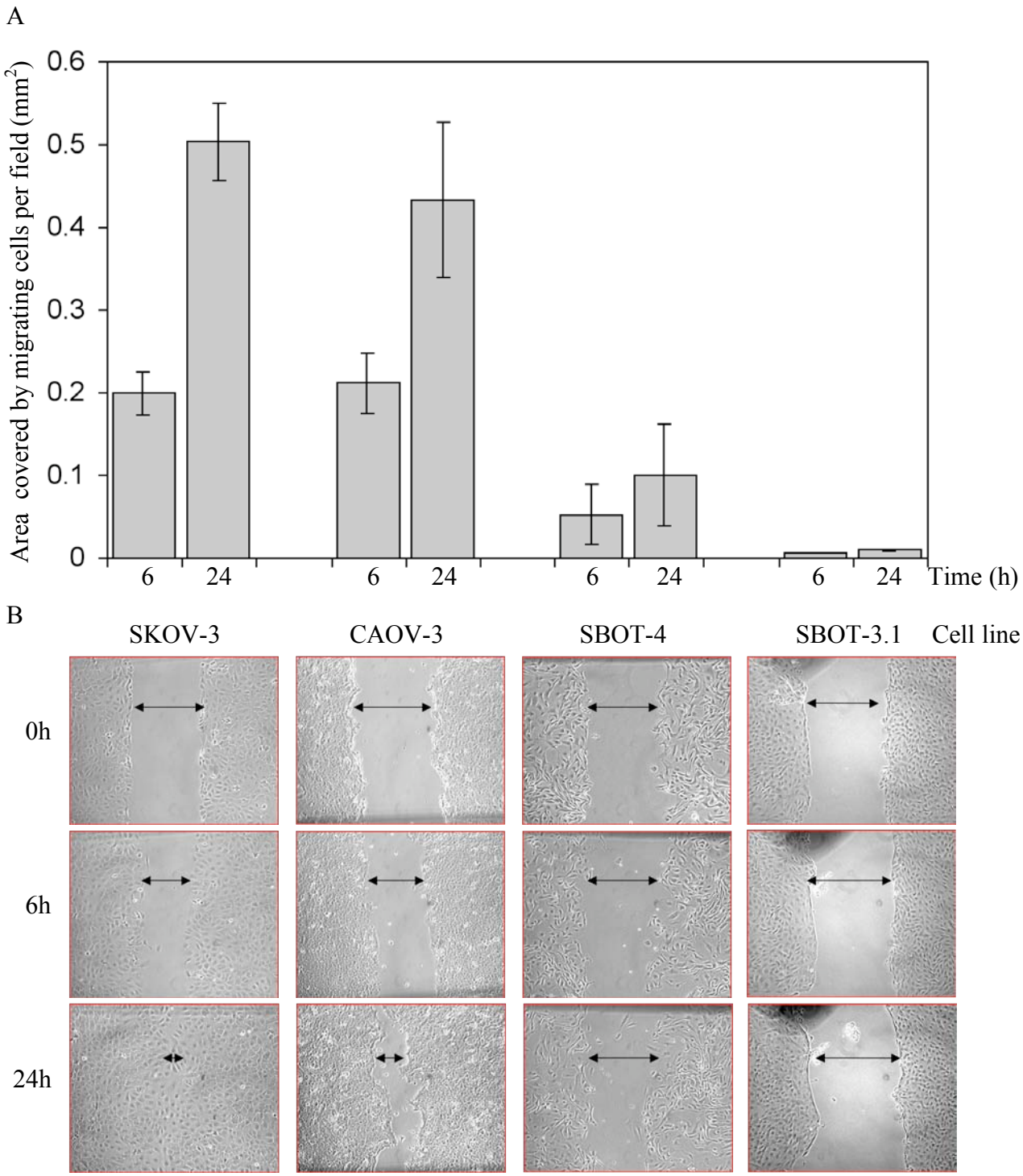

Fig. 14. Wound healing assay with cultured SBOT cells and ovarian cancer cell lines. (A) SBOT cells in culture have limited migratory capacity as compared to the ovarian cancer cell lines, SKOV-3 and CAOV-3. Values shown are the mean of the area covered by migrating cells per field measured from at least five fields per experiment, and are representative of three separate experiments. Bars represent SD. (B) Conflent monolayers cultured in 5% FBS were scratched using a micropipette tip. Photos were taken at the time of scratching (0 h) and, 6 h and 24 h later.

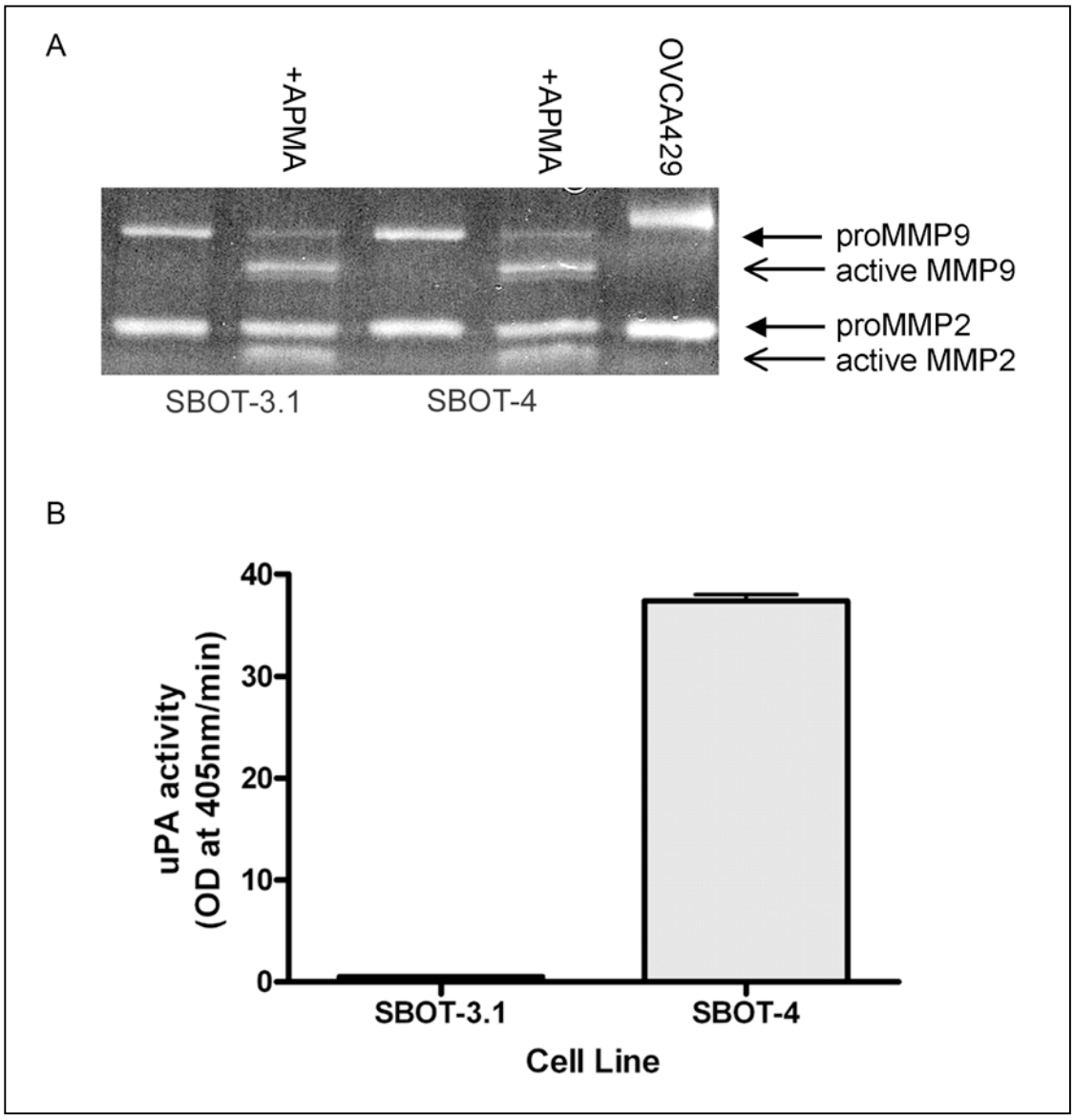

Fig. 15. Protease expression in cultured SBOT cells. (A*)*, expression of the pro-forms and active forms of MMP2 and MMP9 in SBOT cells. Conditioned media from an equal number of SBOT-3.1 and SBOT-4 cells were incubated with and without APMA and then analyzed via gelatin zymography. Conditioned media from the ovarian carcinoma cell line OVCA429 were used as a positive control. (B*)*, uPA activity. Conditioned media were analyzed for uPA activity using a coupled colorimetric plasminogen activation assay based on plasmin hydrolysis of VLKpNA.

independent growth. In addition, the SBOT-3.1 cell line was tested for tumor growth *in vivo*. Over six months, no tumours were observed in the 4 mice.

3.2 Effects of SV40 Early Region Genes on SBOT Cells

3.2.1 SV40 early region genes alter lifespan of SBOT cells

As described in Results Section 3.1, we established a cell/tissue culture model for SBOT by obtaining tissue specimens from women with serous borderline ovarian tumors (SBOT). As the lifespan of these cells in culture had not been previously characterized, we attempted to immortalize or to extend the lifespan of three SBOT lines by introducing the SV40 early region genes, large T (LT) and small t (ST) antigens, which generated lines ISBOT-1.5, -2.2 and -3.3, respectively (Fig. 16). LT exerts its effects by inactivating the cell cycle regulators and apoptosis regulators p53 and pRb, and thus, delays senescence-related growth suppression. However, inactivation of these pathways in the SBOT cells did not result in true immortalization, i.e. indefinite lifespan. Rather, ISBOT-1.5, ISBOT-2.2, and ISBOT-3.3, underwent 94, 56, and 80 population doublings, respectively, before undergoing senescence. Interestingly, one of the untransfected SBOT lines, SBOT-3.1, from which we obtained a pure population of epithelial cells, developed into a permanent line (>100 population doublings) without undergoing senescence or crisis. Inactivation of p53 and pRB induced a loss in their differentiated morphology. and thus, we set out to compare the phenotypic and functional characteristics of the SBOT lines to the SV40 LT/ST antigen-expressing lines.

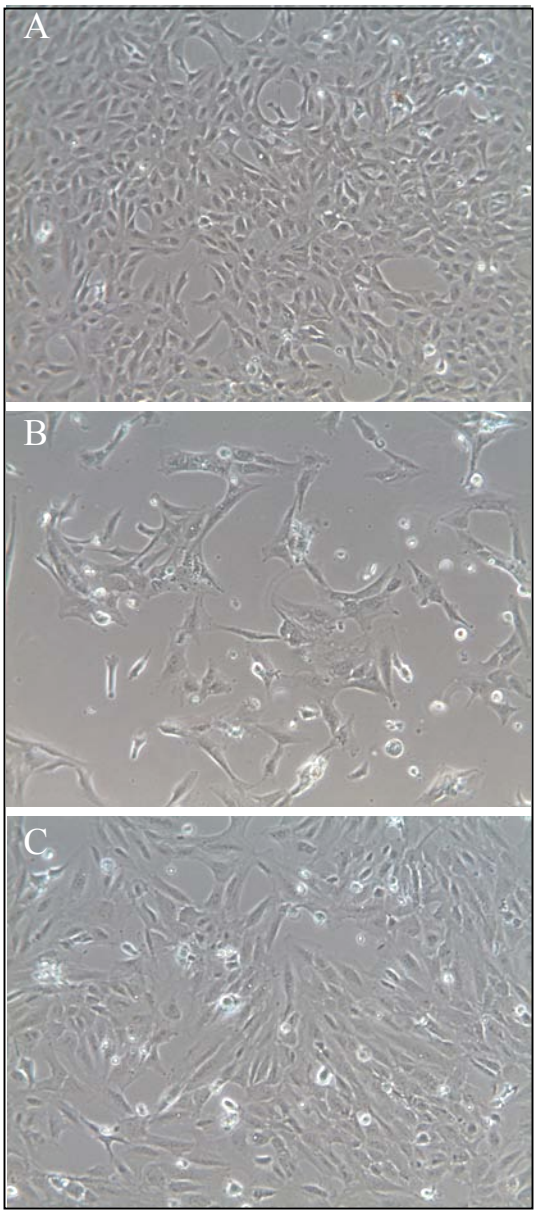

Fig. 16. SV40 early region genes induce a morphological change in the SBOT cells. The cells assume a more atypical and scattered morphology, characteristic of epithelial-mesenchymal transition. Phase photomicrographs of (A) ISBOT-1.5, (B) ISBOT-2.2, and (C) ISBOT-3.3 cell lines.

3.2.2 SV40 early region genes promote epithelio-mesenchymal transition in SBOT cells

Typically, as described in Section 3.1.1, cultured low-passage SBOT cells display an epithelial phenotype and maintain highly organized cell-cell adhesion and columnar-shaped cells, which resemble their characteristics *in vivo* (Fig. 7). However, with the introduction of SV40 LT and ST antigens, the characteristic whorls and tightly packed columnar epithelial cells were replaced by a more atypical and scattered morphology, which is suggestive of an epithelial mesenchymal transition (EMT) (Fig. 16). Such EMT is suggested to contribute to the dissemination of carcinoma cells from epithelial tumors, and therefore, may play an important role in the progression from borderline to invasive cancer (Thiery, 2002). Consequently, we examined molecular alterations associated with EMT. Immunostaining showed that the cells continued to express keratin, an indication of their epithelial origin, but lost the epithelial differentiation marker and adherens junction protein, E-cadherin (Fig. 17). We also observed complete loss of E-cadherin protein by immunoblotting (Fig. 18). In addition, while the SBOT cultures secreted significant levels of CA125, ranging from 304 kU/L to 10 000 kU/L (Table 7), none was detected in the conditioned medium from the ISBOT-1.5, -2.2, or -3.3 cell lines. In contrast, expression of the mesenchymal marker, N-cadherin, whose expression has been shown to correlate positively with EMT, was strongly induced (Fig. 17 and 18). Hence, both the morphological and molecular changes in the SV40 LT/ST-expressing cells demonstrated that these cells had undergone at least a partial EMT.

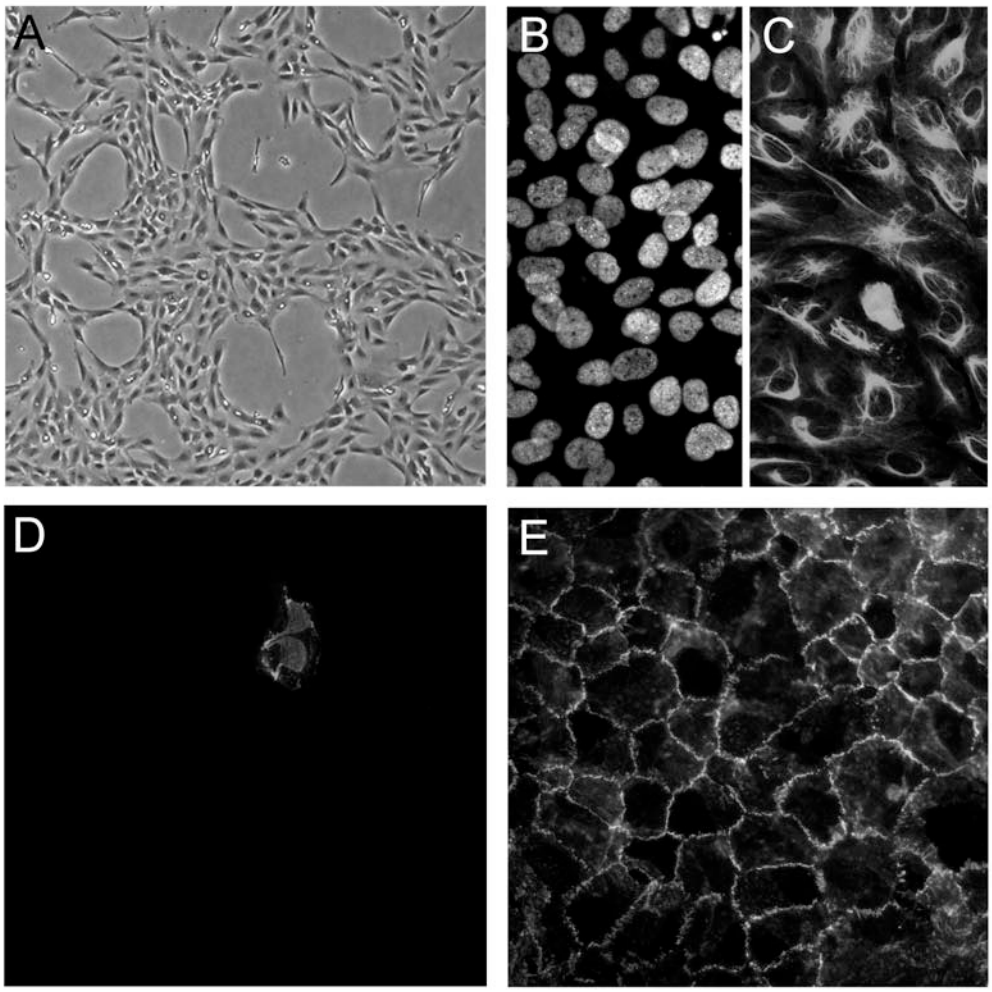

Fig. 17. Immunofluorescence staining for T-antigen, keratin, E- and N-cadherin in cultured SBOT cells transfected with SV40 early region genes. (A) Phase microscopy, (B) T-antigen, (C) keratin, (D) E-cadherin and (E), N-cadherin expression of SBOT-3 cells transfected with SV40 early region genes, ISBOT-3.3. These cells express T-antigen and retained the epithelial marker, keratin. SV40 early region genes induced the expression of N-cadherin concomitantly with a loss of E-cadherin expression.

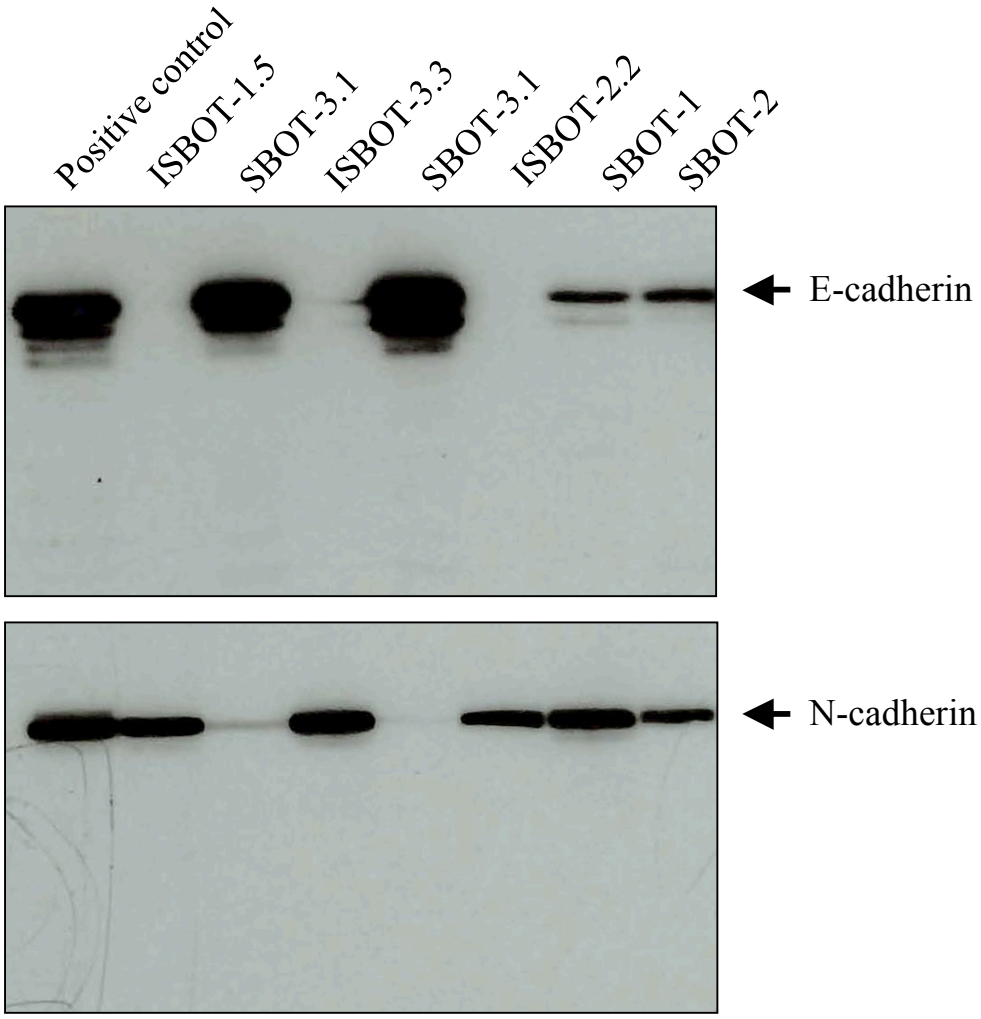

Fig. 18. Western blot analysis of E- and N-cadherin in SBOT cells transfected with SV40 early region genes. SV40 early region genes induced a switch from E- to N-cadherin expression in the SBOT cells. Western blot analysis of (A) E-cadherin and (B) N-cadherin expression in ISBOT and SBOT lines. E-cadherin positive control, OVCAR-3. N-cadherin positive control, IOSE-80pc. Note the expression of N-cadherin in SBOT-1 and -2 cells is most likely due to contamination by fibroblast cells as the majority of keratin-positive cells are N-cadherin negative (data not shown). An equal amount of protein was loaded in each lane.

3.2.3 SV40 early region genes increase invasiveness and cell motility of SBOT cells

Next, we wanted to determine whether the loss of epithelial but a gain in mesenchymal characteristics was associated with a gain in motility and invasiveness. We previously reported that many characteristics of SBOT, including their inability to invade, as observed clinically, were retained in culture. As shown in Fig. 19, all three SV40 LT/ST-transfected lines displayed a significant increase in the number of cells that invaded the ECM barrier in comparison to untransfected SBOT cells. In parallel, SV40 caused an increase in cell motility (Fig. 20). These results indicate that LT and/or ST antigen can induce an invasive and migratory behavior in SBOT cells, suggesting that SBOT cells have the potential to progress to invasive carcinoma and that signaling pathways altered by LT and/or ST can contribute to the phenotype of invasion.

3.2.4 SV40 early region genes are not associated with *in vivo* tumorigenicty but induce anchorage independence of SBOT cells

To determine whether the SV40 early region genes have transforming capabilities in SBOT cells *in vitro*, anchorage independence assays were performed. SBOT-3.1 and SBOT-4 cells were examined but did not form colonies in soft agar, whereas all three SV40-transfected cell lines acquired a significant degree of anchorage independence (Fig. 21). Next, we assessed whether SV40 early region genes can facilitate the transformation of SBOT cells *in vivo* by determining their ability to form tumours in SCID mice. We injected SBOT-3.1 and ISBOT-3.3 cells into the SCID mice but despite the ability for SBOT cells to grow and survive in patients, neither the permanent SBOT-3.1 line nor the ISBOT-3.3

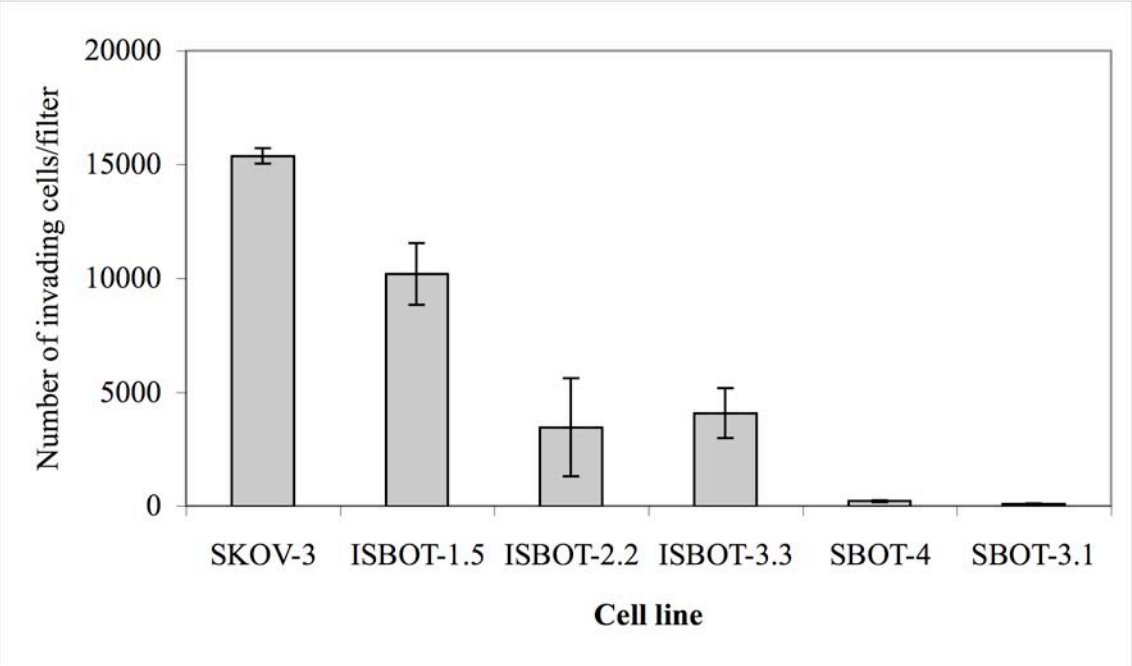

Fig. 19. Induction of invasion of SBOT cells by SV40 ER genes. ISBOT-1.5, -2.2, and -3.3 display varying degrees of invasiveness but are comparably more invasive than SBOT cells. Approximately 10^5 cells were seeded on Matrigel-coated Boyden chambers against a gradient of 10% FBS. After 24 h, the number of cells traversing the filter was determined by staining with Hoechst 33258. Values shown are the mean of the total number of cells per filter for triplicate transwells from one experiment and are representative of 3 individual experiments. Bars represent SD.

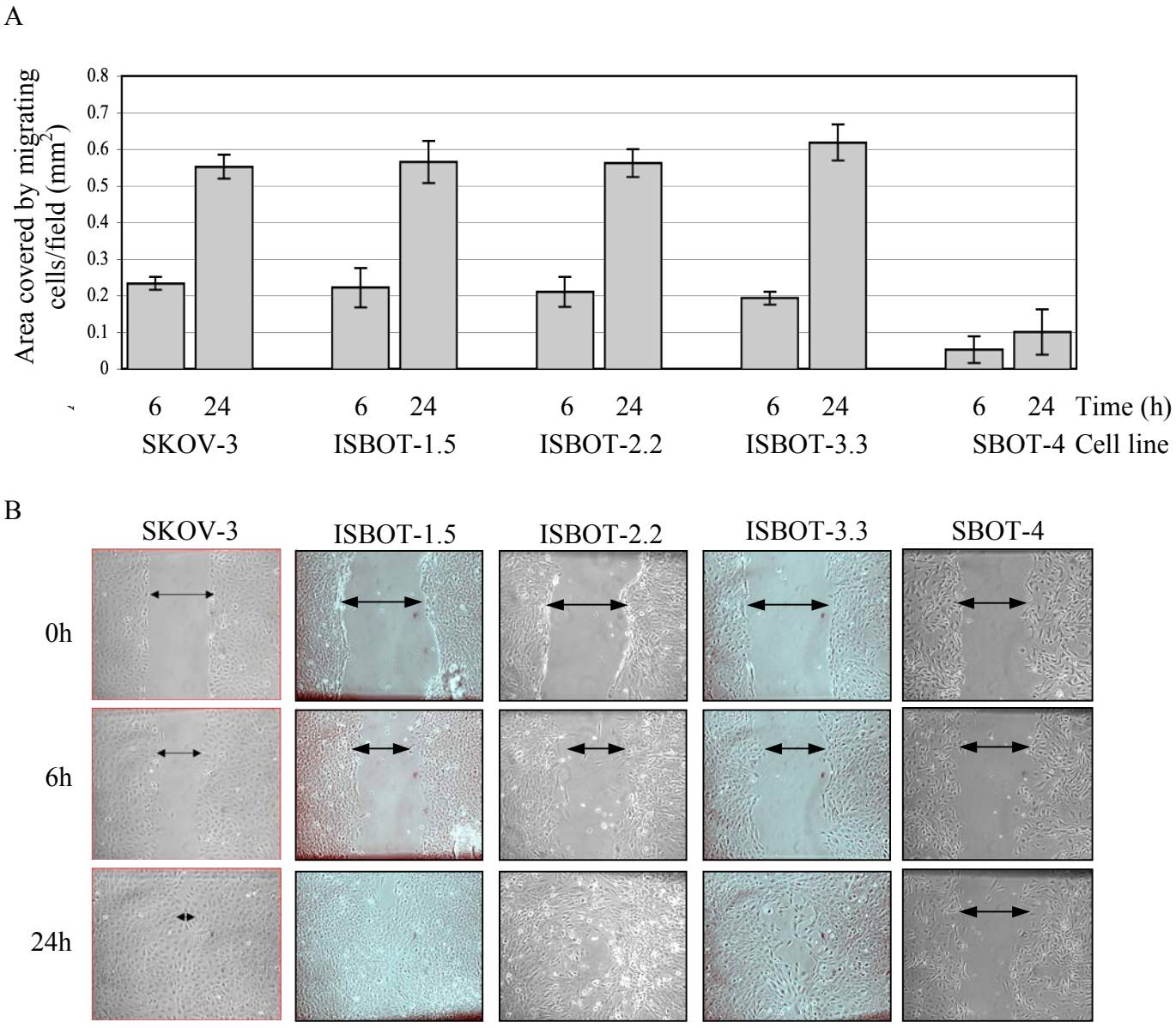

Fig. 20. SV40 early region genes increase the migratory capacity of SBOT cells. (A) Results of a wound healing assay with ISBOT cells. Values shown are the mean of the area covered by migrating cells per field measured from at least five fields and are representative of 3 independent experiments. Bars represent SD. (B) Confluent monolayers were scratched using a micropipette tip. Photos were taken at the time of scratching (0 h) and 6 h and 24 h later.

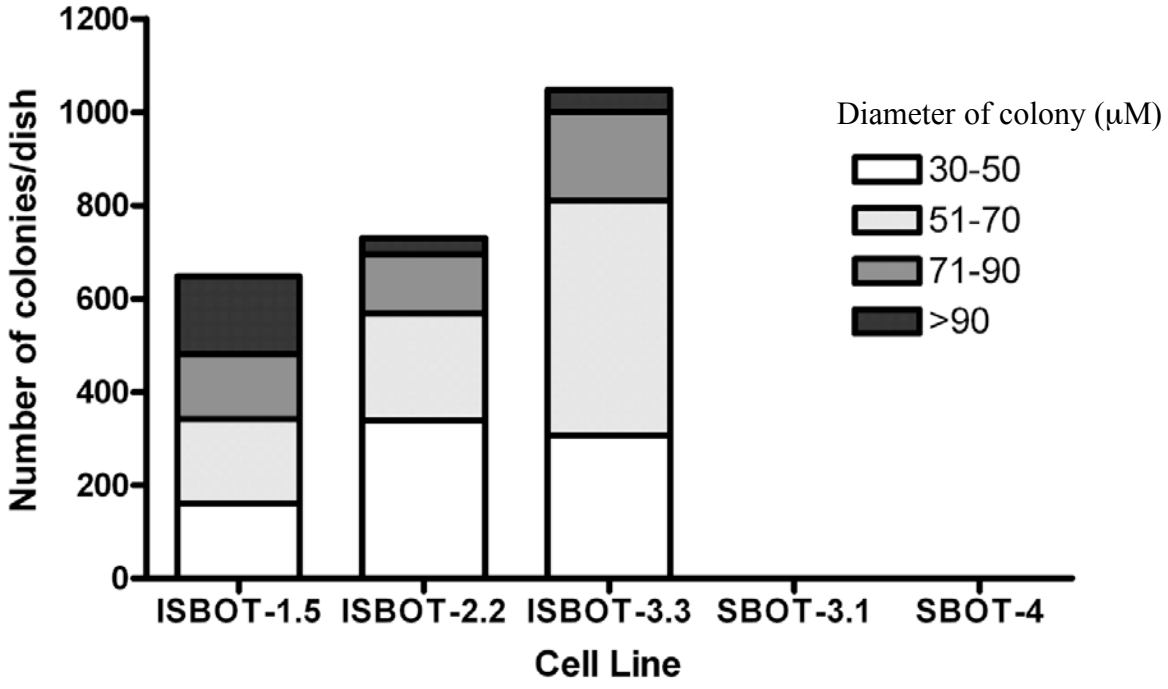

Fig. 21. Anchorage-independent growth of SBOT cells transfected with SV40 LT and ST antigens. All three ISBOT lines formed colonies in soft agar whereas neither the SBOT-3.1 nor SBOT-4 cultures were anchorage-dependent. Approximately 1.3 X 10^4 cells in 2 mL of complete medium with 0.33% agarose were suspended on top of 5.0 mL of solidified 0.5% agarose/medium in 60 mm culture dishes. Triplicate cultures for each cell type were maintained for 3 weeks at 37^{o}C in 5% CO_2/air with 2 mL of fresh medium added once a week. The colonies were then sized (μm) and counted. Values represent mean number of colonies from triplicate cultures in one experiment and are representative of three separate experiments.

cells developed into tumours in mice over 6 months.

3.2.5 Invasion and migration of SV40 LT/ST-transfected SBOT cells are not associated with a change in protease secretion

Since transfection with SV40 LT and ST antigens resulted in highly significant increases in motility and invasiveness, the conditioned media from the three ISBOT lines were analyzed for changes in MMP2, MMP9, and uPA activity, proteases important in ovarian cancer invasion. The three ISBOT cell lines all expressed different levels of proMMP2 (Fig. 22A) which were quantified by ELISA (Fig. 22B). ISBOT 2.2 cells expressed the most total MMP2 followed by the ISBOT 1.5 and ISBOT 3.3 cells, respectively. Similar trends were observed in the levels of uPA activity among these three immortalized cell lines (Fig. 22C). Levels of uPA activity in the ISBOT-2.2 cells were similar to that of SBOT-4 cells while ISBOT-1.5 and ISBOT-3.3 expressed little uPA similar to SBOT-3 cells. In addition, weak expression of proMMP9 could be detected in all cell lines. Both the SBOT-3 and SBOT-4 cell lines also expressed proMMP2 and proMMP9. Thus, in spite of the differences in levels of protease activity among the three ISBOT lines and their similarities to SBOT-3.1 and SBOT-4 lines, there does not seem to be a clear relationship between protease expression and invasive capability.

3.2.6. Overexpression of N-cadherin or suppression of E-cadherin expression in SBOT cells does not induce an invasive phenotype

As the introduction of SV40 LT and ST antigens to the SBOT cells caused a switch from E- to N-cadherin which was associated with an increase in invasion and

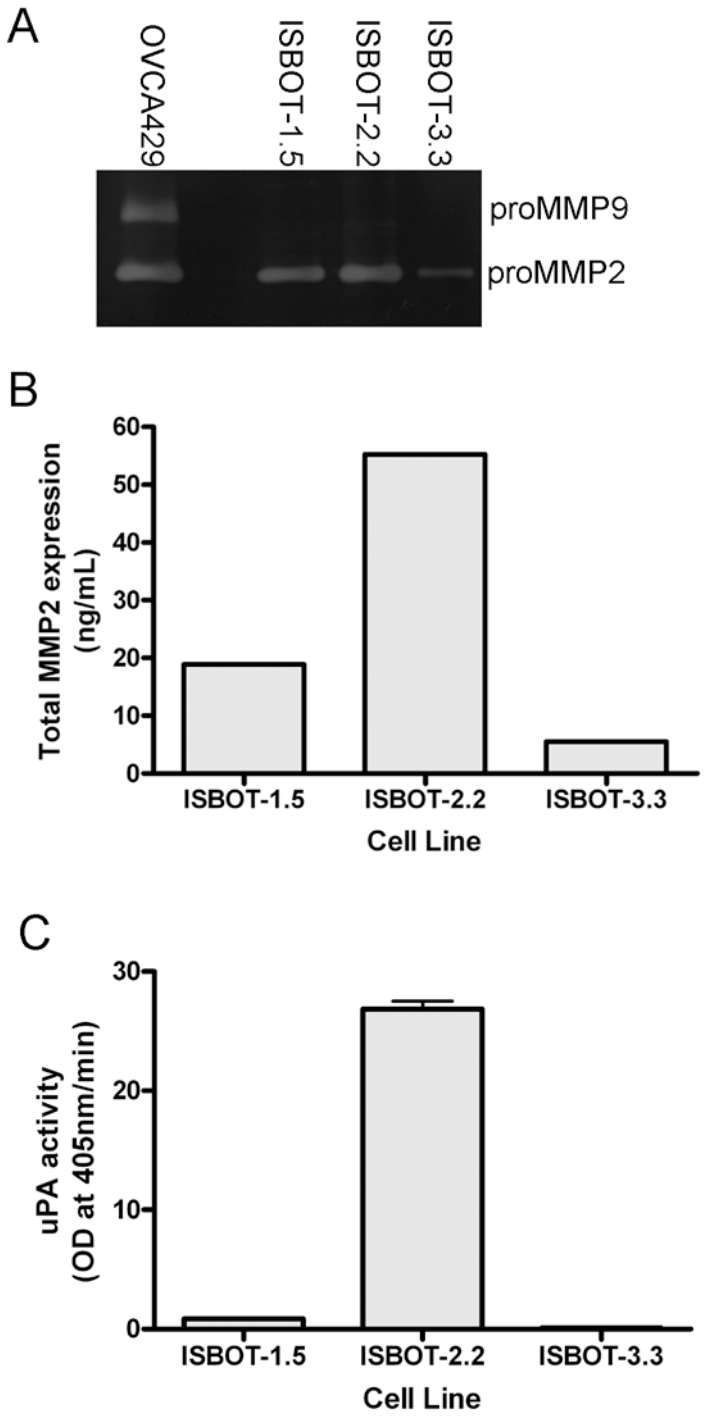

Fig. 22. Protease activity of SBOT cells transfected with SV40 LT and ST antigens. All three ISBOT lines secreted proMMP2 (A, B) while only line ISBOT-2.2 secreted uPA (C). Despite the variation in protease activity amongst the three ISBOT lines, all three lines were invasive. This is in contrast to SBOT cultures which are noninvasive. MMP-2 and MMP-9 were analyzed by gelatin zymography, total MMP2 was analyzed using the Quantikine MMP2 ELISA kit (R&D Systems), and net plasminogen activator activity was quantified using a coupled assay to monitor plasminogen activation, as indicated in the Materials and Methods.

motility, we investigated whether manipulation of their cadherin profile would alter their invasive potential, as has been reported for other epithelial cell types (Nieman *et al.*, 1999; Hazan *et al.*, 2000). To overexpress N-cadherin, we transiently expressed the gene in SBOT cells by adenoviral infection (Fig. 23). E-cadherin staining was unchanged as compared to the EGFP control. However, there was no significant increase in invasiveness in the N-cadherin overexpressing SBOT cells, indicating that such increased expression is insufficient to trigger invasiveness in these cells (Fig. 24). However, the epithelial colonies appeared to be more dispersed or dissociated after the introduction of N-cadherin, as observed in Fig. 23. This was also shown quantitatively as the internuclear distance was overall greater in the N-cadherin overexpressing group compared to the EGFP control (Fig. 25). In addition, disrupting the cell-cell adhesion by blocking the extracellular domain of E-cadherin with a neutralizing anti-E-cadherin antibody which is effective in dissociating C4-II epithelial colonies (Fig. 26), was also insufficient in inducing invasion of the SBOT cells (data not shown).

3.3 Oviduct-Specific Glycoprotein Expression in the Normal Ovary and Ovarian Cancer

3.3.1 Expression of oviduct-specific glycoprotein in the normal ovarian surface epithelium and epithelial inclusion cysts

A rabbit polyclonal antibody against human OVGP1 was generated and characterized previously by Rapisarda *et al.* (1993). As shown in Fig. 27, the antibody binds specifically to the epithelial cells of mid- and late-proliferative phase

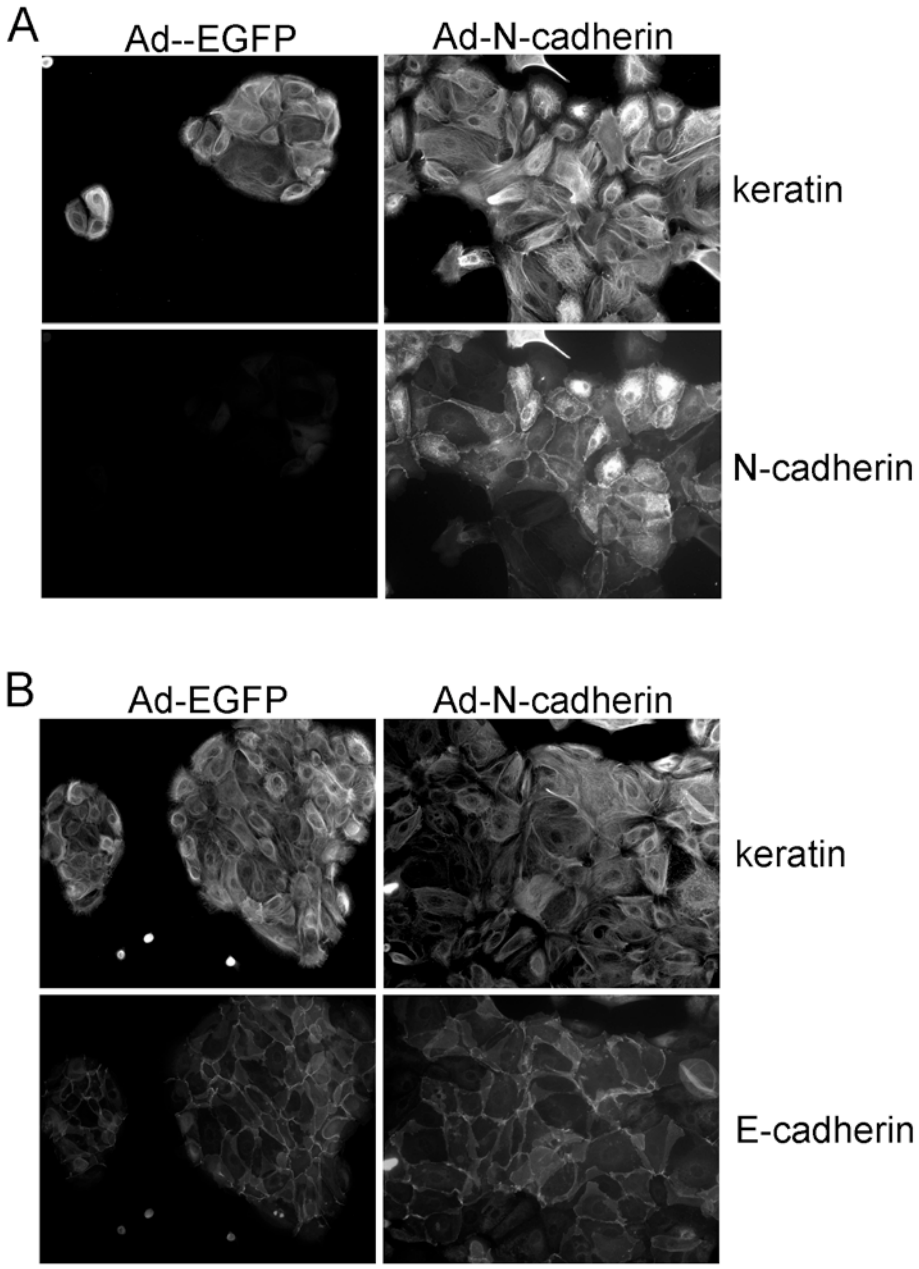

Fig. 23. Immunofluorescence staining for (A) N-cadherin and (B) E-cadherin expression of SBOT cells infected with EGFP control adenovirus or N-cadherin adenovirus. No change in E-cadherin or keratin was observed while abundant N-cadherin appeared following the overexpression of N-cadherin. Note the dispersed phenotype of the colonies in the Ad-N-cadherin infected cultures compared to the compact colonies of the Ad-EGFP infected cultures. For infection, cells were trypsinized, infected with recombinant adenoviruses (either EGFP-virus or N-cadherin virus) for 1 h in suspension, replated and cultured for 24-72 hours.

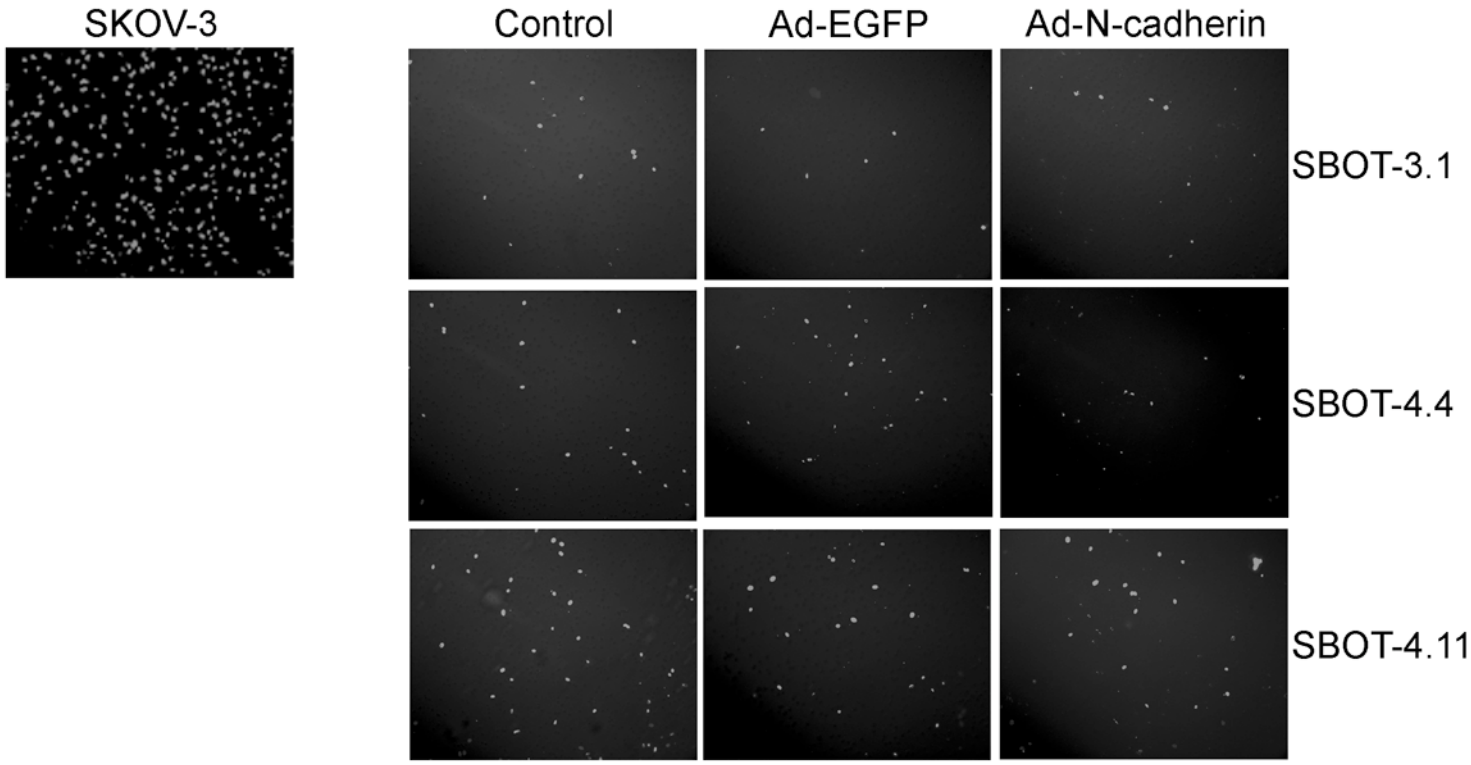

Fig. 24. Hoechst staining of invaded SBOT cells in Matrigel-coated Boyden chambers. Overexpression with N-cadherin adenovirus does not promote invasion of SBOT cells compared to control (no adenovirus) and EGFP adenovirus. Matrigel invasion assays were carried out 72 h post-infection. SKOV-3 cells are highly invasive.

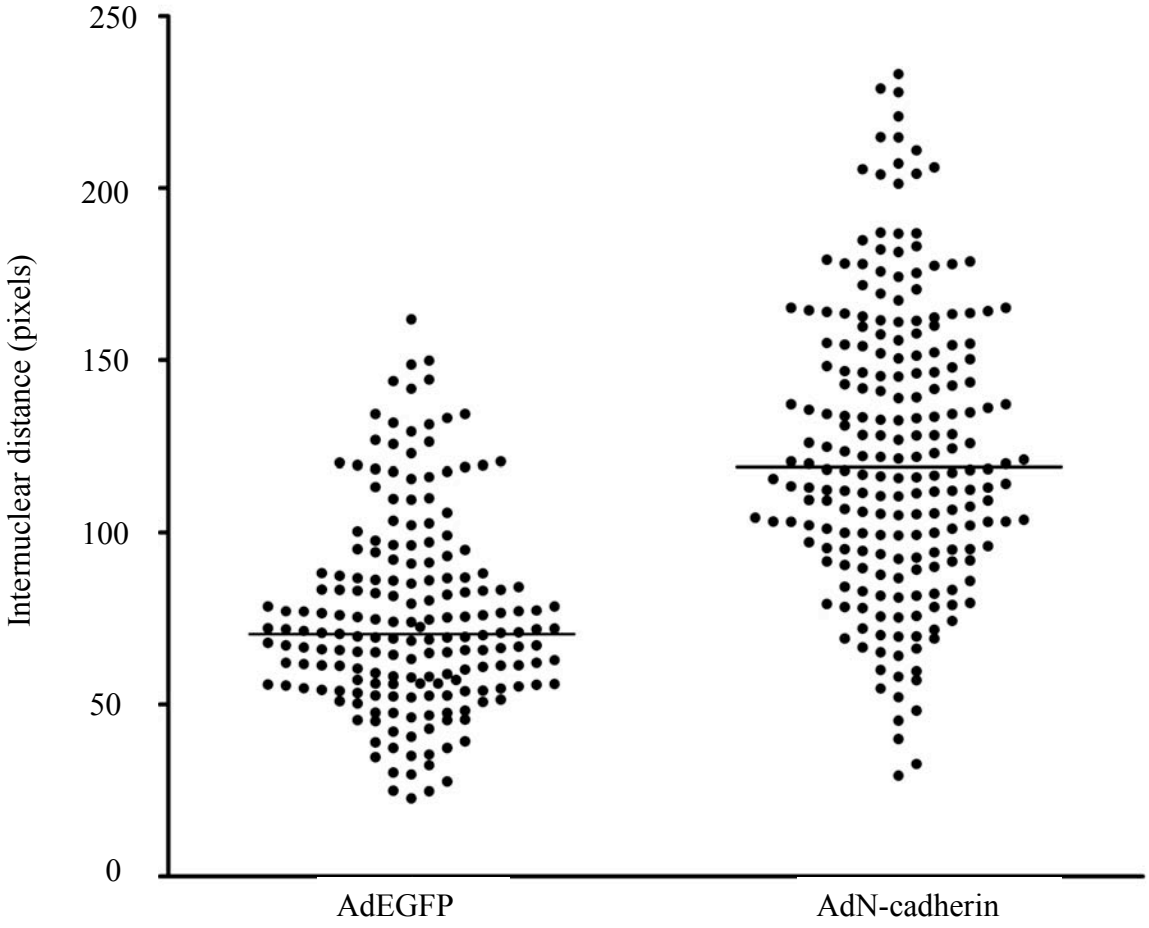

Fig. 25. Internuclear distance of SBOT cells infected with AdEGFP or AdN-cadherin. Overexpression of N-cadherin caused dissociation of the SBOT colonies as measured by their internuclear distances. Each point represents the internuclear distance between two adjacent cells measured in arbitrary units (pixels) using the Northern Eclipse 6.0 software. Bars represent the median of all internuclear distances measured in one experiment from at least 75 cells and are representative of 3 separate experiments.

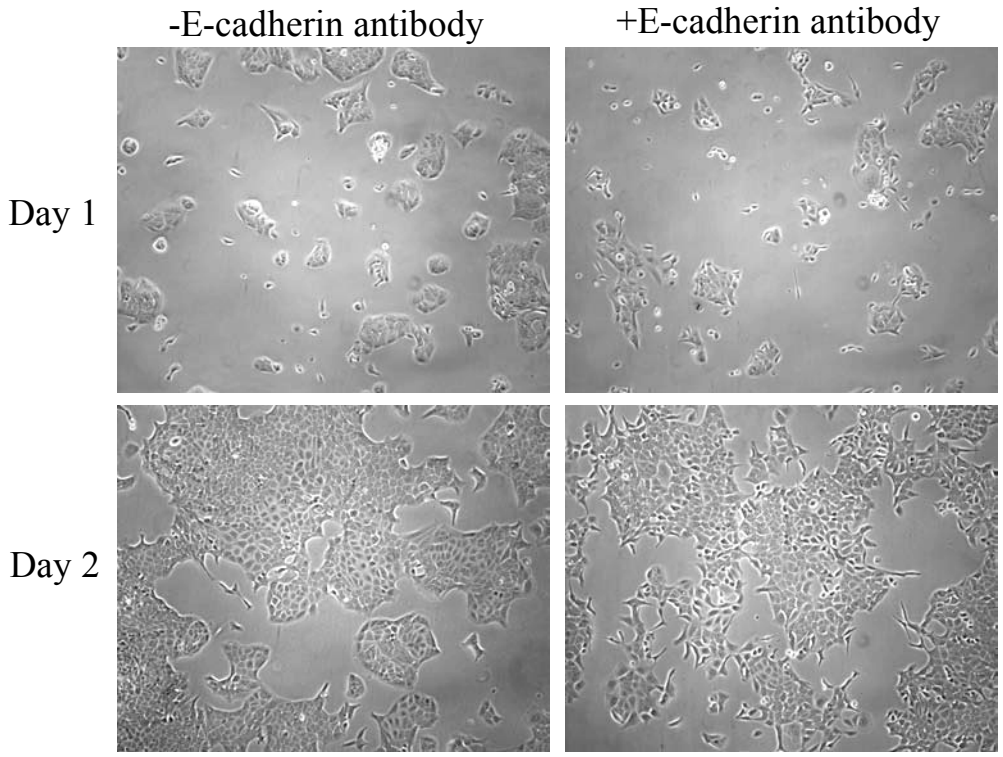

Fig. 26. Efficacy of the E-cadherin blocking antibody, MB2, as examined by cell dispersion of C4-II cells. Cells were trypsinized as small clusters and preincubated with or without the E-cadherin antibody, MB2, at a dilution of 1:15 for 20 minutes. After 1 day in culture, the contours of the colonies were more irregular in the cultures treated with the E-cadherin antibody. After 2 days in culture, there was extensive scattering of the cells in the antibody treated cultures suggesting that the antibody was effective in blocking E-cadherin.

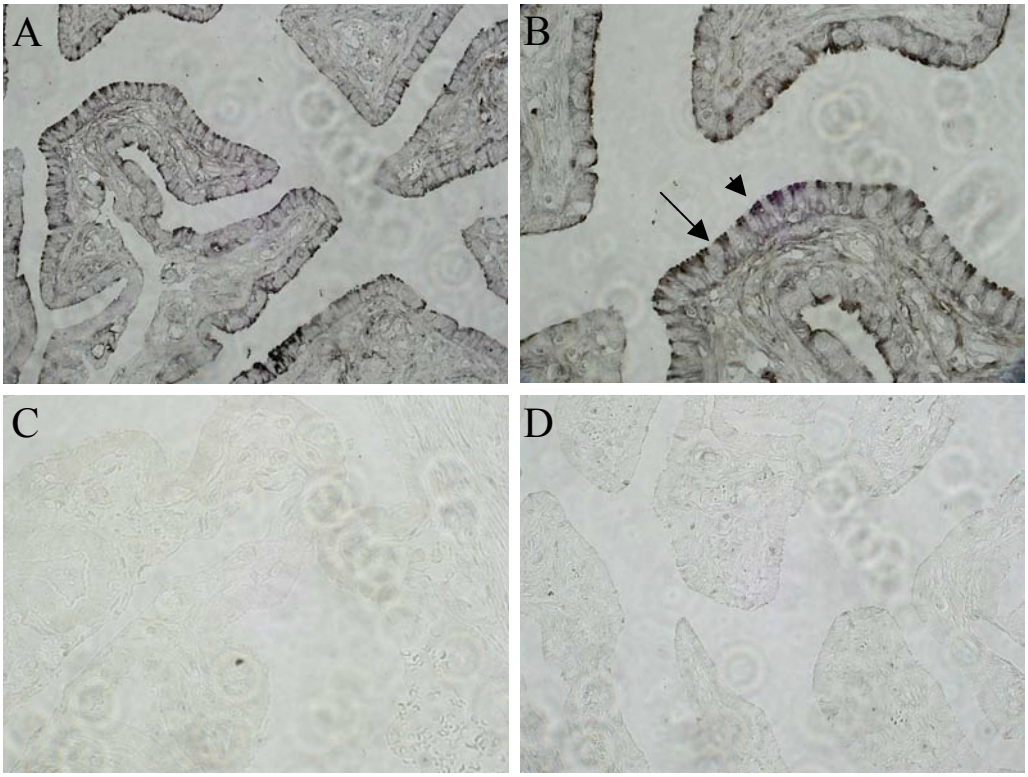

Fig. 27. Immunohistochemical staining of OVGP1 in the oviduct. OVGP1 is expressed in mid- to late- proliferative phase oviductal secretory epithelial cells (A, low power; B, high power) but absent in secretory phase oviductal epithelium (C), as detected by the rabbit polyclonal anti-human OGP antibody (Rapisarda *et al.*, 1993). Note the specific staining of the antibody in the secretory epithelial cells (arrowhead) and the absence of staining in the ciliated epithelial cells (arrow) and stroma. (D) No staining was observed in mid-proliferative phase oviduct incubated with pre-immune serum. Sections were incubated in primary antibody overnight at 4^{o}C and developed with DAB and nickel.

oviduct whereas it is absent in secretory phase oviduct. The staining is in the apical region of the secretory cells as opposed to the ciliated cells as observed in the mid-proliferative phase oviduct. In the late-proliferative phase oviduct, most of the staining appears to be outside of the cells suggesting that most of the OVGP1 has been secreted. No staining was observed in the stromal tissue.

No staining was observed in the connective tissue stroma or in the follicles of the ovarian cortex. OVGP1 was also absent in normal OSE (Fig. 28A,B). Of the 19 ovaries examined, 7 had 31 inclusion cysts. Staining for OVGP1 was intense in the cells and lumen of 22 epithelial inclusion cysts lined with metaplastic OSE (Fig. 28C,D), moderate in 6 inclusion cysts with cuboidal OSE (Fig. 28E,F), and absent in flat OSE from 3 inclusion cysts (Fig. 28G,H).

3.3.2 Expression of oviduct-specific glycoprotein in ovarian tumours

Histologic classification (WHO), grade (FIGO), and results of the OVGP1 analysis are given in Tables 8 and 9. Our analysis included 283 malignant ovarian adenocarcinomas, of which 50 were positively stained for OVGP1. Thus, most invasive ovarian carcinomas did not express OVGP1 (Fig. 29). Of the 50 positively staining tumours, 26 were serous, 9 were mucinous, 10 were endometrioid, 1 was undifferentiated, and 4 were clear cell carcinomas. No staining was observed in seromucinous, transitional cell, or Krukenberg carcinomas (one case each).

The majority of serous benign cystadenomas (13 of 14 cases, 93%) and serous borderline tumours (46 of 65 cases, 71%) (Fig. 30) were OVGP1 positive. Among invasive tumours, only 26 of 184 serous adenocarcinomas staining positively for OVGP1. These included 5 of 8 (63%) grade 1, 7 of 41 (17%) grade 2, and 14 of 134

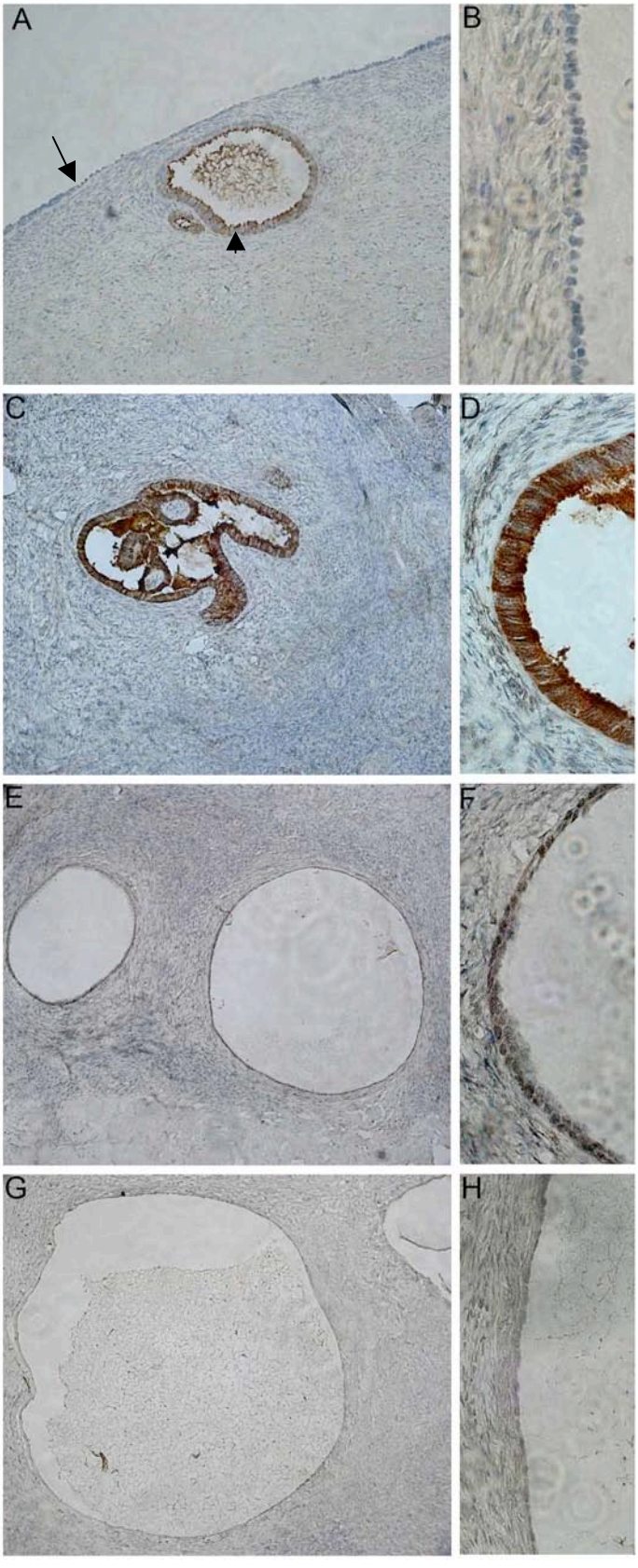

Fig. 28. Expression of OVGP1 in normal and metaplastic OSE. (A) OVGP1 is absent in normal OSE (arrow) but present in epithelial inclusion cysts (arrowhead) which have undergone tubal metaplasia. Note OVGP1 staining in the lumen of the cyst. (B) Higher-power image of normal OSE in A, arrow. (C, D) Metaplastic, (E, F) Cuboidal, and (G, H) Squamous OSE in epithelial inclusion cysts. D, F, and H are high-powered images of OSE-lined inclusion cysts of C, E, and G. Tissues were stained overnight at 4^{o}C with the polyclonal anti-HuOGP antibody, developed in DAB and counterstained with hematoxylin.

Table 8. OVGP1 expression in benign, borderline, and malignant ovarian tumours

Subtype	Positive/total	%
Serous		
Benign	13/14	93
Borderline	46/65	71
Malignant		
Grade 1	5/8	63
Grade 2	7/41	17
Grade 3	14/134	10
Total Malignant	26/183	14
Seromucinous		
Borderline	3/5	60
Malignant	0/1	0
Mucinous		
Benign	0/3	0
Borderline	7/14	50
Malignant		
Grade 1	6/9	67
Grade 2	2/2	100
Grade 3	1/4	25
Total Malignant	9/15	60
Endometrioid		
Borderline	1/5	20
Malignant		
Grade 1	3/13	31
Grade 2	3/16	19
Grade 3	4/10	40
Total Malignant	10/39	26
Undifferentiated		
Malignant		
Grade 2	1/2	50
Grade 3	0/7	0
Total Malignant	1/9	11
Clear cell		
Malignant		
Grade 2	1/1	100
Grade 3	3/33	9
Total Malignant	4/34	12
Transitional cell		
Malignant	0/1	0
Krukenberg		
Malignant	0/1	0

Table 9. Characteristics of OVGP1 immunohistochemical staining in ovarian carcinomas

Subtype	Positive/total no. of cases	%	Localization				Intensity				Percentage of positive cells/case					
			Apical		Cytoplasmic		Weak		Strong		<20%		20-80%		>80%	
Serous																
Grade 1	5/8	63	4/5	80	1/5	20	2/5	40	3/5	60	3/5	60	2/5	40	0/5	0
Grade 2	7/41	17	5/7	71	2/7	29	2/7	29	5/7	71	1/7	14	5/7	71	1/7	14
Grade 3	14/134	10	9/14	64	5/14	36	5/14	36	9/14	64	8/14	57	6/14	43	0/14	0
Total	26/184	14	18/26	69	8/26	31	9/26	35	17/26	65	12/26	46	13/26	50	1/26	4
Mucinous																
Grade 1	6/9	67	4/6	67	2/6	33	1/6	17	5/6	83	1/6	17	2/6	33	3/6	50
Grade 2	2/2	100	2/2	100	0/2	0	0/2	0	2/2	100	1/2	50	0/2	0	1/2	50
Grade 3	1/4	25	0/1	0	1/1	100	1/1	100	0/1	0	0/1	0	0/1	0	1/1	100
Total	9/15	60	6/9	67	3/9	33	2/9	22	7/9	78	2/9	22	2/9	22	4/9	56
Endometrioid																
Grade 1	3/13	31	3/3	100	0/3	0	0/3	0	3/3	100	3/3	100	0/3	0	0/3	0
Grade 2	3/16	19	2/3	67	1/3	33	2/3	67	1/3	33	1/3	33	1/3	33	1/3	33
Grade 3	4/10	40	0/4	0	4/4	100	4/4	100	0/4	0	0/4	0	0/4	0	4/4	100
Total	10/39	26	5/10	50	5/10	50	5/10	50	5/10	50	4/10	40	1/10	10	5/10	50

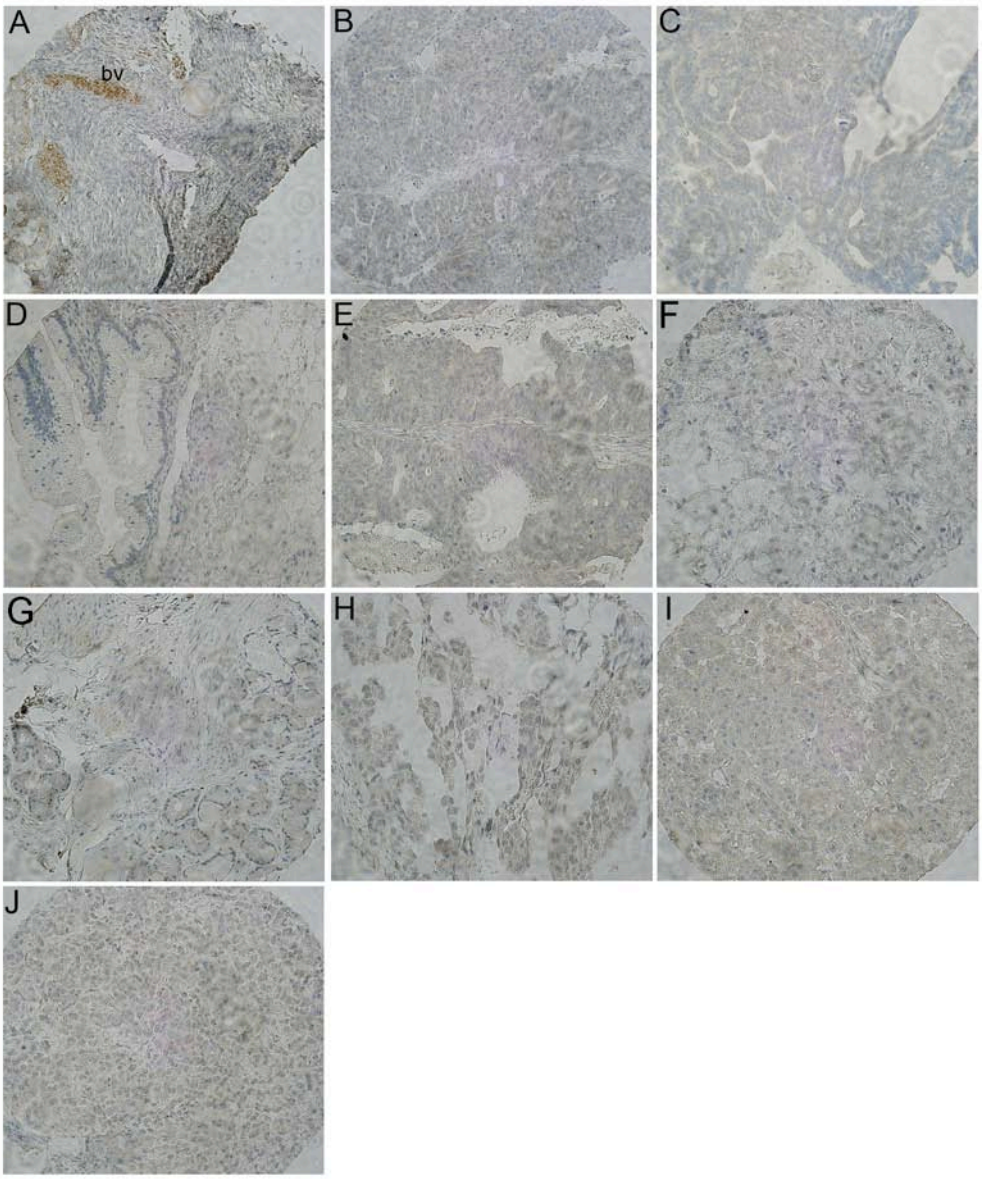

Fig. 29. OVGP1 is absent in most invasive ovarian cancers and in some non-invasive ovarian tumours. The following are examples of negative OVGP1 staining in both epithelial (A-E) and non-epithelial ovarian tumours (F-J): (A) Serous borderline ovarian tumour. Note non-specific staining of red blood cells in blood vessels, bv. (B) Serous carcinoma, Grade 3, (C) Serous carcinoma, Grade 2, (D) Benign mucinous cystadenoma, (E) Endometrioid carcinoma, Grade 3, (F) Malignant teratoma, (G) Benign germ cell tumour, (H) Malignant yolk sac tumour, (I) Malignant cord stromal, steroid cell tumour and, (J) Malignant cord stromal, granulosa cell tumour. Tissues were stained overnight at 4^{o}C with the polyclonal anti-HuOGP antibody, developed in DAB and counterstained with hematoxylin.

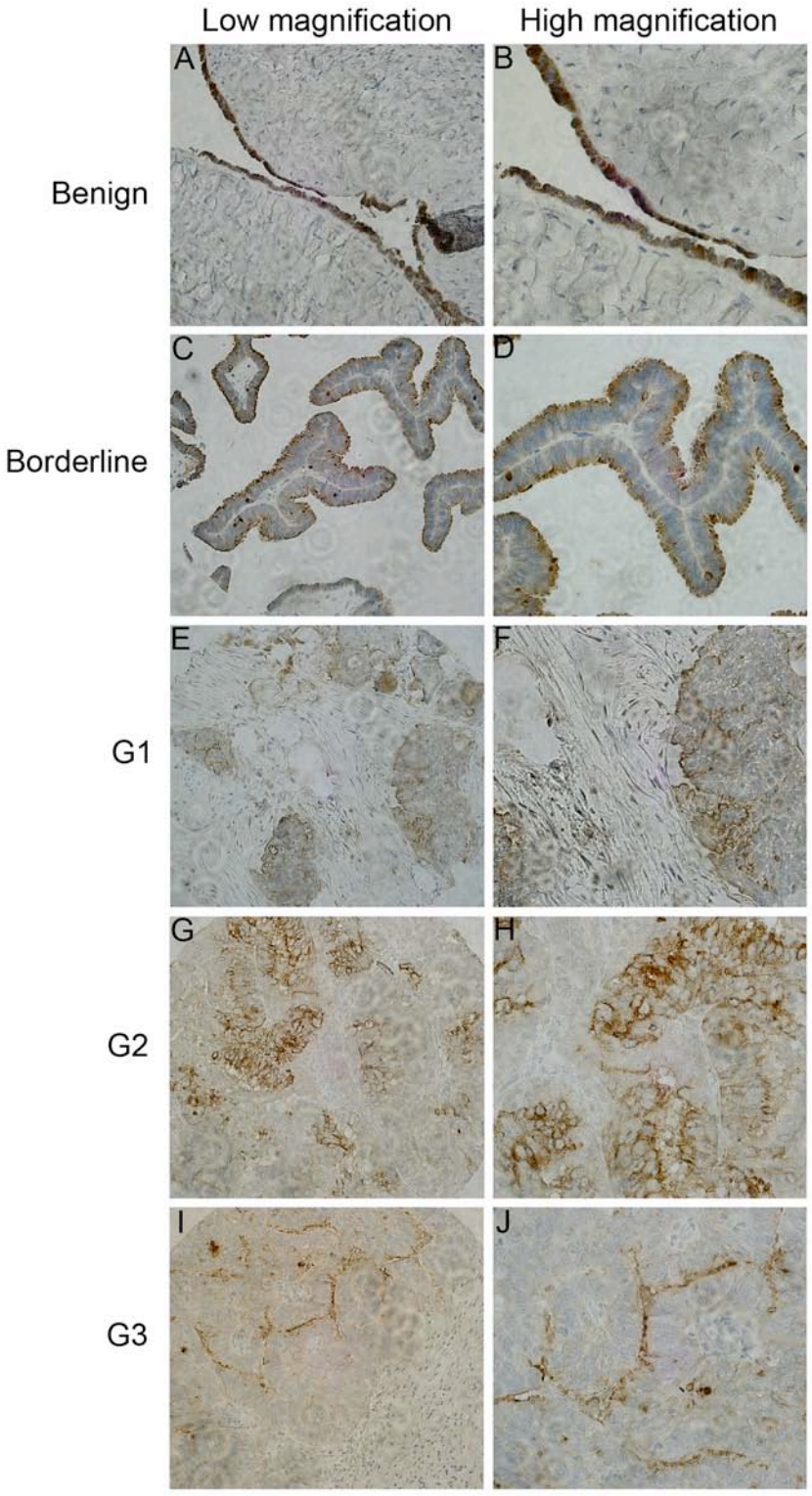

Fig. 30. Expression of OVGP1 in serous ovarian tumours. (A, B) Benign cystadenoma, (C, D) Borderline, (E, F) Grade 1, (G, H) Grade 2, and (I, J) Grade 3. The majority of benign, borderline and Grade 1 serous tumours are positively stained for OVGP1 compared to high-grade serous tumours. B, D, F, H and J are higher power images of A, C, E, G and I. Tissues were stained overnight at 4^{o}C with the polyclonal anti-HuOGP antibody, developed in DAB and counterstained with hematoxylin.

(10%) grade 3 serous carcinomas (Fig. 30). In addition, OVGP1 was also present in borderline and low-grade mucinous tumours but absent in three mucinous cystadenomas (Fig. 31). About 25% of the endometrioid borderline and malignant tumours also expressed OVGP1 (Fig. 32).

In most of the positively stained tumours, OVGP1 staining was apical, sometimes with evidence of secretion. All of the epithelial cells were positively stained for OVGP1 in serous borderline tumours and in all but one benign serous cystadenoma, while the percentage of positive cells in the carcinoma tissues varied (Table 9). Connective tissue in the tumour tissues did not stain.

3.4 Expression of Oviduct-Specific Glycoprotein in Other Normal Tissues and Cancers

No reactivity was found in 41 types of normal tissues, while the oviduct, as described previously, and the mucus-secreting epithelia of salivary gland, duodenum, and ileum reacted weakly with the antibody. In a multi-tumour tissue array, 46 types of nongynecologic neoplasms were OVGP1 negative (Fig. 33). Among other gynecologic carcinomas, 3 of 56 (5%) endometrial carcinomas and 2 of 47 (4%) cervical carcinomas were positive for OVGP1 while all 11 carcinomas of the vulva were negative.

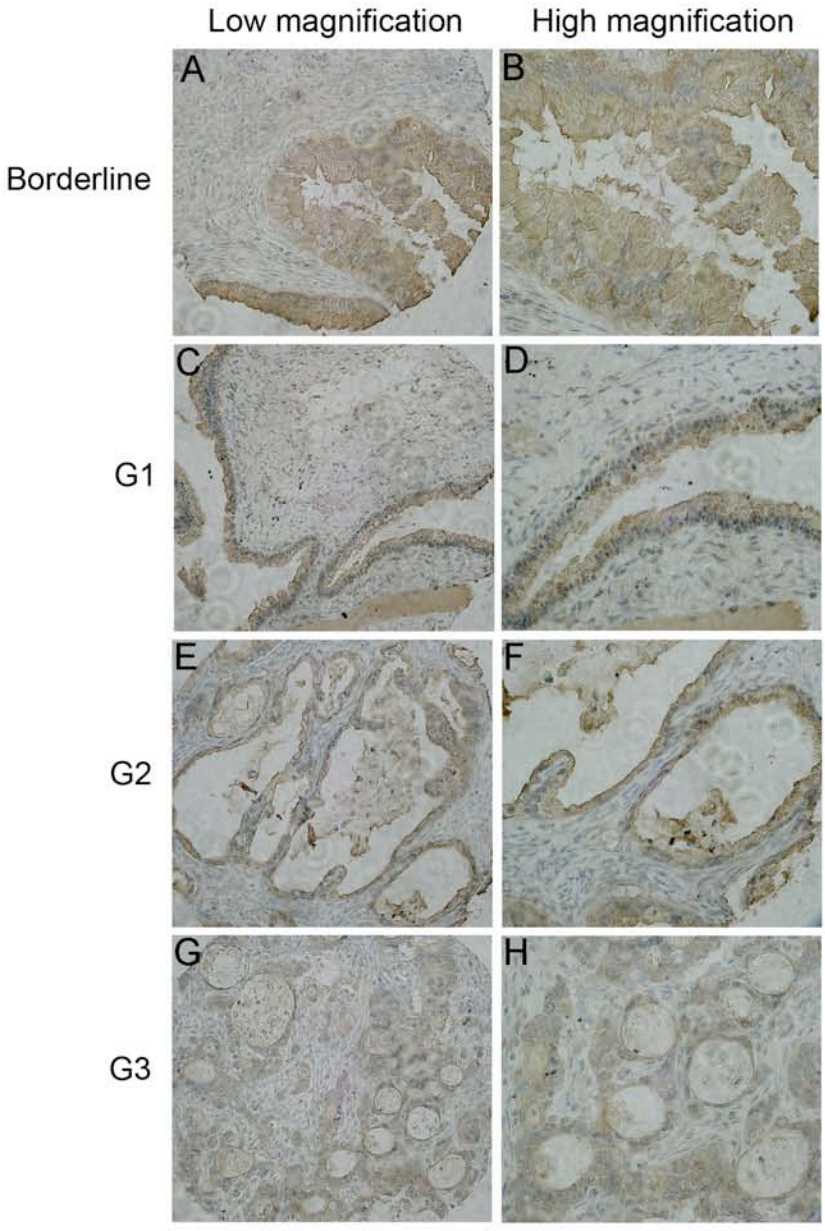

Fig. 31. Expression of OVGP1 in mucinous ovarian tumours. (A, B) Borderline, (C, D) Grade 1, (E, F) Grade 2, and (G, H) Grade 3. Seven of 14 borderline, 6 of 9 Grade 1, 2 of 2 Grade 2, and 1 of 4 Grade 3 mucinous tumors positively stained for OVGP1. B, D, F, H and J are higher power images of A, C, E, G and I. Tissues were stained overnight at 4^{o}C with the polyclonal anti-HuOGP antibody, developed in DAB and counterstained with hematoxylin.

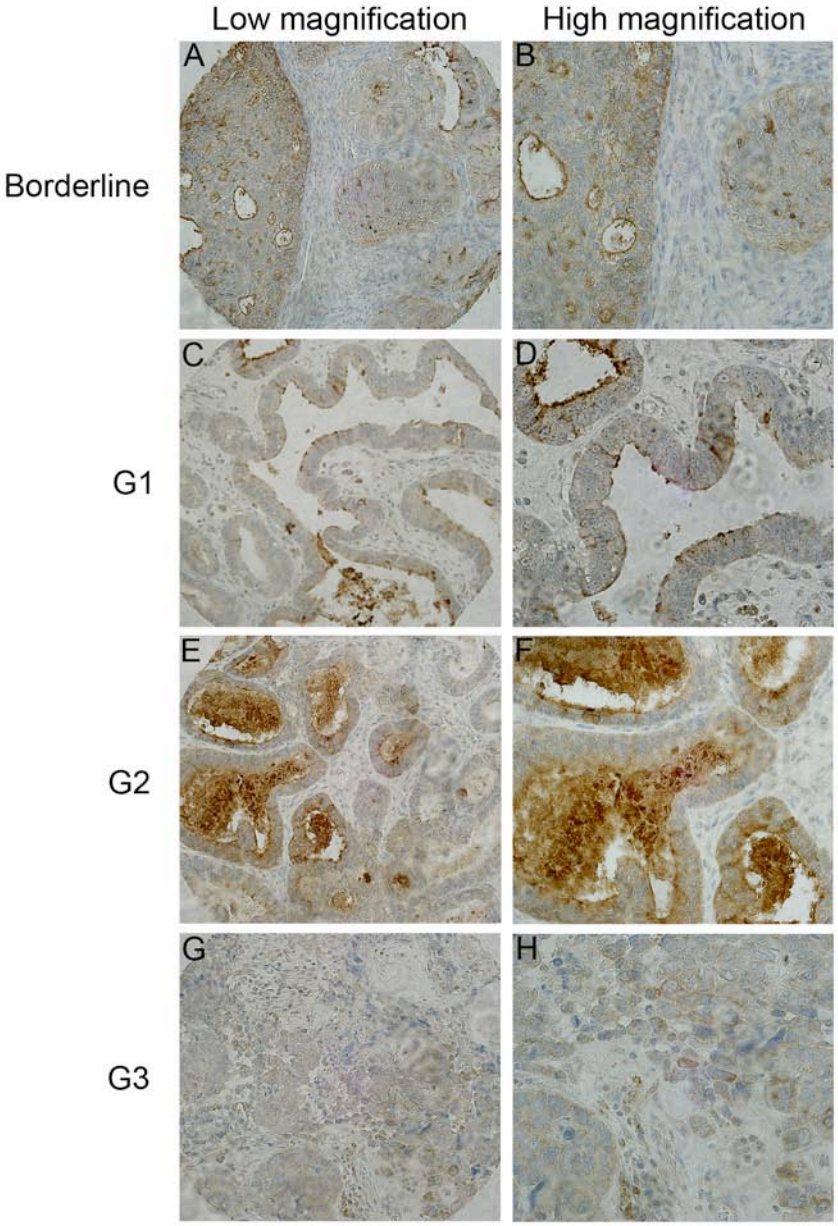

Fig. 32. Expression of OVGP1 in endometrioid ovarian tumours. (A, B) Borderline, (C, D) Grade 1, (E, F) Grade 2, (G, H) Grade 3, and (I, J) Grade 3. B, D, F, and H are higher power images of A, C, E, and G. Tissues were stained overnight at 4^{o}C with the polyclonal anti-HuOGP antibody, developed in DAB and counterstained with hematoxylin.

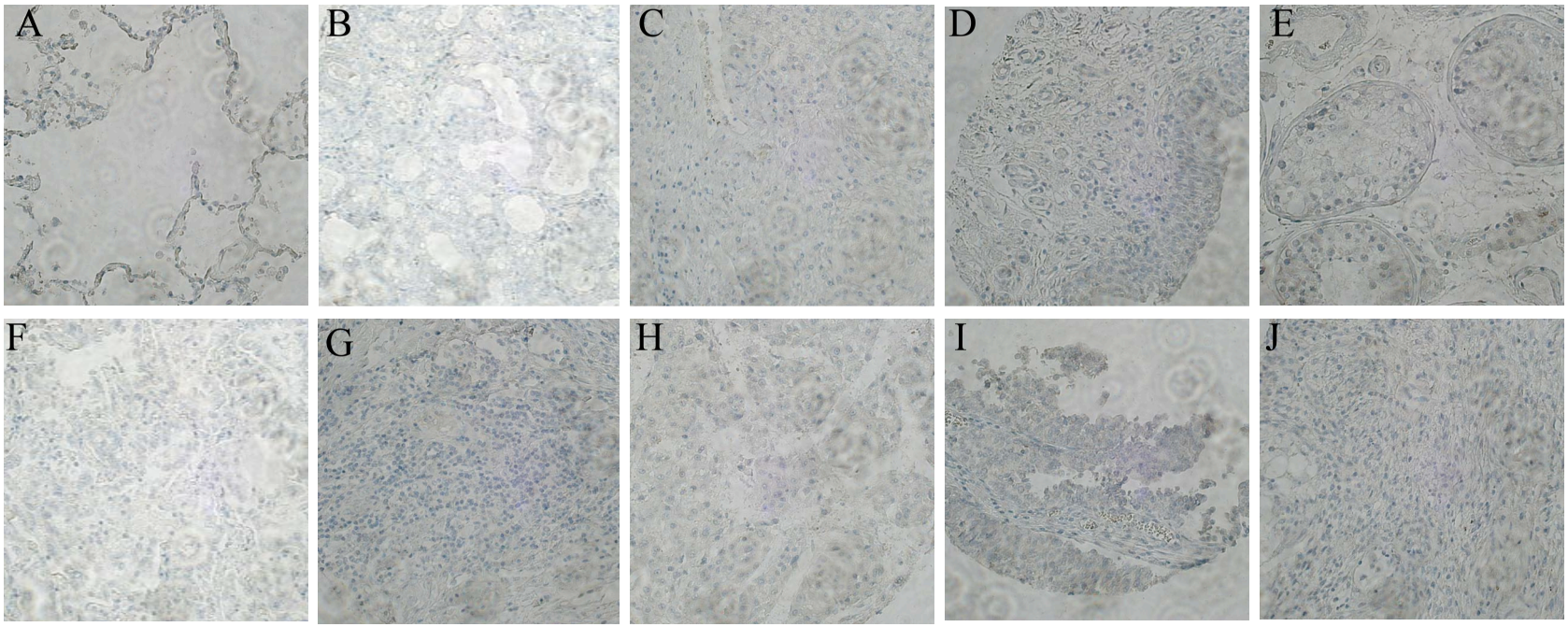

Fig. 33. OVGP1 was absent in most other normal tissues and their malignant counterparts. Examples of such tissues include: (A) Lung, (B) Breast, (C) Liver, (D) Bladder, (E) Testis. (F-J) are the corresponding malignancies of (A-E).

3.5 Detection of Oviduct-Specific Glycoprotein in Serum From Women With Ovarian Cancer

Immunohistochemical staining of ovarian carcinomas suggested that OVGP1 may be secreted and thus, may be a potential serum marker. Therefore, a monoclonal antibody against OVGP1 was produced in collaboration with Dr. Robert Molday (University of British Columbia, Vancouver, BC) to develop a serum-based assay.

3.5.1 Production of oviduct-specific glycoprotein

To generate the monoclonal antibody, OVGP1 was overexpressed in a mammalian culture system. The overexpression of OVGP1 was first tested using attached HEK-293 cells. The OVGP1 cDNA was tagged with 6x histidine to allow for purification of the protein from the conditioned medium using cobalt columns, initially, for use as the antigen in monoclonal antibody production. However, a successful clone was ultimately produced through the use of OVGP1 protein fragments generated as E. coli expressed fusion proteins. As conditioned medium containing OVGP1 was used by us for testing the clones, its production and optimization of expression will be described. Using an antibody against 6x-histidine, it was shown that OVGP1 was secreted into the conditioned medium of HEK-293 cells at the correct molecular weight of 110-130 kDa as compared to vector controls and untransfected HEK-293 cells (Fig. 34). The anti-histidine antibody also detected a lower sized band, at approximately 75 kDa, in the cell lysate of OVGP1-6xHis transfected HEK-293 cells. This band most likely corresponds to the unglycosylated form of the protein. The polyclonal anti-human

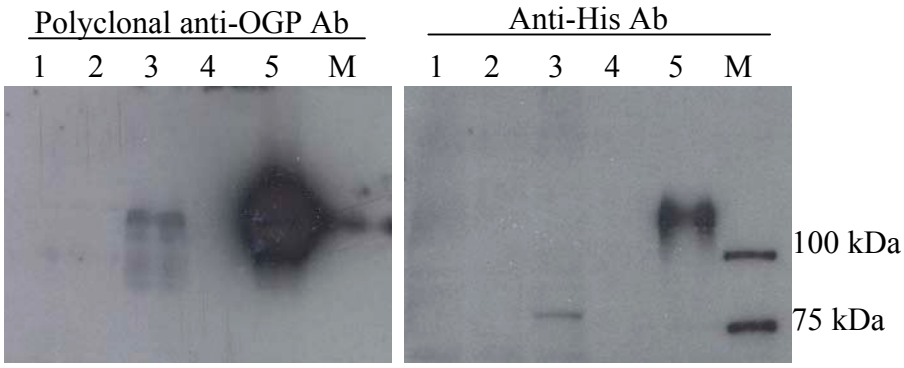

Fig. 34. Expression of OVGP1 in the cell lysate and conditioned medium of HEK-293 cells transfected with OVGP1-6xHis cDNA. Lane 1, untransfected cell lysate; 2, control vector transfected cell lysate; 3, OVGP1-6xHis transfected cell lysate; 4, control vector transfected conditioned medium; 5, OVGP1-6xHis transfected conditioned medium; M, His ladder. By immunoblotting, the polyclonal anti-OGP Ab recognizes a band at approximately 110-130 kDa while the anti-His Ab also recognizes a lower band at approximately 75 kDa in cell lysates which may be the unglycosylated form of the protein.

OGP antibody detected only the glycosylated form of the antibody as the bands appear only at 110-130kDa. The polyclonal antibody also appears to be very sensitive as it can detect the glycosylated form of the protein in the cell lysates which was not detected by the anti-histidine antibody (Fig. 34).

A cell suspension approach was subsequently used which allows for greater amounts of protein to be produced in a smaller volume. To optimize the amount of protein secreted into the conditioned medium of HEK-293F cells (suspension cultures), conditioned medium was collected and fresh medium was replaced every day for 5 days or samples were collected every day over a period of five days to see if the protein can be accumulated in the conditioned medium. As observed in Fig. 35, collecting the conditioned medium and replacing with fresh medium every day yielded larger quantities of OVGP1, as detected using the anti-His antibody.

As Dr. Robert Molday's lab developed the Rho tag and the antibody against the tag (Rho), the OVGP1 gene was tagged with Rho which was used for transfection of HEK-293F cells. OVGP1 can be detected in all the different batches of conditioned medium using the both Rho-1D4 antibody (Fig. 36) and the polyclonal anti-human OGP antibody (data not shown). The conditioned medium was subquently used for testing of the hybridomas to determine which clones could recognize OVGP1.

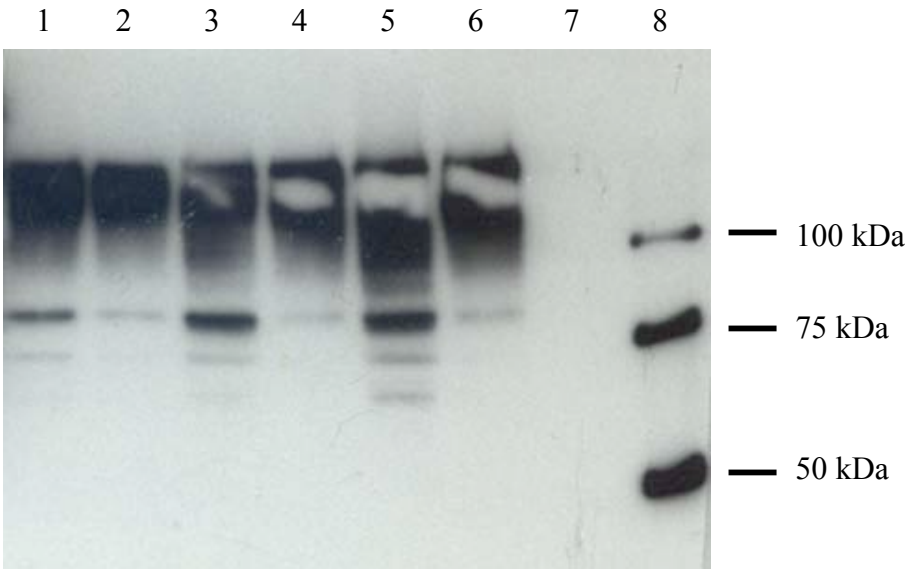

Fig. 35. OVGP1 levels in conditioned medium of HEK-293F cells cultured for different number of days. Immunoblot analysis of OVGP1 using the anti-His antibody: Lane 1, 24 h post-transfection; lane 2, 24 h post-transfection and replace media; lane 3, 48 h post-transfection; lane 4, 48 h post-transfection and replace media; lane 5, 72 h post-transfection; lane 6, 72 h post-transfection and replace media; lane 7, no transfection; lane 8, His-ladder.

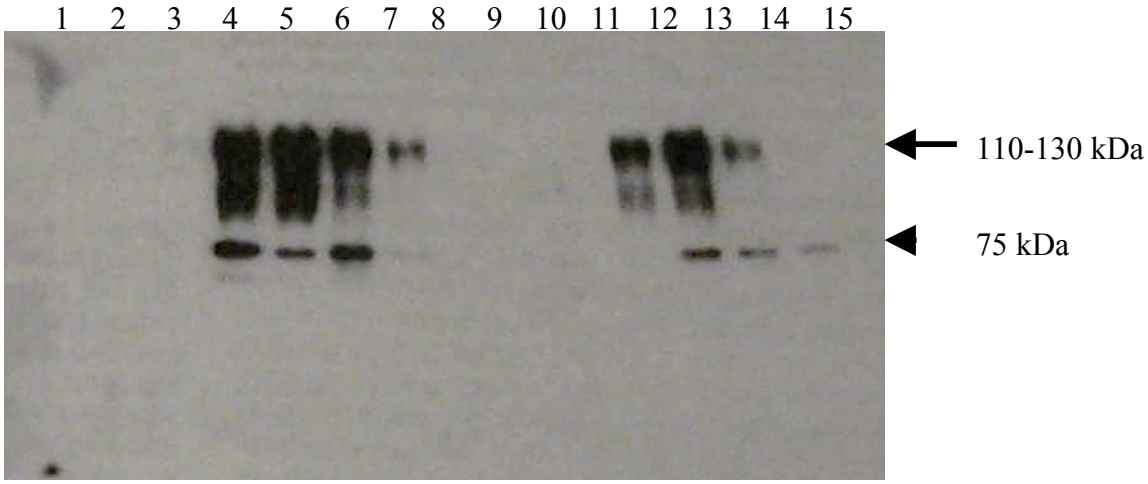

Fig. 36. Expression of OVGP1-Rho in the conditioned medium of HEK-293F cells transiently transfected with OVGP1-Rho cDNA, collected every day and fresh medium replaced every day over a period of 6 days, as detected by the Rho-1D4 antibody using Western blot analysis. Lane 1, marker; 2, untransfected CM on day 1; 3-7 first batch of CM from OVGP1-rho transfected cells; 8, positive control; 9, blank; 10-14 second batch of CM from OVGP1-rho 1D4 transfected cells; 15, blank. Lanes 3 and 10, 1 day post-transfection; 4 and 11, 2 days post-tranfection; 5 and 12, 4 days post-transfection; 6 and 13, 5 days post-transfection; 7 and 14, 6 days post-transfection. Based on the size of the bands, the rho-1D4 antibody appears to detect both the glycosylated (arrow) and unglycosylated (arrowhead) forms of the protein. The presence of unglycosylated OVGP1 may be the result of residual cells leftover in the conditioned medium.

3.5.2 Characterization of a new monoclonal antibody against oviduct-specific glycoprotein

Monoclonal antibodies were generated in Dr. Robert Molday's laboratory using recombinant fusion protein fragments of OVGP1 produced in *E. coli* (Fig. 37A and B). The N-terminal (aa 22-102) and C-terminal (aa 567-678) protein fragments were combined and injected into mice. Several hundred clones were tested by dot blot assay in Dr. Robert Molday's laboratory and positive clones were subsequently tested by Western blot analysis using the OVGP1-Rho conditioned medium. Clone 7E10 recognizes a specific band by Western blot analysis and identifies the C-terminal region of the protein (Fig. 37C). By immunohistochemistry, we showed that the 7E10 clone positively and specifically stained the cytoplasm of secretory epithelial cells of the mid-proliferative phase oviduct (Fig. 37D). Interestingly, the staining pattern is different from the polyclonal antibody which stains the cells apically.

3.5.3 Characterization of ovarian tumours using clone 7E10

As determined using the polyclonal anti-human OGP antibody, OVGP1 is present in most low-grade serous tumours (Woo et *al.*, 2004a). Clone 7E10 was used to stain a different series of ovarian tumour tissue arrays. As these experiments are still ongoing and the data require further analysis, only the preliminary results will be summarized here.

The 7E10 monoclonal antibody recognized a greater portion of invasive ovarian carcinomas as compared to the polyclonal anti-OGP antibody (Table 10) which detected OVGP1 in only 50 of 286 malignant ovarian carcinomas. As the

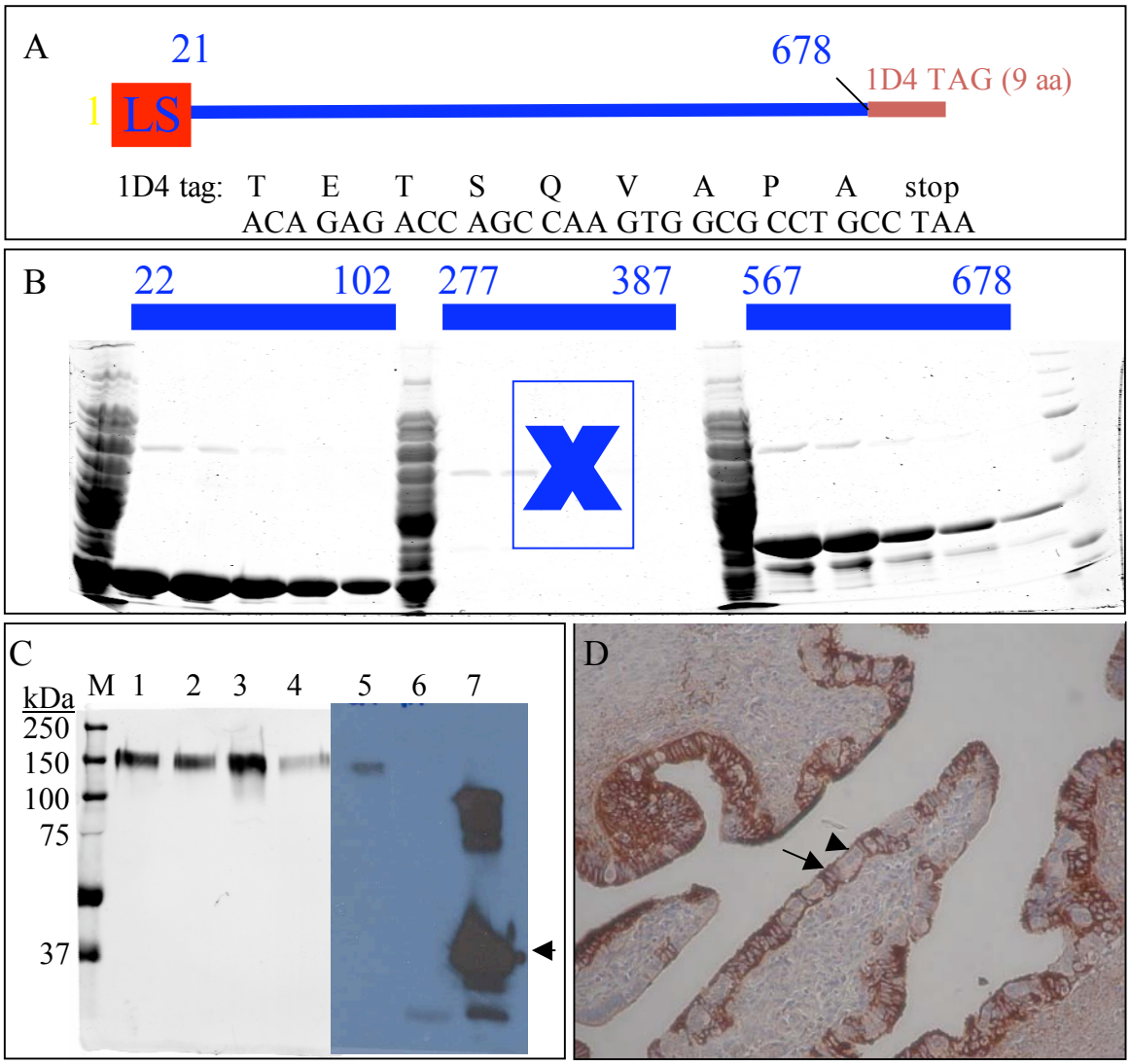

Fig. 37. Generation and characterization of the clone 7E10 monoclonal antibody against OVGP1. (A) Schematic of OVGP1 sequence containing the Rho tag used for screening positive clones. (B) GST fusion proteins from the N-terminal and C-terminal of OVGP1 were purified from *E. coli* and injected into mice. The first lane is the unpurified protein and the 5 lanes after are the elutions of OVGP1 fusion protein from the glutathione beads. X: Note the absence of protein from the central region (aa 277-387) of OVGP1. (C) Western blot analysis of clone 7E10 monoclonal antibody. Clone 7E10 recognized OVGP1-Rho conditioned medium (lanes 1 and 5). Lane 2, unbound to 1D4 beads; 3, 1D4 peptide elution; 4, SDS elution. Clone 7E10 binds to the C-terminal fusion protein (lane 7, arrowhead) and not the N-terminal fusion protein (lane 6). (D) Immunohistochemical staining of OVGP1 in the oviduct using clone 7E10. It binds specifically to the secretory epithelial cells (arrow) of the mid-proliferative phase oviduct. Note absence of staining in the ciliated epithelial cells (arrowhead) and the stroma. Sections were incubated in primary antibody overnight at 4^{o}C, developed with DAB and counterstained with hematoxylin.

Table 10. OVGP1 expression in ovarian carcinomas stained using clone 7E10 monoclonal anti-OVGP1 antibody

Subtype	OVGP1 staining intensity and pattern				
	Negative	Weak diffuse	Strong patchy	Strong diffuse	Total
Serous	21 (10.8%)	94 (48.2%)	32 (16.4%)	48 (24.6%)	195 (100%)
Low grade	4 (40.0%)	3 (30.0%)	0 (0%)	3 (30.0%)	10 (100%)
High grade	17 (9.2%)	91 (49.2%)	32 (17.3%)	45 (24.3%)	185 (100%)
Mucinous	3 (13.0%)	15 (65.2%)	2 (8.7%)	3 (13.0%)	23 (100%)
Endometrioid	12 (11.1%)	71 (65.7%)	19 (17.6%)	6 (5.6%)	108 (100%)
Clear cell	14 (12.1%)	87 (75.0%)	10 (8.6%)	5 (4.3%)	116 (100%)

clinical outcome was available for the set of patients used to construct the tissue array stained using the 7E10 antibody, OVGP1 staining was compared among different histological groups and correlated to clinical outcome. Fig. 38A shows representative figures of negative and positive staining for OVGP1 in ovarian tumors using clone 7E10. We found that in the high-grade serous carcinoma group, which generally have an overall poor prognosis, OVGP1 staining was associated with a more favourable outcome (Fig. 38B). This did not appear to be determined by the staining intensity and localization of the staining as patients with different categories of OVGP1 staining in their tumours had the same survival pattern (Fig. 38C). However, it did appear that OVGP1 was only a predictor of a more favourable clinical outcome in the patients with high-grade serous carcinomas as OVGP1 staining could not differentiate poor vs. good outcome in either the endometrioid or clear cell carcinoma groups (Fig. 39).

3.5.4 Oviduct-specific glycoprotein is present in serum from women with low-grade ovarian cancer

An ELISA-based assay was developed using the 7E10 monoclonal antibody and the polyclonal OGP antibody. Currently only 40 cases of serum from women with ovarian cancer have been collected and tested. Once again, this study is ongoing and only the preliminary results are reported here. Sera from women without ovarian cancer were considered as controls and having baseline OVGP1 levels. Serum from women with borderline, low-grade ovarian carcinoma, high-grade ovarian carcinoma, endometrial hyperplasia, endometrial carcinoma, and other cancers were tested for OVGP1. As shown in Fig. 40, most of the patients with low-grade ovarian carcinoma

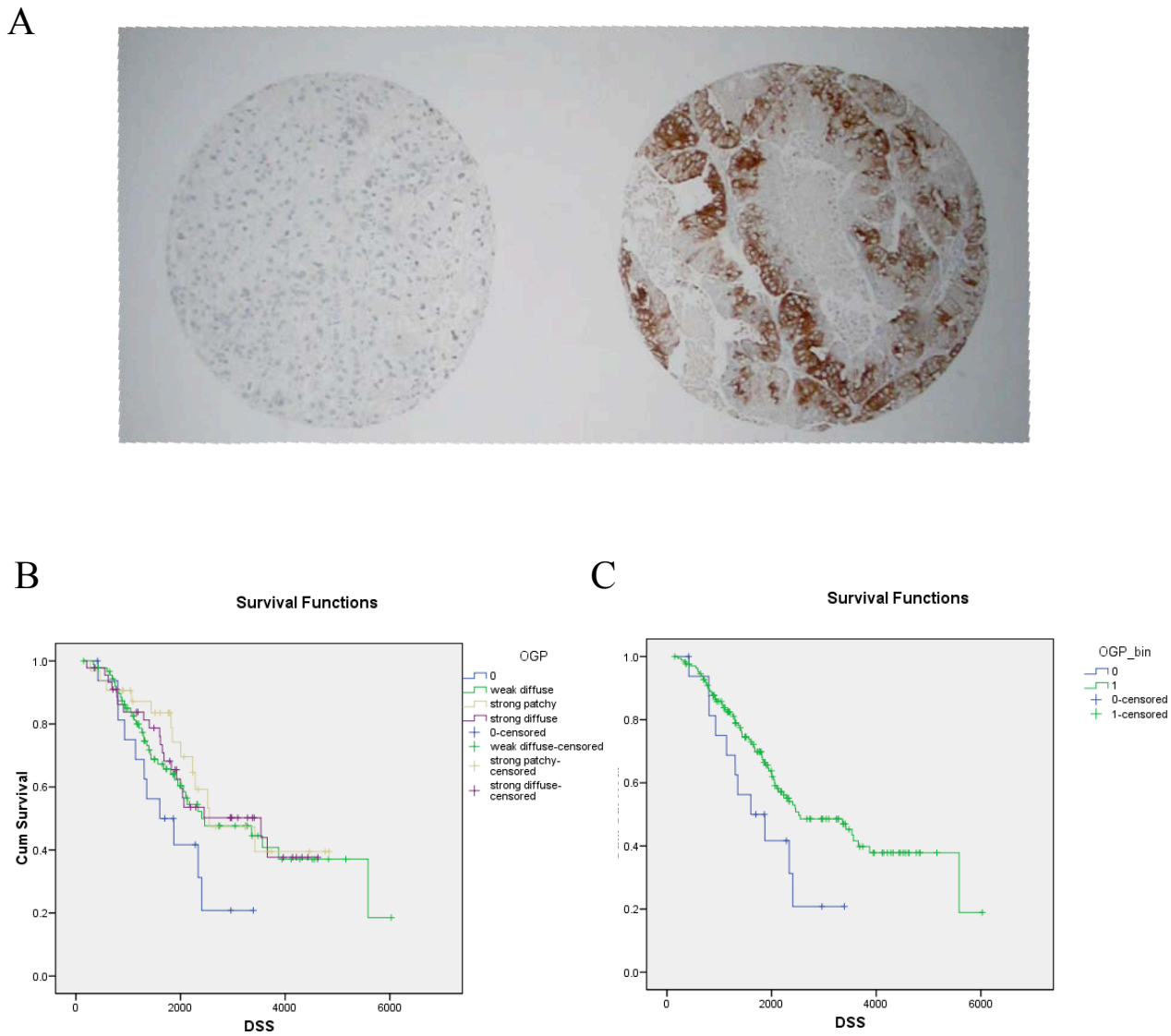

Fig. 38. OVGP1 staining and Kaplan-Meier curve showing survival in days for high-grade serous carcinomas. (A) Representative immunohistochemical staining of ovarian adenocarcinomas for OVGP1 using clone 7E10 monoclonal antibody. Left panel, negative staining. Right panel, positive staining. (B, C) Kaplan-Meier curve showing survival in days for OVGP1 staining of high-grade serous carcinomas (n=185). (B) Survival is separated according to weak diffuse, strong patchy, and strong diffuse pattern of OVGP1 staining while (C) shows the survival as a function of OVGP1 staining versus no staining ($p<0.05$, log rank statistics).

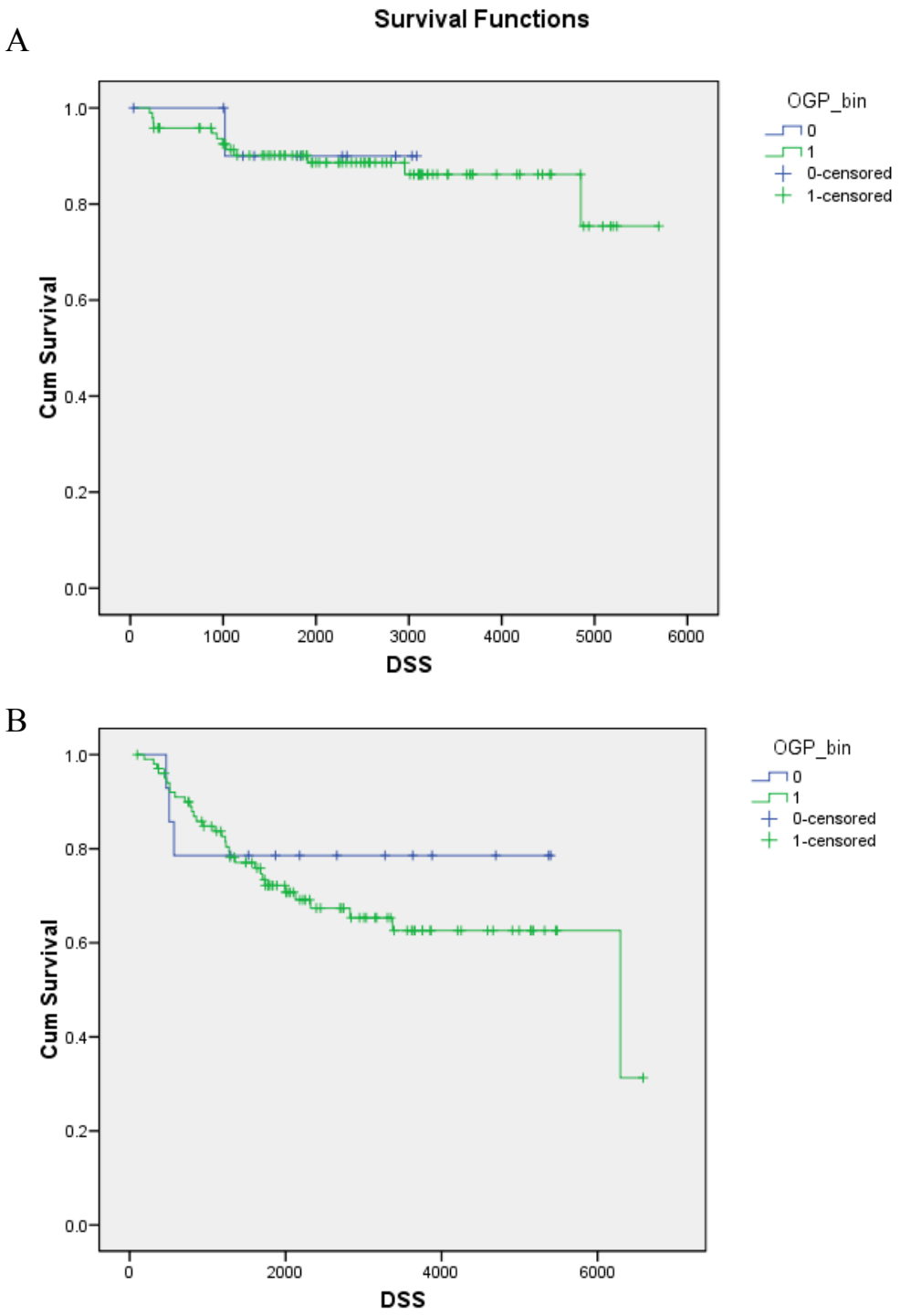

Fig. 39. Kaplan-Meier curve showing survival in days for OVGP1 staining of (A) endometrioid ovarian carcinomas (n=108) and (B) clear cell carcinomas (n=116). The tissues were stained for OVGP1 expression with the clone 7E10 monoclonal antibody.

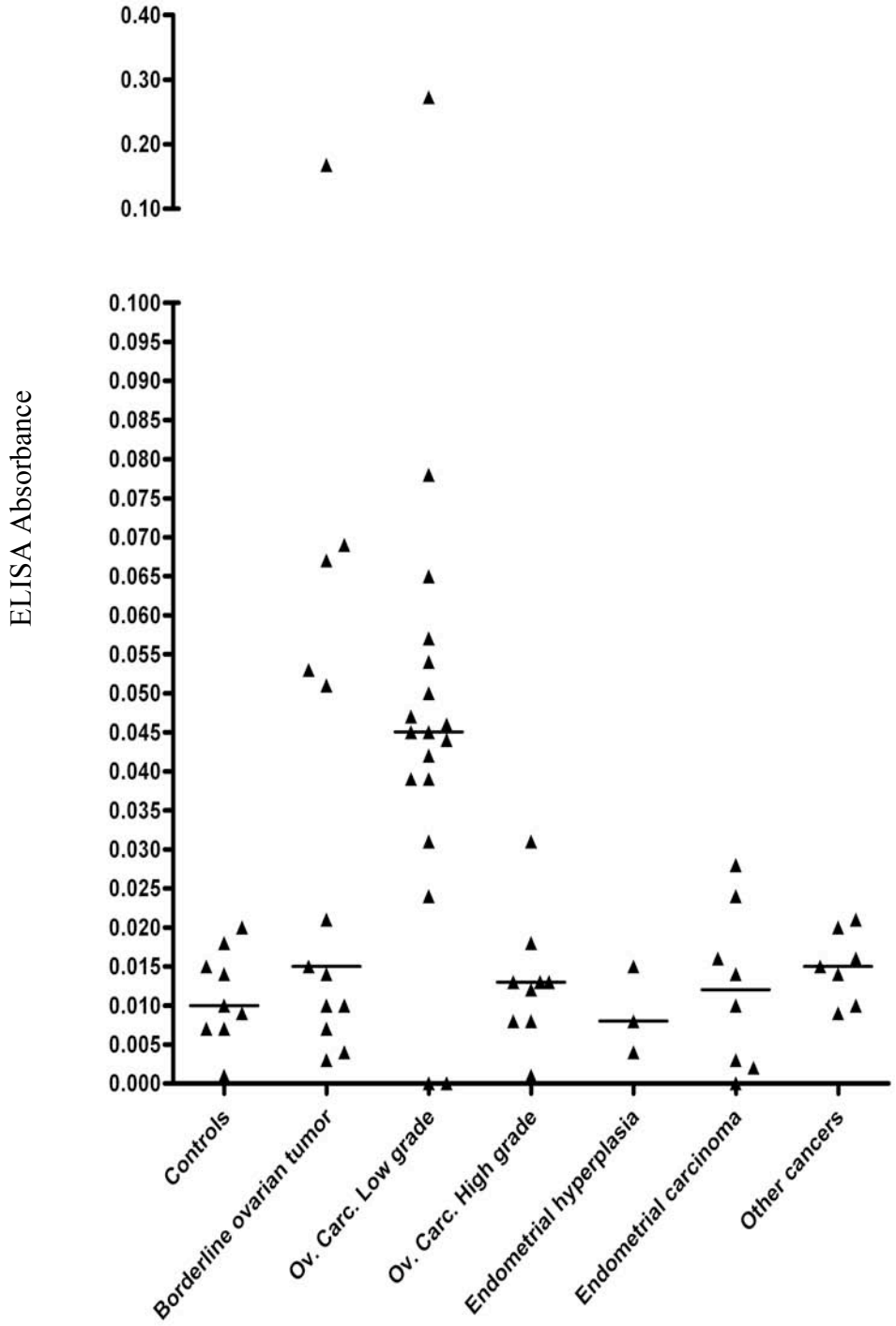

Fig. 40. OVGP1 occurs at higher levels in the sera from patients with low grade ovarian carcinoma. Serum levels of OVGP1 were detected using the clone 7E10 monoclonal antibody and polyclonal OGP antibody in an ELISA assay. Sera from women without cancer were used as controls and considered having baseline levels of OVGP1 in serum. Bars indicate the median of the samples in each group.

had elevated levels of OVGP1 while 5 of 13 patients with borderline ovarian tumours also had elevated levels of OVGP1. Although OVGP1 is expressed in most endometrial hyperplasias and low-grade endometrial carcinomas (Woo *et al.*, 2004b), the levels of OVGP1 in the sera from women with these conditions do not seem to be elevated. In addition, women with cancers in other tissues had OVGP1 concentrations similar to baseline levels.

3.6 Oviduct-Specific Glycoprotein, Estrogen Receptor and PTEN Expression in the Normal Endometrium and Endometrial Cancer

When different tissues were assayed for OVGP1 using the polyclonal OGP antibody, preliminary results showed that 3 of 56 cases of endometrial cancer and 6 of 17 cases of atypical endometrial hyperplasias stained positively for OVGP1 based on examination of 0.6mm tissue cores. On the basis of these observations, we hypothesized that OVGP1 may be a marker of the development and progression of atypical hyperplasias, which are known precursors of endometrial cancer. In the present study, whole sections of normal, hyperplastic, and malignant endometrium were examined, in addition to a tissue microarray of endometrial cancer cases which had follow-up data. All sections were stained using the polyclonal OGP antibody as these studies were performed prior to obtaining the 7E10 clone.

3.6.1 Oviduct-specific glycoprotein expression

The glandular epithelium of normal endometrium stained weakly positive in 10 of 15 (67%) of cases, with a mean staining index of 1.0, whereas the luminal

epithelium was OVGP1 negative in every case. Most of the staining was observed in the basalis layer (Fig. 41), where the stem cells reside, and in some adjacent glands in the functionalis layer. The expression of OVGP1 was focal, and no difference was observed between stages of the menstrual cycle. OVGP1 was expressed in 41 of 43 (95%) cases of endometrial hyperplasia. The intensity of staining was more pronounced in atypical hyperplasia compared with hyperplasia without atypia (P = 0.017; Figs. 41 & 42A), whereas there was no difference in the percentages of positively stained cells (Fig. 42B). Of 16 cases of hyperplasia without atypia, 15 were positive for OVGP1, with a mean staining index of 4.73. Twenty-six of 27 cases of atypical hyperplasia were positive for OVGP1 with a mean staining index of 5.50. This difference in staining indices is not significant.

OVGP1 immunostaining was done on whole sections of 32 endometrial carcinomas. Fifteen (47%) of the tumours were OVGP1 positive and 53% (n = 17) were OVGP1 negative. In the OVGP1 positive group, 80% (n = 12) showed weak (staining index $\leq$ 4) and 20% showed strong staining (staining index > 4).

Figure 43 shows the staining index of all (n = 90) cases where OVGP1 staining cases of hyperplasia (atypical or nonatypical) compared with normally cycling endometrium ($P < 0.0001$). Progression to carcinoma was associated with a decrease in OVGP1 expression compared with hyperplasia ($P < 0.0001$). A significant difference ($P < 0.001$) was observed between the staining index of atypical hyperplasia and well-differentiated (grade 1) endometrioid carcinoma. There was also a significant correlation between OVGP1 expression and tumour grade.

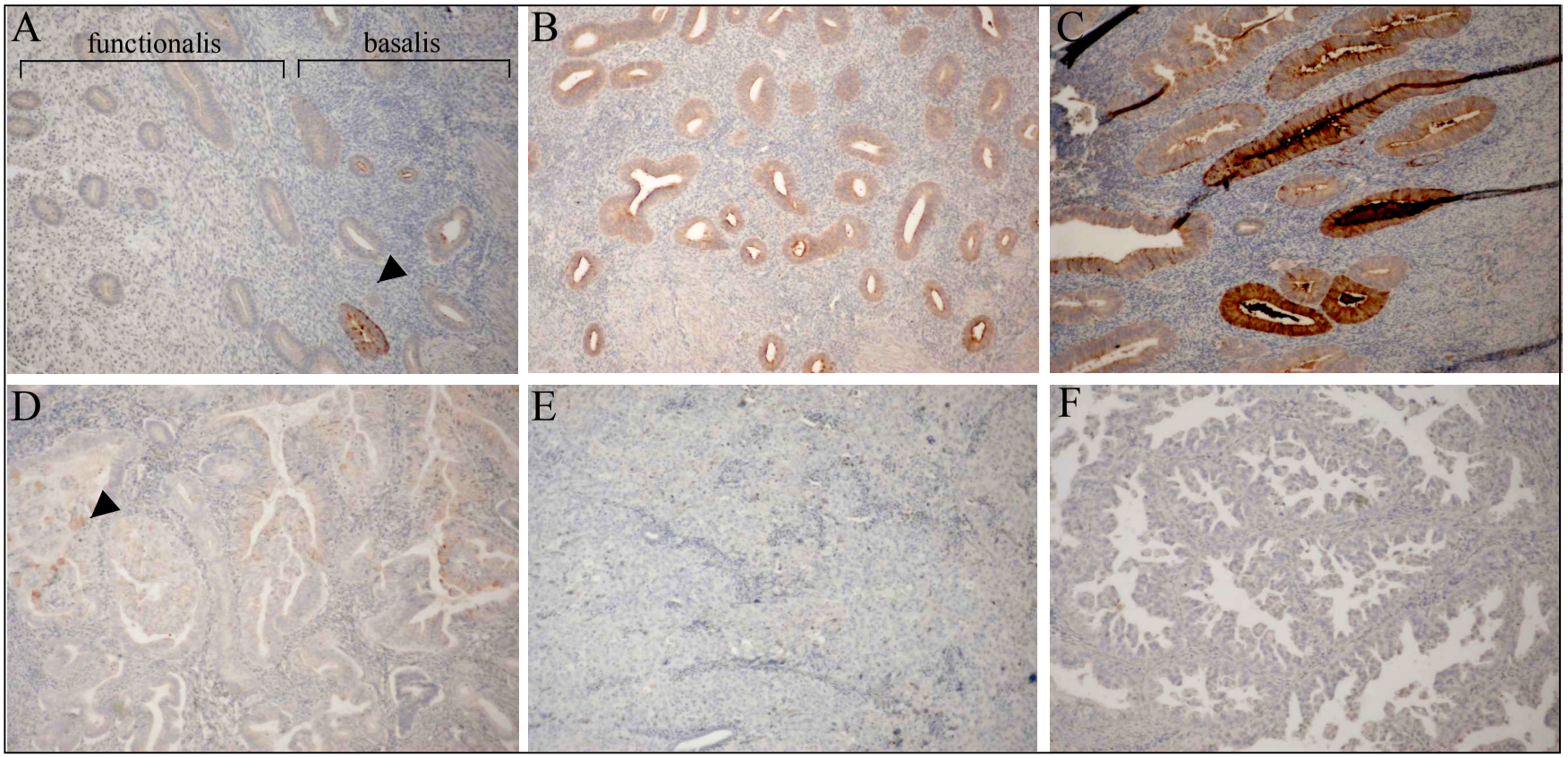

Fig. 41. OVGP1 staining in normal, hyperplastic and malignant endometrial tissue. In normal endometrium (A), focal staining (arrowhead) is observed in the basalis layer, where the stem cells reside. On average, non-atypical hyperplastic endometria (B) stained less intensely than atypical hyperplastic endometria (C). OVGP1 levels fall with progression to carcinoma, (D) EEC Grade I, (E) EEC Grade III, and (F) UPSC. Tissues were stained overnight at 4^{o}C with the polyclonal anti-HuOGP antibody, developed in DAB and counterstained with hematoxylin. All photos were taken at the same magnification.

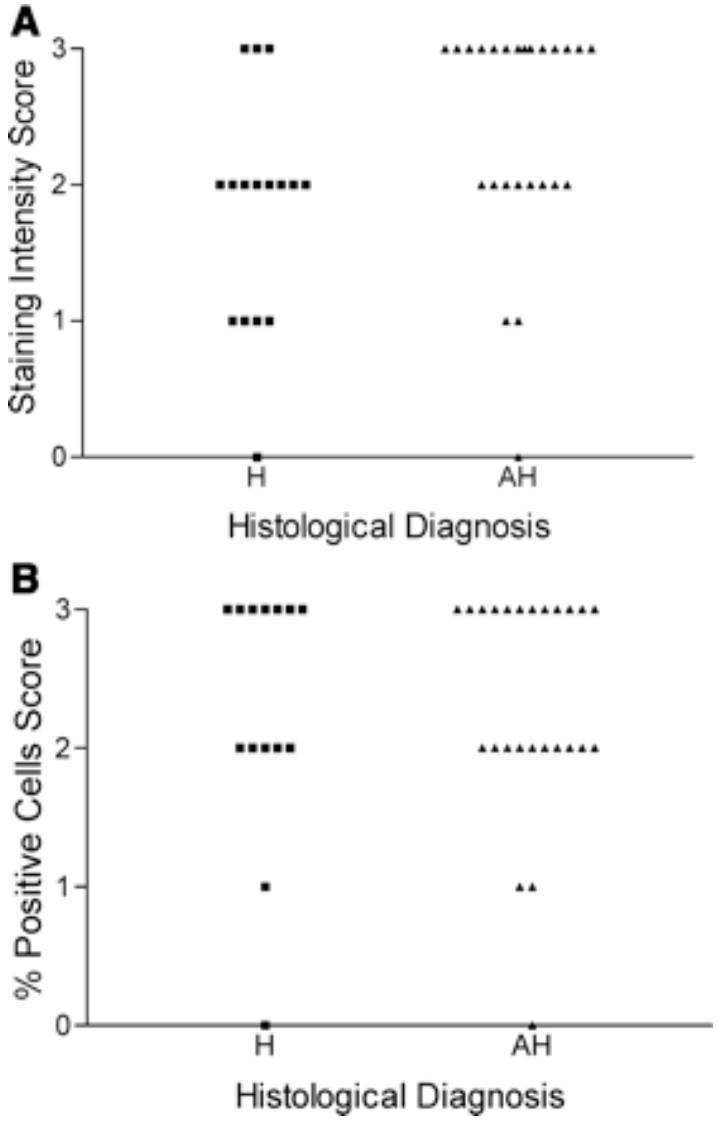

Fig. 42. Comparison of the staining intensity (A) and percentage of positive cells (B) in hyperplasias with and without cytological atypia. Atypical hyperplasias (AHs) stained more intensely than nonatypical hyperplasias (Hs; $P = 0.017$), although the distribution of the percentage of positive cells was not significantly different. Scores for the expression of oviduct-specific glycoprotein were assigned semiquantitatively according to the intensity of staining (no staining, score 0; weak, score 1; moderate, score 2; and strong, score 3) and the percentage of cells stained (no positive cells, score 0; <5%, score 1; 5 to 50%, score 2; and >50%, score 3).

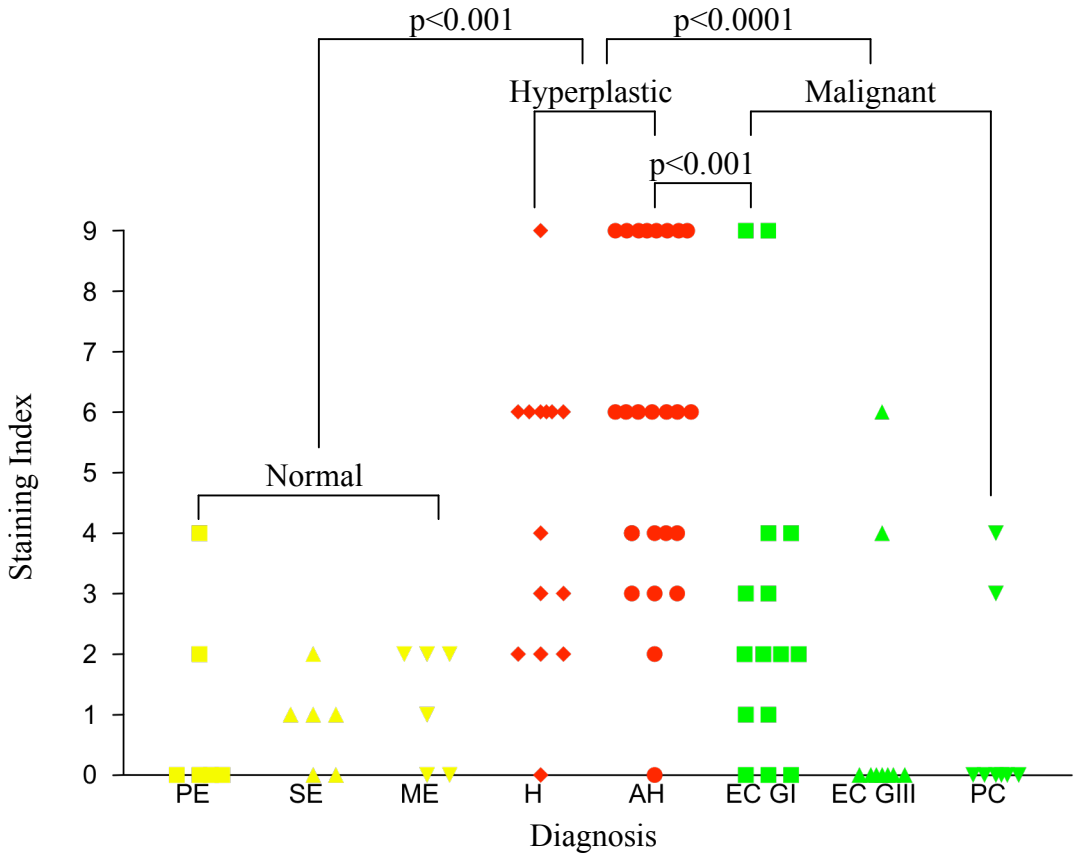

Fig. 43. OVGP1 staining indices for normal, hyperplastic and malignant endometria. There were significant differences between all normal cases vs. all hyperplasias ($p<0.001$, Mann-Whitney *U* rank sum or Kruskal-Wallis nonparametric tests). PE, proliferative endometrium; ME, menstrual endometrium; SE, secretory endometrium; H, non-atypical hyperplasia; AH, atypical hyperplasia; EC GI, endometrioid carcinoma Grade I; EC GIII, endometrioid carcinoma Grade III; PC, papillary serous carcinoma. Sections were stained with the anti-OGP polyclonal antibody, developed with DAB and scored according to staining intensity and percentage of positive cells. The two scores were multiplied to get the staining index.

Percentages of OVGP1 positive tumours were as follows: grade 1 endometrioid carcinoma, 80% OVGP1 positive; grade 3 endometrioid carcinoma, 13% OVGP1 positive; uterine papillary serous carcinoma, 7% OVGP1 positive, with OVGP1 staining index correlating significantly higher in patients with low-grade disease (grade 1 endometrioid carcinoma) compared with those from high grade tumours (grade 3 endometrioid carcinoma and uterine papillary serous carcinoma; $P < 0.05$).

3.6.2 Oviduct-specific glycoprotein expression is related to better survival

Analysis of the endometrial cancer tissue microarray showed that the patients with strong OVGP1-positive tumours had better survival rates compared with OVGP1 weak or negative tumours, but the difference did not reach statistical significance ($P = 0.1$; Fig. 44). All (n = 11) of the strongly OVGP1 positive tumours were grade 1 endometrioid carcinomas with 100% survival for at least 11 years. The 20-year survival rate of patients with OVGP1 weak or negative tumours was ~70%.

3.6.3 Comparison of estrogen receptor expression to oviduct-specific glycoprotein in malignant endometrial tissue

Because OVGP1 is regulated by estrogen, ER immunohistochemistry was done on the endometrial cancer tissue microarray (O'Day-Bowman *et al.*, 1994; Lok *et al.*, 2002). There was no significant correlation between ER expression and OVGP1 staining, although a trend was observed ($P = 0.138$; Table 11).

3.6.4 Comparison of PTEN expression to oviduct-specific glycoprotein in malignant endometrial tissue

The appearance of PTEN somatic mutations or deletions is common in low grade endometrioid carcinomas (Risinger *et al.*, 1997). There was a significant

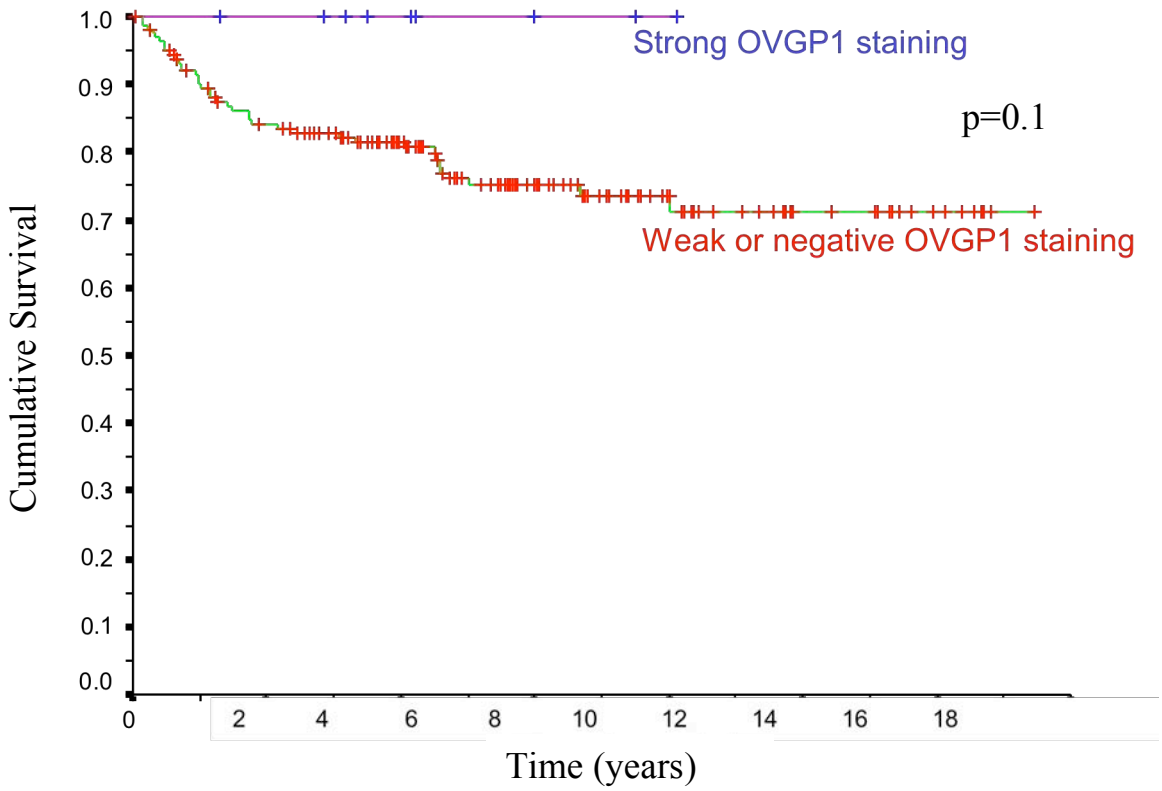

Fig. 44. Kaplan-Meier curve showing survival in years for strong OVGP1 staining vs. weak or negative OVGP1 staining. In an endometrial cancer tissue array, 200 cases with known prognoses were examined for OVGP1 expression. Of 139 EECs, 11 cases were strongly OVGP1 positive while the other 128 cases were negative or weakly positive. All 37 cases of non-endometrioid carcinomas were negative. Analysis with log rank statistics showed a trend towards significance for strong OVGP1 staining being a predictor of good prognosis (p=0.1).

correlation (P = 0.004) between the presence of PTEN-null glands and positive OVGP1 staining in cases on the endometrial cancer tissue microarray (Table 11).

Table 11. Comparison of OVGP1 with ER and PTEN staining in endometrial carcinomas

		OVGP1	
		Negative	Positive
ER			
	Negative	27	0
	Positive	131	11
PTEN			
	Negative	88	11
	Positive	63	0

3.7 Morphogenesis of OSE and Ovarian Cancer Cells

The following two sections present preliminary data describing additional studies which are unfinished but were undertaken to examine early events in ovarian carcinogenesis, and in particular, to replicate *in vitro* the differentiated phenotype of ovarian carcinomas. Specifically, the roles of E-cadherin and hepatocyte growth factor in glandular differentiation, and the effects of a differentiation factor, retinoic acid, on pre(neoplastic) OSE were investigated.

3.7.1 Role of E-cadherin and HGF in branching morphogenesis

In an attempt to reproduce in culture the differentiated phenotype of ovarian carcinomas, i.e. tubal differentiation, OSE at different stages of neoplastic progression were cultured in 3-Dimensional collagen gels. Others have shown that tissues such as the kidney, lung, and mammary gland can undergo branching morphogenesis in 3-D collagen gels, thus mimicking their development *in vivo*

(Comoglio *et al.*, 2007). This study tested the hypothesis that E-cadherin and HGF, which are elevated in ovarian neoplasia, play a role in the branching morphogenesis that is a part of the Mullerian differentiation of OSE cells. Our lab has previously shown that in collagen gel cultures, normal OSE cells scatter and the E-cadherin expressing ovarian cancer cell line OVCAR-3 form round aggregates irrespective of the presence of HGF but a hybrid between OVCAR-3 and IOSE-29 cell lines, IOSE-Ov29, formed branching tubules resembling Mullerian ducts (Wong *et al.*, 2004). This project aimed at testing additional cell lines in an attempt to determine at which stage of neoplasia would branching morphogenesis occur. The experimental model included the IOSE-Ov29 hybrid cell line and OSE at progressive stages of neoplastic transformation, created by sequentially introducing SV40 early region genes (IOSE) and E-cadherin (IOSE-EC) into normal OSE via transfection (Fig. 45). These lines have been previously characterized in our lab in terms of morphology, keratin and CA125 expression, life span, anchorage independence, and tumorigenicity in SCID mice (unpublished data) and are summarized in Table 12.

This project has not yet been completed but our preliminary results show that different ovarian cancer, IOSE and IOSE-EC cell lines formed various morphologies in collagen gels. The morphologies were classified into 5 classes: (Fig. 46A) dispersed, single cells; (Fig. 46B) round aggregrates; (Fig. 46C) single-file rows; (Fig. 46D) networks; and (Fig. 46E) branching tubules. Figure 46F shows the extensive branching structures formed by C4-II cells, an E-cadherin positive cervical cancer cell line, used as a control, cultured in the presence of HGF (Wong *et al.*, 2000). The SKOV-3 and IOSE-Ov29 ovarian cancer cell lines formed various

morphologies (Table 12) while the OVCAR-3 cells formed round aggregates in the presence or absence of HGF. IOSE-Ov29(EC--) is an E-cadherin negative cell line selected by repeated passaging of the IOSE-Ov29 cells and thus, are distinguished from the parental E-cadherin expressing line, termed IOSE-Ov29(EC++) in Table 13. The presence of E-cadherin enabled the IOSE-Ov29 (EC++) cells to form branching tubules. Injection of the IOSE-Ov29 line intraperitoneally into SCID mice gave rise to peritoneal tumours which were subsequently cultured, one of which gave rise to the IOSE-Ov29T4 line. In comparison to its parental line, a larger proportion (exact percentage was not determined and will require further investigation) of the IOSE-Ov29T4 cells formed branching tubules in the presence of HGF. As this line formed branching structures, it was subsequently used for studying the role of retinoic acid in branching morphogenesis. IOSE-118 cells lack E-cadherin but a small percentage of the cells also formed branching tubules. Interestingly, its post-crisis line, IOSE-118pc acquired E-cadherin spontaneously and was tumourigenic in SCID mice but the acquisition of these neoplastic properties did not render the cells more prone to branching morphogenesis suggesting that E-cadherin alone is insufficient for branching morphogenesis. In addition, IOSE-118 and IOSE-118pc had the capability to form branching tubular structures in collagen gels, irrespective of HGF, suggesting that they may secrete HGF and thus form an autocrine regulatory loop. HGF and its receptor, c-Met were present in all the lines tested (Fig. 47). Our results suggest that neither E-cadherin nor HGF are sufficient in inducing branching morphogenesis of OSE cells and that other factors are necessary for this process. The ovarian cancer

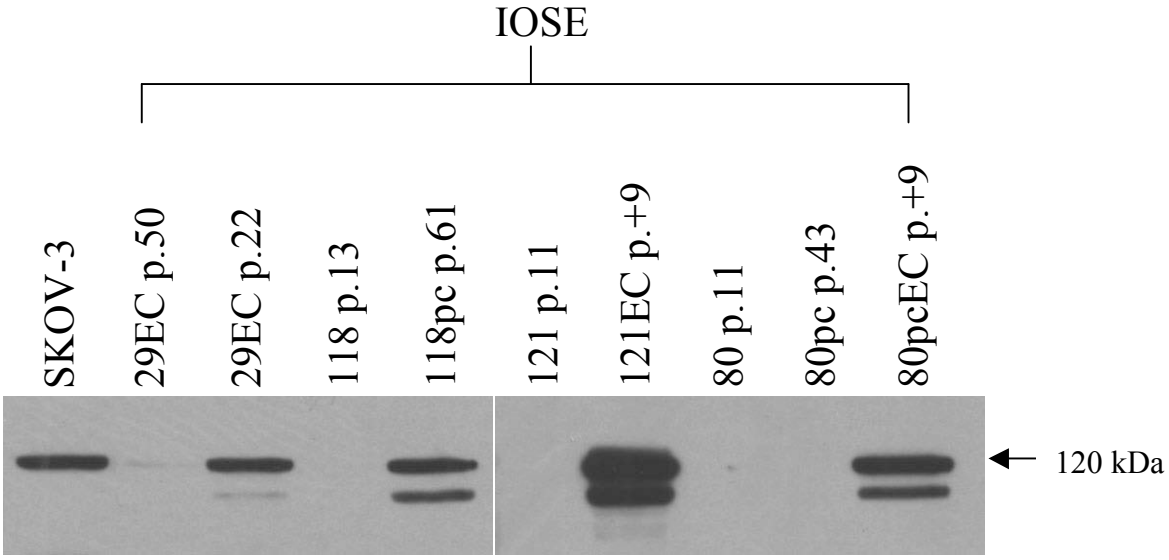

Fig. 45. Western blot analysis of E-cadherin protein expression in IOSE and IOSE-EC lines. Twenty micrograms of protein were loaded per lane, separated by SDS-PAGE, and immunoblotted with an anti-E-cadherin antibody (clone 36, BD Transduction Laboratory) which identifies a 120 kDa band corresponding to E-cadherin. The ovarian cancer cell line, SKOV-3 expresses abundant E-cadherin. E-cadherin was overexpressed in lines IOSE-29, IOSE-121 and IOSE-80pc. IOSE-118 spontaneously expressed E-cadherin post-crisis (IOSE-118pc). Note passage numbers.

Table 12. Characterization of OSE cells transfected with SV40 ER genes and E-cadherin

Cell Type	IOSE				IOSE/EC	pcIOSE		pcIOSE/EC
Cell Line	80	111	118	121	121EC	80pc	118pc	80pcEC
E-cadherin	No	Yes	No	No	Yes	No	Yes	Yes
Keratin %	>90	>90	>90	30	80	>90	100	>90
Morphology	epi f	epi f	epi f	atyp	epi +atyp	epi c+f	epi	epi c
Life Span	15	15	ND	15	15	>40	>40	>40
Anchorage Independence	Yes	No	No	No	Yes	No	Yes	Yes
Tumourigenic	No	ND	No	No	No	No	Yes	ND

Note: IOSE-118 was derived from OSE with a family history of ovarian cancer
IOSE = OSE transfected with SV40 ER genes
IOSE/EC = IOSE transfected with E-cadherin
pc = post-crisis
epi = epithelial
atyp = atypical
c = cobblestone
f = flat
ND = not determined

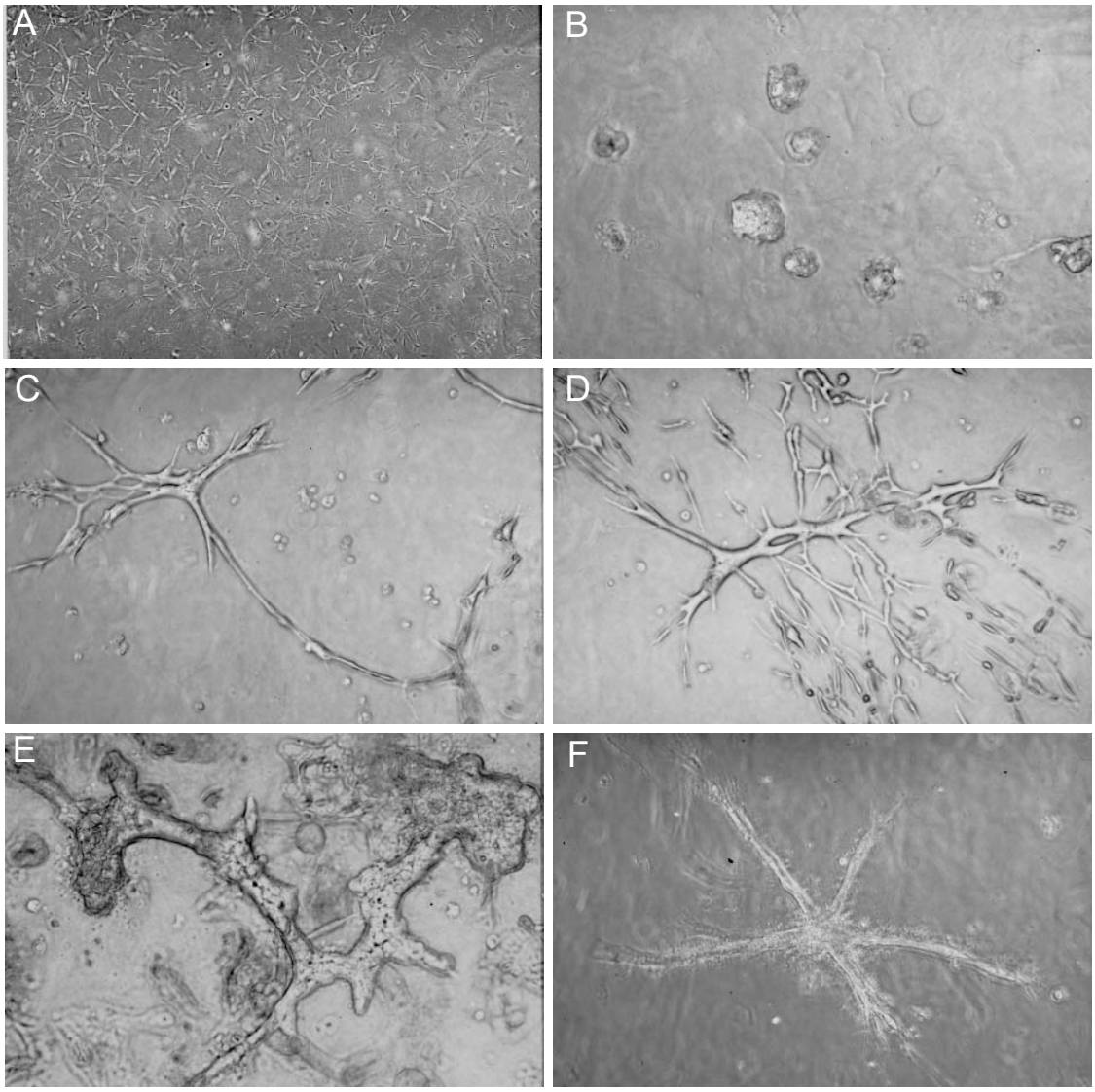

Fig. 46. Examples of the classification of the morphologies displayed by (pre)neoplastic OSE cells cultured in collagen gels. Cells were cultured in the absence or presence of HGF. The morphologies of the cultures were categorized into five classes: (A) dispersed, single cells; (B) round aggregates; (C) single-file rows; (D) networks; and (E) branching tubules. (F) shows the extensive branching structure formed by C4-II cells in the presence of HGF. Light or phase microscopy.

Table 13. Different ovarian cancer, IOSE and IOSE-EC cell lines display various morphologies in 3-dimensional collagen gel cultures in the presence or absence of HGF.

Morphology	Dispersed, single cells		Round aggregates		Single-file rows		Networks		Branching tubules	
	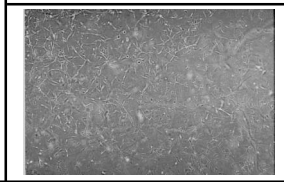		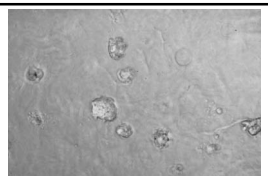		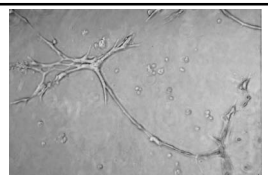		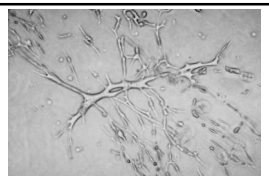		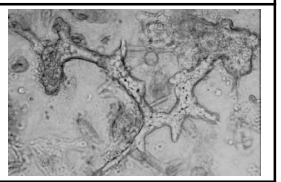	
Cell Line	-HGF	+HGF	-HGF	+HGF	-HGF	+HGF	-HGF	+HGF	-HGF	+HGF
SKOV-3	10%	70%	-	-	10%	10%	10%	20%	70%	tr
OVCAR-3	-	-	100%	100%	-	-	-	-	-	-
IOSE-Ov29(EC--)	10%	>90%	-	-	20%	5%	70%	5%	-	-
IOSE-Ov29(EC++)	-	90%	10%	-	-	10%	80%	-	10%	tr
IOSE-118	20%	70%	-	-	10%	10%	65%	10%	5%	5%
IOSE-118pc	30%	50%	-	-	30%	30%	35%	20%	5%	5%
IOSE-121	70%	100%	-	-	20%	-	10%	-	-	-
IOSE-121EC	30%	>95%	-	-	20%	-	50%	5%	tr	-
IOSE-80	80%	90%	-	-	10%	5%	10%	5%	-	-
IOSE-80pc	<20%	>50%	-	-	>50%	30%	30%	<30%	-	-
IOSE-80pcEC	100%	100%	-	-	tr	tr	-	tr	-	-
IOSE-111	>90%	100%	-	-	<10%	tr	-	-	-	-

tr, trace amounts

cell lines, OVCAR-5 and OVCAR-8 cells were also shown to form branching tubules but their ability to form the different categories of morphogenesis and the percentage in each category have not yet been determined. Upon further characterization of these lines, they may be useful in future studies on defining the mechanisms responsible for branching morphogenesis.

3.7.2 Role of retinoic acid in ovarian carcinogenesis

Retinoic acid causes differentiation of a number of different tissues (Fujiwara, 2006; Rawson & LaMantia, 2006; Romand *et al.*, 2006) and has been shown to effectively treat acute promyelocytic leukemia through its action as a differentiation factor (Huang *et al.*, 1988; Castaigne *et al.*, 1990). Emergence of retinoic acid and its analogues, retinoids, as a chemopreventive agent of ovarian cancer resulted from a randomized clinical study conducted at the Instituto Nazionale Tumori in Italy where statistically significantly fewer ovarian cancers developed in women who received the retinoid analogue, fenretinide, following surgery for breast cancer (De Palo *et al.*, 1995). Their chemopreventive properties may include the induction of apoptosis and/or induction of differentiation. This study tested the role of retinoic acid as a differentiation factor and growth inhibitory factor in ovarian carcinogenesis. analogues, retinoids, as a chemopreventive agent of ovarian cancer resulted from a randomized clinical study conducted at the Instituto Nazionale Tumori in Italy where statistically significantly fewer ovarian cancers developed in women who received the retinoid analogue, fenretinide, following surgery for breast cancer (De Palo *et al.*, 1995). Their chemopreventive properties may include the induction of apoptosis

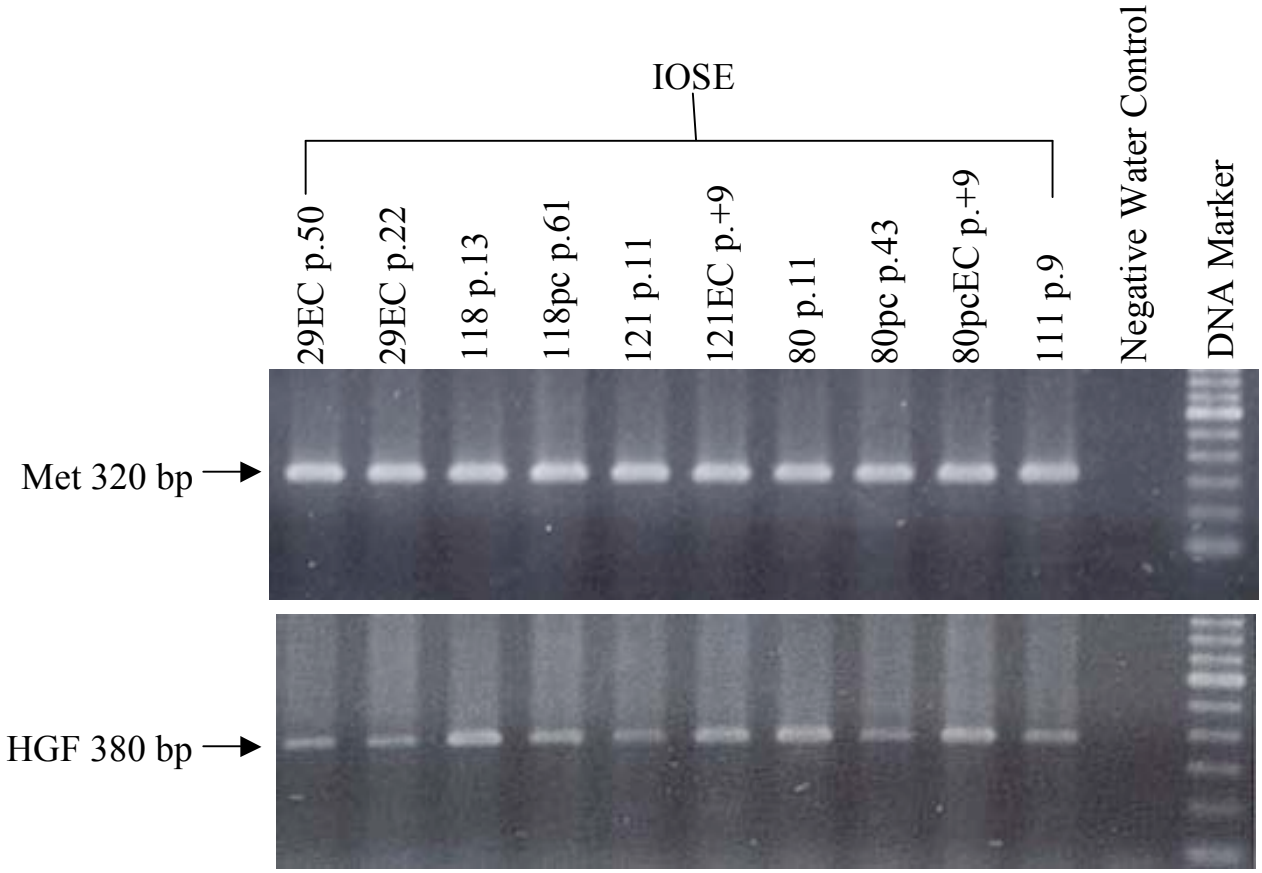

Fig. 47. Met and HGF expression in cultured human IOSE. RT-PCR analysis of (A) Met and (B) HGF in IOSE and IOSE-EC lines. Note that Met and HGF mRNA are detected in all IOSE and IOSE-EC lines.

and/or induction of differentiation. This study tested the role of retinoic acid as a differentiation factor and growth inhibitory factor in ovarian carcinogenesis.Although our study has yet to be completed, our preliminary data suggest that there was no significant effect of ATRA on apoptosis or on the morphology of OSE and IOSE cells cultured on plastic (data not shown). In addition, ATRA alone did not induce branching morphogenesis of IOSE-Ov29T4 cells, nor did treatment in combination with HGF significantly alter the response of these cells (data not shown). However, ATRA inhibited the proliferation of 2 of 3 cases of normal OSE cells and 1 of 3 cases of the premalignant IOSE cells (Fig. 48). The decrease in proliferation of retinoid-treated cultures ranged from 26-38% compared to the DMSO-treated cultures. In addition, there was no effect of ATRA on proliferation of the hybrid ovarian cancer cell line, IOSE-Ov29. Based on preliminary data observed by Dr. Thomas Grunt (University of Innsbruck, Innsbruck, Austria) in Dr. Steven Pelech's laboratory (University of British Columbia, Vancouver, BC), we examined whether ATRA can alter the levels and phosphorylation of the MAPKs extracellular signal-regulated kinases ERK1 and -2, key signaling molecules regulating proliferation. As the availability of normal OSE cells is limited, we first examined the phosphorylation and expression pattern of ERK1/2 in IOSE cells in response to 1μM ATRA at different time points. Our initial results suggested that ATRA was able to increase the phosphorylation of ERK1/2 but upon a more detailed examination of phosphorylation levels in response to ATRA compared to DMSO as a control at all time points, the effects seemed to be mediated by DMSO. As shown in Figs. 49 and

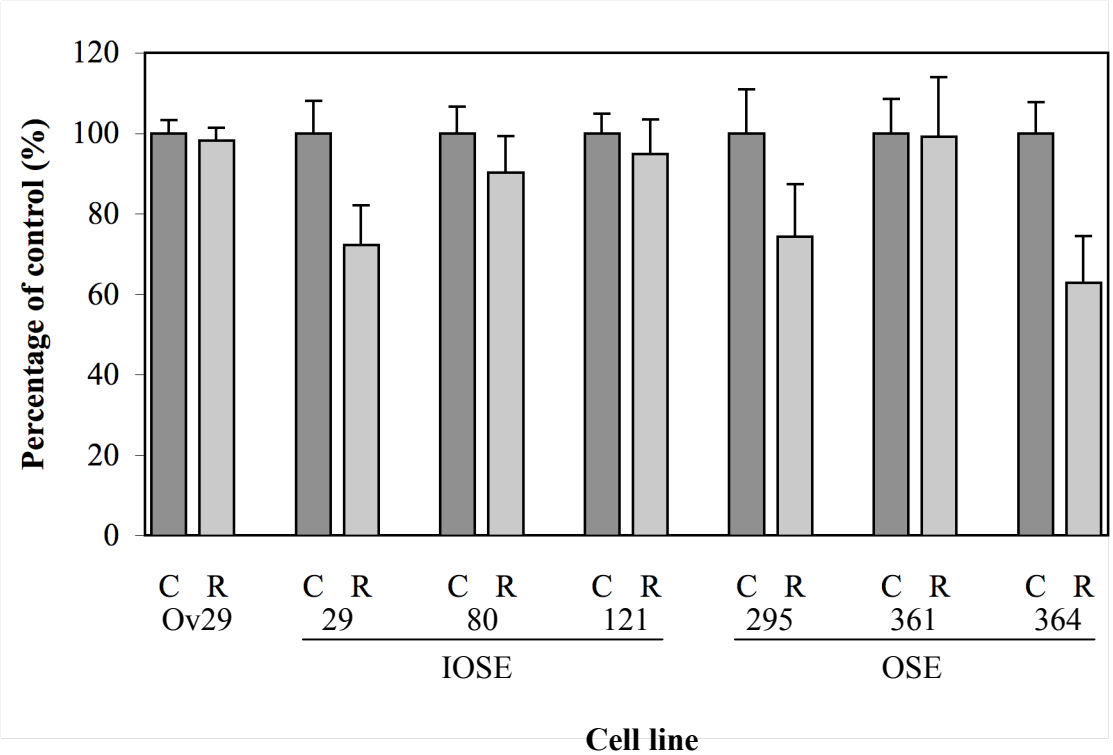

Fig. 48. Effect of retinoic acid on proliferation of normal OSE and IOSE cells. There was a differential response among different cases of IOSE and normal OSE cells to all-trans retinoic acid (ATRA). One micromolar ATRA inhibited the proliferation of IOSE-29 cells and two of three normal OSE cultures (OSE-295 and -364). ATRA had no effect on proliferation of the hybrid ovarian cancer cell line, IOSE-Ov29. Cells were cultured in 96-well plates and treated with 0.1% DMSO (C, control) or 1μM ATRA (R) for 6 days. Cells were fixed in methanol, stained with Hoechst 33258 and measured at wavelengths of 360/40 and 460/40 (Fluorescence Plate Reader FL600). All values have been converted to percentage of control for each case and represent the mean ± S.D. of 8 wells. Representative of 3 individual experiments.

50, 1μM ATRA had no effect on expression or phosphorylation of ERK1/2 in IOSE-29, IOSE-80 and IOSE-121 cells. As such, further examination of normal OSE cells was not carried out.

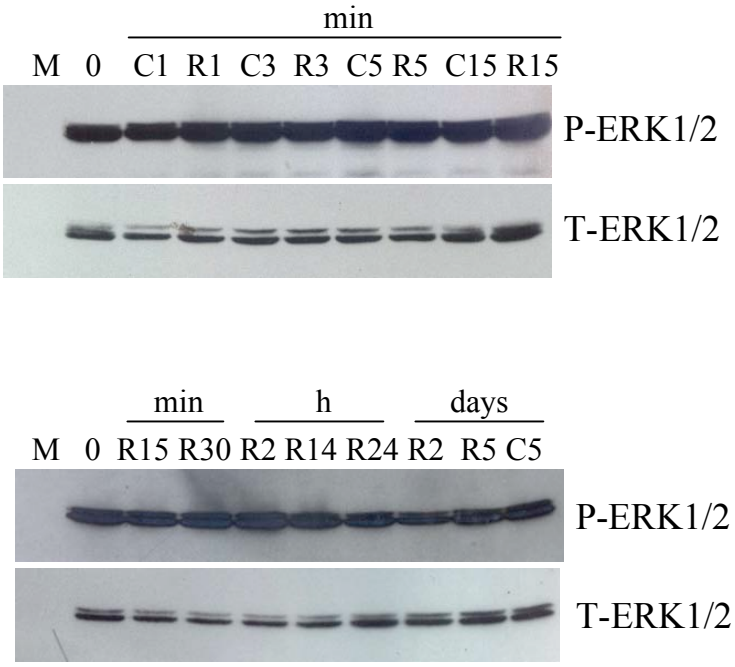

Fig. 49. Effects of short- and long-term treatment with retinoic acid on p44/42 MAP kinase expression and phosphorylation in IOSE-29 cells. Cells were treated with 0.1% DMSO (control, C) or 1μM ATRA (R) for the indicated times (min, h, days). No changes in total or phospho-p44/42 MAPK was observed. Protein were separated by SDS-PAGE and immunoblotted with a p44/42 MAP kinase antibody which detects total MAPK (T-ERK1/2) and a Phospho-p44/42 MAP kinase antibody which detects the phosphorylated form of the protein (P-ERK1/2). M, marker.

A. IOSE-80

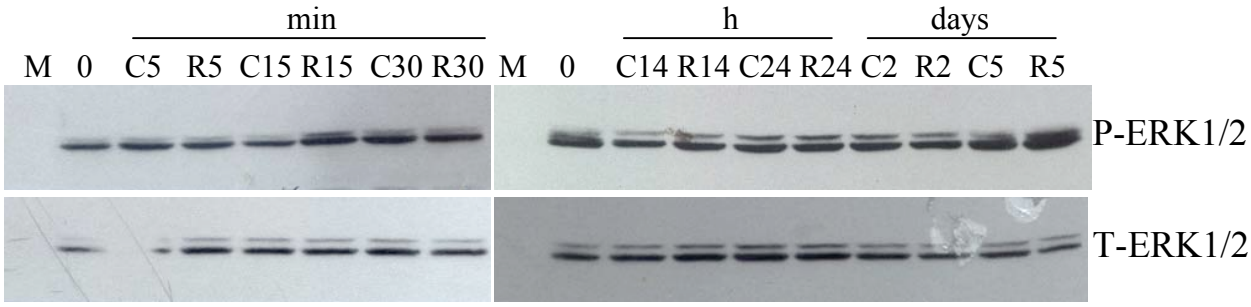

B. IOSE-121

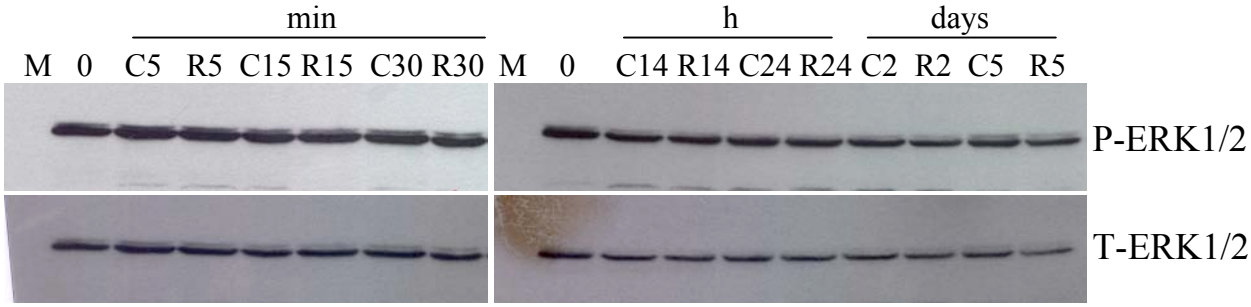

Fig. 50. Effects of short- and long-term treatment with retinoic acid on p44/42 MAP kinase expression and phosphorylation in IOSE-80 and IOSE-121 cells. (A) IOSE-80 and (B) IOSE-121 cells were treated with 0.1% DMSO (control, C) or 1μM ATRA (R) for the indicated times (min, h, days). No change in either total or phospho-p44/42 MAPK was observed. Protein were separated by SDS-PAGE and immunoblotted with a p44/42 MAP kinase antibody which detects total MAPK (T-ERK1/2) and a Phospho-p44/42 MAP kinase antibody which detects the phosphorylated form of the protein (P-ERK1/2). M, marker.

4. DISCUSSION

Mullerian differentiation occurs in a high proportion of and is consistently observed in ovarian cancers suggesting that it may confer a selective advantage on the transforming cells. The aim of this study was to investigate the role of Mullerian differentiation in early ovarian carcinogenesis and to examine whether Mullerian epithelial characteristics can help us discover new predictive markers for the early detection of ovarian cancer. Our findings show that preneoplastic OSE cells can undergo glandular differentiation in culture and SBOT cells maintain their differentiated phenotype *in vitro*, thus mimicking early ovarian neoplasia *in vivo*. In addition, we have demonstrated that OVGP1, a tubal differentiation marker, is an indicator of early ovarian epithelial neoplasia and can be detected in the sera from women with early ovarian cancer.

4.1 Morphogenesis of Ovarian Surface Epithelial Cells Occurs During Neoplastic Progression

4.1.1 Role of E-cadherin and HGF in branching morphogenesis

Mullerian duct epithelia are characterized by branching and glandular structures as in the oviduct and endometrium. These tissues are also characterized by the presence of the epithelial differentiation marker, E-cadherin, which is also a distinguishing characteristic of metaplastic OSE. It has previously been reported that the E-cadherin expressing hybrid IOSE-Ov29 ovarian cancer cell line can undergo branching morphogenesis in the presence of hepatocyte growth factor (Maines-Bandiera *et al.*, 2004; Wong *et al.*, 2004). Branching morphogenesis is mediated in

part by HGF during different developmental stages of tissues such as the kidney, lung, mammary gland and others (Tamagnone & Comoglio, 1997; Zhang & Vande Woude, 2003; Kolatsi-Joannou et al., 1996). Therefore, this study tested the hypothesis that E-cadherin and HGF, which are elevated in ovarian neoplasia, play a role in the branching morphogenesis that is a part of the Mullerian differentiation of OSE cells. Most of the ovarian cancer cell lines, and one of the IOSE lines, pre- and post-crisis, were found to undergo branching morphogenesis. Other morphologies were more frequently observed, including the formation of branching networks and single-file rows. These results suggest that although the cells can adhere to one another in the collagen gels, unlike normal OSE cells which normally scatter, their ability to form tubules is limited. Rather, branching morphogenesis appears to play a role in the neoplastic progression of OSE but E-cadherin and HGF are neither sufficient nor necessary and that other factors appear to be involved in the Mullerian differentiation of these cells. During development, HGF regulates organ and branching development (Sonnenberg *et al.*, 1993; Pepper *et al.*, 1995) through the ability of HGF to induce cells to invade the matrix and grow to form polarized tubular structures as demonstrated in 3-Dimensional cultures such as collagen gels (Naldini *et al.*, 1991; Montesano *et al.*, 1991; Sonnenberg et al., 1993; Medico et al., 1996). In malignant growths, activation of this pathway also leads to invasive growth and metastasis (Tamagnone & Comoglio, 1997; Comoglio *et al.*, 2007) suggesting that branching morphogenesis observed in ovarian carcinogenesis may be a form of invasive growth. It is not known whether the collagen gel would have induced E-cadherin expression in the IOSE line that formed branching tubules which would

facilitate cell to cell adhesion. Interestingly, the E-cadherin negative IOSE line IOSE-118, gave rise to a tumourigenic, E-cadherin positive line post-crisis, and thus may represent a cell line possessing preneoplastic characteristics. Another possible explanation as to why HGF may not be required may be the fact that all of the IOSE and IOSE-EC lines expressed HGF as well as its receptor, c-met, suggesting the possibility of an autocrine/paracrine regulatory loop already established in these cells. It has previously been reported that c-met is expressed in normal OSE from women with and without a family history of ovarian cancer but its expression in cell culture only persists in OSE from patients with family histories (Wong *et al.*, 2001). In addition, HGF is not normally expressed in normal OSE, whereas a high proportion of OSE from women with family histories express HGF. This autocrine HGF-Met loop has been implicated in tumourigenic transformation, and suggests that this change in OSE from women with family histories may play a role in the enhanced susceptibility to ovarian carcinogenesis in women with hereditary ovarian cancer syndromes (Wong *et al.*, 2001). The introduction of SV40 early region genes to the OSE cells appear to advance the neoplastic stage of the cells as they acquired increased neoplastic properties which include one or more of the following: expression of E-cadherin, an HGF-Met loop, the ability to undergo branching morphogenesis, and/or anchorage-independence. Only line IOSE-118pc was tumourigenic. Thus, despite the acquisition of these neoplastic properties, the cell lines were non-tumourigenic *in vivo* suggesting that E-cadherin and HGF are insufficient for transformation but do appear to promote neoplastic progression.

4.1.2 Role of retinoic acid in ovarian carcinogenesis

Retinoic acid is another factor which plays a role in differentiation of other epithelial tissues. This compound and its synthetic derivatives, retinoids, received greater attention following a randomized clinical trial conducted at the Instituto Nazionale Tumori in Italy where statistically significantly fewer ovarian cancers developed in women who received the retinoid analogue, fenretinide (4-HPR, N-(4-Hydroxyphenyl)-retinamide), following surgery for breast cancer (De Palo *et al.*, 1995). It has been postulated that 4-HPR may act as a chemopreventive agent through its induction of apoptosis and/or induction of differentiation in ovarian cancer cells as well-differentiated ovarian tumours are less aggressive than poorly differentiated ovarian carcinomas (Brewer *et al.*, 2003). In this study, we did not observe a significant effect of ATRA on apoptosis or on the morphology of OSE and IOSE cells cultured on plastic. Exposure to different concentrations of retinoic acid may render a differential response in the cells as was observed by Brewer *et al.* (2005). In addition, ATRA alone did not induce branching morphogenesis of IOSE-Ov29T4 cells, nor did treatment in combination with HGF significantly alter the response of these cells. A study published at the same time while we were undertaking this study showed that well-formed glandular structures were observed consistently in retinoid-treated OVCAR-3 and CAOV-3 cultures (Guruswamy *et al.*, 2001). They observed 27 glandular structures in 458 colonies (6%) in sections of retinoid-treated cultures and none in the untreated cultures. Therefore, in retrospect, it may be necessary to do a detailed analysis of the colonies to observe these slight but significant differences. A significant finding in our study was that ATRA

inhibited the proliferation of normal OSE cells and the premalignant IOSE cells, but not the hybrid ovarian cancer cell line, IOSE-Ov29, suggesting a possible mechanism by which it may act as a chemopreventive agent. Normal OSE cells are very sensitive to 4-HPR and undergo apoptosis while IOSE cells are not as sensitive to 4-HPR and are more resistant to apoptosis (Brewer *et al.*, 2005). In our study, apoptosis did not occur in either the normal OSE or IOSE cells in response to ATRA as compared to 4-HPR as observed by Brewer *et al.* (2005) suggesting different mechanisms of action. The lack of effect of ATRA on cellular proliferation of ovarian cancer cell lines has also been shown by others (Supino *et al.*, 1996). It has been reported that 4-HPR is more effective than ATRA in suppressing growth of four ovarian cancer cell lines (Um *et al.*, 2001). The anti-proliferative effect on OSE cells observed in our study, however, was not observed in all cases suggesting an inherent difference in the cells. Whether this is related to differential receptor expression in the OSE from different women is unclear and whether the response translates to chemopreventive effects is also unclear. A study of ovarian cancer cell lines showed that 4-HPR had the strongest apoptotic effect in A2780 cells which express RARβ and the highest levels of RARα and RARγ (Supino *et al.*, 1996). Differential expression of nuclear retinoid receptors in normal, premalignant and malignant tissues have been demonstrated by others (Xiao-Chun *et al.*, 1994; Jiang *et al.*, 1999). Because it has been reported that 4-HPR has non-receptor mediated effects and based on preliminary data on ATRA signaling in IOSE cells observed by Dr. Thomas Grunt (University of Innsbruck, Innsbruck, Austria) in Dr. Steven Pelech's laboratory (University of British Columbia, Vancouver, BC), we examined whether ATRA can alter signaling events

such as the MAPK pathway which is a key signaling molecule of cellular proliferation. Our results demonstrated that neither short- nor long-term culture with ATRA altered the phosphorylation and activation of MAPK. 4-HPR induces apoptosis and inhibits growth of normal OSE cells through activation of the p53 pathway while the response is largely mediated via a mitochondrial-dependent pathway in ovarian cancer cells (Cuello *et al.*, 2004).

4.2 Serous Borderline Ovarian Tumors in Long-Term Culture: Phenotypic and Genotypic Distinction From Invasive Ovarian Carcinomas

To examine whether the differentiated phenotype of early ovarian neoplasms alters invasiveness, we established the first permanent cell line for serous borderline ovarian tumours. SBOTs present a unique phenotype as they have already acquired the differentiated phenotype of oviductal epithelia and other neoplastic properties such as oncogenic mutations but differ from serous carcinomas in that they are noninvasive. The divergence in their invasive phenotype allows us to study the mechanisms of differentiation separately from those of invasion. Although differentiation in these tumours precedes invasion, a large proportion of SBOTs recur as low-grade invasive carcinomas (Silva *et al.*, 2006). The majority of SBOTs and of low-grade invasive carcinomas contains either *KRAS* or *BRAF* activating mutations, suggesting that these two forms of ovarian neoplasms have a common origin. However, the molecular changes leading to these early invasive events, and in particular the roles of *KRAS* and *BRAF*, are virtually unknown. In this study, we developed the first permanent SBOT cell line, and compared its characteristics to

three short-term SBOT cultures. The permanent SBOT cell line, SBOT-3.1, and one short-term culture, SBOT-4, were characterized more extensively to determine whether the genetic differences between these cell populations were reflected in properties related to neoplastic progression. The SBOT-4 cell line contained a BRAF mutation but seemed otherwise genetically stable, while the SBOT-3.1 cell line lacked KRAS and BRAF mutations but was genetically unstable.

Oncogenic forms of KRAS and BRAF, which are members of the RAS-RAF-mitogen/extracellular signal-regulated kinase (MEK), extracellular signal-regulated kinase (ERK), and mitogen-activated protein kinase (MAPK) cascade pathway, mediate cellular responses to growth signals and have been identified in many human cancers, including ovarian neoplasms. Activating mutations in *KRAS* and *BRAF* are usually found exclusive of one another, and occur in at least 60% of serous borderline tumors (36% B*RAF*, 30% *KRAS*) and low-grade ovarian tumours, but are uncommon in high-grade ovarian tumours (Singer *et al.*, 2003; Sieben *et al.*, 2004). The V600E mutation is a common one, accounting for at least 80% of *BRAF* mutations, and occurs in the kinase domain, which normally protects the substrate-binding site. Recent reports have shown that tumours with a mutation in either *BRAF* or *KRAS* were more sensitive to the MEK inhibitor CI-1040, for growth inhibition and apoptosis than those without such mutations (Collisson *et al.*, 2003; Pohl *et al.*, 2000). This raises the possibility of using drugs that target the RAS-RAF-MEK-MAPK cascade in the treatment of serous tumours with *BRAF* and *KRAS* mutations, which are generally not responsive to conventional chemotherapeutic agents. Thus, the different mutational status of the SBOT lines established in this study provides a

unique system with which to study the role of the RAS-RAF-MAPK cascade in ovarian cancer progression and therapy.

In contrast to the SBOT-4 cells, which had very few copy number alterations, the SBOT-3.1 cell line displayed numerical and structural cytogenetic abnormalities, with multiple chromosomal amplifications and losses that are important in ovarian neoplastic progression. Previous studies on the cytogenetics of SBOT have revealed multiple recurrent numerical chromosome abnormalities, however the cytogenetics of such cancers are less complex than those of high-grade serous carcinomas (Rao *et al.*, 2002), and SBOTs also differ from high-grade serous carcinomas in terms of gene expression (Bonome *et al.*, 2005; Ouellet *et al.*, 2005). Cytogenetic changes include but are not limited to gain of chromosome 8 and, to a lesser degree, gain of chromosome 12 (Wolf *et al.*, 1993; Helou *et al.*, 2006). It may be significant that aCGH analysis of SBOT-3.1 demonstrated a loss at the HRAS locus, which may have resulted in disregulated functions of the RAS gene family. A deletion of chromosomal region 1p36, as demonstrated by aCGH in SBOT-3.1 has previously been identified in numerous types of cancers (Zahn *et al.* 2006; Lahortiga *et al.*, 2006), including SBOT (Hu *et al.*, 2002), and is more common in poorly differentiated ovarian cancers than in well or moderately differentiated cases (Alvarez *et al.*, 2001). To the best of our knowledge the translocation observed in the SBOT-3.1 cell line is the first translocation observed in SBOT. Our initial analysis using mFISH and aCGH suggested that this was a balanced translocation. However, further analysis using a 385,000 oligonucleotide array (NimbleGen Systems Inc., Madison, WI) revealed this to be a complex rearrangement with multiple regions of loss on

both partner chromosomes. Taken together, the different genetic make-up of these two lines implicates either different etiologies or different stages of progression. The former explanation is supported by cytogenetic differences, such as the presence of a BRAF mutation in SBOT-4 only, while the latter explanation is supported by the occurrence of a low grade serous carcinoma in the other patient two years after SBOT-3 was obtained. SBOT-3 was harvested six years and SBOT-4 two years after the initial presentation and both had a low degree of genomic abnormalities compared to that reported for high grade serous tumors.

Interestingly, in spite of the major differences in their genetic make-up, the phenotypes of the two lines were strikingly similar, indicating that in many aspects, phenotypic regulation by environmental ad/or epigenetic influences predominated over the consequences of genetic variability.

In the course of neoplastic progression, epithelial ovarian carcinomas acquire morphological and functional characteristics of the specialized epithelia of Mullerian duct origin, *viz.* the oviduct, endometrium and endocervix *in vivo* (Auersperg *et al.*, 2001; Auersperg & Woo, 2004; Woo *et al.*, 2004) and in culture (Maines-Bandiera & Auersperg, 1997; Sundfeldt *et al.*, 1997; Bast *et al.*, 1998). In this study, such epithelial characteristics of the SBOT lines were readily apparent morphologically and as they expressed keratin, E-cadherin, CA-125, and OVGP1.

Another important event during the course of early neoplasia and cellular immortalization is the expression and activation of the catalytic subunit of human telomerase, hTERT (Kilian *et al.*, 1997; Meyerson *et al.*, 1997). Telomerase activity is present in most ovarian carcinomas, in 60-100% of SBOT and absent in most

benign cystadenomas (Datar *et al.*, 1999; Wan *et al.*, 1997). In our study, both the SBOT-3.1 and SBOT-4 cell lines tested positive for telomerase activity. Despite the activation of hTERT, only the SBOT-3.1 culture continued to grow for over 100 population doublings in comparison to 10-12 population doublings for SBOT-4 cells, suggesting that hTERT activation alone was insufficient to produce a permanent cell line. It should be noted, however, that most carcinoma specimens, of many origins, have limited life spans when explanted into culture, although most of them exhibit activated telomerase. Telomerase activation alone also expands the growth potential and prolongs the lifespan of human OSE in culture but does not result in permanent cell lines (Oishi *et al.*, 1998; Yang *et al.*, 2007a; Yang *et al.*, 2007b). Luo and colleagues (1997) found that transfection of SBOT cells with an adenoviral expression vector for SV40-T antigen also prolonged their lifespan but did not result in immortalization. It is most likely that the limited life spans of the SBOT cultures, as well as of other tumor cultures, are due, at least in part, to deficient tissue culture conditions. Histopathologically, it is clear that SBOTs *in vivo* are normally closely associated with their underlying stroma. The stromal microenvironment is a critical determinant of benign versus malignant growth in other tumour cell types (Cunha *et al.*, 2003; Kenny *et al.*, 2007). However, the role of stromal cells in the development and maintenance of the SBOT phenotype has not been previously studied. In this study, we briefly investigated the possible roles of stromal factors on cultured SBOT cells. We demonstrated that fibronectin, an extracellular matrix molecule which is normally synthesized and deposited by stromal fibroblasts, promoted adhesion of the SBOT cells while 3T3 feeder layers promoted SBOT cell growth. In addition,

cultured SBOT cells lacked the capacity to form tumours in immunodeficient mice which paralleled their anchorage dependence suggesting that these cells lack the capacity to supply the autocrine growth factors and/or extracellular matrix components that form the basis for anchorage independent growth and likely contribute to tumourigenicity *in vivo*. These results indicate that stromal influences may alter the behavior of SBOT cells and therefore, further investigation into the role of the microenvironment and in particular, the interaction between stroma and SBOT cells is warranted.

Despite the dependence on stromal factors for growth, the limited invasive capacity displayed by the SBOT cultures seemed to be independent of stromal factors, as the presence of isogenous fibroblasts in early passage cultures did not alter their invasive capacity (data not shown). The inability to invade appeared to be related to their limited cell motility but does not seem to be related to a lack of matrix-degrading proteinases as both lines expressed both proMMP2 and proMMP9, and the SBOT-4 cells also expressed uPA. MMP2 and MMP9 are produced by several ovarian carcinoma cell lines, but not in detectable amounts by normal OSE (Moser *et al.*, 1994), and uPA was reported to be expressed at levels 17 to 38 fold higher in malignant ovarian epithelial cells compared to normal ovarian epithelium (Young *et al.*, 1994). Previous studies have shown MMP2, MMP9, and uPA to be expressed in borderline ovarian tumours, but at lower levels compared to more malignant ovarian neoplasms (van der Burg *et al.*, 1996; Sakata *et al.*, 2000).

4.3 SV40 Early Region Genes Promote Neoplastic Progression of Serous Borderline Ovarian Tumour Cells

As mentioned previously, serous borderline ovarian tumours represent a unique model with which to study the mechanism of invasion in early ovarian cancer as the cells are in the early stages of tumourigenesis and are metaplastic but have not yet acquired the capacity to invade and to undergo malignant transformation. Recurrence of SBOT as a low-grade invasive carcinoma is associated with a significantly worse prognosis (Silva *et al.*, 2006). Relatively little is known, however, about the nature of SBOT and their relationship to invasive carcinoma, because, until recently, very few experimental systems for its study were available (Luo *et al.*, 1997; Lee *et al.*, 2005). Here, we report that in an attempt to immortalize cultured SBOT cells with SV40 LT and ST antigens, the cells lost their differentiated morphology and lost the expression of differentiation markers. The cells acquired other characteristics associated with increased neoplastic progression including anchorage-independence, motility and invasiveness.

Transformation of the SBOT cells to a more aggressive phenotype may, in part, be mediated by p53 and protein phosphatase 2A (PP2A), targets of the SV40 early genes. It is firmly established that LT antigen contributes to cell transformation by inactivating the p53 and the retinoblastoma protein (pRB) tumour suppressor proteins (Ahuja *et al.*, 2005; Arroyo & Hahn, 2005). These proteins have been studied principally for their functions in cell cycle arrest and apoptosis. Growing evidence suggests that perturbation of these pathways, in particular p53, not only modulates their anti-proliferative activities, but also has a potential role in cell

motility, a crucial step in invasion and metastasis (Arroyo & Hahn, 2005; Roger *et al.*, 2006). The unconventional role of p53 in the regulation of cell migration is largely mediated through the regulation of Rho GTPases, thereby controlling actin cytoskeletal organization and EMT which participates in the progression of epithelial tumors (Lozano *et al.*, 2003). Our observations also showed that SV40 induced a morphologic change in the SBOT cells, suggestive of EMT. In addition, we found that the cells lost the epithelial marker, E-cadherin, while gaining the mesenchymal marker, N-cadherin. These results are particularly interesting in view of recent observations indicating that the transition from SBOT to low-grade invasive carcinomas is associated with a reduction of p53 (Bonome *et al.*, 2005) which is one of the genes inactivated by LT antigen. They suggest that p53 and p53-modulated genes may be responsible for maintaining the distinct phenotype of these non-invasive, low-proliferative cancers. In addition to p53, PP2A which is targeted by ST antigen, may also mediate the cell motility effects observed in the SBOT cells (Arroyo & Hahn, 2005). PP2A is required for the proper localization of E-cadherin and β-catenin to the plasma membrane (Gotz *et al.*, 2000). Taken together these results suggest that inactivation of p53, and possibly PP2A, may play a critical role in the enhanced migratory and invasive activity of SBOT cells and therefore contribute to the progression of invasive ovarian cancers.

The different SBOT and ISBOT lines expressed varying proteinase levels, but we found no association between neoplastic characteristics and the expression of the three proteinases. Luo and colleagues (1997) found that uPA and tPA were secreted by ovarian carcinoma cells when compared to borderline tumour cells transfected

with SV40 T-antigen suggesting that uPA and tPA may play a role in the malignant phenotype. However, in our system, the ISBOT lines were able to invade regardless of uPA activity.

The invasive phenotype was accompanied by a transition from E- to N-cadherin expression which is characteristic of EMT. N-cadherin may play an important role in the cell migration of SBOT cells as it can promote motility and invasion in other epithelial cell types, including breast carcinoma and oral squamous cell carcinoma-derived cells (Islam *et al.*, 1996; Hazan *et al.*, 1997; Nieman *et al.*, 1999). To test this hypothesis, N-cadherin was transiently expressed in SBOT cells, but such forced expression of N-cadherin was not sufficient to generate an invasive phenotype. It is possible that the exogenous expression of N-cadherin using an adenoviral approach did not induce long-term changes to the cells vital for EMT and the invasive process. It was observed, however, that N-cadherin induced cell spreading as the colony morphology was less compact and the internuclear distances were greater in the N-cadherin overexpressing cells (Savagner *et al.*, 2005.). However, this may not have been sufficient to induce invasion as EMT is a process involving not only the expression of N-cadherin, but also changes to the cytoskeleton and, usually, loss of E-cadherin. In many epithelial tumours, E-cadherin is down-regulated (Schipper *et al.*, 1991; Bringuier *et al.*, 1993; Dorudi *et al.*, 1993; Mayer *et al.*, 1993; Oka *et al.*, 1993; Umbas *et al.*, 1994). It is well established that the loss of the adhesive function of E-cadherin and disruption of its downstream pathways is a critical step in the promotion of epithelial cells to an invasive phenotype. Exogenous expression of N-cadherin can induce the invasive process, concomitant with or

without a reduction in E-cadherin levels (Hazan *et al.*, 1997; Nieman *et al.*, 1999; Hazan *et al.*, 2000). In this study, overexpression of N-cadherin in the SBOT cells did not alter E-cadherin levels. Our study also showed that blocking E-cadherin was also insufficient in promoting invasion. Down-regulation of E-cadherin, possibly in conjunction with N-cadherin expression, may be necessary for enhanced motility and invasiveness of this cell type and therefore, warrants further investigation.

4.4 Oviduct-Specific Glycoprotein is A New Differentiation-Based Indicator of Early Ovarian Epithelial Neoplasia

The tendency for OSE to undergo aberrant Mullerian differentiation during tumorigenesis led us to examine the expression of a specific differentiation marker for oviductal epithelium, oviduct-specific glycoprotein (OVGP1), in normal and neoplastic OSE. Using the polyclonal OGP antibody, OVGP1 was absent in normal OSE, present in inclusion cysts and in the majority of benign and borderline serous tumours, but absent in most invasive serous adenocarcinomas. The expression of OVGP1 was almost entirely limited to ovarian neoplasms. This specificity may help to distinguish ovarian tumours from those originating at other sites.

Developmentally, OSE arises from the mesodermal coelomic epithelium, as do the Mullerian duct-derived epithelia of the oviduct, endometrium, and endocervix. However, unlike these latter complex tissues, OSE lacks many of their differentiated epithelial markers (Auersperg *et al.*, 2001). Possibly the most important differentiation marker discovered to date is CA125, which has clinically proven to be an important diagnostic tool for ovarian cancer (Bast *et al.*, 1998). In this report, we

have focused on another protein, OVGP1 which, like CA125, is a highly glycosylated secreted protein (Verhage *et al.*, 1998). Unlike CA125, OVGP1 expression in Mullerian duct-derived normal epithelia is almost entirely limited to the oviduct (Arias *et al.*, 1994), except for rare glands in the basalis layer of the endometrium (Woo et al., 2004b). We have shown that OVGP1, like CA125, is absent in OSE but present in metaplastic OSE lining epithelial inclusion cysts which have undergone tubal differentiation, and in the majority of benign cystadenomas and borderline tumours. However, whereas CA125 is present in the majority of ovarian serous carcinomas (Bast *et al.*, 1998), the expression of OVGP1 is rare in these neoplasms.

Although our results show that the highest proportion (63%) of invasive serous adenocarcinomas that express OVGP1 is grade 1, this value is based on too few cases to warrant conclusions about its significance. However, since OVGP1 is also expressed in most epithelial inclusion cysts, which are believed to be the preferential sites for the initiation of malignant transformation (Scully, 2000; Auersperg *et al.*, 2001), OVGP1 may also represent an early indicator of neoplastic events. A study of additional low-grade serous carcinomas is required to examine this possibility. The proportion of benign and borderline serous epithelial tumours that progress to high-grade invasive neoplasms is still not defined but may be quite low (Scully, 2000; Scully *et al.*, 1998; Hu *et al.*, 2002). Yet, benign and borderline serous tumours adopt a similar phenotype to serous adenocarcinomas in terms of tubal differentiation, suggesting that the common mechanisms which regulate differentiation in all these tumour types diverge from those responsible for the invasive phenotype.

The ectopic expression of OVGP1 in ovarian epithelial tumours further supports the idea that OSE is a developmentally immature epithelium, which has retained the capacity to alter its state of differentiation under physiologic and pathologic conditions (Auersperg *et al.*, 2001; Auersperg & Woo, 2004). On the other hand, expression of OVGP1 may also indicate a tubal origin of serous carcinomas, in particular the high-grade serous carcinomas, whereby the neoplastic cells have retained this differentiation marker. It has been postulated that epithelial inclusion cysts may arise from epithelial cells of the fimbria which have seeded onto the ovarian surface and later become incorporated into the stroma (Piek *et al.*, 2004). In this regard, it is conceivable that OVGP1 expressed in the columnar epithelial cells of inclusion cysts observed in this study may be of tubal origin, rather than of metaplastic OSE, and that the weak or lack of OVGP1 staining in cuboidal and squamous cells may indicate the ovarian surface epithelium as the source of these cysts. However, there is little other data to support a tubal origin for low-grade ovarian tumours which are believed to arise from the ovary. Low-grade tumours are more likely to be discovered in the substance of the ovary, and are often confined to one or more cysts. It is known that the pathogenesis of low-grade serous tumours are distinct from high-grade serous carcinomas (Shih & Kurman, 2004) which has been attributed to distinct alterations in molecular pathways but may also indicate a difference in tissue of origin. Thus, OVGP1 staining in serous cystadenomas, serous borderline tumours and low-grade serous tumours would support the hypothesis that OSE gains properties of Mullerian duct epithelium during ovarian neoplasia.

4.5 Oviduct-Specific Glycoprotein: An Early Detection Marker for Ovarian Cancer?

Based on our immunohistochemical study of OVGP1 in ovarian tumour tissues using the polyclonal OGP antibody, we hypothesized that OVGP1 may be secreted and therefore, may be a potential serum marker for ovarian cancer. We recently established a new monoclonal antibody, clone 7E10, against OVGP1 for the development of a serum-based assay. Clone 7E10 recognizes the C-terminal region of OVGP1. It is specific as indicated by the exclusive binding of the antibody to the secretory epithelial cells of the mid- to late-proliferative phase oviduct. By Western blot analysis, clone 7E10 recognizes a specific band in the region between 110-130 kDa, the correct size of OVGP1. Using the new monoclonal antibody, preliminary results show that expression of OVGP1 is associated with a more favourable outcome among the high-grade serous carcinoma group of patients. It is not clear whether the expression of OVGP1 is related to stage as five-year survival rates for grade 3 disease range from 64% for early stage (I and II) to 19% for late stage (III and IV) disease (Pecorelli *et al.*, 1998). The findings in the high grade serous carcinoma group did not apply to the endometrioid type of ovarian carcinomas. Generally speaking, the histology of the carcinoma is not of prognostic significance except for clear cell carcinomas, which are associated with a worse prognosis than the other histologic types (Silverberg, 1989). It has also been suggested that high-grade serous carcinomas and high grade endometrioid carcinomas can be clustered together as a single entity as there are no differences between the two in terms of treatment and outcome (Gilks, 2004). Our results suggest that the two histological subtypes are

different biologically. It is not clear as to why only a portion of the high-grade serous carcinomas express OVGP1 or how OVGP1 is regulated in high-grade serous carcinomas. It may be that OVGP1 is detecting the more differentiated carcinomas within this group.

We do know that there is an intimate relationship between estrogen and the expression of OVGP1 based on both the results of this report on endometrial cancer (Woo *et al.*, 2004b) and the results of others in the fallopian tube epithelium (O'Day-Bowman *et al.*, 1995; Agarwal *et al.*, 2002; Lok *et al.*, 2002). Whether the expression of OVGP1 is related to estrogen responsiveness in the high grade serous carcinomas remains to be determined. In addition, whether this translates to an effective treatment option is also unclear, as hormonal therapy is not used for ovarian carcinoma because it is usually ineffective despite frequent estrogen receptor expression by tumour cells (reviewed in Zheng *et al.*, 2007). On the other hand, there have been studies that have used the anti-estrogen tamoxifen to treat chemo-resistant ovarian cancer (Hatch *et al.*, 1991; Ahlgren *et al.*, 1993) and more recently, the aromatase inhibitor, Letrozole, which inhibits estrogen synthesis, confers clinical benefit in a sub-group of ovarian cancer patients (Bowman *et al.*, 2002; Papadimitriou *et al.*, 2004; Smyth *et al.*, 2007). Therefore, a second look at the role of estrogen in ovarian cancer may be warranted.

Ultimately, our goal is to determine whether OVGP1 can be used as an early detection marker for ovarian cancer. Using an ELISA-based assay, OVGP1 was detected in the serum from the majority of low-grade ovarian carcinoma cases and in about half of the borderline tumour cases. It appeared to be relatively specific as

serum from women with endometrial cancer and other cancers did not have elevated levels of the protein. Efforts are now underway to collect serum from a larger number of cases from normal controls as well as patients with ovarian cancer, in particular those with low-grade disease.

4.6 Gain of Oviduct-Specific Glycoprotein is Associated with the Development of Endometrial Hyperplasia and Endometrial Cancer

On the basis of the present study of normal, hyperplastic, and malignant endometrial tissues, it appears that a gain of OVGP1 begins under conditions of unopposed estrogen exposure, which is a known risk factor for the development of endometrioid carcinoma.

Although OVGP1 is not normally a secretory product of the normal endometrium, we observed focal staining of the stem cells in the basalis layer with some staining in adjacent glands in the functionalis layer (Rapisarda *et al.*, 1993). The epithelial cells in the functionalis layer shed each month and regenerate during the next menstrual cycle through proliferation of epithelial cells in the intact basalis layer. It has been proposed that genetic alterations that induce endometrial cancer are acquired sequentially by the nonshedding stem cells (Tanaka *et al.*, 2003). Whether the ectopic expression of OVGP1 observed in the stem cells of the normal endometrium is indicative of early changes in endometrial carcinogenesis is not known, but other studies have shown that overtly normal endometrium can harbour genetic and/or epigenetic alterations of genes such as MLH1 and PTEN, which are common in endometrial cancer (Kanaya *et al.*, 2003, Mutter *et al.*, 2000). In this

study, we showed that there was a significant correlation between gain of OVGP1 and loss of PTEN in endometrioid carcinoma. It would be interesting to determine whether OVGP1 is expressed in the same glands where PTEN is inactivated, which would suggest a mechanistic link between loss of PTEN and OVGP1 expression. Another possible factor for contributing to the ectopic expression of OVGP1 in the endometrial basalis could be the close embryonic relationship between the endometrial epithelial cells and oviductal epithelial cells (Auersperg & Woo, 2004). Both are derived from Mullerian-duct epithelia, which in turn originate from the coelomic epithelium, and thus, the stem cells of the basalis may be less differentiated and have retained properties similar to the common embryonic precursor.

In the normal oviduct, OVGP1 secretion is driven by estrogen and changes cyclically during the menstrual cycle (O'Day-Bowman *et al.*, 1996). In this study, we did not observe any significant changes in the levels of OVGP1 in normal endometrial tissues with the menstrual cycle. However, there was a gain in OVGP1 under conditions of prolonged estrogen exposure as indicated by the significantly higher staining indices observed in nonatypical and atypical hyperplastic endometrial tissues compared to normal endometrium. Characterization of the human OVGP1 promoter has revealed eight half-estrogen-responsive elements and an imperfect estrogen-responsive element (Agarwal *et al.*, 2002). Despite the presence of estrogen and its receptors in normal endometrium, it may be insufficient for activation of OVGP1 under normal cycling estrogen levels. This may be due to variations in the relative levels of ER coactivators or corepressors in endometrial epithelium compared with oviductal epithelium (Jordan *et al.*, 2004). However, a recent study showed that

the expression of the coactivators SRC-1 and p300/CBP decreased in endometrial hyperplasia, whereas the corepressor NcoR was elevated (Uchikawa *et al.*, 2003). Despite the lower levels of coactivators and higher levels of the corepressor, Uchikawa *et al.* (2003) showed a topologic correlation between the expression of ER and SRC-1, suggesting that hyperplasias remain responsive to estrogen. On the basis of these findings, we propose that it may be the exposure to prolonged estrogen that is stimulating the ectopic expression of OVGP1 in hyperplasias. With carcinogenesis, there is a dissocation of ER from its coactivators, as well as methylation of ER rendering it inactive (Uchikawa *et al.*, 2003; Sasaki *et al.*, 2001). Thus, many endometrial carcinomas no longer respond to estrogen, which may explain the decrease in levels of OVGP1 expression with progression to carcinoma. Another possibility for the difference in OVGP1 secretion between normal endometrial and oviductal epithelium may be that coactivator interactions are site-specific (Shang & Brown, 2002). Transfection studies have shown a lack of transactivation activity of the OVGP1 gene in ER-positive breast cells, whereas immortalized oviductal cells showed OVGP1 protein activity (Agarwal *et al.*, 2002).

With progression to cancer, there was a significant decrease in OVGP1 expression when compared with hyperplasias, with a significant difference in staining index comparing atypical hyperplasia and well-differentiated endometrioid carcinoma. This raises the possibility of using OVGP1 immunostaining as a diagnostic adjunct. The differences in staining, although statistically significant, are not absolute, and OVGP1 would not be of diagnostic use in individual cases as a single immunomarker. Conceivably, it could be part of a panel of immunomarkers

that could be used to more accurately classify premalignant and early malignant change in the endometrium, improving on the current irreproducible histologic classification system. Comparison of low-grade and high-grade endometrioid endometrial cancers showed a significant difference in OVGP1 staining. In cases from the endometrial cancer tissue microarray, all of the strongly positive tumours were grade 1 with 100% of these patients (n = 11) surviving for at least 11 years. Use of tissue microarrays does not detect all OVGP1 positive tumours as the staining is frequently focal, as seen in the higher frequency of OVGP1 immunostaining in the endometrial cancer cases in which whole sections, rather than 0.6-mm tissue microarray cores, were examined.

These findings indicate that although OVGP1 is differentially expressed during the transformation of endometrial hyperplasia and development of endometrioid carcinoma, it appears to be unrelated to uterine papillary serous carcinoma. Additional studies are required to examine whether the ectopic expression of OVGP1 in the stem cells of histologically normal endometria may indicate early preneoplastic changes.

4.7 Summary

In summary, epithelial ovarian tumors adopt a Mullerian-differentiated phenotype as demonstrated by the ability of metaplastic/neoplastic OSE cells to undergo branching morphogenesis, the differentiated characteristics of SBOT cells in culture, and the presence of OVGP1 in the majority of well-differentiated serous ovarian tumors.

Although this study showed that branching morphogenesis is a part of ovarian neoplastic progression, the factors which regulate this process is not known. Despite the importance of HGF in the branching morphogenesis of other epithelial tissues and the appearance of E-cadherin in Mullerian-differentiated OSE, it appears that E-cadherin and HGF are neither sufficient nor necessary for the glandular differentiation of OSE cells. In addition, retinoic acid appeared to inhibit growth of OSE cells but did not induce differentiation. Therefore, investigating other mechanisms underlying Mullerian differentiation will be important to better understand the etiology of epithelial ovarian neoplasias. As mentioned previously, cues for the malignant potential of OSE may be uncovered by examining the developmental process of OSE and tubal epithelium. A number of genes, such as the homeobox family of genes, are involved in the development of the Mullerian epithelia. A recent study by Naora's group showed that HOXA9, which normally controls differentiation of the Mullerian duct into the fallopian tube, when introduced into an undifferentiated mouse tumour gave rise to papillary tumours resembling serous EOCS (Cheng *et al.*, 2005). In addition, HOXA10 and HOXA11, which normally regulate formation of the uterus and cervix, respectively, were able to induce morphogenesis of endometrioid-like and mucinous-like EOCs. These results suggest that inappropriate inactivation of a molecular program that controls patterning of the reproductive tract could explain the morphologic heterogeneity of EOCs and their assumption of Mullerian-like features (Cheng *et al.*, 2005). Perhaps one of the most crucial question in this study is how enhanced Mullerian differentiation could promote the progression of ovarian carcinogenesis. Using the 3-dimensional collagen

gel assay, OSE at different stages of progression, including SBOTs established in this study, can be cultured and examined for the changes that occur during differentiation and neoplasia.

The study of SBOT cultures *in vitro* showed that in spite of their diverse genotypes, the SBOT cultures resembled one another in terms of morphology, differentiation markers, telomerase activity, protease secretion, lack of invasiveness, limited motility and dependence on stromal factors for growth. The last three characteristics also distinguished them from most ovarian cancer lines and thus mimicked their *in vivo* phenotype, thereby providing a model for studying the nature of this disease and the mechanisms involved in progression to invasive cancer. As SBOT is a disease where residual tumor or recurrence of the tumour is not uncommon but is unresponsive to treatment, the permanent line, SBOT 3.1, also provides a useful tool for helping to identify and evaluate new therapeutic targets.

Although it remains in question whether SBOTs are precursors of ovarian serous adenocarcinomas, our study suggests that at least under experimental conditions SBOT cells have the potential to progress to a more invasive phenotype. Our results indicate, however, that neither disruption of the growth pattern (by trypsinization prior to seeding for invasion assays) nor manipulations of the cadherin profile (exogenous introduction of N-cadherin or blocking E-cadherin) induced invasiveness. Thus, Mullerian differentiation does not directly prevent invasiveness, but it diminishes in parallel with invasion caused by other factors. The lack of invasiveness by SBOT cells may depend on factors that regulate motlity. We have demonstrated that SBOT cells cultured *in vitro* can acquire the ability to undergo cell

migration which is an important process in invasion and metastasis. This may be mediated by the effects of SV40 LT and ST antigens on p53 and PP2A, respectively, which induces EMT in the cells leading to a transition from E-cadherin to N-cadherin and increased cell motility and invasiveness, as well as anchorage-independence. Although the precise mechanism by which SV40 LT and ST antigens promote ovarian cancer cell migration has yet to be defined, these lines provide a unique opportunity to study the pathways targeted by SV40 LT and ST antigen which are important in the invasive process. Further pursuit of the mechanisms underlying invasion in ovarian cancer may help to uncover better markers for predicting tumours that progress to a more aggressive and lethal invasive ovarian cancer.

Our study of Mullerian epithelial differentiation markers led to the identification of OVGP1 as a possible early detection marker for ovarian cancer. Only a small number of grade 1 serous adenocarcinomas have been examined to date; however, a high proportion of these tumours expresses OVGP1, and its consistent presence in metaplastic inclusion cysts suggests that this marker may be an indicator of early events in ovarian carcinogenesis. The presence of an oviductal differentiation marker supports the hypothesis that OSE cells that become entrapped in the ovarian stroma undergo Mullerian metaplasia. On the other hand, if the fallopian tube epithelium is believed to be the source of epithelial ovarian cancer, then the presence of OVGP1 would support the postulation that inclusion cysts are derived from oviductal epithelial cells, especially those on the fimbria that come in close contact with the ovarian surface, which are sometimes seeded on the ovarian

surface and are subsequently included within the ovarian stroma (Piek *et al.*, 2001; Piek *et al.*, 2004).

Our findings on OVGP1 expression in ovarian tumour tissues, led us to develop a new monoclonal antibody for OVGP1 which will be useful for the further study of this protein in not only ovarian and endometrial cancer, but also in reproductive biology. In comparison to the polyclonal anti-human OGP antibody, the 7E10 clone positively stains a larger portion of high-grade ovarian tumours. However, OVGP1 was not detectable in the sera of patients with high-grade serous carcinomas. A possible explanation may be that low-grade ovarian tumours have the ability to secrete the protein as they have polarized epithelia whereas high-grade cancers have a disorganized epithelium and lack the ability to secrete. Others have shown that the distribution and glycosylation of another glycoprotein or mucin, MUC1, in tumour cells differ substantially from that found in normal tissue. Whereas MUC1 is found apically in normal polarized glandular epithelia, it is often expressed in an unorganized fashion throughout the cells in tumours where the architecture of the tissues is usually disrupted (Barratt-Boyes, 1996). MUC1 is also usually underglycosylated in tumours. There are fewer and less complex carbohydrate side chains (Lloyd *et al.*, 1996). This increased production of aberrantly glycosylated mucins has also been observed in ovarian tumours (Yazawa *et al.*, 1986; Dong *et al.*, 1997; Giuntoli *et al.*, 1998). In other tumour tissues, aberrant glycosylation has been implicated in increasing metastatic potential (Wesseling *et al.*, 1995; Regimbald *et al.*, 1996; Wesseling *et al.*, 1996). It will be of interest to determine whether OVGP1, which is also a mucin (MUC9), is differentially glycosylated in ovarian carcinomas,

especially serous carcinomas. Our results indicate that by Western blot analysis, the polyclonal OGP antibody recognizes a high molecular weight protein between 110-130 kDa whereas the anti-His and Rho-1D4 antibodies can detect, in addition to the higher molecular weight form of the protein, a lower molecular weight band at approximately 75 kDa. We speculate that the lower molecular weight band corresponds to the naked form of the protein. Thus, if the polyclonal antibody recognizes primarily the glycosylated form of the protein and if OVGP1 is aberrantly glycosylated in high-grade invasive carcinomas, it is conceivable that only a small proportion of high-grade invasive carcinomas would be positively stained for OVGP1 using the polyclonal OGP antibody. Furthermore, the staining pattern of the polyclonal OGP antibody in the secretory epithelial cells is apical whereas clone 7E10 binds to OVGP1 in the entire cytoplasmic region of the cells. We speculate that the polyclonal OGP antibody identifies OVGP1 localized in the secretory granules in the apical region of the cells or on the periphery outside the cells. In contrast, clone 7E10, which recognizes the C-terminal portion of the core protein, stains OVGP1 throughout the secretory epithelial cells as OVGP1 is being synthesized by the endoplasmic reticulum, processed by the Golgi, and transported out of the cell. These findings may implicate aberrant glycosylation or underglycosylation of OVGP1 in high-grade invasive ovarian cancers, and thus, although it is detectable in tissues, it may not be secreted by these cells, and therefore, undetectable in serum.

Functionally, OVGP1 is believed to play an important role in early fertilization events within the oviduct via binding to the zona pellucida of oocytes and embryos (Verhage *et al.*, 1997; McCauley *et al.*, 2003; O'Day-Bowman *et al.*, 2002).

We observed that OVGP1 staining was present in the lumen and surface of cysts and glandular structures of low-grade ovarian tumours, and OVGP1 could be detected in the serum from low-grade ovarian cancers, indicating that it is also secreted. In the oviduct, OVGP1 likely increases the viscosity of the luminal fluid, which in turn would stabilize the microenvironment immediately surrounding the gametes and embryo, thereby preventing dispersal of essential nutrients and ions (Buhi *et al.*, 2002). OVGP1 within the complex papillary structure of the normal oviduct and of the low-grade serous tumours may similarly contribute to a microenvironment where there is an accumulation of growth promoting factors. However, in high-grade ovarian adenocarcinomas, where OVGP1 is most probably retained within the cell rather than being secreted, it raises the possibility that the cells have acquired increased autonomy and thus no longer require OVGP1 to facilitate their growth. This would also hold true if the source of high-grade serous carcinomas, as some have speculated, is the fallopian tube epithelium. It would indicate that OVGP1 is lost during the transformation from normal oviductal epithelium to high-grade serous adenocarcinomas, suggesting dedifferentiation of the oviductal epithelium. Mucins in other cancers play significant roles in tumour development. For instance, as mucins act as a protective barrier for epithelium, it may contribute to tumour progression by allowing tumor cells to evade immune recognition. In pancreatic cancer, MUC1 and MUC4 are upregulated and are no longer strictly apically localized. Together, the steric hindrance disrupts cell-cell and cell-matrix interactions which facilitates migration and metastasis (Komatsu *et al.*, 1997). In addition, overexpression of MUC1 leads to an increase in the interaction via its cytoplasmic tail with β-catenin,

which disrupts β-catenin and E-cadherin interactions (Li *et al.*, 1998). This results in the disruption of cell-cell contacts and therefore, facilitates the release of the tumour cell from the tissue. Interestingly, recent reports by Kadam *et al.* (2006, 2007) shows that OVGP1 binds directly to non-muscle myosin type IIA, a cytoskeletal protein which regulates cell shape and polarity, in gametes and oviduct. Kadam *et al.* (2007) also showed that OVGP1 can be localized to the tight junctions in differentiating oviductal epithelial cells. This interaction may occur via a PDZ-binding domain in OVGP1. There is growing evidence which shows that mucins, in particular transmembrane mucins, are directly involved in intracellular signaling events through their interactions with signaling molecules and growth factor receptors (Carraway *et al.*, 2007). MUC9 is believed to be part of the secretory group of mucins but recent findings of Kadam *et al.* (2007) indicate that OVGP1 has domains that might enable it to be recruited to intracellular sites other than the secretory pathway.

The question of whether ovarian cancer originates in the ovarian surface epithelium or in tubal epithelium is intriguing and remains in debate but what is clear is that the tubal differentiation marker, OVGP1, is differentially regulated during ovarian neoplasia. Thus, further studies on the expression of OVGP1 in high-grade serous carcinomas and its relation to other events such as stage or the presence of ER would provide further clues as to the prognostic significance of this protein and the mechanisms which regulate it. The five-year overall survival rate of grade 3 ovarian cancers is 75% for early stage disease and 28.5% for late stage disease (Heintz *et al.*, 2006). Thus, it will be important to determine whether OVGP1 is also correlated to the stage of disease. If OVGP1 is correlated with early stage disease, then the use of

this protein in conjunction with CA125, which detects mainly late stage disease, will be particularly interesting as the two markers would be able to detect the majority of ovarian cancers, regardless of progression. In addition, it will be interesting to demonstrate whether ER is related to OVGP1 expression in high-grade serous carcinomas. This is of particular interest since our finding on OVGP1 in endometrial cancer suggested that a gain of OVGP1 begins under conditions of unopposed estrogen exposure, a known risk factor for the development of endometrioid endometrial cancer. A number of studies have demonstrated the presence of ERα and ERβ in epithelial ovarian cancer cells (Sakaguchi *et al.*, 2002; Bardin *et al.*, 2004; Cunat *et al.*, 2004; Lindgren *et al.*, 2004; O'Donnell *et al.*, 2005). Most of these studies have implicated the proliferative response of estrogen to ERα (Cunat *et al.*, 2004; O'Donnell *et al.*, 2005). Bardin *et al.* (2004) showed that ERβ expression strongly inhibited cell proliferation and cell motility, in addition to playing a proapoptotic role. These findings are particularly interesting since ERβ binds to the promoter region of OVGP1 in oviductal epithelial cells (Agarwal *et al.*, 2002). Together, these findings suggest a possible mechanism by which OVGP1 may play a protective role in high-grade serous carcinomas and thus, possibly explain the better prognosis of patients expressing OVGP1 in their tumours. However, the function of OVGP1 in ovarian cancer awaits further investigation.

Despite the dismal prognosis for women with ovarian cancer, there have been no recent advances in the therapeutic treatment for these women or the development of a reliable test for detection. Based on the hypothesis that Mullerian differentiation accompanies ovarian neoplastic progression, our findings on the morphogenesis of

neoplastic OSE and the characterization of SBOT cells *in vitro* have furthered our understanding of the development of this disease and provide a model for testing and identifying new therapeutic targets. It is our hope that OVGP1 may provide us with a new predictive marker for epithelial ovarian cancer which will detect early stages of this disease and hopefully, help save the lives of thousands of women.

5. REFERENCES

1. Agarwal, A., Yeung, W. S., and Lee, K. F. Cloning and characterization of the human oviduct-specific glycoprotein (HuOGP) gene promoter. Mol Hum Reprod, *8:* 167-175, 2002.
2. Ahlgren, J. D., Ellison, N. M., Gottlieb, R. J., Laluna, F., Lokich, J. J., Sinclair, P. R., Ueno, W., Wampler, G. L., Yeung, K. Y., Alt, D., and et al. Hormonal palliation of chemoresistant ovarian cancer: three consecutive phase II trials of the Mid-Atlantic Oncology Program. J Clin Oncol, *11:* 1957-1968, 1993.
3. Ahuja, D., Saenz-Robles, M. T., and Pipas, J. M. SV40 large T antigen targets multiple cellular pathways to elicit cellular transformation. Oncogene, *24:* 7729-7745, 2005.
4. Albini, A., Iwamoto, Y., Kleinman, H. K., Martin, G. R., Aaronson, S. A., Kozlowski, J. M., and McEwan, R. N. A rapid in vitro assay for quantitating the invasive potential of tumor cells. Cancer Res, *47:* 3239-3245, 1987.
5. Alkushi, A., Irving, J., Hsu, F., Dupuis, B., Liu, C. L., Rijn, M., and Gilks, C. B. Immunoprofile of cervical and endometrial adenocarcinomas using a tissue microarray. Virchows Arch, *442:* 271-277, 2003.
6. Alvarez, A. A., Lambers, A. R., Lancaster, J. M., Maxwell, G. L., Ali, S., Gumbs, C., Berchuck, A., and Futreal, P. A. Allele loss on chromosome 1p36 in epithelial ovarian cancers. Gynecol Oncol, *82:* 94-98, 2001.
7. Alvero, A. B., Fishman, D. A., Qumsiyeh, M. B., Garg, M., Kacinski, B. M., and Sapi, E. Telomerase prolongs the lifespan of normal human ovarian surface epithelial cells without inducing neoplastic phenotype. J Soc Gynecol Investig, *11:* 553-561, 2004.
8. Araki, Y., Nohara, M., Yoshida-Komiya, H., Kuramochi, T., Ito, M., Hoshi, H., Shinkai, Y., and Sendai, Y. Effect of a null mutation of the oviduct-specific glycoprotein gene on mouse fertilization. Biochem J, *374:* 551-557, 2003.
9. Arias, E. B., Verhage, H. G., and Jaffe, R. C. Complementary deoxyribonucleic acid cloning and molecular characterization of an estrogen-dependent human oviductal glycoprotein. Biol Reprod, *51:* 685-694, 1994.
10. Arroyo, J. D. and Hahn, W. C. Involvement of PP2A in viral and cellular transformation. Oncogene, *24:* 7746-7755, 2005.
11. Auersperg, N. Histogenetic behavior of tumors. I. Morphologic variation in vitro and in vivo of two related human carcinoma cell lines. J Natl Cancer Inst, *43:* 151-173, 1969.
12. Auersperg, N., Maines-Bandiera, S. L., Dyck, H. G., and Kruk, P. A. Characterization of cultured human ovarian surface epithelial cells: phenotypic plasticity and premalignant changes. Lab Invest, *71:* 510-518, 1994.
13. Auersperg, N., Pan, J., Grove, B. D., Peterson, T., Fisher, J., Maines-Bandiera, S., Somasiri, A., and Roskelley, C. D. E-cadherin induces mesenchymal-to-epithelial transition in human ovarian surface epithelium. Proc Natl Acad Sci U S A, *96:* 6249-6254, 1999.

14. Auersperg, N., Wong, A. S., Choi, K. C., Kang, S. K., and Leung, P. C. Ovarian surface epithelium: biology, endocrinology, and pathology. Endocr Rev, *22:* 255-288, 2001.
15. Auersperg, N. and Woo, M. M. Development and differentiation of ovarian surface epithelium: cues for the basis of its malignant potential., 2nd edition, p. 579-588. San Diego: Elsevier Academic Press, 2004.
16. Balconi, G., Broggini, M., Erba, E., D'Incalci, M., Colombo, N., Mangioni, C., and Bertolero, F. Human ovarian tumors in primary culture: growth, characterization and initial evaluation of the response to cis platinum treatment in vitro. Int J Cancer, *41:* 809-818, 1988.
17. Bardin, A., Hoffmann, P., Boulle, N., Katsaros, D., Vignon, F., Pujol, P., and Lazennec, G. Involvement of estrogen receptor beta in ovarian carcinogenesis. Cancer Res, *64:* 5861-5869, 2004.
18. Barratt-Boyes, S. M. Making the most of mucin: a novel target for tumor immunotherapy. Cancer Immunol Immunother, *43:* 142-151, 1996.
19. Bast, R. C., Jr., Urban, N., Shridhar, V., Smith, D., Zhang, Z., Skates, S., Lu, K., Liu, J., Fishman, D., and Mills, G. Early detection of ovarian cancer: promise and reality. Cancer Treat Res, *107:* 61-97, 2002.
20. Bast, R. C., Jr., Xu, F. J., Yu, Y. H., Barnhill, S., Zhang, Z., and Mills, G. B. CA 125: the past and the future. Int J Biol Markers, *13:* 179-187, 1998.
21. Birk, O. S., Casiano, D. E., Wassif, C. A., Cogliati, T., Zhao, L., Zhao, Y., Grinberg, A., Huang, S., Kreidberg, J. A., Parker, K. L., Porter, F. D., and Westphal, H. The LIM homeobox gene Lhx9 is essential for mouse gonad formation. Nature, *403:* 909-913, 2000.
22. Bleau, G., Massicotte, F., Merlen, Y., and Boisvert, C. Mammalian chitinase-like proteins. Exs, *87:* 211-221, 1999.
23. Blegen, H., Einhorn, N., Sjovall, K., Roschke, A., Ghadimi, B. M., McShane, L. M., Nilsson, B., Shah, K., Ried, T., and Auer, G. Prognostic significance of cell cycle proteins and genomic instability in borderline, early and advanced stage ovarian carcinomas. Int J Gynecol Cancer, *10:* 477-487, 2000.
24. Boatman, D. E., Felson, S. E., and Kimura, J. Changes in morphology, sperm penetration and fertilization of ovulated hamster eggs induced by oviductal exposure. Hum Reprod, *9:* 519-526, 1994.
25. Boice, M. L., McCarthy, T. J., Mavrogianis, P. A., Fazlebas, A. T., and Verhage, H. G. Localization of oviductal glycoproteins within the zona pellucida and perivitelline space of ovulated ova and early embryos in baboons (Papio anubis). Biol Reprod, *43:* 340-346, 1990.
26. Bonome, T., Lee, J. Y., Park, D. C., Radonovich, M., Pise-Masison, C., Brady, J., Gardner, G. J., Hao, K., Wong, W. H., Barrett, J. C., Lu, K. H., Sood, A. K., Gershenson, D. M., Mok, S. C., and Birrer, M. J. Expression profiling of serous low malignant potential, low-grade, and high-grade tumors of the ovary. Cancer Res, *65:* 10602-10612, 2005.
27. Booth, M., Beral, V., and Smith, P. Risk factors for ovarian cancer: a case-control study. Br J Cancer, *60:* 592-598, 1989.
28. Bowman, A., Gabra, H., Langdon, S. P., Lessells, A., Stewart, M., Young, A., and Smyth, J. F. CA125 response is associated with estrogen receptor

expression in a phase II trial of letrozole in ovarian cancer: identification of an endocrine-sensitive subgroup. Clin Cancer Res, *8:* 2233-2239, 2002.
29. Boyd, J. and Rubin, S. C. Hereditary ovarian cancer: molecular genetics and clinical implications. Gynecol Oncol, *64:* 196-206, 1997.
30. Brewer, M., Wharton, J. T., Wang, J., McWatters, A., Auersperg, N., Gershenson, D., Bast, R., and Zou, C. In vitro model of normal, immortalized ovarian surface epithelial and ovarian cancer cells for chemoprevention of ovarian cancer. Gynecol Oncol, *98:* 182-192, 2005.
31. Bringuier, P. P., Umbas, R., Schaafsma, H. E., Karthaus, H. F., Debruyne, F. M., and Schalken, J. A. Decreased E-cadherin immunoreactivity correlates with poor survival in patients with bladder tumors. Cancer Res, *53:* 3241-3245, 1993.
32. Brinkmann, V., Foroutan, H., Sachs, M., Weidner, K. M., and Birchmeier, W. Hepatocyte growth factor/scatter factor induces a variety of tissue-specific morphogenic programs in epithelial cells. J Cell Biol, *131:* 1573-1586, 1995.
33. Buhi, W. C. Characterization and biological roles of oviduct-specific, oestrogen-dependent glycoprotein. Reproduction, *123:* 355-362, 2002.
34. Buhi, W. C., Alvarez, I. M., Choi, I., Cleaver, B. D., and Simmen, F. A. Molecular cloning and characterization of an estrogen-dependent porcine oviductal secretory glycoprotein. Biol Reprod, *55:* 1305-1314, 1996.
35. Buhi, W. C., Alvarez, I. M., and Kouba, A. J. Secreted proteins of the oviduct. Cells Tissues Organs, *166:* 165-179, 2000.
36. Byskov, A. G. Differentiation of mammalian embryonic gonad. Physiol Rev, *66:* 71-117, 1986.
37. Callahan, M. J., Crum, C. P., Medeiros, F., Kindelberger, D. W., Elvin, J. A., Garber, J. E., Feltmate, C. M., Berkowitz, R. S., and Muto, M. G. Primary fallopian tube malignancies in BRCA-positive women undergoing surgery for ovarian cancer risk reduction. J Clin Oncol, *25:* 3985-3990, 2007.
38. Campbell, J. Some unusual gonadal tumours of the fowl. Br J Cancer, *5:* 69-84, 1951.
39. Carraway, K. L., 3rd, Funes, M., Workman, H. C., and Sweeney, C. Contribution of membrane mucins to tumor progression through modulation of cellular growth signaling pathways. Curr Top Dev Biol, *78:* 1-22, 2007.
40. Cass, I., Holschneider, C., Datta, N., Barbuto, D., Walts, A. E., and Karlan, B. Y. BRCA-mutation-associated fallopian tube carcinoma: a distinct clinical phenotype? Obstet Gynecol, *106:* 1327-1334, 2005.
41. Castaigne, S., Chomienne, C., Daniel, M. T., Berger, R., Miclea, J. M., Ballerini, P., and Degos, L. Retinoic acids in the treatment of acute promyelocytic leukemia. Nouv Rev Fr Hematol, *32:* 36-38, 1990.
42. Cheng, W., Liu, J., Yoshida, H., Rosen, D., and Naora, H. Lineage infidelity of epithelial ovarian cancers is controlled by HOX genes that specify regional identity in the reproductive tract. Nat Med, *11:* 531-537, 2005.
43. Cirisano, F. D., Jr., Robboy, S. J., Dodge, R. K., Bentley, R. C., Krigman, H. R., Synan, I. S., Soper, J. T., and Clarke-Pearson, D. L. The outcome of stage I-II clinically and surgically staged papillary serous and clear cell endometrial cancers when compared with endometrioid carcinoma. Gynecol Oncol, *77:*

55-65, 2000.
44. Collisson, E. A., De, A., Suzuki, H., Gambhir, S. S., and Kolodney, M. S. Treatment of metastatic melanoma with an orally available inhibitor of the Ras-Raf-MAPK cascade. Cancer Res, *63:* 5669-5673, 2003.
45. Comoglio, P., Trusolino, L., and Boccaccio, C. Scatter factor-dependent branching morphogenesis: structural and histological features. Eur J Histochem, *51 Suppl 1:* 79-92, 2007.
46. Connolly, D. C., Bao, R., Nikitin, A. Y., Stephens, K. C., Poole, T. W., Hua, X., Harris, S. S., Vanderhyden, B. C., and Hamilton, T. C. Female mice chimeric for expression of the simian virus 40 TAg under control of the MISIIR promoter develop epithelial ovarian cancer. Cancer Res, *63:* 1389-1397, 2003.
47. Crawford, P. A., Sadovsky, Y., and Milbrandt, J. Nuclear receptor steroidogenic factor 1 directs embryonic stem cells toward the steroidogenic lineage. Mol Cell Biol, *17:* 3997-4006, 1997.
48. Crickard, K., Marinello, M. J., Crickard, U., Satchidanand, S. K., Yoonessi, M., and Caglar, H. Borderline malignant serous tumors of the ovary maintained on extracellular matrix: evidence for clonal evolution and invasive potential. Cancer Genet Cytogenet, *23:* 135-143, 1986.
49. Crispens, M. A., Bodurka, D., Deavers, M., Lu, K., Silva, E. G., and Gershenson, D. M. Response and survival in patients with progressive or recurrent serous ovarian tumors of low malignant potential. Obstet Gynecol, *99:* 3-10, 2002.
50. Crum, C. P., Drapkin, R., Miron, A., Ince, T. A., Muto, M., Kindelberger, D. W., and Lee, Y. The distal fallopian tube: a new model for pelvic serous carcinogenesis. Curr Opin Obstet Gynecol, *19:* 3-9, 2007.
51. Cuello, M., Coats, A. O., Darko, I., Ettenberg, S. A., Gardner, G. J., Nau, M. M., Liu, J. R., Birrer, M. J., and Lipkowitz, S. N-(4-hydroxyphenyl) retinamide (4HPR) enhances TRAIL-mediated apoptosis through enhancement of a mitochondrial-dependent amplification loop in ovarian cancer cell lines. Cell Death Differ, *11:* 527-541, 2004.
52. Cunat, S., Hoffmann, P., and Pujol, P. Estrogens and epithelial ovarian cancer. Gynecol Oncol, *94:* 25-32, 2004.
53. Cunha, G. R., Hayward, S. W., Wang, Y. Z., and Ricke, W. A. Role of the stromal microenvironment in carcinogenesis of the prostate. Int J Cancer, *107:* 1-10, 2003.
54. Dalrymple, J. C., Bannatyne, P., Russell, P., Solomon, H. J., Tattersall, M. H., Atkinson, K., Carter, J., Duval, P., Elliott, P., Friedlander, M., and et al. Extraovarian peritoneal serous papillary carcinoma. A clinicopathologic study of 31 cases. Cancer, *64:* 110-115, 1989.
55. Datar, R. H., Naritoku, W. Y., Li, P., Tsao-Wei, D., Groshen, S., Taylor, C. R., and Imam, S. A. Analysis of telomerase activity in ovarian cystadenomas, low-malignant-potential tumors, and invasive carcinomas. Gynecol Oncol, *74:* 338-345, 1999.
56. De Palo, G., Veronesi, U., Camerini, T., Formelli, F., Mascotti, G., Boni, C., Fosser, V., Del Vecchio, M., Campa, T., Costa, A., and et al. Can fenretinide

protect women against ovarian cancer? J Natl Cancer Inst, *87:* 146-147, 1995.
57. DeSouza, M. M. and Murray, M. K. An estrogen-dependent sheep oviductal glycoprotein has glycan linkages typical of sialomucins and does not contain chitinase activity. Biol Reprod, *53:* 1517-1526, 1995.
58. Dietel, M. The histological diagnosis of endometrial hyperplasia. Is there a need to simplify? Virchows Arch, *439:* 604-608, 2001.
59. Dinulescu, D. M., Ince, T. A., Quade, B. J., Shafer, S. A., Crowley, D., and Jacks, T. Role of K-ras and Pten in the development of mouse models of endometriosis and endometrioid ovarian cancer. Nat Med, *11:* 63-70, 2005.
60. Dong, Y., Walsh, M. D., Cummings, M. C., Wright, R. G., Khoo, S. K., Parsons, P. G., and McGuckin, M. A. Expression of MUC1 and MUC2 mucins in epithelial ovarian tumours. J Pathol, *183:* 311-317, 1997.
61. Donnelly, K. M., Fazleabas, A. T., Verhage, H. G., Mavrogianis, P. A., and Jaffe, R. C. Cloning of a recombinant complementary DNA to a baboon (Papio anubis) estradiol-dependent oviduct-specific glycoprotein. Mol Endocrinol, *5:* 356-364, 1991.
62. Dorudi, S., Sheffield, J. P., Poulsom, R., Northover, J. M., and Hart, I. R. E-cadherin expression in colorectal cancer. An immunocytochemical and in situ hybridization study. Am J Pathol, *142:* 981-986, 1993.
63. Dubeau, L. The cell of origin of ovarian epithelial tumors and the ovarian surface epithelium dogma: does the emperor have no clothes? Gynecol Oncol, *72:* 437-442, 1999.
64. Dyck, H. G., Hamilton, T. C., Godwin, A. K., Lynch, H. T., Maines-Bandiera, S., and Auersperg, N. Autonomy of the epithelial phenotype in human ovarian surface epithelium: changes with neoplastic progression and with a family history of ovarian cancer. Int J Cancer, *69:* 429-436, 1996.
65. Dye, F. J. Human life before birth. Amsterdam, Netherlands: Harwood Academic Publishers, 2000.
66. Farrow, D. C., Weiss, N. S., Lyon, J. L., and Daling, J. R. Association of obesity and ovarian cancer in a case-control study. Am J Epidemiol, *129:* 1300-1304, 1989.
67. Fathalla, M. F. Incessant ovulation--a factor in ovarian neoplasia? Lancet, *2:* 163, 1971.
68. Finch, A., Shaw, P., Rosen, B., Murphy, J., Narod, S. A., and Colgan, T. J. Clinical and pathologic findings of prophylactic salpingo-oophorectomies in 159 BRCA1 and BRCA2 carriers. Gynecol Oncol, *100:* 58-64, 2006.
69. Flesken-Nikitin, A., Choi, K. C., Eng, J. P., Shmidt, E. N., and Nikitin, A. Y. Induction of carcinogenesis by concurrent inactivation of p53 and Rb1 in the mouse ovarian surface epithelium. Cancer Res, *63:* 3459-3463, 2003.
70. Fraser, M., Bai, T., and Tsang, B. K. Akt promotes cisplatin resistance in human ovarian cancer cells through inhibition of p53 phosphorylation and nuclear function. Int J Cancer, 2007.
71. Fromm, G. L., Gershenson, D. M., and Silva, E. G. Papillary serous carcinoma of the peritoneum. Obstet Gynecol, *75:* 89-95, 1990.
72. Fujiwara, S. Retinoids and nonvertebrate chordate development. J Neurobiol, *66:* 645-652, 2006.

73. Gelberg, H. B., McEntee, K., and Heath, E. H. Feline cystic rete ovarii. Vet Pathol, *21:* 304-307, 1984.
74. Genadry, R., Parmley, T., and Woodruff, J. D. The origin and clinical behavior of the parovarian tumor. Am J Obstet Gynecol, *129:* 873-880, 1977.
75. Gilks, C. B. Subclassification of ovarian surface epithelial tumors based on correlation of histologic and molecular pathologic data. Int J Gynecol Pathol, *23:* 200-205, 2004.
76. Gilks, C. B., Vanderhyden, B. C., Zhu, S., van de Rijn, M., and Longacre, T. A. Distinction between serous tumors of low malignant potential and serous carcinomas based on global mRNA expression profiling. Gynecol Oncol, *96:* 684-694, 2005.
77. Giuntoli, R. L., 2nd, Rodriguez, G. C., Whitaker, R. S., Dodge, R., and Voynow, J. A. Mucin gene expression in ovarian cancers. Cancer Res, *58:* 5546-5550, 1998.
78. Gondos, B. Surface epithelium of the developing ovary. Possible correlation with ovarian neoplasia. Am J Pathol, *81:* 303-321, 1975.
79. Gotz, J., Probst, A., Mistl, C., Nitsch, R. M., and Ehler, E. Distinct role of protein phosphatase 2A subunit Calpha in the regulation of E-cadherin and beta-catenin during development. Mech Dev, *93:* 83-93, 2000.
80. Grice, J., Ek, M., Greer, B., Koh, W. J., Muntz, H. G., Cain, J., Tamimi, H., Stelzer, K., Figge, D., and Goff, B. A. Uterine papillary serous carcinoma: evaluation of long-term survival in surgically staged patients. Gynecol Oncol, *69:* 69-73, 1998.
81. Grulich, A. E., Swerdlow, A. J., Head, J., and Marmot, M. G. Cancer mortality in African and Caribbean migrants to England and Wales. Br J Cancer, *66:* 905-911, 1992.
82. Guruswamy, S., Lightfoot, S., Gold, M. A., Hassan, R., Berlin, K. D., Ivey, R. T., and Benbrook, D. M. Effects of retinoids on cancerous phenotype and apoptosis in organotypic cultures of ovarian carcinoma. J Natl Cancer Inst, *93:* 516-525, 2001.
83. Hatch, K. D., Beecham, J. B., Blessing, J. A., and Creasman, W. T. Responsiveness of patients with advanced ovarian carcinoma to tamoxifen. A Gynecologic Oncology Group study of second-line therapy in 105 patients. Cancer, *68:* 269-271, 1991.
84. Hazan, R. B., Kang, L., Whooley, B. P., and Borgen, P. I. N-cadherin promotes adhesion between invasive breast cancer cells and the stroma. Cell Adhes Commun, *4:* 399-411, 1997.
85. Hazan, R. B., Phillips, G. R., Qiao, R. F., Norton, L., and Aaronson, S. A. Exogenous expression of N-cadherin in breast cancer cells induces cell migration, invasion, and metastasis. J Cell Biol, *148:* 779-790, 2000.
86. Heintz, A. P., Odicino, F., Maisonneuve, P., Quinn, M. A., Benedet, J. L., Creasman, W. T., Ngan, H. Y., Pecorelli, S., and Beller, U. Carcinoma of the ovary. FIGO 6th Annual Report on the Results of Treatment in Gynecological Cancer. Int J Gynaecol Obstet, *95 Suppl 1:* S161-192, 2006.
87. Hellstrom, I., Raycraft, J., Hayden-Ledbetter, M., Ledbetter, J. A., Schummer, M., McIntosh, M., Drescher, C., Urban, N., and Hellstrom, K. E. The HE4

(WFDC2) protein is a biomarker for ovarian carcinoma. Cancer Res, *63:* 3695-3700, 2003.
88. Helou, K., Padilla-Nash, H., Wangsa, D., Karlsson, E., Osterberg, L., Karlsson, P., Ried, T., and Knutsen, T. Comparative genome hybridization reveals specific genomic imbalances during the genesis from benign through borderline to malignant ovarian tumors. Cancer Genet Cytogenet, *170:* 1-8, 2006.
89. Heussen, C. and Dowdle, E. B. Electrophoretic analysis of plasminogen activators in polyacrylamide gels containing sodium dodecyl sulfate and copolymerized substrates. Anal Biochem, *102:* 196-202, 1980.
90. Hilton, J. L., Geisler, J. P., Rathe, J. A., Hattermann-Zogg, M. A., DeYoung, B., and Buller, R. E. Inactivation of BRCA1 and BRCA2 in ovarian cancer. J Natl Cancer Inst, *94:* 1396-1406, 2002.
91. Hu, J., Khanna, V., Jones, M. M., and Surti, U. Genomic imbalances in ovarian borderline serous and mucinous tumors. Cancer Genet Cytogenet, *139:* 18-23, 2002.
92. Huang, M. E., Ye, Y. C., Chen, S. R., Chai, J. R., Lu, J. X., Zhoa, L., Gu, L. J., and Wang, Z. Y. Use of all-trans retinoic acid in the treatment of acute promyelocytic leukemia. Blood, *72:* 567-572, 1988.
93. Ikeda, Y., Shen, W. H., Ingraham, H. A., and Parker, K. L. Developmental expression of mouse steroidogenic factor-1, an essential regulator of the steroid hydroxylases. Mol Endocrinol, *8:* 654-662, 1994.
94. Islam, S., Carey, T. E., Wolf, G. T., Wheelock, M. J., and Johnson, K. R. Expression of N-cadherin by human squamous carcinoma cells induces a scattered fibroblastic phenotype with disrupted cell-cell adhesion. J Cell Biol, *135:* 1643-1654, 1996.
95. Jacobs, I. J. and Menon, U. Progress and challenges in screening for early detection of ovarian cancer. Mol Cell Proteomics, *3:* 355-366, 2004.
96. Jemal, A., Siegel, R., Ward, E., Murray, T., Xu, J., and Thun, M. J. Cancer statistics, 2007. CA Cancer J Clin, *57:* 43-66, 2007.
97. Jimbo, H., Yoshikawa, H., Onda, T., Yasugi, T., Sakamoto, A., and Taketani, Y. Prevalence of ovarian endometriosis in epithelial ovarian cancer. Int J Gynaecol Obstet, *59:* 245-250, 1997.
98. Jordan, V. C. Selective estrogen receptor modulation: concept and consequences in cancer. Cancer Cell, *5:* 207-213, 2004.
99. Kabawat, S. E., Bast, R. C., Jr., Bhan, A. K., Welch, W. R., Knapp, R. C., and Colvin, R. B. Tissue distribution of a coelomic-epithelium-related antigen recognized by the monoclonal antibody OC125. Int J Gynecol Pathol, *2:* 275-285, 1983.
100. Kadam, K. M., D'Souza, S. J., Bandivdekar, A. H., and Natraj, U. Identification and characterization of oviductal glycoprotein-binding protein partner on gametes: epitopic similarity to non-muscle myosin IIA, MYH 9. Mol Hum Reprod, *12:* 275-282, 2006.
101. Kadam, K. M., D'Souza, S. J., and Natraj, U. Identification of cellular isoform of oviduct-specific glycoprotein: role in oviduct tissue remodeling? Cell Tissue Res, 2007.

102. Kanaya, T., Kyo, S., Maida, Y., Yatabe, N., Tanaka, M., Nakamura, M., and Inoue, M. Frequent hypermethylation of MLH1 promoter in normal endometrium of patients with endometrial cancers. Oncogene, *22:* 2352-2360, 2003.
103. Karseladze, A. I. On the site of origin of epithelial tumors of the ovary. Eur J Gynaecol Oncol, *22:* 110-115, 2001.
104. Kendall, B. S., Ronnett, B. M., Isacson, C., Cho, K. R., Hedrick, L., Diener-West, M., and Kurman, R. J. Reproducibility of the diagnosis of endometrial hyperplasia, atypical hyperplasia, and well-differentiated carcinoma. Am J Surg Pathol, *22:* 1012-1019, 1998.
105. Kenny, P. A., Lee, G. Y., and Bissell, M. J. Targeting the tumor microenvironment. Front Biosci, *12:* 3468-3474, 2007.
106. Kilian, A., Bowtell, D. D., Abud, H. E., Hime, G. R., Venter, D. J., Keese, P. K., Duncan, E. L., Reddel, R. R., and Jefferson, R. A. Isolation of a candidate human telomerase catalytic subunit gene, which reveals complex splicing patterns in different cell types. Hum Mol Genet, *6:* 2011-2019, 1997.
107. Kindelberger, D. W., Lee, Y., Miron, A., Hirsch, M. S., Feltmate, C., Medeiros, F., Callahan, M. J., Garner, E. O., Gordon, R. W., Birch, C., Berkowitz, R. S., Muto, M. G., and Crum, C. P. Intraepithelial carcinoma of the fimbria and pelvic serous carcinoma: Evidence for a causal relationship. Am J Surg Pathol, *31:* 161-169, 2007.
108. Kmet, L. M., Cook, L. S., and Magliocco, A. M. A review of p53 expression and mutation in human benign, low malignant potential, and invasive epithelial ovarian tumors. Cancer, *97:* 389-404, 2003.
109. Kotra, L. P., Zhang, L., Fridman, R., Orlando, R., and Mobashery, S. N-Glycosylation pattern of the zymogenic form of human matrix metalloproteinase-9. Bioorg Chem, *30:* 356-370, 2002.
110. Kreidberg, J. A., Sariola, H., Loring, J. M., Maeda, M., Pelletier, J., Housman, D., and Jaenisch, R. WT-1 is required for early kidney development. Cell, *74:* 679-691, 1993.
111. Kurman, R. J., Zaino, R. J., and Norris, H. J. Endometrial carcinoma. , p. 441. New York: Springer-Verlag, 1994.
112. Lahortiga, I. and Cools, J. Cryptic chromosomal aberrations waiting to be discovered. Leukemia, *20:* 210-211, 2006.
113. Lapensee, L., Paquette, Y., and Bleau, G. Allelic polymorphism and chromosomal localization of the human oviductin gene (MUC9). Fertil Steril, *68:* 702-708, 1997.
114. Lauchlan, S. C. The secondary Mullerian system. Obstet Gynecol Surv, *27:* 133-146, 1972.
115. Lauchlan, S. C. The secondary mullerian system revisited. Int J Gynecol Pathol, *13:* 73-79, 1994.
116. Lax, S. F. Molecular genetic pathways in various types of endometrial carcinoma: from a phenotypical to a molecular-based classification. Virchows Arch, *444:* 213-223, 2004.
117. Lee, C. H., Xue, H., Sutcliffe, M., Gout, P. W., Huntsman, D. G., Miller, D. M., Gilks, C. B., and Wang, Y. Z. Establishment of subrenal capsule

xenografts of primary human ovarian tumors in SCID mice: potential models. Gynecol Oncol, *96:* 48-55, 2005.
118. Lee, Y., Medeiros, F., Kindelberger, D., Callahan, M. J., Muto, M. G., and Crum, C. P. Advances in the recognition of tubal intraepithelial carcinoma: applications to cancer screening and the pathogenesis of ovarian cancer. Adv Anat Pathol, *13:* 1-7, 2006.
119. Leese, H. J., Tay, J. I., Reischl, J., and Downing, S. J. Formation of Fallopian tubal fluid: role of a neglected epithelium. Reproduction, *121:* 339-346, 2001.
120. Li, A. J., Elmore, R. G., Pavelka, J. C., and Karlan, B. Y. Hyperandrogenism, mediated by obesity and receptor polymorphisms, promotes aggressive epithelial ovarian cancer biology. Gynecol Oncol, 2007.
121. Li, Y., Bharti, A., Chen, D., Gong, J., and Kufe, D. Interaction of glycogen synthase kinase 3beta with the DF3/MUC1 carcinoma-associated antigen and beta-catenin. Mol Cell Biol, *18:* 7216-7224, 1998.
122. Lindgren, P. R., Cajander, S., Backstrom, T., Gustafsson, J. A., Makela, S., and Olofsson, J. I. Estrogen and progesterone receptors in ovarian epithelial tumors. Mol Cell Endocrinol, *221:* 97-104, 2004.
123. Liu, J., Yang, G., Thompson-Lanza, J. A., Glassman, A., Hayes, K., Patterson, A., Marquez, R. T., Auersperg, N., Yu, Y., Hahn, W. C., Mills, G. B., and Bast, R. C., Jr. A genetically defined model for human ovarian cancer. Cancer Res, *64:* 1655-1663, 2004.
124. Lloyd, K. O., Burchell, J., Kudryashov, V., Yin, B. W., and Taylor-Papadimitriou, J. Comparison of O-linked carbohydrate chains in MUC-1 mucin from normal breast epithelial cell lines and breast carcinoma cell lines. Demonstration of simpler and fewer glycan chains in tumor cells. J Biol Chem, *271:* 33325-33334, 1996.
125. Lok, I. H., Briton-Jones, C. M., Yuen, P. M., and Haines, C. J. Variable expression of oviductin mRNA at different stages of human reproductive cycle. J Assist Reprod Genet, *19:* 569-576, 2002.
126. Longacre, T. A., Chung, M. H., Jensen, D. N., and Hendrickson, M. R. Proposed criteria for the diagnosis of well-differentiated endometrial carcinoma. A diagnostic test for myoinvasion. Am J Surg Pathol, *19:* 371-406, 1995.
127. Longacre, T. A., Kempson, R. L., and Hendrickson, M. R. Well-differentiated serous neoplasms of the ovary. Pathology (Phila), *1:* 255-306, 1993.
128. Lozano, E., Betson, M., and Braga, V. M. Tumor progression: Small GTPases and loss of cell-cell adhesion. Bioessays, *25:* 452-463, 2003.
129. Luo, M. P., Gomperts, B., Imren, S., DeClerck, Y. A., Ito, M., Velicescu, M., Felix, J. C., and Dubeau, L. Establishment of long-term in vitro cultures of human ovarian cystadenomas and LMP tumors and examination of their spectrum of expression of matrix-degrading proteinases. Gynecol Oncol, *67:* 277-284, 1997.
130. Lynch, H. T. and Lynch, J. F. Hereditary cancer: family history, diagnosis, molecular genetics, ecogenetics, and management strategies. Biochimie, *84:* 3-17, 2002.
131. Maeda, T., Tashiro, H., Katabuchi, H., Begum, M., Ohtake, H., Kiyono, T.,

and Okamura, H. Establishment of an immortalised human ovarian surface epithelial cell line without chromosomal instability. Br J Cancer, *93:* 116-123, 2005.

132. Maines-Bandiera, S. L. and Auersperg, N. Increased E-cadherin expression in ovarian surface epithelium: an early step in metaplasia and dysplasia? Int J Gynecol Pathol, *16:* 250-255, 1997.
133. Maines-Bandiera, S. L., Huntsman, D., Lestou, V. S., Kuo, W. L., Leung, P. C., Horsman, R. D., Wong, A. S., Woo, M. M., Choi, K. K., Roskelley, C. D., and Auersperg, N. Epithelio-mesenchymal transition in a neoplastic ovarian epithelial hybrid cell line. Differentiation, *72:* 150-161, 2004.
134. Maines-Bandiera, S. L., Kruk, P. A., and Auersperg, N. Simian virus 40-transformed human ovarian surface epithelial cells escape normal growth controls but retain morphogenetic responses to extracellular matrix. Am J Obstet Gynecol, *167:* 729-735, 1992.
135. Malette, B., Filion, B., St-Jacques, S., Kan, F. W., and Bleau, G. Hormonal control of the biosynthesis of hamster oviductin. Microsc Res Tech, *31:* 470-477, 1995.
136. Marshall, J. T., Nancarrow, C. D., and Brownlee, A. G. Cloning and sequencing of a cDNA encoding an ovine oestrus-associated oviducal protein. Reprod Fertil Dev, *8:* 305-310, 1996.
137. Mayer, B., Johnson, J. P., Leitl, F., Jauch, K. W., Heiss, M. M., Schildberg, F. W., Birchmeier, W., and Funke, I. E-cadherin expression in primary and metastatic gastric cancer: down-regulation correlates with cellular dedifferentiation and glandular disintegration. Cancer Res, *53:* 1690-1695, 1993.
138. Mazurek, A., Niklinski, J., Laudanski, T., and Pluygers, E. Clinical tumour markers in ovarian cancer. Eur J Cancer Prev, *7:* 23-35, 1998.
139. McCauley, T. C., Buhi, W. C., Wu, G. M., Mao, J., Caamano, J. N., Didion, B. A., and Day, B. N. Oviduct-specific glycoprotein modulates sperm-zona binding and improves efficiency of porcine fertilization in vitro. Biol Reprod, *69:* 828-834, 2003.
140. McKenney, J. K., Balzer, B. L., and Longacre, T. A. Patterns of stromal invasion in ovarian serous tumors of low malignant potential (borderline tumors): a reevaluation of the concept of stromal microinvasion. Am J Surg Pathol, *30:* 1209-1221, 2006.
141. Medeiros, F., Muto, M. G., Lee, Y., Elvin, J. A., Callahan, M. J., Feltmate, C., Garber, J. E., Cramer, D. W., and Crum, C. P. The tubal fimbria is a preferred site for early adenocarcinoma in women with familial ovarian cancer syndrome. Am J Surg Pathol, *30:* 230-236, 2006.
142. Medico, E., Mongiovi, A. M., Huff, J., Jelinek, M. A., Follenzi, A., Gaudino, G., Parsons, J. T., and Comoglio, P. M. The tyrosine kinase receptors Ron and Sea control "scattering" and morphogenesis of liver progenitor cells in vitro. Mol Biol Cell, *7:* 495-504, 1996.
143. Meyerson, M., Counter, C. M., Eaton, E. N., Ellisen, L. W., Steiner, P., Caddle, S. D., Ziaugra, L., Beijersbergen, R. L., Davidoff, M. J., Liu, Q., Bacchetti, S., Haber, D. A., and Weinberg, R. A. hEST2, the putative human

telomerase catalytic subunit gene, is up-regulated in tumor cells and during immortalization. Cell, *90:* 785-795, 1997.
144. Miller, C., Pavlova, A., and Sassoon, D. A. Differential expression patterns of Wnt genes in the murine female reproductive tract during development and the estrous cycle. Mech Dev, *76:* 91-99, 1998.
145. Mink, P. J., Sherman, M. E., and Devesa, S. S. Incidence patterns of invasive and borderline ovarian tumors among white women and black women in the United States. Results from the SEER Program, 1978-1998. Cancer, *95:* 2380-2389, 2002.
146. Montesano, R., Matsumoto, K., Nakamura, T., and Orci, L. Identification of a fibroblast-derived epithelial morphogen as hepatocyte growth factor. Cell, *67:* 901-908, 1991.
147. Moore, K. L. and Persaud, P. V. N. The developing human. Clinically oriented embryology. Philadelphia, PA: W.B. Saunders Company, 1998.
148. Morais da Silva, S., Hacker, A., Harley, V., Goodfellow, P., Swain, A., and Lovell-Badge, R. Sox9 expression during gonadal development implies a conserved role for the gene in testis differentiation in mammals and birds. Nat Genet, *14:* 62-68, 1996.
149. Moser, T. L., Young, T. N., Rodriguez, G. C., Pizzo, S. V., Bast, R. C., Jr., and Stack, M. S. Secretion of extracellular matrix-degrading proteinases is increased in epithelial ovarian carcinoma. Int J Cancer, *56:* 552-559, 1994.
150. Mutter, G. L. Diagnosis of premalignant endometrial disease. J Clin Pathol, *55:* 326-331, 2002.
151. Mutter, G. L., Ince, T. A., Baak, J. P., Kust, G. A., Zhou, X. P., and Eng, C. Molecular identification of latent precancers in histologically normal endometrium. Cancer Res, *61:* 4311-4314, 2001.
152. Mutter, G. L., Lin, M. C., Fitzgerald, J. T., Kum, J. B., Baak, J. P., Lees, J. A., Weng, L. P., and Eng, C. Altered PTEN expression as a diagnostic marker for the earliest endometrial precancers. J Natl Cancer Inst, *92:* 924-930, 2000.
153. Naldini, L., Weidner, K. M., Vigna, E., Gaudino, G., Bardelli, A., Ponzetto, C., Narsimhan, R. P., Hartmann, G., Zarnegar, R., Michalopoulos, G. K., and et al. Scatter factor and hepatocyte growth factor are indistinguishable ligands for the MET receptor. Embo J, *10:* 2867-2878, 1991.
154. Nicosia, S. V., Ku, N. K., Oliveros-Saunders, B., Giacomini, G., Pierro, E., Mayer, J., and Nicosia, R. F. Ovarian mesothelium (surface epithelium) in normal, pathological and experimental conditions. Rome, Italy: Antonio Delfino Editore, 1997.
155. Nicosia, S. V., Saunders, B. O., Acevedo-Duncan, M. E., Setrakian, S., and Degregorio, R. Biopathology of ovarian mesothelium. Boston, MA: Kluwer Academic Publishers, 1991.
156. Nieman, M. T., Prudoff, R. S., Johnson, K. R., and Wheelock, M. J. N-cadherin promotes motility in human breast cancer cells regardless of their E-cadherin expression. J Cell Biol, *147:* 631-644, 1999.
157. Nieman, M. T., Prudoff, R. S., Johnson, K. R., and Wheelock, M. J. N-cadherin promotes motility in human breast cancer cells regardless of their E-cadherin expression. J Cell Biol, *147:* 631-644, 1999.

158. Noguera, R., Piqueras, M., Subramaniam, M., Cruz, J., Canete, A., Bosch, A. L., and Navarro, S. Immunohistochemical evaluation of a novel clone of monoclonal anti-MYCN antibody B8.4B in neuroblastic tumours: a correlation with MYCN gene status. Virchows Arch, *449:* 277-278, 2006.
159. O'Day-Bowman, M. B., Mavrogianis, P. A., Fazleabas, A. T., and Verhage, H. G. A human oviduct-specific glycoprotein: synthesis, secretion, and localization during the menstrual cycle. Microsc Res Tech, *32:* 57-69, 1995.
160. O'Day-Bowman, M. B., Mavrogianis, P. A., Minshall, R. D., and Verhage, H. G. In vivo versus in vitro oviductal glycoprotein (OGP) association with the zona pellucida (ZP) in the hamster and baboon. Mol Reprod Dev, *62:* 248-256, 2002.
161. O'Day-Bowman, M. B., Mavrogianis, P. A., Reuter, L. M., Johnson, D. E., Fazleabas, A. T., and Verhage, H. G. Association of oviduct-specific glycoproteins with human and baboon (Papio anubis) ovarian oocytes and enhancement of human sperm binding to human hemizonae following in vitro incubation. Biol Reprod, *54:* 60-69, 1996.
162. O'Donnell, A. J., Macleod, K. G., Burns, D. J., Smyth, J. F., and Langdon, S. P. Estrogen receptor-alpha mediates gene expression changes and growth response in ovarian cancer cells exposed to estrogen. Endocr Relat Cancer, *12:* 851-866, 2005.
163. Oishi, T., Kigawa, J., Minagawa, Y., Shimada, M., Takahashi, M., and Terakawa, N. Alteration of telomerase activity associated with development and extension of epithelial ovarian cancer. Obstet Gynecol, *91:* 568-571, 1998.
164. Oka, H., Shiozaki, H., Kobayashi, K., Inoue, M., Tahara, H., Kobayashi, T., Takatsuka, Y., Matsuyoshi, N., Hirano, S., Takeichi, M., and et al. Expression of E-cadherin cell adhesion molecules in human breast cancer tissues and its relationship to metastasis. Cancer Res, *53:* 1696-1701, 1993.
165. Oliveira, C., Westra, J. L., Arango, D., Ollikainen, M., Domingo, E., Ferreira, A., Velho, S., Niessen, R., Lagerstedt, K., Alhopuro, P., Laiho, P., Veiga, I., Teixeira, M. R., Ligtenberg, M., Kleibeuker, J. H., Sijmons, R. H., Plukker, J. T., Imai, K., Lage, P., Hamelin, R., Albuquerque, C., Schwartz, S., Jr., Lindblom, A., Peltomaki, P., Yamamoto, H., Aaltonen, L. A., Seruca, R., and Hofstra, R. M. Distinct patterns of KRAS mutations in colorectal carcinomas according to germline mismatch repair defects and hMLH1 methylation status. Hum Mol Genet, *13:* 2303-2311, 2004.
166. Oreal, E., Mazaud, S., Picard, J. Y., Magre, S., and Carre-Eusebe, D. Different patterns of anti-Mullerian hormone expression, as related to DMRT1, SF-1, WT1, GATA-4, Wnt-4, and Lhx9 expression, in the chick differentiating gonads. Dev Dyn, *225:* 221-232, 2002.
167. Orsulic, S., Li, Y., Soslow, R. A., Vitale-Cross, L. A., Gutkind, J. S., and Varmus, H. E. Induction of ovarian cancer by defined multiple genetic changes in a mouse model system. Cancer Cell, *1:* 53-62, 2002.
168. Osterberg, L., Akeson, M., Levan, K., Partheen, K., Zetterqvist, B. M., Brannstrom, M., and Horvath, G. Genetic alterations of serous borderline tumors of the ovary compared to stage I serous ovarian carcinomas. Cancer

Genet Cytogenet, *167:* 103-108, 2006.
169. Ouellet, V., Provencher, D. M., Maugard, C. M., Le Page, C., Ren, F., Lussier, C., Novak, J., Ge, B., Hudson, T. J., Tonin, P. N., and Mes-Masson, A. M. Discrimination between serous low malignant potential and invasive epithelial ovarian tumors using molecular profiling. Oncogene, *24:* 4672-4687, 2005.
170. Pan, J., Roskelley, C. D., Luu-The, V., Rojiani, M., and Auersperg, N. Reversal of divergent differentiation by ras oncogene-mediated transformation. Cancer Res, *52:* 4269-4272, 1992.
171. Papadimitriou, C. A., Markaki, S., Siapkaras, J., Vlachos, G., Efstathiou, E., Grimani, I., Hamilos, G., Zorzou, M., and Dimopoulos, M. A. Hormonal therapy with letrozole for relapsed epithelial ovarian cancer. Long-term results of a phase II study. Oncology, *66:* 112-117, 2004.
172. Papadimitriou, E. and Lelkes, P. I. Measurement of cell numbers in microtiter culture plates using the fluorescent dye Hoechst 33258. J Immunol Methods, *162:* 41-45, 1993.
173. Paquette, Y., Merlen, Y., Malette, B., and Bleau, G. Allelic polymorphism in the hamster oviductin gene is due to a variable number of mucin-like tandem repeats. Mol Reprod Dev, *42:* 388-396, 1995.
174. Parker, K. L. and Schimmer, B. P. Steroidogenic factor 1: a key determinant of endocrine development and function. Endocr Rev, *18:* 361-377, 1997.
175. Parker, R. L., Clement, P. B., Chercover, D. J., Sornarajah, T., and Gilks, C. B. Early recurrence of ovarian serous borderline tumor as high-grade carcinoma: a report of two cases. Int J Gynecol Pathol, *23:* 265-272, 2004.
176. Parr, B. A. and McMahon, A. P. Sexually dimorphic development of the mammalian reproductive tract requires Wnt-7a. Nature, *395:* 707-710, 1998.
177. Pelliniemi, L. J., Frojdman, K., Sundstrom, J., Pollanen, P., and Kuopio, T. Cellular and molecular changes during sex differentiation of embryonic mammalian gonads. J Exp Zool, *281:* 482-493, 1998.
178. Pepper, M. S., Soriano, J. V., Menoud, P. A., Sappino, A. P., Orci, L., and Montesano, R. Modulation of hepatocyte growth factor and c-met in the rat mammary gland during pregnancy, lactation, and involution. Exp Cell Res, *219:* 204-210, 1995.
179. Piek, J. M., Kenemans, P., and Verheijen, R. H. Intraperitoneal serous adenocarcinoma: a critical appraisal of three hypotheses on its cause. Am J Obstet Gynecol, *191:* 718-732, 2004.
180. Piek, J. M., van Diest, P. J., Zweemer, R. P., Kenemans, P., and Verheijen, R. H. Tubal ligation and risk of ovarian cancer. Lancet, *358:* 844, 2001.
181. Piver, M. S., Baker, T. R., Piedmonte, M., and Sandecki, A. M. Epidemiology and etiology of ovarian cancer. Semin Oncol, *18:* 177-185, 1991.
182. Pohl, G., Ho, C. L., Kurman, R. J., Bristow, R., Wang, T. L., and Shih Ie, M. Inactivation of the mitogen-activated protein kinase pathway as a potential target-based therapy in ovarian serous tumors with KRAS or BRAF mutations. Cancer Res, *65:* 1994-2000, 2005.
183. Pollock, P. M., Harper, U. L., Hansen, K. S., Yudt, L. M., Stark, M., Robbins, C. M., Moses, T. Y., Hostetter, G., Wagner, U., Kakareka, J., Salem, G.,

Pohida, T., Heenan, P., Duray, P., Kallioniemi, O., Hayward, N. K., Trent, J. M., and Meltzer, P. S. High frequency of BRAF mutations in nevi. Nat Genet, *33:* 19-20, 2003.

184. Powell, C. B., Kenley, E., Chen, L. M., Crawford, B., McLennan, J., Zaloudek, C., Komaromy, M., Beattie, M., and Ziegler, J. Risk-reducing salpingo-oophorectomy in BRCA mutation carriers: role of serial sectioning in the detection of occult malignancy. J Clin Oncol, *23:* 127-132, 2005.
185. Prat, J. Pathology of the ovary. Philadelphia: Saunders, 2004.
186. Prat, J. and De Nictolis, M. Serous borderline tumors of the ovary: a long-term follow-up study of 137 cases, including 18 with a micropapillary pattern and 20 with microinvasion. Am J Surg Pathol, *26:* 1111-1128, 2002.
187. Pritchard-Jones, K., Fleming, S., Davidson, D., Bickmore, W., Porteous, D., Gosden, C., Bard, J., Buckler, A., Pelletier, J., Housman, D., and et al. The candidate Wilms' tumour gene is involved in genitourinary development. Nature, *346:* 194-197, 1990.
188. Quattropani, S. L. Serous cysts of the aging guinea pig ovary. I. Light microscopy and origin. Anat Rec, *188:* 351-360, 1977.
189. Quattropani, S. L. Serous cysts of the aging guinea pig ovary. II. Scanning and transmission electron microscopy. Anat Rec, *190:* 285-298, 1978.
190. Quattropani, S. L. Serous cystadenoma formation in guinea pig ovaries. J Submicrosc Cytol, *13:* 337-345, 1981.
191. Rajagopalan, H., Bardelli, A., Lengauer, C., Kinzler, K. W., Vogelstein, B., and Velculescu, V. E. Tumorigenesis: RAF/RAS oncogenes and mismatch-repair status. Nature, *418:* 934, 2002.
192. Ramakrishna, V., Negri, D. R., Brusic, V., Fontanelli, R., Canevari, S., Bolis, G., Castelli, C., and Parmiani, G. Generation and phenotypic characterization of new human ovarian cancer cell lines with the identification of antigens potentially recognizable by HLA-restricted cytotoxic T cells. Int J Cancer, *73:* 143-150, 1997.
193. Rao, P. H., Harris, C. P., Yan Lu, X., Li, X. N., Mok, S. C., and Lau, C. C. Multicolor spectral karyotyping of serous ovarian adenocarcinoma. Genes Chromosomes Cancer, *33:* 123-132, 2002.
194. Rapisarda, J. J., Mavrogianis, P. A., O'Day-Bowman, M. B., Fazleabas, A. T., and Verhage, H. G. Immunological characterization and immunocytochemical localization of an oviduct-specific glycoprotein in the human. J Clin Endocrinol Metab, *76:* 1483-1488, 1993.
195. Rawson, N. E. and LaMantia, A. S. Once and again: retinoic acid signaling in the developing and regenerating olfactory pathway. J Neurobiol, *66:* 653-676, 2006.
196. Regimbald, L. H., Pilarski, L. M., Longenecker, B. M., Reddish, M. A., Zimmermann, G., and Hugh, J. C. The breast mucin MUCI as a novel adhesion ligand for endothelial intercellular adhesion molecule 1 in breast cancer. Cancer Res, *56:* 4244-4249, 1996.
197. Riman, T., Persson, I., and Nilsson, S. Hormonal aspects of epithelial ovarian cancer: review of epidemiological evidence. Clin Endocrinol (Oxf), *49:* 695-707, 1998.

198. Risch, H. A. and Howe, G. R. Pelvic inflammatory disease and the risk of epithelial ovarian cancer. Cancer Epidemiol Biomarkers Prev, *4:* 447-451, 1995.
199. Risinger, J. I., Hayes, A. K., Berchuck, A., and Barrett, J. C. PTEN/MMAC1 mutations in endometrial cancers. Cancer Res, *57:* 4736-4738, 1997.
200. Rodriguez-Burford, C., Barnes, M. N., Berry, W., Partridge, E. E., and Grizzle, W. E. Immunohistochemical expression of molecular markers in an avian model: a potential model for preclinical evaluation of agents for ovarian cancer chemoprevention. Gynecol Oncol, *81:* 373-379, 2001.
201. Roger, L., Gadea, G., and Roux, P. Control of cell migration: a tumour suppressor function for p53? Biol Cell, *98:* 141-152, 2006.
202. Romand, R., Dolle, P., and Hashino, E. Retinoid signaling in inner ear development. J Neurobiol, *66:* 687-704, 2006.
203. Rutgers, J. L. and Scully, R. E. Cysts (cystadenomas) and tumors of the rete ovarii. Int J Gynecol Pathol, *7:* 330-342, 1988.
204. Sainz de la Cuesta, R., Eichhorn, J. H., Rice, L. W., Fuller, A. F., Jr., Nikrui, N., and Goff, B. A. Histologic transformation of benign endometriosis to early epithelial ovarian cancer. Gynecol Oncol, *60:* 238-244, 1996.
205. Sakaguchi, H., Fujimoto, J., Aoki, I., Toyoki, H., Khatun, S., and Tamaya, T. Expression of oestrogen receptor alpha and beta in uterine endometrial and ovarian cancers. Eur J Cancer, *38 Suppl 6:* S74-75, 2002.
206. Sakata, K., Shigemasa, K., Nagai, N., and Ohama, K. Expression of matrix metalloproteinases (MMP-2, MMP-9, MT1-MMP) and their inhibitors (TIMP-1, TIMP-2) in common epithelial tumors of the ovary. Int J Oncol, *17:* 673-681, 2000.
207. Sasaki, M., Kotcherguina, L., Dharia, A., Fujimoto, S., and Dahiya, R. Cytosine-phosphoguanine methylation of estrogen receptors in endometrial cancer. Cancer Res, *61:* 3262-3266, 2001.
208. Satoh, T., Abe, H., Sendai, Y., Iwata, H., and Hoshi, H. Biochemical characterization of a bovine oviduct-specific sialo-glycoprotein that sustains sperm viability in vitro. Biochim Biophys Acta, *1266:* 117-123, 1995.
209. Savagner, P., Kusewitt, D. F., Carver, E. A., Magnino, F., Choi, C., Gridley, T., and Hudson, L. G. Developmental transcription factor slug is required for effective re-epithelialization by adult keratinocytes. J Cell Physiol, *202:* 858-866, 2005.
210. Schipper, J. H., Frixen, U. H., Behrens, J., Unger, A., Jahnke, K., and Birchmeier, W. E-cadherin expression in squamous cell carcinomas of head and neck: inverse correlation with tumor dedifferentiation and lymph node metastasis. Cancer Res, *51:* 6328-6337, 1991.
211. Schmidt, A., Mavrogianis, P. A., O'Day-Bowman, M. B., Jaffe, R. C., and Verhage, H. G. Characterization of antibodies generated against a conserved portion of oviductal glycoprotein (OGP) and endogenous hamster OGP and their ability to decrease sperm binding to the zona pellucida in vitro. Am J Reprod Immunol, *38:* 377-383, 1997.
212. Scully, R. E. Influence of origin of ovarian cancer on efficacy of screening. Lancet, *355:* 1028-1029, 2000.

213. Scully, R. E., Young, R. H., and Clement, P. B. Atlas of Tumor Pathology. Washington, D.C.: Armed Forces Institute of Pathology, 1996.
214. Sendai, Y., Abe, H., Kikuchi, M., Satoh, T., and Hoshi, H. Purification and molecular cloning of bovine oviduct-specific glycoprotein. Biol Reprod, *50:* 927-934, 1994.
215. Sendai, Y., Komiya, H., Suzuki, K., Onuma, T., Kikuchi, M., Hoshi, H., and Araki, Y. Molecular cloning and characterization of a mouse oviduct-specific glycoprotein. Biol Reprod, *53:* 285-294, 1995.
216. Shang, Y. and Brown, M. Molecular determinants for the tissue specificity of SERMs. Science, *295:* 2465-2468, 2002.
217. Shaw, L. M. Tumor cell invasion assays. Methods Mol Biol, *294:* 97-105, 2005.
218. Sherman, M. E., Berman, J., Birrer, M. J., Cho, K. R., Ellenson, L. H., Gorstein, F., and Seidman, J. D. Current challenges and opportunities for research on borderline ovarian tumors. Hum Pathol, *35:* 961-970, 2004.
219. Sherman, M. E., Bitterman, P., Rosenshein, N. B., Delgado, G., and Kurman, R. J. Uterine serous carcinoma. A morphologically diverse neoplasm with unifying clinicopathologic features. Am J Surg Pathol, *16:* 600-610, 1992.
220. Shih Ie, M. and Kurman, R. J. Molecular pathogenesis of ovarian borderline tumors: new insights and old challenges. Clin Cancer Res, *11:* 7273-7279, 2005.
221. Sieben, N. L., Macropoulos, P., Roemen, G. M., Kolkman-Uljee, S. M., Jan Fleuren, G., Houmadi, R., Diss, T., Warren, B., Al Adnani, M., De Goeij, A. P., Krausz, T., and Flanagan, A. M. In ovarian neoplasms, BRAF, but not KRAS, mutations are restricted to low-grade serous tumours. J Pathol, *202:* 336-340, 2004.
222. Silva, E. G., Gershenson, D. M., Malpica, A., and Deavers, M. The recurrence and the overall survival rates of ovarian serous borderline neoplasms with noninvasive implants is time dependent. Am J Surg Pathol, *30:* 1367-1371, 2006.
223. Silverberg, S. G. Prognostic significance of pathologic features of ovarian carcinoma. Curr Top Pathol, *78:* 85-109, 1989.
224. Silverberg, S. G. Problems in the differential diagnosis of endometrial hyperplasia and carcinoma. Mod Pathol, *13:* 309-327, 2000.
225. Sinclair, A. H. Human sex determination. J Exp Zool, *281:* 501-505, 1998.
226. Singer, G., Oldt, R., 3rd, Cohen, Y., Wang, B. G., Sidransky, D., Kurman, R. J., and Shih Ie, M. Mutations in BRAF and KRAS characterize the development of low-grade ovarian serous carcinoma. J Natl Cancer Inst, *95:* 484-486, 2003.
227. Singer, G., Stohr, R., Cope, L., Dehari, R., Hartmann, A., Cao, D. F., Wang, T. L., Kurman, R. J., and Shih Ie, M. Patterns of p53 mutations separate ovarian serous borderline tumors and low- and high-grade carcinomas and provide support for a new model of ovarian carcinogenesis: a mutational analysis with immunohistochemical correlation. Am J Surg Pathol, *29:* 218-224, 2005.
228. Sivridis, E. and Giatromanolaki, A. Prognostic aspects on endometrial

hyperplasia and neoplasia. Virchows Arch, *439:* 118-126, 2001.
229. Smyth, J. F., Gourley, C., Walker, G., MacKean, M. J., Stevenson, A., Williams, A. R., Nafussi, A. A., Rye, T., Rye, R., Stewart, M., McCurdy, J., Mano, M., Reed, N., McMahon, T., Vasey, P., Gabra, H., and Langdon, S. P. Antiestrogen therapy is active in selected ovarian cancer cases: the use of letrozole in estrogen receptor-positive patients. Clin Cancer Res, *13:* 3617-3622, 2007.
230. Society, American Cancer. www.cancer.org.
231. Sonnenberg, E., Weidner, K. M., and Birchmeier, C. Expression of the met-receptor and its ligand, HGF-SF during mouse embryogenesis. Exs, *65:* 381-394, 1993.
232. Stack, S., Gonzalez-Gronow, M., and Pizzo, S. V. Regulation of plasminogen activation by components of the extracellular matrix. Biochemistry, *29:* 4966-4970, 1990.
233. Stadel, B. V. Letter: The etiology and prevention of ovarian cancer. Am J Obstet Gynecol, *123:* 772-774, 1975.
234. Sundfeldt, K., Piontkewitz, Y., Ivarsson, K., Nilsson, O., Hellberg, P., Brannstrom, M., Janson, P. O., Enerback, S., and Hedin, L. E-cadherin expression in human epithelial ovarian cancer and normal ovary. Int J Cancer, *74:* 275-280, 1997.
235. Supino, R., Crosti, M., Clerici, M., Warlters, A., Cleris, L., Zunino, F., and Formelli, F. Induction of apoptosis by fenretinide (4HPR) in human ovarian carcinoma cells and its association with retinoic acid receptor expression. Int J Cancer, *65:* 491-497, 1996.
236. Suzuki, K., Sendai, Y., Onuma, T., Hoshi, H., Hiroi, M., and Araki, Y. Molecular characterization of a hamster oviduct-specific glycoprotein. Biol Reprod, *53:* 345-354, 1995.
237. Swerdlow, A. J., Marmot, M. G., Grulich, A. E., and Head, J. Cancer mortality in Indian and British ethnic immigrants from the Indian subcontinent to England and Wales. Br J Cancer, *72:* 1312-1319, 1995.
238. Tamagnone, L. and Comoglio, P. M. Control of invasive growth by hepatocyte growth factor (HGF) and related scatter factors. Cytokine Growth Factor Rev, *8:* 129-142, 1997.
239. Tanaka, M., Kyo, S., Kanaya, T., Yatabe, N., Nakamura, M., Maida, Y., Okabe, M., and Inoue, M. Evidence of the monoclonal composition of human endometrial epithelial glands and mosaic pattern of clonal distribution in luminal epithelium. Am J Pathol, *163:* 295-301, 2003.
240. Tashiro, H., Blazes, M. S., Wu, R., Cho, K. R., Bose, S., Wang, S. I., Li, J., Parsons, R., and Ellenson, L. H. Mutations in PTEN are frequent in endometrial carcinoma but rare in other common gynecological malignancies. Cancer Res, *57:* 3935-3940, 1997.
241. Taylor, H. S., Vanden Heuvel, G. B., and Igarashi, P. A conserved Hox axis in the mouse and human female reproductive system: late establishment and persistent adult expression of the Hoxa cluster genes. Biol Reprod, *57:* 1338-1345, 1997.
242. Thiery, J. P. Epithelial-mesenchymal transitions in tumour progression. Nat

Rev Cancer, *2:* 442-454, 2002.
243. Tibiletti, M. G., Bernasconi, B., Taborelli, M., Facco, C., Riva, C., Capella, C., Franchi, M., Binelli, G., Acquati, F., and Taramelli, R. Genetic and cytogenetic observations among different types of ovarian tumors are compatible with a progression model underlying ovarian tumorigenesis. Cancer Genet Cytogenet, *146:* 145-153, 2003.
244. Uchikawa, J., Shiozawa, T., Shih, H. C., Miyamoto, T., Feng, Y. Z., Kashima, H., Oka, K., and Konishi, I. Expression of steroid receptor coactivators and corepressors in human endometrial hyperplasia and carcinoma with relevance to steroid receptors and Ki-67 expression. Cancer, *98:* 2207-2213, 2003.
245. Um, S. J., Lee, S. Y., Kim, E. J., Han, H. S., Koh, Y. M., Hong, K. J., Sin, H. S., and Park, J. S. Antiproliferative mechanism of retinoid derivatives in ovarian cancer cells. Cancer Lett, *174:* 127-134, 2001.
246. Umbas, R., Isaacs, W. B., Bringuier, P. P., Schaafsma, H. E., Karthaus, H. F., Oosterhof, G. O., Debruyne, F. M., and Schalken, J. A. Decreased E-cadherin expression is associated with poor prognosis in patients with prostate cancer. Cancer Res, *54:* 3929-3933, 1994.
247. Vainio, S., Heikkila, M., Kispert, A., Chin, N., and McMahon, A. P. Female development in mammals is regulated by Wnt-4 signalling. Nature, *397:* 405-409, 1999.
248. Van den Steen, P. E., Opdenakker, G., Wormald, M. R., Dwek, R. A., and Rudd, P. M. Matrix remodelling enzymes, the protease cascade and glycosylation. Biochim Biophys Acta, *1528:* 61-73, 2001.
249. van der Burg, M. E., Henzen-Logmans, S. C., Berns, E. M., van Putten, W. L., Klijn, J. G., and Foekens, J. A. Expression of urokinase-type plasminogen activator (uPA) and its inhibitor PAI-1 in benign, borderline, malignant primary and metastatic ovarian tumors. Int J Cancer, *69:* 475-479, 1996.
250. Verhage, H. G., Fazleabas, A. T., and Donnelly, K. The in vitro synthesis and release of proteins by the human oviduct. Endocrinology, *122:* 1639-1645, 1988.
251. Verhage, H. G., Fazleabas, A. T., Mavrogianis, P. A., O'Day-Bowman, M. B., Schmidt, A., Arias, E. B., and Jaffe, R. C. Characteristics of an oviductal glycoprotein and its potential role in fertility control. J Reprod Fertil Suppl, *51:* 217-226, 1997.
252. Verhage, H. G., Mavrogianis, P. A., O'Day-Bowman, M. B., Schmidt, A., Arias, E. B., Donnelly, K. M., Boomsma, R. A., Thibodeaux, J. K., Fazleabas, A. T., and Jaffe, R. C. Characteristics of an oviductal glycoprotein and its potential role in the fertilization process. Biol Reprod, *58:* 1098-1101, 1998.
253. Wan, M., Li, W. Z., Duggan, B. D., Felix, J. C., Zhao, Y., and Dubeau, L. Telomerase activity in benign and malignant epithelial ovarian tumors. J Natl Cancer Inst, *89:* 437-441, 1997.
254. Watanabe, T., Kobori, K., Miyashita, K., Fujii, T., Sakai, H., Uchida, M., and Tanaka, H. Identification of glutamic acid 204 and aspartic acid 200 in chitinase A1 of Bacillus circulans WL-12 as essential residues for chitinase activity. J Biol Chem, *268:* 18567-18572, 1993.
255. Weiss, N. S. and Peterson, A. S. Racial variation in the incidence of ovarian

cancer in the United States. Am J Epidemiol, *107:* 91-95, 1978.
256. Wesseling, J., van der Valk, S. W., and Hilkens, J. A mechanism for inhibition of E-cadherin-mediated cell-cell adhesion by the membrane-associated mucin episialin/MUC1. Mol Biol Cell, *7:* 565-577, 1996.
257. Wesseling, J., van der Valk, S. W., Vos, H. L., Sonnenberg, A., and Hilkens, J. Episialin (MUC1) overexpression inhibits integrin-mediated cell adhesion to extracellular matrix components. J Cell Biol, *129:* 255-265, 1995.
258. Whittemore, A. S., Harris, R., and Itnyre, J. Characteristics relating to ovarian cancer risk: collaborative analysis of 12 US case-control studies. IV. The pathogenesis of epithelial ovarian cancer. Collaborative Ovarian Cancer Group. Am J Epidemiol, *136:* 1212-1220, 1992.
259. Williams, T. I., Toups, K. L., Saggese, D. A., Kalli, K. R., Cliby, W. A., and Muddiman, D. C. Epithelial ovarian cancer: disease etiology, treatment, detection, and investigational gene, metabolite, and protein biomarkers. J Proteome Res, *6:* 2936-2962, 2007.
260. Wilson, J. Adeno-carcinomata in hens kept in a constant environment. Poult Sci, *37:* 1253, 1958.
261. Wolf, N. G., Abdul-Karim, F. W., Farver, C., Schrock, E., du Manoir, S., and Schwartz, S. Analysis of ovarian borderline tumors using comparative genomic hybridization and fluorescence in situ hybridization. Genes Chromosomes Cancer, *25:* 307-315, 1999.
262. Wong, A. S., Leung, P. C., and Auersperg, N. Hepatocyte growth factor promotes in vitro scattering and morphogenesis of human cervical carcinoma cells. Gynecol Oncol, *78:* 158-165, 2000.
263. Wong, A. S., Leung, P. C., Maines-Bandiera, S. L., and Auersperg, N. Metaplastic changes in cultured human ovarian surface epithelium. In Vitro Cell Dev Biol Anim, *34:* 668-670, 1998.
264. Wong, A. S., Maines-Bandiera, S. L., Rosen, B., Wheelock, M. J., Johnson, K. R., Leung, P. C., Roskelley, C. D., and Auersperg, N. Constitutive and conditional cadherin expression in cultured human ovarian surface epithelium: influence of family history of ovarian cancer. Int J Cancer, *81:* 180-188, 1999.
265. Wong, A. S., Pelech, S. L., Woo, M. M., Yim, G., Rosen, B., Ehlen, T., Leung, P. C., and Auersperg, N. Coexpression of hepatocyte growth factor-Met: an early step in ovarian carcinogenesis? Oncogene, *20:* 1318-1328, 2001.
266. Wong, A. S., Roskelley, C. D., Pelech, S., Miller, D., Leung, P. C., and Auersperg, N. Progressive changes in Met-dependent signaling in a human ovarian surface epithelial model of malignant transformation. Exp Cell Res, *299:* 248-256, 2004.
267. Woo, M. M., Alkushi, A., Verhage, H. G., Magliocco, A. M., Leung, P. C., Gilks, C. B., and Auersperg, N. Gain of OGP, an estrogen-regulated oviduct-specific glycoprotein, is associated with the development of endometrial hyperplasia and endometrial cancer. Clin Cancer Res, *10:* 7958-7964, 2004.
268. Woo, M. M., Gilks, C. B., Verhage, H. G., Longacre, T. A., Leung, P. C., and Auersperg, N. Oviductal glycoprotein, a new differentiation-based indicator present in early ovarian epithelial neoplasia and cortical inclusion cysts.

Gynecol Oncol, *93:* 315-319, 2004.
269. Woo, M. M., Salamanca, C. M., Minor, A., and Auersperg, N. An improved assay to quantitate the invasiveness of cells in modified Boyden chambers. In Vitro Cell Dev Biol Anim, *43:* 7-9, 2007.
270. Wu, R., Hendrix-Lucas, N., Kuick, R., Zhai, Y., Schwartz, D. R., Akyol, A., Hanash, S., Misek, D. E., Katabuchi, H., Williams, B. O., Fearon, E. R., and Cho, K. R. Mouse model of human ovarian endometrioid adenocarcinoma based on somatic defects in the Wnt/beta-catenin and PI3K/Pten signaling pathways. Cancer Cell, *11:* 321-333, 2007.
271. Xu, X. C., Ro, J. Y., Lee, J. S., Shin, D. M., Hong, W. K., and Lotan, R. Differential expression of nuclear retinoid receptors in normal, premalignant, and malignant head and neck tissues. Cancer Res, *54:* 3580-3587, 1994.
272. Yang, G., Rosen, D. G., Colacino, J. A., Mercado-Uribe, I., and Liu, J. Disruption of the retinoblastoma pathway by small interfering RNA and ectopic expression of the catalytic subunit of telomerase lead to immortalization of human ovarian surface epithelial cells. Oncogene, *26:* 1492-1498, 2007.
273. Yang, G., Rosen, D. G., Mercado-Uribe, I., Colacino, J. A., Mills, G. B., Bast, R. C., Jr., Zhou, C., and Liu, J. Knockdown of p53 combined with expression of the catalytic subunit of telomerase is sufficient to immortalize primary human ovarian surface epithelial cells. Carcinogenesis, *28:* 174-182, 2007.
274. Yazawa, S., Abbas, S. A., Madiyalakan, R., Barlow, J. J., and Matta, K. L. N-acetyl-beta-D-glucosaminyltransferases related to the synthesis of mucin-type glycoproteins in human ovarian tissue. Carbohydr Res, *149:* 241-252, 1986.
275. Yoshida, H., Broaddus, R., Cheng, W., Xie, S., and Naora, H. Deregulation of the HOXA10 homeobox gene in endometrial carcinoma: role in epithelial mesenchmal transition. Cancer Res, *66*: 889-897, 2006.
276. Young, T. N., Rodriguez, G. C., Moser, T. L., Bast, R. C., Jr., Pizzo, S. V., and Stack, M. S. Coordinate expression of urinary-type plasminogen activator and its receptor accompanies malignant transformation of the ovarian surface epithelium. Am J Obstet Gynecol, *170:* 1285-1296, 1994.
277. Zahn, S., Sievers, S., Alemazkour, K., Orb, S., Harms, D., Schulz, W. A., Calaminus, G., Gobel, U., and Schneider, D. T. Imbalances of chromosome arm 1p in pediatric and adult germ cell tumors are caused by true allelic loss: a combined comparative genomic hybridization and microsatellite analysis. Genes Chromosomes Cancer, *45:* 995-1006, 2006.
278. Zand, L., Qiang, F., Roskelley, C. D., Leung, P. C., and Auersperg, N. Differential effects of cellular fibronectin and plasma fibronectin on ovarian cancer cell adhesion, migration, and invasion. In Vitro Cell Dev Biol Anim, *39:* 178-182, 2003.
279. Zhang, Y. W. and Vande Woude, G. F. HGF/SF-met signaling in the control of branching morphogenesis and invasion. J Cell Biochem, *88:* 408-417, 2003.
280. Zheng, H., Kavanagh, J. J., Hu, W., Liao, Q., and Fu, S. Hormonal therapy in ovarian cancer. Int J Gynecol Cancer, *17:* 325-338, 2007.

6. APPENDIX

6.1 UBC Research Ethics Approval Form

The University of British Columbia
Office of Research Services
Clinical Research Ethics Board – Room 210, 828 West 10th Avenue, Vancouver, BC V5Z 1L8

ETHICS CERTIFICATE OF EXPEDITED APPROVAL: RENEWAL

PRINCIPAL INVESTIGATOR:	DEPARTMENT:	UBC CREB NUMBER:
Nelly Auersperg	UBC/Medicine, Faculty of/Obstetrics & Gynaecology	H87-70219

INSTITUTION(S) WHERE RESEARCH WILL BE CARRIED OUT:

Institution	Site
Vancouver Coastal Health (VCHRI/VCHA)	Vancouver General Hospital
Children's and Women's Health Centre of BC (incl. Sunny Hill)	Children's and Women's Health Centre of BC (incl. Sunny Hill)

Other locations where the research will be conducted:
Child and Family Research Institute

CO-INVESTIGATOR(S):
N/A

SPONSORING AGENCIES:
British Columbia Health Research Foundation - "Molecular Characterization of Receptors for GnRH and Activin in Epithelial Ovarian Carcinomas" - "Regulatory Interactions Between the Surface Epithelium and Follicular Cells in the Human Ovary"
British Columbia Ministry of Advanced Education - "CA125 as a Predictive Marker for Familial Ovarian Cancer"
Cancer Research Society - "Ovarian Carcinogenesis: Preneoplastic Changes and Early Detection"
Medical Research Council - "Early Changes in Ovarian Carcinogenesis" - "Microenvironmental and Familial Factors in Ovarian Carcinogenesis"
National Cancer Institute of Canada - "Microenvironmental and Familial Factors in Ovarian Carcinogenesis" - "Microenvironmental and familial factors in ovarian carcinogenesis"
National Institutes of Health - "Biology of Ovarian Cancer"

PROJECT TITLE:
Microenvironmental and familial factors in ovarian carcinogenesis

EXPIRY DATE OF THIS APPROVAL: December 17, 2008

APPROVAL DATE: December 17, 2007

CERTIFICATION:
In respect of clinical trials:
1. The membership of this Research Ethics Board complies with the membership requirements for Research Ethics Boards defined in Division 5 of the Food and Drug Regulations.
2. The Research Ethics Board carries out its functions in a manner consistent with Good Clinical Practices.
3. This Research Ethics Board has reviewed and approved the clinical trial protocol and informed consent form for the trial which is to be conducted by the qualified investigator named above at the specified clinical trial site. This approval and the views of this Research Ethics Board have been documented in writing.

The Chair of the UBC Clinical Research Ethics Board has reviewed the documentation for the above named project. The research study, as presented in the documentation, was found to be acceptable on ethical grounds for research involving human subjects and was approved for renewal by the UBC Clinical Research Ethics Board.

Approval of the Clinical Research Ethics Board by:

Dr. James McCormack

Dr. James McCormack, Associate Chair